CORA Cork Open Research Archive
Cartlann Taighde Oscailte Chorcaí

Title	A study into the properties and applications of bacterial microcompartments and polyphosphate metabolism
Authors	McCarthy, Karen Christine
Publication date	2015
Original Citation	McCarthy, K. C. 2015. A study into the properties and applications of bacterial microcompartments and polyphosphate metabolism. PhD Thesis, University College Cork.
Type of publication	Doctoral thesis
Rights	© 2015, Karen Christine McCarthy. - http://creativecommons.org/licenses/by-nc-nd/3.0/
Download date	2026-11-07 02:57:44
Item downloaded from	https://hdl.handle.net/10468/3811

UCC
University College Cork, Ireland
Coláiste na hOllscoile Corcaigh

A study into the properties and applications of bacterial microcompartments and polyphosphate metabolism.



Ollscoil na hÉireann, Corcaigh

NATIONAL UNIVERSITY OF IRELAND, CORK

A Thesis presented to the National University of Ireland for the Degree of Doctor of Philosophy by

Karen Christine McCarthy, B.Sc.

School of Microbiology and Alimentary Pharmabiotic Centre, Ireland

University College Cork

Supervisor: Prof. Michael B. Prentice

Head of School: Prof. Gerald F. Fitzgerald

September 2015

Declaration

I hereby declare that the research presented in this thesis is my own work and effort and that it has not been submitted for any other degree, either at University College Cork or elsewhere. Wherever contributions of others are involved, every effort is made to indicate this clearly, with due reference to the literature and acknowledgement of collaborative research and discussions.

This work was completed under the guidance of Prof. Michael B. Prentice at the School of Microbiology, in association with the Alimentary Pharmabiotic Centre, University College Cork.

Signature:.....

Date:.....

Table of Contents

Thesis Abstract **5**

List of Abbreviations **7**

Chapter I **9**

A study of bacterial microcompartments and phosphate metabolism in bacteria and humans

Chapter II **80**

A study of polyphosphate kinases and phosphate uptake in *Lactobacillus* and *E. coli.*

Chapter III **142**

Investigation into the use of a biological phosphate removal system *in vivo.*

Chapter IV **189**

Investigation into changes in buoyant cell density of bacterial cells following induction of ethanolamine (Eut*)* and propanediol (Pdu) microcompartments

Chapter V **230**

Extraction and imaging of bacterial microcompartments.

Chapter VI **266**

Conclusions and Future Directions

Acknowledgments **273**

Thesis Abstract

Bacterial microcompartments were initially observed in the 1950s and since that time, research in the field has focused on the unique properties of their proteinaceous structures and their role in the bacterial cell.

This thesis investigates the properties of the propanediol utilization (Pdu) and ethanolamine (Eut) utilization microcompartments and applications of their components in the cells of *Lactobacillus reuteri,* and *Escherichia coli* predominantly, with additional investigation into *Yersinia spp.*

The experimental chapters of this thesis initially investigate the application of bacterial microcompartments as tools for compartmentalizing metabolic reactions, in particular regarding the uptake of phosphate from extracellular environment and the retention of polyphosphate intracellularly. This was observed experimentally through the engineering of recombinant constructs containing genes encoding microcompartment-directed polyphosphate kinase enzyme. Bacterial phenotypes conferred by these constructs with respect to enhanced net uptake of phosphate from the environment were defined, and potential applications as a clinical therapy addressed in an animal trial, which utilized the phosphate-uptake constructs which had been created. In the trial, recombinant bacteria expressing these constructs were successfully delivered in therapeutic quantities to the target (small intestine) of rats experiencing induced renal failure, with no adverse effects were observed. However inter-group animal variation regarding baseline blood mineral content was larger than the expected therapeutic effect and therefore no therapeutic effect could be demonstrated.

Additionally, novel phenotypic differences conferred by induction of Pdu and Eut microcompartments and empty recombinant microcompartments on host cells were identified. These identified an observable phenotypic difference in buoyant density between strains expressing the *Pdu* and *Eut* microcompartments. Futher investigation into the potential function and phenotypic differences of strains expressing microcompartments were supported by methodological developments including the use of imaging instruments such as the FIB-SEM, and microcompartment extraction from cells. These technical developments enabled additional observations regarding the characteristics of microcompartments and provided novel information.

List of Abbreviations (alphabetical order)

(3-HPA) Beta-hydroxypropionaldehyde

(6-PG/PK) the 6-phosphogluconate/phosphoketolase

(ADPN) Adiopectin

(AmpR) Ampicillin resistance

(ATP) Adeno-Tri-Phosphate

(B-PER) Bacterial protein extraction reagent

(BMC) Bacterial microcompartment

(BSA) Bovine serum albumin

(BSIC) BioSciences Imaging Centre

(CKD) Chronic kidney disease

(CmR) Chloramphenicol resistance

(cob) Cobalamin genes

(EAL) ethanolamine ammonia-lyase

(EBPR) Enhanced Biological Phosphorus Removal

(ECOR) E. coli reference library

(EHEC) Enterohaemorrhagic E. coli

(EmR) Erythromycin resistance

(EPEC) Enteropathogenic E. coli

(ESRD) End-stage renal disease

(ETEC) Entrotoxigenic E. coli

(Eut) Ethanolamine

(DAPI) 4',6-diamidino-2-phenylindole

(FIB-SEM) Focused ion beam – scanning electron microscopy

(LB) Luria Bertani broth

(LTU) Long-term usage(MBD) Mineral & bone disease

(MCP) Microcompartment

(MLM) Minimal Lactobacillus Medium

(MLST) Multi locus sequencing technology

(MRS MOD) de Man-Rogosa-Sharpe Modified

(MRS) de Man-Rogosa-Sharpe

(MW) Molecular weight

(P) Phosphorus

(p)ppGpp) Guanosine pentaphosphate phosphohydralase

(PAP) Polyphosphate :AMP phosphotransferase

(PBS) Phosphate buffered saline

(Pdu) Propanediol

(polA) DNA repair polymerase

(PolyP) Polyphosphate

(ppGpp) Guanosine 3,5-bispyrophosphate

(PPK) Polyphosphate kinase

(PPX) Exopolyphosphate

(PTH) Parathyroid hormone

(RuBisCO) Ribulose-1,5-bisphosphate carboxylase/oxygenase

(SDS-PAGE) Sodium dodecyl sulfate-polyacrylamide gel electrophoresis

(SMR) Suspended microchannel resonator

(STEM) Scanning transmission electron microscope

(TEM) Transmission electron microscopy

(xylA) Xylose isomerase gene A

(Y-PER) Yeast protein extraction reagent

Chapter I

A study of bacterial microcompartments and phosphate metabolism in bacteria and humans.

.

Literature Review

Contents

1.0. Abstract

1.1. Discovery and identification of microcompartments

1.1.1. The function of the microcompartment

1.1.2. The common structure of the microcompartment

1.1.3. Why compartmentalize?

1.2. Propanediol (Pdu) microcompartment

1.2.1. Identification

1.2.2. Genetics

1.2.3. Structure

1.2.4. Metabolism of 1,2-Propanediol

1.3. Ethanolamine (*eut*) microcompartment

1.3.1. Role of ethanolamine

1.3.2. Identification

1.3.3. Genetics

1.3.4. Structure and function

1.3.5. Metabolism of ethanolamine

1.4. Phosphorus & Phosphate

1.4.1. The phosphorus cycle

1.4.2. Polyphosphate in nature

1.4.3. The role of polyphosphate in bacteria

1.4.3.1. PolyP as an energy source

1.4.3.2. PolyP as a phosphate source

1.4.3.3. PolyP as a regulator

1.5. Polyphosphate kinases

1.5.1. Polyphosphate kinase 1

1.5.2. Polyphosphate kinase 2

1.5.3. Exophosphates

1.6. Polyphosphate metabolism

1.6.1. Polyphosphate metabolism in bacteria

1.6.2. Polyphosphate metabolism in humans

1.7. Hyperphosphatemia

1.7.1. Association with renal failure and cardiovascular

1.7.2. Prevention and therapies

1.7.2.1. Phosphorus absorption

1.7.2.2. Polyphosphate absorption

1.7.2.3. Phosphate binders

1.8. References

1.0. Abstract

Bacterial microcompartments (MCPs) offer promise for the future of synthetic biology and metabolic engineering. The ability to offer increased reaction and enzymatic efficacy through cellular compartmentalization is common in eukaryotes, but was presumed non-existent in prokaryotes. However, levels of compartmentalization offer benefits to natural, and potentially synthetically engineered bacterial systems. The possible retention of toxic intermediates, or volatile metabolites are all possible roles discussed for native microcompartments, which have been identified in many diverse bacterial genera, including pathogens and commensals, Gram positives and Gram negatives.

Those genera that produce microcompartments attribute a large number of genes to their generation and the identification of >50 microcompartments within a single bacterial cell under electron microscopy indicates an important role in the limited spatial arrangement of the bacterial cell.

Knowledge of mechanisms by which bacteria gain energy and resources from microcompartment-mediated metabolism may illustrate potential vulnerabilities in the processes by which some pathogens multiply in the gut, or alternatively may indicate potentially biotechnological or clinical applications such as the ability to accumulate intracellular phosphate within a microcompartment, which is to be a focus point in the experimental chapters of this thesis.

Phosphate and polyphosphate act within the prokaryotic bacterial cell to regulate aspects of metabolic and stress responses. Within the human body, phosphate levels are regulated in parallel with calcium by the parathyroid hormone, and a

resulting dysfunction in this balance can lead to disruption of the blood and renal system, resulting in the illness hyperphosphatemia. This accumulation of phosphate in the blood requires treatment using a variety of interventions including the use of oral phosphate binders, and dietary control of phosphate intake.

The potential to apply a microcompartment-mediated uptake system, expressed in a probiotic host, may offer some alternative options for relieving excess phosphate and hyperphosphataemia.

Sections 1.1-1.3 will discuss the functionality and characteristics of bacterial microcompartments, particularly focusing on the Pdu and Eut microcompartments. Sections 1.4-1.7 will then discuss the role of phosphate within bacteria and the human body, and how excess phosphate in the body is typically treated.

1.1. Discovery of bacterial microcompartments

Bacterial microcompartments (MCPs) are small proteinaceous structures originally observed within bacterial cells in the 1950s (Drews & Niklowitz, 1956). They possess a distinct polygonal shape, which triggered their identification by electron microscopy. This unusual geometric shape caused MCPs to be initially mistaken for phage capsids (Peters, 1974). However expanding research into the structures and their properties identified MCPs as being distinctive novel structures.

Initially observed in the cyanobacterium *Phormidium uncinatum* in 1956 (Drews & Niklowitz, 1956) these MCPs were dismissed as being inclusion bodies or aggregates. After some time, their distinct polygonal shape was identified in many more bacterial species, primarily cyanobacteria including *Nostoc punctiforme* (Yeates *et al.,* 2010) However since the early 1970s, microcompartments have been identified, through genome sequencing, in approximately 400 genomes, including diverse genera such as *Lactobacillus*, *Clostridia*, *Klebsiella,* and *Salmonella* (Kerfeld *et al.,* 2010).

Due to their distinct proteinaceous composition, it is possible to extract microcompartments as a distinct fraction from the bacterial cell, originally through the use of sucrose density gradient centrifugation, which produced the first extracted MCP from *Halothiobacillus neapolitanus* in 1973 (Shively *et al.,* 1973).

On extraction, the unique structure now associated with MCPs could be identified, distinguishing them from inclusion bodies or other vacuoles. These polyhedral structures were then denoted as carboxysomes, due to the presence of

ribulose-1,5-bisphosphate carboxylase/oxygenase (RuBisCO) within the MCP (Shively *et al.,* 1973).

1.1.1. The function of the microcompartment

Due to the wide range of bacteria that produce bacterial MCPs, they appear to have varying functions, mainly centered on either anabolic (building up) or catabolic (breaking down) activities. This division into anabolic (typically carboxysomes) and catabolic (typically metabolosomes) is dependent upon their cargo enzymes (Aussignargues *et al.,* 2014).

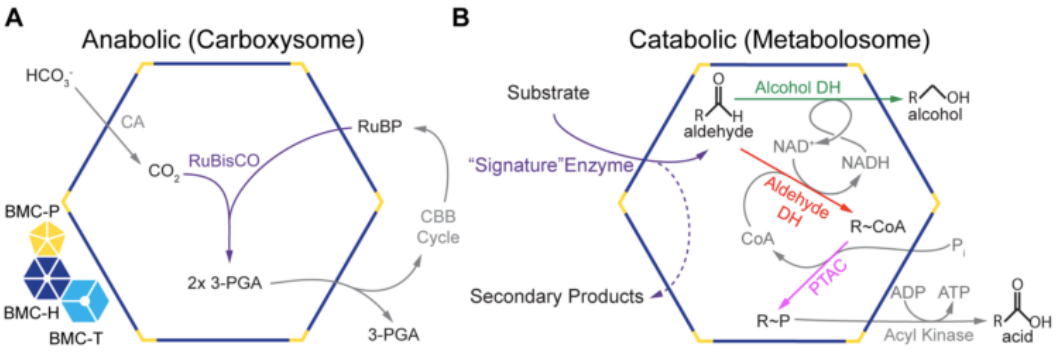


Figure 1.1. *Schematic illustrating the anabolic and catabolic MCPs (Axen et al., 2014)*

For carboxysomes, which are predominantly observed in autotrophs, their role is primarily anabolic carbon-fixation, particularly in cyanobacteria. Cyanobacteria are one of the key contributors to the global carbon cycle, where they play roles in marine and terrestrial ecosystems (Cameron *et al.,* 2013). The carboxysome plays a key role in the Calvin-Benson-Bassham cycle, where it is a core factor in the carbon concentrating mechanism (Price *et al.,* 1992). In the carboxysome, CO_2 fixation is enhanced through the encapsulation of key enzymes ribulose 1,5-bisphosphate carboxylase/oxygenase (RuBisCO), a carbon fixing enzyme, and

carbonic anhydrase. This shift reduces the reaction with O_2, which is a competitive substrate (Heinhorst *et al.,* 2006).

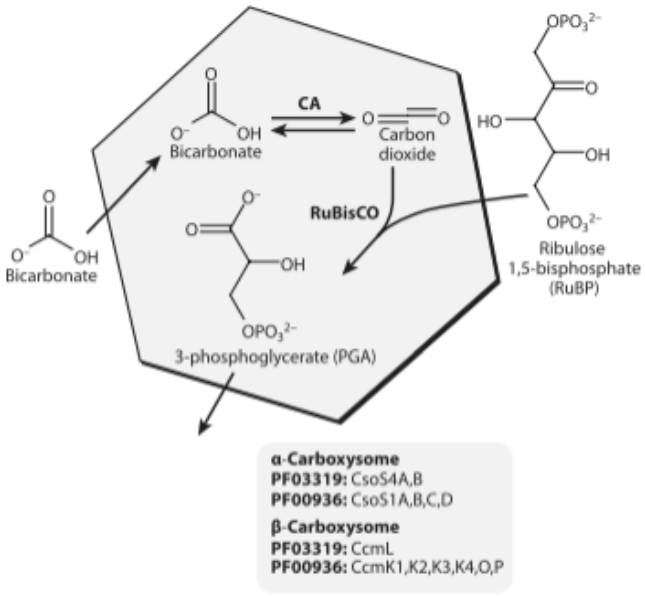


Figure 1.2. *Illustration of the carboxysome microcompartment (Kerfeld et al., 2010)*

In contrast, in heterotrophic bacteria, the two most common MCPs are the propanediol (Pdu*)* and the ethanolamine (Eut*)* microcompartments. As mentioned, these MCPs are more directly focused on catabolic activity - breaking down substrates within their enclosed shells.

1.1.2. The common structure of the microcompartment

A unifying structural feature of the MCPs is a thin enclosing shell composed mainly of thousands of small protein subunits, which all belong to a family of homologous BMC (bacterial microcompartment) shell proteins. The BMC shell proteins have been identified across many bacteria; originally in the carboxysome (English *et al.,* 1994) and then subsequently in the *pdu* operon of *Salmonella* (Chen *et al.,* 1994) and also the ethanolamine (*eut*) operon of

Salmonella (Stojiljkovic *et al.,* 1995). Currently, 1700 unique BMC-containing proteins have been identified, in 10 different phyla (Yeates *et al.,* 2011). The typical length of the commonest BMC domain is approximately 90 amino acids, with an alpha/beta fold (Kerfeld *et al.,* 2005). The shell proteins form hexamers that go on to act as the foundation of the shell (Figure 2.1). The commonest BMC proteins (hexameric shell subunits) contain a single copy of the Pfam domain PF00936, and are called BMC-H. Longer shell proteins (BMC-T) are a fusion of two of the PF00936 domains and form trimers (pseudohexamers). Another non-homologous Pfam domain PF03319 is associated with a minority of shell proteins including some that form pentamers (BMC-P) (Axen *et al.,* 2014).

Each hexamer has a two-sided shape, with a prominent bowl-shaped depression on the side containing the N-termini and C-termini (Yeates *et al.,* 2010). A narrow pore also exists through the middle of the hexamer, along the six-fold axis of symmetry (Yeates *et al.,* 2011).

The carboxysome typically assumes an icosahedral shape, which is guided by the homologous proteins CcmL and CsoS4A (PF03319, BMC-P), which form a small proportion of the overall shell proteins and are present in different carboxysome types. These are pentamers and are hypothesized to form the vertices of the MCP shell, resulting in the distinct and recognizable icosahedral shape (Tanaka *et al.,* 2008), which was identified using EM cryotomography (Schmid *et al.,* 2006). However in structural assembly studies of Pdu and Eut MCPs, these pentameric proteins proved more difficult to crystallise. In fact *Salmonella* EutN, which is homologous to CcmL, was found to form hexamers on crystallization (Tanaka *et al.,* 2008). However, charge-based native gel

separation shows EutN from *E. coli* is pentameric in solution, despite this hexameric crystal structure (Wheatley *et al.,* 2013) and it has been proposed that these proteins should be called BMV (bacterial microcompartment vertex proteins).

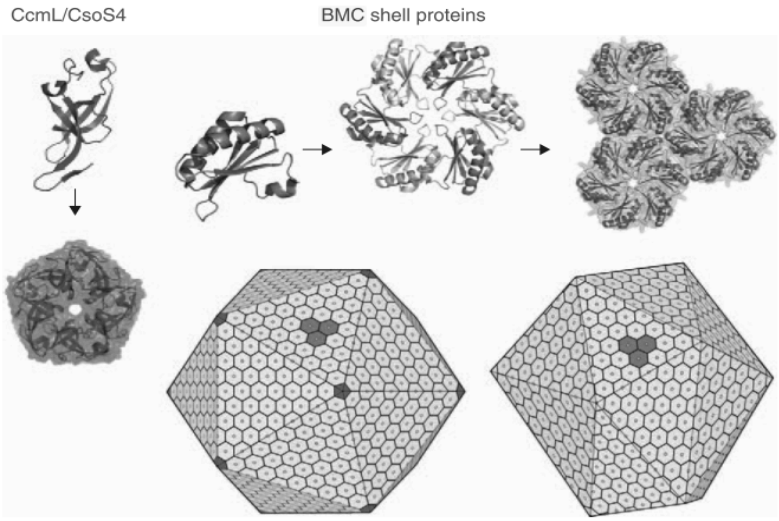


Figure 1.3. *Figure illustrating simplified microcompartment shell assembly*

(credit: Yeates et al., 2011)

Surprisingly, within the various BMC domain proteins, there is a large degree of variation regarding confirmation and tomography. Many of the BMC proteins contain tandem-BMC domains, which have been identified in all MCPs (e.g. PduT, EutN, PduB) These tandem-BMC domains result in the construct of a symmetric trimer with pseudo six-fold symmetry (Klein *et al.,* 2009). These variants have been observed to cause conformational changes which affect the central pore of the hexamer. In addition, there both single and tandem-domain BMC can be permuted shell proteins (PduU, EutS, EtuB), which result in the production of the N-terminus and C-terminus at different spatial locations, and allow the blocking of the pore by an extended 6-stranded beta barrel tail (Tanaka *et al.,* 2009).

To build further on these findings, different tandem-BMC domain proteins can be arranged in opposite order in the pseudohexamer, including those assembled from two circularly permuted domains (EutL, EutD) and two canonical BMC domains (PduT); (Crowley *et al.,* 2010) (Tanaka *et al.,* 2010). Other variations include enzyme components and co-factors. Recent bioinformatics analysis has found 23 different types of BMCs encoded in 30 distinct locus subtypes found in 23 bacteria phyla (Axen *et al.,* 2014). The focus of this study will be however primarily be on the Pdu and Eut MCPs, and their genetics, structure and metabolic roles are further detailed further in the sections below.

α-Carboxysome (*e.g. Halothiobacillus neapolitanus*)		
CsoS1A	Single-BMC domain hexamer	Major shell component (Tsai *et al.,* 2007)
CsoS1C	Single-BMC domain hexamer	Major shell component (Tsai *et al.,* 2009)
CsoS1D	Tandem-BMC domain (permuted) trimer	Trimers stack to form a hexamer with D3 symmetry; open and closed conformations suggest gated transport (Klein *et al.,* 2009)
CsoS4A/B	Pentamer (non-BMC domain)	Minor shell component; believed to form icosahedral vertices.
β-Carboxysome (*e.g. Synechocystis PCC6803*)		
CcmK1	Single-BMC domain hexamer	Major shell component (Tanaka *et al.,* 2008)
CcmK2	Single-BMC domain hexamer	Major shell component (Samborska & Kimber, 2012)
CcmK4	Single-BMC domain hexamer	Minor shell component (Kerfeld *et al.,* 2005)
CcmL	Pentamer (non-BMC domain)	Minor shell component; believed to form icosahedral vertices.
Pdu Microcompartment (*e.g. Salmonella enterica, Lactobacillus reuteri*)		
PduA	Single-BMC domain hexamer	Major shell component (Pang *et al.,* 2014)
PduB	Tandem-BMC domain trimer	Major shell component, subunit pore rather than central pore (Pang *et al.,* 2012)
PduT	Tandem-BMC domain trimer	Pore likely involved in electron transport or Fe-S cluster transport (Pang *et al.,* 2011)
PduU	Single-BMC domain hexamer (permuted)	Minor shell component; pore is blocked by 6-stranded β-barrel in crystal structure (Crowley *et al.,* 2008)
Eut Microcompartment (*e.g. S. enterica & E. coli*)		
EutK	Single-BMC domain fused to helix-turn-helix (HTH) domain	HTH motif with positively charged surface suggests role in nucleic acid binding (Tanaka *et al.,* 2009*)*
EutL	Tandem-BMC domain trimer	Pore observed in open and closed conformations; probable role in gated transport (Sagermann *et al.,* 2009)
EutM	Single-BMC domain hexamer	Major shell component (Tanaka *et al.,* 2009*)*
EutN	Non-BMC domain hexamer	Crystallizes as a hexamer despite homology to pentameric CcmL/CsoS4 family; pentameric association from gel.
EutS	Single-BMC domain (permuted) hexamer	Hexamer forms bent structure with C2 symmetry; possible role in edge formation within shell (Tanaka *et al.,* 2009*)*
Other Microcompartments		
EtuB	Tandem-BMC domain (permuted) trimer	Part of presumptive ethanol utilization microcompartment in Clostridium kluyveri.
PduT homolog	Tandem-BMC domain trimer	Part of microcompartment of uncharacterized function in De sulfitobacterium halfniense.

Table 1.1. *Table illustrating known structures of shell proteins from bacterial microcompartments (Yeates et al., 2011)*

1.1.3. Why compartmentalize?

In bacteria that produce MCPs, they often dedicate a large amount of genetic information to its function – *Salmonella* has 40 genes encoding the Pdu MCP (Bobik *et al.,* 1999). The BMC domains, which encode for the MCP shell, are also highly conserved across MCP-associated species. There are benefits for cellular compartmentalization; enzymes like RuBisCO can have slow reaction turnover, which could be alleviated by access to a local concentration gradients of substrates (Eichelmann *et al.,* 2009). Metabolites can also be required to participate in many competing reactions, which can reduce their availability and lead to pathway bottlenecks (Xu *et al.,* 2011).

In eukaryotes, this method of metabolic compartmentalisation is not uncommon – the perixosome is a membrane organelle that contains reactions relating to the catabolism of hydrogen peroxide (Gehrmann & Elsner, 2011). Bacterial MCPs, due to their hexameric shell proteins, contain a number of pores postulated to regulate substrate transport (Klein *et al.,* 2009). This allows isolation of reaction intermediates from the rest of the cell, providing high concentrations of substrates, removing the problem of enyzmes such as RuBisCo.

Compared to the cytoplasm as a whole, quantification calculations indicate that there is a significant concentration effects which apply to enzyme kinetics within the MCP. A bacterial MCP is approximately 1000^{th} the volume of a bacterial cell (a typical *E. coli* cell is approximately $1\mu m^3$), (Vendeville *et al.,* 2011). Utilising Avogadro's number (6.02×10^{23}) and calculating 1 litre = 1.0×10^{15} μm^3, this indicates that in the cytoplasm, a single enzyme molecular represents an enzyme

concentration of approximately 10^{-9} M (nanomolar), whilst the same molecule within the MCP actually is equivalent to micromolar concentration.

In addition, based on stochastic modeling, classical Michaelis-Menten kinetic calculations likely underestimated the rates of catalyzed reactions occurring within the MCP (Conrado *et al.,* 2007), (Grima, 2009). This information indicates that the fundamental effects of molecular crowding prompt the process of compartmentalization within the MCP.

This is also research indicating that the presence of MCPs within a cell is associated with spatial organisation. Carboxysomes align themselves along the main axis of the cell, with the cytoskeletal component ParA required for this correct alignment to occur (Cornejo *et al.,* 2014). This connection is still not fully elucidated, but may provide information that could aid the design of novel synthetic structures (Chen & Silver, 2012).

There is also evidence for a contribution of the Pdu and Eut microcompartments to the mitigation of potentially toxic aldehyde intermediates (Penrod & Roth, 2006), (Sampson & Bobik, 2008). The relevant studies for each microcompartment are included under their individual sections.

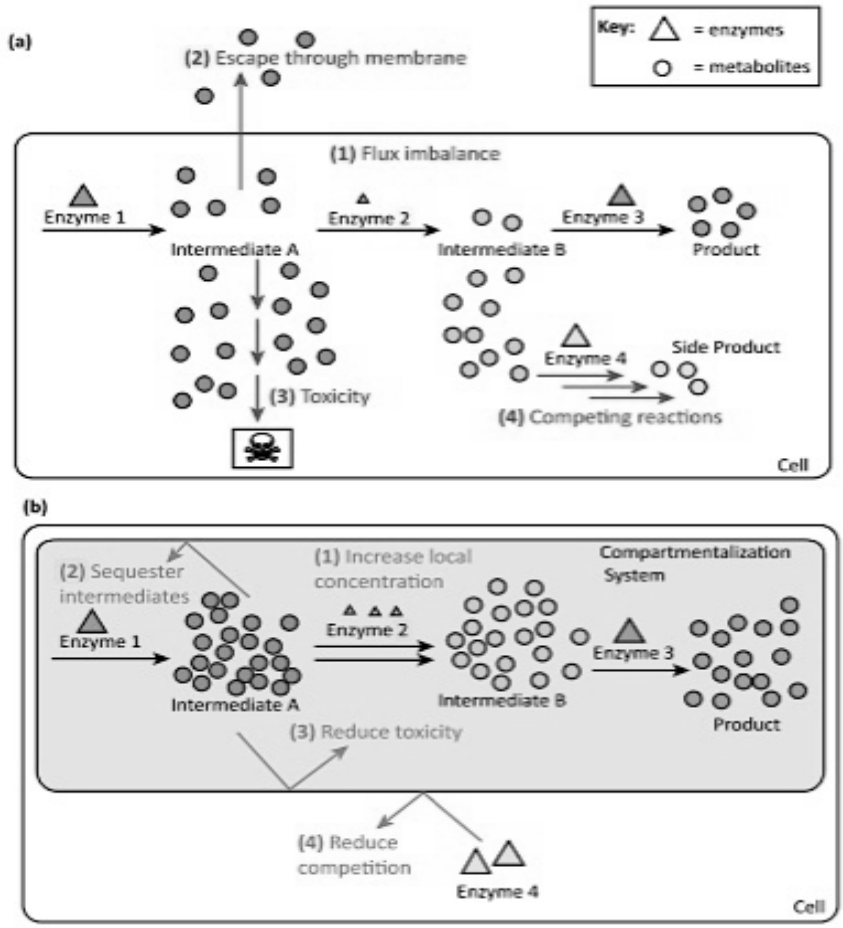


Figure 1.4. *(1) Differing enzyme kinetics may result in flux imbalances. (2) Intermediates may be lost through the cell membrane. (3) Toxic intermediates can result in growth inhibition. (4) Competing reactions can divert flux through undesired pathways. (b) Compartmentalization systems specifically solve challenges 1–4, respectively, by: (1) creating areas of local concentrations to favour reaction kinetics; (2) sequestering intermediates; (3) reducing toxicity; and (4) reducing competition. (Credit: Lee et al., 2012; Chen & Silver, 2012).*

1.2. Propanediol utilization (Pdu*)* Microcompartment

1.2.1. Identification

The propanediol utilization *(*Pdu*)* microcompartment was initially identified in 1994, when homologues of carboxysome shell proteins were identified in a gene cluster associated with the metabolism of 1,2-propanediol in the strain *Salmonella enterica* serovar Typhimurium (Chen *et al.,* 1994). This coenzyme-B12 dependent metabolism was hypothesized to take place within the encapsulation of the proteinaceous MCP, thus protecting the cell from the toxic intermediate, propionaldehyde (Havemann *et al.,* 2002). This demonstrated that bacterial MCPs were involved in additional metabolic processes beyond CO_2 fixation, and heralded the discovery of the Pdu microcompartment in the presence of 1,2-propanediol.

1.2.2. Genetics

The *Pdu* operon is approximately 19kbp long, encoding for up to 23 genes with products related to the metabolism of 1,2-propanediol (Crowley *et al.,* 2010). The breakdown of this operon can be observed in Table 3.1.

The Pdu microcompartment appears more complex than its related counterpart, the carboxysome, with more enzymatic capabilities. It contains the key enzymes for 1,2-propanediol metabolism (Parsons *et al.,* 2010). The genes encoding 1,2-propanediol utilization can be identified in a contiguous cluster (*pocR*, *pduF*, and *pduABB'CDEGHJKLMNOPQSTUVWX*), which encodes enzymes for the breakdown of 1,2-propanediol and cobalamin recycling, along with the formation proteins for the MCP (Bobik *et al.,* 1997).

No. of genes	Genes	Encoding	Source
7	*pduA, pduB, pduB', pduJ, pduK, pduN, pduU, pduT**	Eight shell proteins (further details Table 2.1)	Frank *et al.,* 2013
7	*pduCDE, pduL, pduP, pduQ, pduW*	Metabolic enzymes	Leal *et al.,* 2003; Liu *et al.,* 2007
4	*pduGH, pduO, pduS**	Cobalamin & dehydratase reactivation	Bobik *et al.,* 1997; Cheng and Bobik, 2010; Johnson *et al.,* 2001; Parsons *et al.,* 2010b
1	*pduX*	Cobalamin synthesis	Fan and Bobik, 2008
1	*pduF*	Propanediol diffusion faciliator	Chen *et al.,* 1994
1	*pduV*	MCP/cytoskeleton interaction	Parsons *et al.,* 2010a
1	*pduM*	Structural protein	Sinha *et al.,* 2012

Table 1.2. *Table indicating the gene breakdown of the Pdu microcompartment (Frank et al., 2013)*

** not present in L. reuteri Pdu MCP (Sriramulu et al., 2008)*

1.2.3. Structure

Appearing relatively heterogeneous in size, the Pdu microcompartments have been observed as being between 120-160 nm in diameter (Havemann *et al.,* 2003). Their shape, as previously mentioned in Section 2.1.2., is less regular than that of the icosahedral carboxysome, and tends be appear more polyhedral with various irregular facets (Kerfeld *et al.,* 2005). The MCP shell is estimated to contain approximately 4000 protein subunits (Yeates *et al.,* 2008), which surround an additional <15,000 protein molecules (Cheng et al., 2008). In the Pdu microcompartment, the first shell protein to be crystalized was PduU (Crowley *et al.,* 2008).



Figure 1.5. *The Pdu operon, including structural and enzymatic genes. (Crowley et al., 2010)*

As mentioned in Section 2.1.2., and Table 2.1., the Pdu MCP shell is formed by the paralogous structural proteins belonging to BMC Pfam domain PF00936 PduA,B,J,K,T and U, and PduN (Pfam 033190). This involvement of multiple distinct BMC domains appears to be a highly conserved feature amongst the MCP family (Beeby *et al.,* 2009).

A distinct feature of the Pdu microcompartment is the presence of two forms of PduB; PduB and PduB'. The difference between these two forms is a mere 37 amino acids, and occurs due to two translation start sites on the polycistronic message (Parsons et al., 2008). This produces a slight variance in protein size; PduB is 28kDa, whilst PduB' is 24kDa. This can be identified by SDS-PAGE analysis. The crystal structure relates to the full length PduB (Pang *et al.,* 2012).

Targeting of a heterologous protein to a microcompartment has been achieved by fusion with the N-terminal 42 AA of PduV (Parsons *et al.,* 2010). Sequence alignment suggested the presence of an 18 amino acid extension in the N-terminal of the propionaldehyde dehydrogenase (PduP) protein only present in homologues associated with MCP function (BMC proximal) and not homologues of PduP which were not MCP-associated (Figure 3.2) (Fan *et al.,* 2010). The 18 amino acid sequence, present in the N-terminal of the propionaldehyde dehydrogenase (PduP) protein, was necessary and sufficient when fused with fluorescent proteins (e.g. GFP) or other heterologous proteins to localize the

targeted protein within the Pdu microcompartment (Fan *et al.,* 2010). In order to demonstrate that this PduP peptide is important for encapsulation within the microcompartment, PduP mutants that lacked these distinct N-terminal amino acids were engineered. Once purified, these mutant MCPs had far less PduP vs the wild-type strain. This observation demonstrated that the deletion or removal of these N-terminal amino acids from PduP impaired its association to the MCP (Fan *et al.,* 2010).

The structure of the p18 sequence from PduP (aldehyde dehydrogenase) of *Citrobacter freundii* has since been reported (Lawrence *et al.,* 2014), indicating a well-defined helical conformation along its whole length. Further studies have also since indicated that these target sequences are not limited to the N-terminus, with the C-terminal region of an α-carboxysomal protein (CcmN) interacting with the shell (Kinney *et al.,* 2012), (Field *et al.,* 2015).

Peptides, mostly derived from viruses or prions, are recognized for organelle-targeting within eukaryotic cells, and protein export target sequences are well recognized in bacteria, but physiological internal peptide targeting is novel for bacterial cells. There are more of these specific enzyme targeting sequences across the MCP systems, with a number of proteins successfully directed into the MCP using terminal targeting peptides (Lawrence *et al.,* 2014).

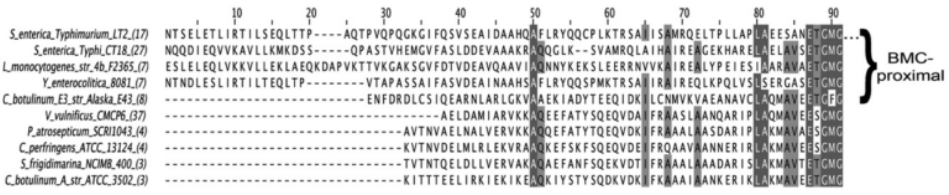


Figure 1.6. *Multiple sequence alignment highlighting the extended N-terminal sequences seen in 4 out of 5 microcompartment-associated aldehyde dehydrogenase PduP and absent in 5 homologues which are not MCP-associated (Fan et al., 2010)*

Recently, a key structural requirement for three or four conserved residues exposed on the edges of assembled hexamers for shell assembly has been demonstrated (Pang *et al.,* 2014), (Sinha *et al.,* 2014).

1.2.4. Metabolism of 1,2-Propanediol

The *pdu* operon in *Salmonella* was originally regarded as being unimportant to the overall metabolic and competitive capacity of the bacteria, despite the fact that *Salmonella* maintains approximately 40 genes for the metabolism of propanediol and biosynthesis of cobalamin B12 (*cob* genes) (Bobik *et al.,* 1999). The utilization of 1,2-propanediol did not appear to offer an *in vivo* competitive advantage, as it is not readily available in the environment and required the use of an electron acceptor (Bobik *et al.,* 1997).

The observation that the electron acceptor tetrathionate in the presence of a functioning tetrathionate reductase operon not only could support the anaerobic use of 1,2-propanediol as a sole carbon and energy source via the use of endogenously synthesized B12 , but actually lead to increased growth on this source (Price-Carter *et al.,* 2001), was finally integrated into the enteric pathogenesis strategies of *Salmonella* in an *in vivo* model. This model showed that the production of tetrathionate, from the reaction of thiosulphate resulting from anaerobic bacterial metabolism with reactive oxygen species produced by inflammatory damage to the large intestine, provided the necessary electron acceptor to allow anaerobic respiration of 1,2-propanediol produced from fucose catabolism and offered a major growth advantage to *Salmonella* over commensal bacteria (Winter *et al.,* 2010). Microcompartment-mediated metabolism is thus

an important contributor to the dysbiosis of intestinal infection (Winter & Baumler, 2013) .

In *Salmonella* and *Lactobacillus reuteri,* the Pdu MCP is formed in response to the presence of 1,2-propanediol, which acts as a transcriptional control. 1,2-propanediol is a fermentative product of the sugars rhamnose and fucose (Obradors *et al.,* 1998). Fucose is present in the glycoconjugates of intestinal cell where it plays a role in host-parasite interactions in the digestive tract (Bry *et al.,* 1996). As such, 1,2-propanediol is hypothesized to act as a persistent carbon and energy source for aerobic and anaerobic metabolism in enteric bacteria (Bobik 2006).

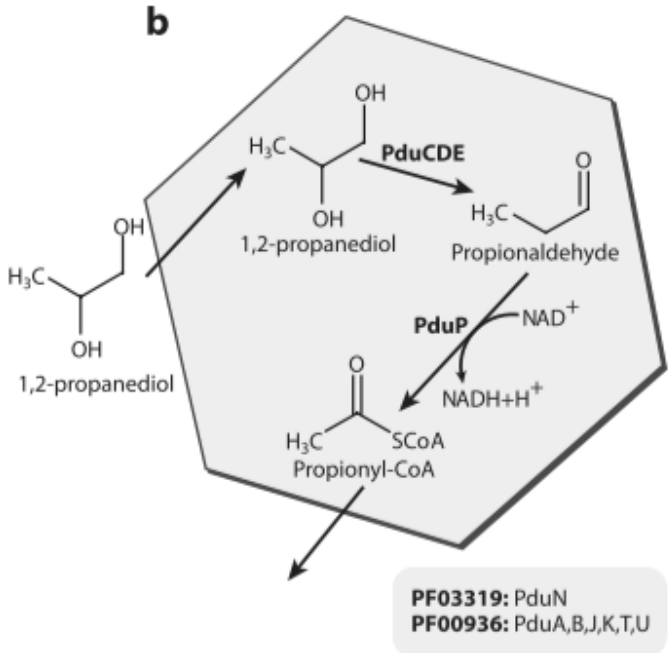


Figure 1.7. *Schematic illustrating the metabolic processes of the Pdu MCP. (Kerfeld et al., 2010)*

The Pdu MCP provides an encapsulated space for the initial enzymatic steps for 1,2-propanediol metabolism; i) 1,2-propanediol is first converted to

propionaldehyde by the B12 dependant diol dehydratase enzyme and ii) this toxic intermediate propionaldehyde is further converted to propionyl-CoA, by the actions of coenzyme-A and NAD^+-dependant propionaldehyde dehydrogenase (Bobik *et al.,* 1997).

There are a number of additional enzymes present in the Pdu MCP which are involved in 1,2-propanediol metabolism; an NADH-dependent cob(II/III) alamin reductase, an ATP-dependent adenosyltransferase which triggers the activation of coenzyme B12 and finally an ATP-dependent diol dehydratase reactivase, which releases deactivated B12 (Crowley *et al.,* 2010). Because there is no means of ATP generation within the microcompartment, for these enzymes to function means that ATP must be able to access the microcompartment interior from outside.

In *L. reuteri,* PduCDE contributes to the formation of beta-hydroxypropionaldehyde (3-HPA) from glycerol co-fermentation, which is the foundation (through its monomeric and dimeric forms) of the production of the antimicrobial agent reuterin (Morita *et al.,* 2008). The *L. reuteri* Pdu MCP differs from that of *Salmonella* by an association of the *L. reuteri* PduL enzyme with the MCP structure (Sriramulu *et al.,* 2008) and by the absence of PduS and PduT (a single electron channel) (Pang *et al.,* 2011).

1.2.5. The role of the Pdu microcompartment

Synthesizing the many thousands of proteins required for the formation of the Pdu MCP is a large energy investment by the cell, therefore its formation is typically strictly limited to environments containing 1,2-propanediol – a fact

which has hampered research into its functionality in bacteria such as *Salmonella* (Bobik *et al.,* 1997).

Although much research focuses on the pathogenic association of the presence of the Pdu MCP, it has also been identified in the commensal probiotic *Lactobacillus reuteri* DSM 20016, where it degrades 1,2-propanediol to propionaldehyde (Sriramulu *et al.,* 2008). The production of aldehydes within MCPs has lead to hypotheses regarding a potential role in the presence of the MCP in mitigating aldehyde toxicity. This idea was initially based upon comparative genomics (Stojilkovic *et al.,* 1995), as both the 1,2-propanediol and ethanolamine degradation pathways proceed via aldehyde intermediates. Studies involving the deletion of the *pduA* gene indicated that when MCP formation was prevented, culture growth was halted at high concentrations of 1,2-propanediol, suggesting that a toxic metabolite (propionaldehyde) was accumulating from the catabolism of 1,2-propanediol (Havemann *et al.,* 2003). In this study, *pdu* mutants (*pduJ, pduK, pduB)* also released significant amounts of propionaldehyde versus the wild-type strain, indicating a potential structural role for the MCP in the retention of the aldehyde.

In contrast, other studies proposed an alternative role for MCP based on the Eut microcompartment, suggesting the role of the MCP was to prevent acetaldehyde loss from the cell, which can occur due its volatile state as a gas (Penrod & Roth, 2006). (Cheng *et al.,* 2011), (Huseby & Roth, 2013). In either case, the mechanism of retention of small aldehyde molecules within a protein structure is not fully understood.

Horizontal transfer of the MCP is possible by cloning (Parsons *et al.,* 2008), with the use of an artificial operon, which contains the core structural genes, allowing the expression of an empty structurally viable MCP (Parsons *et al.,* 2010). This key observations forms the basis of experimental chapters Chapter II and III of this thesis.

1.3. Ethanolamine utilization (*eut)* Microcompartment

1.3.1. The role of ethanolamine

Ethanolamine is an amino alcohol produced in the gastrointestinal tract of mammals as a product of the degradation of phosphatidyl ethanolamine, which is present in large quantities in eukaryotic membranes. Due to rapid turnover of membrane cells in the digestive tract – approx. 25% of enterocytes per day are released into the gut per day – ethanolamine is present at high levels in the mammalian gut (Snoeck *et al.,* 2005). Ethanolamine is a valuable source of key nutrients such as carbon and nitrogen, which may offer a competitive advantage amongst the many bacteria present in the mammalian gut (Thiennimitr *et al.,* 2011), particularly some pathogenic bacteria such as enterohaemorrhagic *E. coli* (EHEC) (Bertin *et al.,* 2011). For pathogens capable of metabolizing, ethanolamine, like 1,2-propanediol, can be respired by the cell through the availability of tetrathionate (as an electron acceptor) (Price-Carter *et al.,* 2001) in an inflamed gut (Thiennimitr *et al.,* 2011). Expression of the eut operon is quantitatively greater in enterohaemorrhagic *E. coli* (EHEC) than commensal *E. coli* on exposure to ethanolamine (Bertin *et al.,* 2011).

In *E. coli* O157:H7, free ethanolamine has been identified to act as a nitrogen source, which had been previously observed in *Salmonella* (Penrod & Roth, 2006), (Stojilkovic *et al.,* 1995). A functional ethanolamine ammonia-lyase (EAL) is required for nitrogen metabolism, whilst acetaldehyde dehydrogenase, alcohol dehydrogenase and phosphotransacetylase do not appear to contribute to the process (Bertin *et al.,* 2011).

1.3.2. Identification

The ethanolamine utilization (Eut*)* microcompartment and its gene cluster were initially identified in *E. coli* in 1995 (Stojiljkovic *et al.,* 1995). Its dependence on the presence of B12 was noted and its association with the presence of genes encoding a bacterial microcompartment. The *eut* operon has been identified in a number of enteric bacterial genera, typically pathogenic. The complete *eut* cluster has been identified in a number of *E. coli* strains; particularly those associated with mammalian enteric infection *e.g.* EHEC (enterohaemorragic *E. coli*), EPEC (enteropathogenic *E. coli)* and ETEC (enterotoxigenic *E. coli)*. However this same gene cluster was also identified in a number of commensal or K-12 strains including MG1655 (Bertin *et al.,* 2011), other Enterobacteriaceae such as *Salmonella,* and Gram positives such as *Listeria* (Korbel *et al.,* 2005) and *Enterococcus*. Despite the consistent presence of the Eut operon in *E. coli*, images of the Eut microcompartment in *E. coli* are rare (Shively *et al.,* 1998) but they seem similar to Pdu microcompartments.

1.3.3. Genetics

The arrangement of the *eut* operon in *E. coli* is highly similar to the *pdu* operon. The *eut* operon contains a number of BMC domain genes that are identifiable across MCP-producing bacteria (Section 2.1.2., Table 2.1.).

No. of genes	Genes	Encoding	Source
1	*EutT*	Corrinoid adenosyltransferase & cobalamin recycling	Kofoid *et al.,* 1999
1	*EutD*	Phosphotransacetylase	Kofoid *et al.,* 1999
1	*EutE*	Aldehyde dehydrogenase	Kofoid *et al.,* 1999
1	*EutJ*	Possible chaperone function	Kofoid *et al.,* 1999
1	*EutG*	Alcohol dehydrogenase	Kofoid *et al.,* 1999
1	*EutH*	Permease	Kofoid *et al.,* 1999
1	*EutA*	Ethanolamine ammonia-lyase reactivase	Kofoid *et al.,* 1999
2	*EutB, EutC*	Ethanolamine ammonia lyase	Kofoid *et al.,* 1999
1	*EutR*	Transcription activator	Kofoid *et al.,* 1999

Table 1.3. *Table indicating the gene breakdown of the eut microcompartment. (Yeates et al., 2008)*

In total, the *eut* operon contains 17 encoding genes, with a number of these involved in the transport and metabolism of ethanolamine (Roof & Roth, 1992). Key genes include *eutR*, which acts a transcriptional activator for the expression of the *eut* operon in response to the presence of ethanolamine (Yeates *et al.,* 2008) and the structural genes *eutS, eutM, eutN, eutL* and *eutK,* which encode the formative shell proteins (Kofoid *et al.,* 1999). Recent studies have indicated an unexpected importance for *eutD* with regards to long-term growth on ethanolamine (Huseby & Roth, 2013). It has also been observed that in strains with defective MCP shell genes, excess acetaldehyde is released versus the wild-type, indicating a role for the MCP in acetaldehyde retention (Penrod & Roth, 2006).

1.3.4. Function of the Eut microcompartment

The main role of the Eut microcompartment, like the Pdu microcompartment (Section 3.1.5.) is a matter of debate; one hypothesis is that its role is in the

retention of the volatile aldehyde intermediate, which would otherwise be lost during the gas phase (Penrod & Roth, 2006). This is similar to the retention of the less volatile aldehyde propionaldehyde in the Pdu microcompartment but the advantage drawn from it is different. Penrod and Roth suggested that the mechanism of aldehyde retention may be that all microcompartments sustain an internal pH lower than that of the exterior cytoplasm. This acid environment may promote the conversion of aldehydes to less volatile acetals. A primary advantage of microcompartment enclosure in preventing aldehyde metabolite loss rather than cytoplasmic toxicity was supported by lack of acetaldehyde toxicity in mutants unable to form the Eut MCP (Penrod & Roth, 2006).

Other studies have indicated a role of the Eut MCP in the sequestering of toxic aldehyde (Brinsmade *et al.,* 2005). *polA* (DNA repair polymerase) mutants were unable to grow on ethanolamine (Rondon *et al.,* 2005). However, the possibility of increased ethanolamine sensititity in these mutants (at non-toxic levels for the wild-type) was indicated by a later study (Penrod & Roth, 2006).

The *eut* operon genes have also been identified in *Listeria monocytogenes,* where knockout studies of *eutB* (required for ethanolamine metabolism) illustrated intracellular growth of *Listeria* in mammalian tissue culture is greatly reduced (Joseph *et al,* 2005) and the *eut* operon is strongly induced in infecting Listeria (Archambaud *et al.,* 2012) .

1.3.5. Metabolism

Ethanolamine is metabolized in the *eut* microcompartment in two steps; i) Ethanolamine ammonia-lyase initially requires the co-factor adenosyl cobalamin which is synthesized in anaerobic conditions, but crucially transported under

aerobic conditions (Jeter *et al.,* 1984). Once B12 is present, ii) ethanolamine is then cleaved to produce ammonia plus acetaldehyde, which is further converted to acetyl-coenzyme A (acetyl Co-A) by oxidoreductase, which is NAD-dependent. Within Chapter IV, there is further detail concerning ethanolamine metabolism with respects to its importance and contribution to the cell.

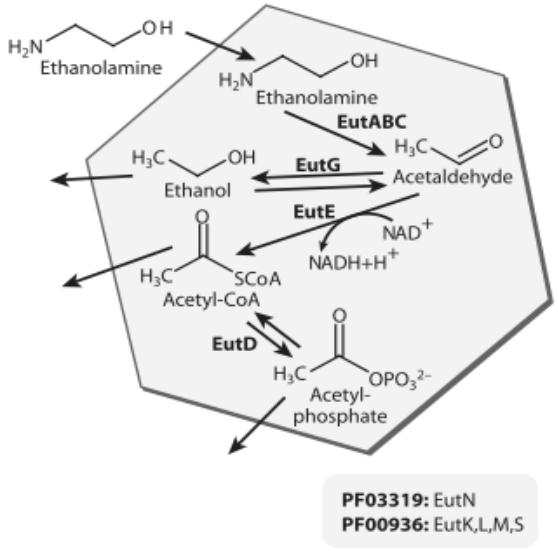


Figure 1.8. *Schematic illustrating the metabolic processes of the eut MCP. (Kerfeld et al., 2010)*

1.4. Phosphorus and Phosphate

Rarely existing as a free chemical, phosphorus (P) is an element that is predominantly identified within nature as part of the phosphate molecule (PO_4). Organic phosphate is typically defined as phosphate associated with a carbon-based molecular structure, such as animal tissue. In contrast inorganic phosphate is any available phosphate not associated with organic material, and is the dominant source within nature.

1.4.1. The phosphorus cycle

The phosphorus cycle typically begins through plant matter assimilating inorganic phosphorus and converting this to organic phosphorus. Through the consumption and decomposition of these plants, animals can then obtain this converted organic phosphorus. Continuing the cycle, as animals excrete waste and die, their consumed organic phosphorus dissolves into the soil bed or water table, where bacterial saprophytes reconvert it back to inorganic phosphorus. This is then once again available for assimilation by plant matter, and the cycle continues anew (EPA.gov.usa).

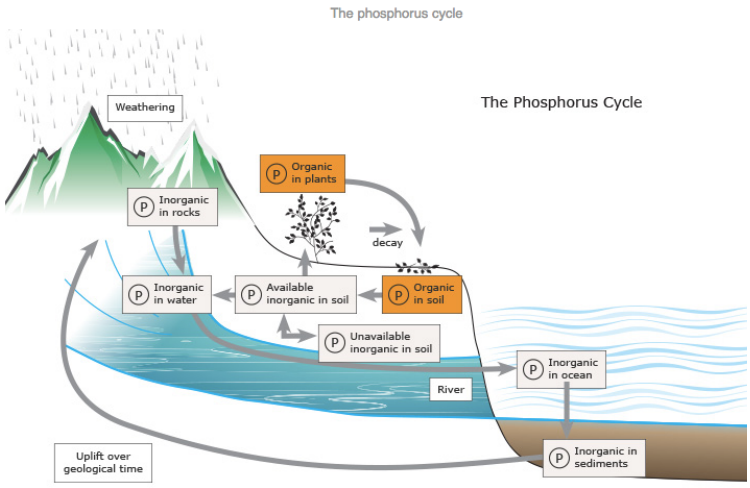


***Figure 1.9**. Image illustrating the natural cycle of phosphorus (Science Learning Hub, University of Waikato, 2013)*

Terrestrial phosphorus cycle is predominantly influenced by agricultural practices, with increasing off-flow accumulation in rivers and soils threaten eutrophication (Bennett *et al,* 2001). Few minerals bear enough phosphorus in meaningful quantities. In igneous rock, fluorapatite, which is typically associated with ferromagnesian minerals, is one of the main phosphorus-bearers, whilst in sedimentary rock, the majority of phosphorus is present in authigenic (formed in situ) carbonate-fluorapatite (Fillipelli, 2008).

Within the ocean, authigenic formation of calcium phosphate minerals in sediments results in a large phosphorus sink. The source for apatite in oceanic phosphate sediments in some coastal regions is thought to be polyphosphate from the giant sulphur bacterium *Thiomargarita namibiensis* (Schulz & Schulz, 2005) and a significant proportion of apatite in all oceanic sediments may derive from deposition of polyphosphate-containing diatoms (Diaz *et al*, 2008),

1.4.2. Polyphosphate in nature

Inorganic polyphosphate (polyP) exists as a linear chain of hundreds of phosphate residues linked by energy-rich phosphoanhydride bonds, the same as those found in adeno-tri-phosphate (ATP), which is the molecular energy currency of cells.

Highly conserved across nature, and stable over a range of temperatures, pH and oxidants (Rao *et al,* 2009), polyP is present in bacterial, animal, fungal and plant cells (Brown & Kornberg, 2004). Within nature, polyP has been identified in deep oceanic vents and volcanoes, where it has been generated through the dehydration of orthophosphate or phosphate rock, at elevated temperatures

(Kornberg, 1995). Orthophosphates are the inorganic forms of phosphate, such PO_4^-, HPO_4^- and $H_2PO_4^-$, and the most common form used for fertilizers (Johnson *et al,* 2007).

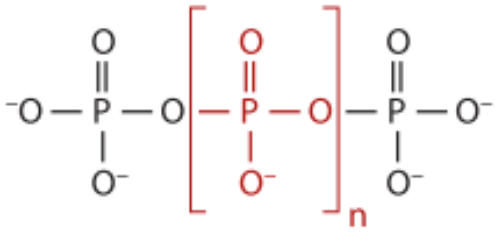


Figure 1.10. *Inorganic polyphosphate (PolyP). The value of n, the number of PO_3^- residues, may vary from 3 to over 1,000.* (Rao *et al*, 2009).

1.4.3. The role of polyP in bacterial cells

PolyP was initially observed as metachromatic granules within the bacterium *Spirillum volutans*, which lead to the term "volutin granules" being bequeathed on these unusual clusters. These clusters could be stained pink using toluidine blue (Meyer, 1904). Using microscopy, the volutin granules could be correlated against the presence of polyP, an observation that led to the renaming from volutin to polyP granules, nearly 50 years after their initial discovery (Wiame, 1937). Typically in prokaryotes, polyP granules are composed of acid-insoluble, long chain polyP and present in the cytoplasm (Wood & Clark, 1988), (Kulaev & Vagabov, 1983). In some bacteria cells however, acid-soluble, short chain polyP can also be identified beyond the cytoplasm, in cellular compartments such as the periplasm or plasma membrane (Wood & Clark, 1988). In *Helicobacter pylori*, polyP granules have been observed in the cell membrane (Achbergerova & Nahalka, 2011) and in the sporulating prespore of *Acetonema longum* (Tocheva *et al.,* 2013).

1.4.3.1. PolyP as an energy source

As previously mentioned, polyP is a rich source of energy. Within the microbial cell, granules of polyP act as reservoirs for energy and phosphate storage, which can be degraded to release ATP or phosphate (Achbergerová & Nahálka, 2011). It has been observed in polyP-deficient cells, that cells compensate for this energy gap by increasing the flow of energy generating pathways such as the citric acid cycle and oxidative phosphorylation (Varela *et al,* 2010). There are a number of key enzymes involved in this important process of polyP metabolism, including polyphosphate kinases (PPK), (Kornberg *et al,* 1956) and exopolyphosphatases (PPX) (Akiyama *et al,* 1993).

1.4.3.2. PolyP as a phosphate source

In prokaryotes, polyPs are the dominant regulators of intracellular phosphate. The amount of polyP within a bacterial cell typically depends on its surrounding environment, with bacteria associated with wastewater typically exhibiting high levels of polyP (Kulaev & Kulakovskaya, 2000). However to ensure a standard, stable level of intracellular phosphate, a polyP reservoir which can be changed to phosphate via exopolyphosphatases, is essential. PolyP, due to its polymeric form, is ideal to act as a large-scale phosphate sink within the cell, as its aggregations have little effect on cellular osmotic pressure (Kulaev *et al,* 2004). As phosphorus is a life-limiting factor, this ability to uptake and retain vast amounts of phosphate in the form of polyP is crucial for cell survival, particularly in environments where phosphate is limited (Kulaev and Vagabov, 1983).

1.4.3.3. PolyP as a regulator

Due to important contribution of polyP storage and phosphate metabolism to cellular function, polyPs contribute to the regulation of enzymatic activities and gene expression. This influence can be observed in stress conditions and on adaptation into the stationary-growth phase (Kulaev *et al,* 2004). There is a close responsive relationship between polyP and the alarmone guanosine 3,5-bispyrophosphate (ppGpp), a key factor in the bacterial stringent response (Kulaev *et al,* 2004). The crucial role that polyP kinase (PPK) plays in cellular survival under stress and starvation was highlighted by PPK-mutant studies (Crooke *et al,* 1994).

PolyP has been observed to have an impactful role in the oxidative stress response in both prokaryotic and eukaryotic cells (Gray & Jakob, 2015). Previous studies demonstrated increased stress sensitivity from heat and H_2O_2 when the polyphosphate kinase gene (PPK) of *Escherichia coli* was disrupted (Akiyama *et al,* 1992), and polyP deficiency was also observed to be associated with increased sensitivity in *Mycobacterium tuberculosis* on exposure to nitrosative stress (Singh *et al.,* 2013). Studies on *Proteus mirabilis* additionally identified loss of colonization ability, along with a loss of swarming and biofilm formation where attenuation of the *ppk* gene had occurred (Peng *et al.,* 2015).

More recently, similar stress sensitivity has been identified in *Lactobacillus* spp., where again, disruption of the PPK gene led to diminished growth under extreme conditions (high salt or low pH) and an increased sensitivity to oxidative stress (Alcantara *et al,* 2014).

1.5. Polyphosphate kinases (PPK)

As previously mentioned, in bacteria, the main enzyme known to be involved in polyP synthesis is polyphosphate kinase (PPK), which, in an ATP-dependent reaction, catalyzes the creation of a phosphoanhydride bond between a polyP chain and orthophosphate (Rao *et al,* 2009). Due to this connection with the utilization of ATP, PPKs are key enzymes within the cell, as they are capable of alternating the balance of energy and phosphate, from storage to consumption (Achbergerova & Nahalka, 2011).

$$2\ PO_4^{3-} + 2\ H^+ \rightleftharpoons P_2O_7^{4-} + H_2O$$

Figure 1.11. *Equation illustrating the condensation reaction resulting in the production of polyphosphates. Equilibrium status is given as the opposite hydrolytic reaction is also possible.*

The typical reaction leading to the formation of polyP within the cell essentially arises from the polymerization of phosphoric acid derivatives. This condensation reaction is energy consuming (ATP-dependent) and consists of two phosphate molecules together forming polyphosphate.

This forward reaction can continually repeat, with an additional phosphate added at each step. The reaction is reversible, with a hydrolytic reverse reaction, but predominantly the reaction favors polyP synthesis (Rao *et al*, 2009). This reaction is catalyzed by what was originally perceived as the only PPK, but when PPK knockout studies in *Pseudomonas* spp., still displayed up to 20% of polyP levels, the novel PPK2 was identified, leading to the reclassification of the "original" PPK as PPK1. (Ishige *et al,* 2002).

1.5.1. Polyphosphate kinase 1 (PPK1)

PPK1 (EC 2.7.4.1) was the first PPK identified, and is the key catalyzer of the polymerization of the terminal phosphate of ATP into a polyP chain (Kornberg et al, 1956). Across the majority of species, prokaryotic and eukaryotic, PPKs have been identified (Achbergerova & Nahalka, 2011), although no definitive proof has demonstrated their presence in mammalian cells (Pavlov *et al.,* 2010). In particular, PPK1 and its homologues have been identified in >100 species, across pathogens like *Klebsiella pneumoniae sp pneumoniae* and probiotics like *Lactobacillus delbrueckii* (Rao et al, 2009). This makes PPK1 the most highly conserved enzyme involved in polyP metabolism.

PPK2	PPK1 only	Neither PPK1 nor PPK2
PPK2 and PPK1	**Genome complete**	*Aeropyrum pernix*
Agrobacterium tumefaciens	*Bacillus anthracis*	*Aquifex aeolicus*
Brucella melitensis	*Bacillus halodurans*	*Archaeoglobus fulgidus*
Burkholderia fungorum(2)	*Clostridium acetobutylicum*	*Bacillus subtilis*
Campylobacter jejuni	*E. coli*	*Borrelia burgdorferi*
Caulobacter crescentus	*Helicobacter pylori*	*Buchnera aphidicola str. Sg*
Chlorobium tepidum	*Mycobacterium leprae*	*Buchnera sp. APS*
Chloroflexus aurantiacus	*Neisseria meningitidis*	*Chlamydia muridarum*
Deinococcus radiodurans	*Salmonella typhi*	*Chlamydia trachomatis*
Magnetospirillum magnetotacticum (2)	*Salmonella typhimurium*	*Chlamydophila pneumoniae*
Mesorhizobium loti(2)	*Xylella fastidiosa*	*Clostridium perfringens*
Methanosarcina acetivorans(2)	*Yersinia pestis*	*Fusobacterium nucleatum*
Methanosarcina mazei(2)		*Haemophilus influenzaeRd*
Mycobacterium tuberculosis	**Genome incomplete**	*Halobacterium sp. NRC-1*
Myxococcus xanthus	*Acidithiobacillus ferrooxidans*	*Lactococcus lactis*
Nostoc punctiforme (2)	*Acinetobacter baumannii*	*Listeria innocua*
Nostoc sp. PCC7120 (2)	*Acinetobacter calcoaceticus*	*Listeria monocytogenes*
Prochlorococcus marinus	*Acinetobacter sp. ADP1*	*Methanococcus jannaschi*
Pseudomonas aeruginosa(3)	*Aphanizomenon sp. TR183*	*Methanopyrus kandleri*
Pseudomonas fluorescens(2)	*Aphanizomenon baltica*	*Methanothermobacter*
Ralstonia metallidurans (5)	*Arthrobacter sp. KM*	*thermautotrophicus*
Ralstonia solanacearum	*Bordetella pertussis*	*Mycoplasma genitalium*
Rhodobacter sphaeroides (2)	*Burkholderia cepacia*	*Mycoplasma pneumoniae*
Rhodopseudomonas palustris	*Campylobacter coli*	*Mycoplasma pulmonis*
Rhodospirillum rubrum	*Cytophaga hutchinsonii*	*Pasteurella multocida*
Sinorhizobium meliloti(3)	*Dictyostelium discoideum*	*Pyobaculum aerophilum*
Streptomyces coelicolor	*Geobacter sulfurreducens*	*Pyrococcus abyssi*
Synechococcus sp. WH 8102	*Haloferax volcanii*	*Pyrococcus furiosus*
Synechocystis sp. PCC6803	*Klebsiella aerogenes*	*Pyrococcus horikoshii*
Thermosynechococcus elongatus	*Leuconostoc mesenteroides*	*Rickettsia conorii*
Vibrio cholerae	*Microbulbifer degradans*	*Rickettsia prowazekii*
Xanthomonas axonopodis	*Mycobacterium marinum*	*Saccharomyces cerevisiae*
Xanthomonas campestris	*Mycobacterium ulcerans*	*Schizosaccharomyces pombe*
	Neisseria gonorrhoeae	*Staphylococcus aureus*
	Nitrosomonas europaea	*Streptococcus pneumoniae*
PPK2 only	*Nodularia spumigena*	*Streptococcus pyogenes*
Corynebacterium glutamicum(2)	*Oenococcus oeni*	*Sulfolobus solfataricus*
MagnetococcusMC-1 (2)	*Porphyromonas gingivalis*	*Sulfolobus tokodaii*
Plectonema boryanum	*Propionibacterium shermanii*	*Thermoanaerobacter tengcongensis*
	Rhodocyclus tenuis	*Thermoplasma acidophilum*
	Salmonella Dublin	*Thermoplasma volcanium*
	Serratia marcescens	*Thermotoga maritima*
	Shigella flexneri	*Treponema pallidum*
	Streptomyces griseus	*Ureaplasma urealyticum*
	Streptomyces lividans	
	Thermobifida fusca	

Table 1.4. *Table indicating PPK1 and PPK2 homologues among microorganisms (credit: Zhang et al, 2002)*

Structurally, PPK1 a homotetramer, formed from 80kDa monomers, which interlock together as a dimer. Within a highly conserved structural tunnel, the

enzymatic active site is located and is likely the accommodation site for freshly synthesized polyP (Zhu et al, 2005).

This tunnel is a crucial feature in the functionality of PPK1, where it accommodates ATP and highly conserved, charged residues. These residues interact with polyP during polyP chain elongation (Zhu *et al,* 2005). Purified recombinant PPK catalyses the elongation of polyP, resulting in termination of polyP synthesis when the chain reaches approximately 750 phosphate groups (Kumble *et al,* 1996).



Figure 1.12. *Crystal structure of E. coli* PPK1 dimer. *Each monomer of ppk1 contains amino terminal domain (N) (red), the "head" domain (H) (yellow) and two carboxyterminal domains (C1 and C2) (blue and green).* (Achbergerová & Nahálka, 2011)

1.5.2. Polyphosphate kinase 2 (PPK2)

However, PPK1 is not the only universal polyP-associated enzyme. PPK2 is a polyphosphate-dependent ATP/GTP regenerating enzyme, which was first identified in *Pseudomonas aeruginosa* (Zhang et al, 2002). This novel PPK2 was initially identified whilst observing PPK1-null *Pseudomonas* mutants, which retained polyP granulations despite the enzyme knockout. In contrast to PPK1, which is completely ATP-dependent, PPK2 can utilize both ATP and GTP to

synthesis polyP (Ishige et al, 2002). However, PPK1-deficient cells have been observed to lack functionality in abilities such as quorum sensing and virulence (Rashid & Kornberg, 2000). Structurally, PPK2 is diverse depending on its state and role. On isolation from the cell, it appears as a 44kDa protein, however this differs *in vivo* depending on polyP (Ishige et al, 2002). In *Pseudomonas aeruginosa,* two 1-domain (dimeric) and one 2-domain (tetrameric) PPK2 proteins are produced, the latter probably resulting from a gene duplication (Nocek *et al*, 2008). One domain PPK2 catalyzes ATP and GTP synthesis from the respective nucleoside diphosphates and polyP, while the 2-domain PPK2 catalyzes ADP and GDP synthesis from nucleoside monophosphates and polyp (Nocek *et al*, 2008). *A. phosphatis* widely associated with enhanced biological phosphorus removal (EBPR) systems, contains multiple *ppk2* paralogues in a representative metagenome, leading to a suggestion that the metabolism of polyP by PPK2 is important for its survival in such a system (Martin *et al,* 2006). A recent study (Motomura *et al*, 2014) (Fig 3.5) has identified a new subfamily of PPK2, which is phylogenetically distinct from the 1-domain and 2-domain PPK2. This subfamily appears to catalyse both nucleoside monophosphate and nucleoside diphosphate phosphorylation.

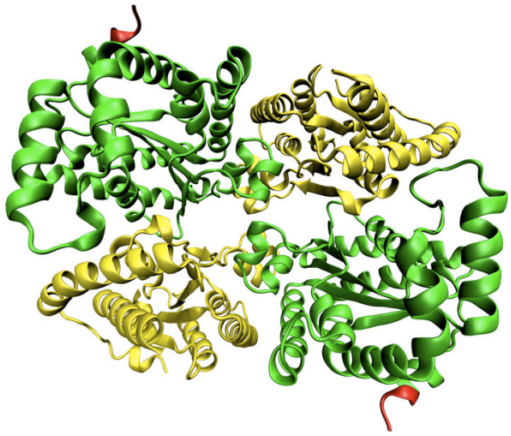


Figure 1.13. *P. aeruginosa PPK2 contains two monomers. Each monomer contains two domains coloured in yellow and green connected by a flexible linker coloured in red (Achbergerová & Nahálka, 2011).*

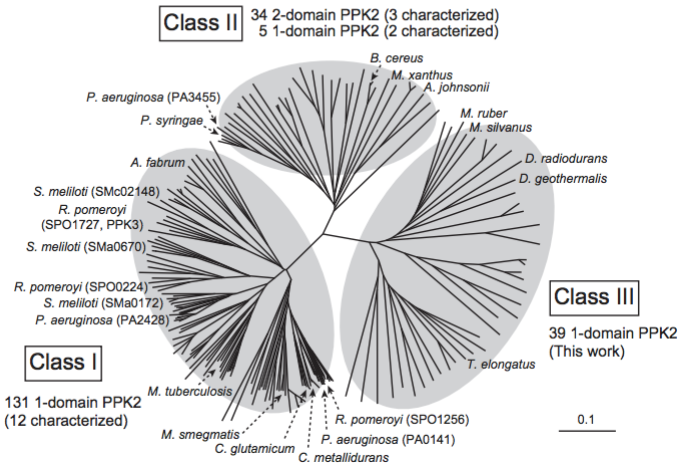


Figure 1.14. *Unrooted phylogenetic tree of PPK2, generated by ClustalW and GeneDoc programs using amino acid sequences of 17 characterized and 192 putative PPK2 homologs ((Motomura et al, 2014)*

$$NTP + polyP_n \leftrightarrow NDP + polyP_{n+1}$$
$$NDP : ADP > GDP > UDP > CDP$$

Figure 1.15. *PPK1 and its phosphorylation efficacy, where ADP is preferentially used to all others*

(Achbergerova & Nahalka, 2011)

$$NTP + polyP_n \leftrightarrow NDP + polyP_{n+1}$$
$$NDP : GDP, ADP$$

Figure 1.16.*. PPK2 and its phosphorylation efficacy, where both GDP and ADP can be utilized.*

(Achbergerova & Nahalka, 2011)

1.5.3 Exopolyphosphatases (PPX)

As previously mentioned, polyP synthesis typically occurs in the forward condensation reaction as PPK1 catalyzes this reaction. However the reverse hydrolytic reaction can be carried out by a specific enzymatic class, the exopolyphosphatases (EC 3.6.1.11), which split phosphate from the ends of poly-P chains (Akiyama *et al,* 1993). So far, two types of these enzymes have been

classified; those encoded by the *ppx* gene, and those guanosine pentaphosphate (pppGpp) phosphohydrolase (GppA; EC 3.6.1.40). These two classes produce enzymes which are sequentially related, but with differing actions. PPX typically splits long-chain polyP, whilst GppaA is also involved in the hydrolysis of (p)ppGpp, which are alarming compounds involved in the trigger of the stringent response (Potrykus & Cashel, 2008).

1.6. Polyphosphate metabolism

1.6.1. Metabolism in bacteria

As previously mentioned, polyP is strongly associated with the stress and stringent response in a number of microorganisms, due to its direct linkage with numerous physiological processes such as mobility and virulence (Rashid & Kornberg, 2000). These subsequent studies have broadened the interpretation and importance of polyP beyond the role of a phosphate and energy storage molecule. However, no one mechanism illustrates how polyP influences such various cellular processes and response.

Within the bacteria cell, polyP has many biologically advantageous properties. Due to its polymer structure, it is an osmotically neutral form of phosphorus and can also readily form complexes with cellular components such as nucleic acids or proteins, influencing their biological activities (Kulakovskaya *et al*, 2012). In *E. coli*, polyP can form a complex with the ATP-dependant Lon protease, leading to the degradation of free ribosomal proteins (Kuroda, 2006), whilst polyP-RNA complexes have been isolated from many different organisms (Kulaev *et al,* 2004).

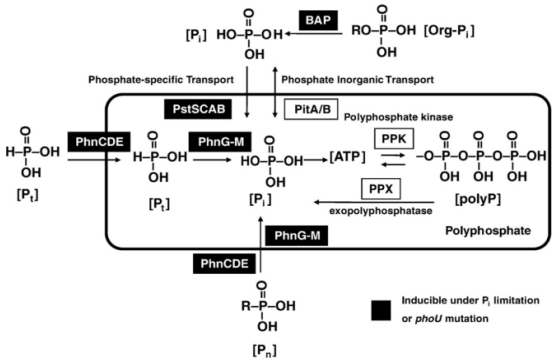


Figure 1.17. *Uptake of phosphate and intracellular polyP metabolism (Hirota et al. 2010)*

Within the cell, the production of polyP can be manipulated through the introduction of additional copies of the *ppk* gene and inducing these recombinant inserts (Smolke, 2010). Previous studies analyzing over-expression of PPK1 have demonstrated increased polyP:AMP phosphotransferase (PAP) activity (Ishige & Noguchi, 2000), and also the observance of an accumulation of adenylate kinase and phosphatases, and inclusion bodies (Nahálka *et al,* 2006). This highlights the ability to manipulate and influence the intracellular metabolism of polyP within the bacterial cell.

1.6.2. Metabolism in humans

Within humans and mammalian cells, polyP also plays an identifiable role. Previous studies have recognized polyP as being an influential regulator of blood homeostasis (Morrissey *et al*, 2012). PolyP can be identified within granules in platelets, where their function has been well elucidated (Mueller *et al*, 2009). Within platelets, the role of polyP is part of the response to endothelial damage. Platelets are alerted to the site of damage, where secreted granules of polyP aid in the blood coagulation process.

The body relies heavily on access to phosphorus via polyphosphate, as phosphorus to essential to develop and maintain bones and teeth, in parallel with calcium. Approx. 85% of phosphorus is stored within the bones and teeth (Cupisti *et al,* 2013). This relationship with calcium is also clinically important, as calcium and phosphate work conversely; as phosphate levels increase in the blood, calcium levels fall. This balance is overseen by the parathyroid hormone (PTH), but this relationship can be disrupted due to illness.

1.7. Hyperphosphatemia

The distribution of electrolytes and minerals within the body is a delicate balance. An excess or depletion of one can have an enormous effect on the body, and can indicate more serious health issues. Hyperphosphatemia is the excess accumulation of phosphate within the body. In the kidneys, the majority of inorganic phosphorus is ultra-filterable at the glomerulus, with approximately 7g of phosphorus filtered daily. Reabsorption occurs in the renal tubules, with the remainder excess excreted in urine (Knox *et al,* 2006). Under normal conditions, parathyroid hormone (PTH) influences phosphate balance by preventing the kidneys from re-absorbing excess phosphate, directing its excretion into urine. It acts as a mediator of phosphate excretion per nephron, regulating phosphate ion loss in urine. Serum PTH level, which is central to calcium homeostasis, also plays a key role in phosphate homeostasis. When renal function declines, and chronic kidney disease (CKD) develops, phosphate retention levels increase and lead to a dysfunction of the phosphate-calcium-PTH balance (Peacock, 2010). Hyperphosphatemia is therefore indicative of renal disruption or failure, as the kidneys fail to excrete phosphate into urine.

1.7.1. Association with renal failure and cardiovascular disease

In chronic kidney disease, hyperphosphatemia is associated with decreased serum calcium levels and vascular calcification; this is referred to as mineral and bone disorder associated with chronic kidney disease (CKD-MBD) (Guo *et al,* 2013). Observation of patients suffering from end-stage renal disease (ESRD) also indicate the population are highly vulnerable to infection due to their immunocompromised state, which can be observed by a notable decrease in the

killing capacity of neutrophils (Anding, 2003). Therefore, despite the fact that hyperphosphatemia is a consequential condition of ESRD, it requires its own intensive treatment to alleviate its effects – typically in the form of oral phosphate binders (Guo *et al,* 2013).

Cardiovascular morbidity and mortality is also clinically associated with hyperphosphatemia, particularly in patients undergoing dialysis treatment (Kendrick & Chonchol, 2011). According to literature, the leading cause of death in patients with chronic kidney disease (CKD) is in fact cardiovascular disease, with the progression of vascular calcification acting as a key impact factor (Andrade & Ignaszewski, 2008), (McCabe *et al,* 2013). Adiponectin (ADPN), a secretory protein from the adipose tissue, can be observed in the serum of ESRD patients at high levels, and is associated with a number of cardiovascular risk factors including heightened HDL cholesterol levels (Zoccali *et al,* 2002).

1.7.2. Prevention and Therapies

Control and prevention of hyperphosphatemia is difficult, particularly if patients are involved in dialysis treatment, with previous data observing increased mortality in patients in patients suffering from ESRD and receiving dialysis (Block & Port, 2000). This is likely due to inadequate phosphate removal through conventional dialysis treatment, which often displays a consequential post-dialysis rebound from mobilization of intracellular phosphate (Coladonato, 2005). Typical treatment options therefore consist of optimal dialysis removal, methodical use of oral phosphate binders, and dietary control of phosphorus intake all in unison (Cupisti et al, 2013).

1.7.2.1. Phosphorus absorption

Guidelines issued by the Food and Nutrition Board of the Institute of Medicine (a division of the National Academies of Sciences, Engineering, and Medicine, USA) have indicated a recommended dietary allowance of 700 mg/d of phosphorus in healthy adults. In pregnant women, this allowance increases to <1250 mg/d (Food & Nutrition Board, 1997). Within the body, phosphorus is primarily removed by two systems; the gastrointestinal tract (150mg/day) and via urine excretion (800mg/day) (Hruska *et al,* 2008). In a healthy individual, after the body ingests phosphorus, phosphatonins such as PTH trigger phosphaturia (phosphate excretion in urine) to regulate the body's phosphorus balance (Isakova *et al*, 2009).

As previously mentioned, his process becomes dysfunctional with a decrease in renal function, with decreased glomerular filteration of phosphorus and attempted compensation with decreased tubular reabsorption (González-Parra *et al*, 2012)

1.7.2.2. Polyphosphate absorption

In mammals, absorption of polyP occurs in the small intestine, where it is degraded to orthophosphate by the alkaline phosphatase of the intestinal wall (Lorenz & Schroder, 2001). Intestinal absorption proceeds via a co-transport system for active sodium/phosphate co-transporters. This gastrointestinal interaction provides an opportunity for phosphate intake control via dietary restrictions and oral medication. The main factors governing the rate of phosphate absorption via the small intestine include i) the amount of phosphorus

in the diet, ii) its bioavailability and iii) the presence of natural or pharmacologic phosphorus binders (Noori *et al,* 2010).

Inorganic phosphate is obtained by the body mainly through the ingestion of food, particularly processed food, with estimations that up to 50% of our dietary phosphorus intake is from phosphorus-containing food additives, which are rarely quantified on food labels (Winger *et al*, 2012). In addition, polyphosphate is often used as a preservative additive (E452). This is due to its high buffering capacity, helping to maintain optimal pH and its polyanion status, which are all beneficial technological properties. (Kulakovskaya *et al*, 2012). Phosphate is also naturally present abundantly in food in the form of phospholipids and phosphoproteins (Massey, 2003). This consistent presence in food makes the avoidance or restriction of phosphate very difficult for patient management.

However in dialysis patients with ESRD, the largest complication regarding control of dietary polyP intake is the correlation between phosphate and protein intake. Dietary protein is a major source of phosphorus and phosphate (Boaz & Smetana, 1996), however recent literature has indicated that dietary restriction of phosphate intake can have a negative effect on protein intake as a result, leading to potentially increased mortality (Shinaberger *et al*, 2008). Therefore dietary control is not alone sufficient in the majority of cases.

1.7.2.3. Phosphate binders

Regarding the use of phosphate binders, as dialysis and dietary is rarely sufficient; there is a large reliance upon the use of medicinal intervention. The most frequently used phosphate binders can be arranged into three property-

based classifications: i) aluminium-based binders, ii) calcium-based binders and iii) aluminum and calcium-free binders (Cupisti *et al,* 2013), *(Table 5.1).*

In previous years, aluminium-based binders were a popular choice for the treatment of hyperphosphataemia, however more recently they have fallen out of favour due to concerns regarding their long-term usage (LTU). Longitudinal studies have linked LTU of aluminum-based phosphate binders with aluminum accumulation causing induced osteomalacia (KDIGO, 2009).

Calcium-based binders have also been a popular choice since the 1980s, and appear well tolerated across the majority of patient groups. Degree of dosage is once again an aspect of concern however, due to the sensitivity of PTH to the calcium-phosphate balance. A positive increase toward calcium can lead to hypercalcemia causing vascular calcification, which can in turn lead in increased cardiovascular disease (McCabe *et al,* 2013).

An improvement from the traditional failings of calcium-based binders is lanthanum carbonate, a novel non-calcium, non-aluminum binder. Literature studies have identified lanthanum carbonate as beneficial in reducing the risk of vascular calcification and reducing serum phosphate levels (Neven *et al,* 2009). Sevalamer is an ion exchange resin made in Waterford (Genzyme, now Sanofi) with worldwide sales of over 800 million euro per annum. It is also used in therapy of hyperphosphataemia (ref) However the requirement for oral medication increases pill burden on patients and adds to an increased medication load (Chiu *et al*, 2009). Therefore treatment of hyperphosphatemia remains a multi-disciplinary approach between clinician, dietician and the patient.

Table 1.5. *Table indicating the advantages and disadvantages of the three major phosphate binders*

(credit : Cupisti et al, 2013

1.8. References

- Achbergerova, L., Nahálka, J. (2013). Polyphosphate - an ancient energy source and active metabolic regulator. Microbial Cell Factories 10, 1–14.
- Akiyama M, Crooke E, Kornberg A (1992) The polyphosphate kinase gene of Escherichia coli. Isolation and sequence of the ppk gene and membrane location of the protein. J Biol Chem 267:22556-22561. 7.
- Akiyama M, Crooke E, Kornberg A (1993) An exopolyphosphatase of Escherichia coli. The enzyme and its ppx gene in a polyphosphate operon. J Biol Chem 268:633-639
- Albaaj F, Hutchison A. (2003) Hyperphosphataemia in renal failure: causes, consequences and current management. Drugs. 63: 577–596.
- Alcantara, C., Blasco, A., Zuniga, M., Monedero, V. (2014). Accumulation of Polyphosphate in *Lactobacillus* spp. and Its Involvement in Stress Resistance. Applied and Environmental Microbiology 80, 1650–1659.
- Anding K (2003) The influence of uraemia and haemodialysis on neutrophil phagocytosis and antimicrobial killing. Nephrology Dialysis Transplantation 18:2067-2073
- Andrade J, Ignaszewski AA. (2008) Cardiovascular risk assessment: identification of individuals at increased risk. BCMJ; 50: 246–251.
- Archambaud, C., Nahori, M., Soubigou, G., Becavin, C., Laval, L., Lechat, P., Smokvina, T., Langella, P., Lecuit, M., Cossart, P. (2012). Impact of lactobacilli on orally acquired listeriosis. Proceedings of the National Academy of Sciences 109, 16684-16689.

- Aussignargues C, Paasch B, Gonzalez-Esquer R, Erbilgin O, Kerfeld C (2015) Bacterial microcompartment assembly: The key role of encapsulation peptides. Communicative & Integrative Biology 8:e1039755
- Axen, S., Erbilgin, O., Kerfeld, C. (2014). A Taxonomy of Bacterial Microcompartment Loci Constructed by a Novel Scoring Method. PLoS Compututational Biology 10, e1003898.
- Beeby M, Bobik T, Yeates T (2008) Exploiting genomic patterns to discover new supramolecular protein assemblies. Protein Science 18:69-79
- Bennett E, Carpenter S, Caraco N (2001) Human Impact on Erodable Phosphorus and Eutrophication: A Global Perspective. BioScience 51:227
- Bertin Y., Girardeau J., Chaucheyras-Durand F., Lyan B., Pujos-Guillot E., Harel J., Martin C. (2010) Enterohaemorrhagic *Escherichia coli* gains a competitive advantage by using ethanolamine as a nitrogen source in the bovine intestinal content. Environmental Microbiology 13:365-377.
- Block G, Port F (2000) Re-evaluation of risks associated with hyperphosphatemia and hyperparathyroidism in dialysis patients: Recommendations for a change in management. American Journal of Kidney Diseases 35:1226-1237
- Boaz M, Smetana S (1996) Regression Equation Predicts Dietary Phosphorus Intake from Estimate of Dietary Protein Intake. Journal of the American Dietetic Association 96:1268-1270

- Bobik T, Havemann G, Aldrich. H, Busch R, Williams D, Aldrich H (1999) The propanediol utilization (pdu) operon of *Salmonella enterica* serovar Typhimurium LT2 includes genes necessary for formation of polyhedral organelles involved in coenzyme B12-dependent 1,2-propanediol degradation. Journal of Bacteriology 181:5967–5975
- Bobik T, Xu Y, Jeter R, Otto K, Roth J (1999) Propanediol Utilization Genes (pdu) of *Salmonella typhimurium*: Three Genes for the Propanediol Dehydratase. Journal Of Bacteriology, 6633–6639
- Bobik, T., Lehman, B., Yeates, T. (2015). Bacterial microcompartments: widespread prokaryotic organelles for isolation and optimization of metabolic pathways. Molecular Microbiology
- Bobik, T.A. (2006). Polyhedral organelles compartmenting bacterial metabolic processes. Applied Microbiology and Biotechnology. 70:517–525.
- Brinsmade S, Paldon T, Escalante-Semerena J (2005) Minimal Functions and Physiological Conditions Required for Growth of *Salmonella enterica* on Ethanolamine in the Absence of the Metabolosome. Journal of Bacteriology 187:8039-8046
- Bry, L., Falk, P. G., Midtvedt, T., Gordon J. I. (1996) A model of host-microbial interactions in an open mammalian ecosystem. Science 273: 1380–1383.

- Cameron J, Wilson S, Bernstein S, Kerfeld C (2013) Biogenesis of a Bacterial Organelle: The Carboxysome Assembly Pathway. Cell 155:1131-1140
- Chen A, Silver P (2012) Designing biological compartmentalization. Trends in Cell Biology 22:662-670
- Chen, P., Andersson, D. I., Roth, J. R. The control region of the Pdu/cob regulon in *Salmonella typhimurium*. Journal of Bacteriology 176, 5474–5482 (1994).
- Cheng S, Sinha S, Fan C, Liu Y, Bobik T (2011) Genetic Analysis of the Protein Shell of the Microcompartments Involved in Coenzyme B12-Dependent 1,2-Propanediol Degradation by *Salmonella*. Journal of Bacteriology 193:1385-1392
- Cheng, S., Liu, Y., Crowley, C.S., Yeates, T.O., Bobik, T.A., (2008) Bacterial microcompartments: their properties and paradoxes. BioEssays: News and Reviews in Molecular, Cellular and Developmental Biology 30:1084–1095
- Chiu Y, Teitelbaum I, Misra M, de Leon E, Adzize T, Mehrotra R (2009) Pill Burden, Adherence, Hyperphosphatemia, and Quality of Life in Maintenance Dialysis Patients. Clinical Journal of the American Society of Nephrology 4:1089-1096
- Coladonato J (2005) Control of Hyperphosphatemia among Patients with ESRD. Journal of the American Society of Nephrology 16:S107-S114
- Conrado R, Mansell T, Varner J, DeLisa M (2007) Stochastic reaction–diffusion simulation of enzyme compartmentalization reveals improved

catalytic efficiency for a synthetic metabolic pathway. Metabolic Engineering 9:355-363

- Crooke E, Akiyama M, Rao NN,Kornberg A. (1994) Genetically altered levels of inor- ganic polyphosphate in Escherichia coli. J. Biol. Chem. 269:6290–95
- Crowley C, Cascio D, Sawaya M, Kopstein J, Bobik T, Yeates T (2010) Structural Insight into the Mechanisms of Transport across the *Salmonella enterica* Pdu Microcompartment Shell. Journal of Biological Chemistry 285:37838-37846
- Crowley C, Sawaya M, Bobik T, Yeates T (2008) Structure of the PduU Shell Protein from the Pdu Microcompartment of *Salmonella*. Structure 16:1324-1332
- Cupisti, A., Gallieni, M., Rizzo, M. A., Carla, S., Meola, M., Bolasco, P. (2013). Phosphate control in dialysis. International Journal Nephronology and Renovascular Disease 193.
- Diaz J, Ingall E, Benitez-Nelson C, Paterson D, de Jonge M, McNulty I, Brandes J (2008) Marine Polyphosphate: A Key Player in Geologic Phosphorus Sequestration. Science 320:652-655
- Drews G, Niklowitz W. 1956. Beitrage zur Cytologie der Blaualgen. Archives of Microbiology 24:147–62
- Eichelmann H, Talts E, Oja V, Padu E, Laisk A (2009) Rubisco in planta kcat is regulated in balance with photosynthetic electron transport. Journal of Experimental Botany 60:4077-4088

- English R.S., Lorbach S.C., Qin X., Shively J.M. (1994) Isolation and characterization of a carboxysome shell gene from *Thiobacillus neapolitanus*. Molecular Microbiology 12:647-654.
- Field, L., Delehanty, J., Chen, Y., Medintz, I. (2015). Peptides for Specifically Targeting Nanoparticles to Cellular Organelles: Quo Vadis? Accounts of Chemical Research 48, 1380-1390.
- Filippelli G (2008) The Global Phosphorus Cycle: Past, Present, and Future. Elements 4:89-95
- Food and Nutrition Board: Phosphorus. In: Dietary Reference Intakes: Calcium, Phosphorus, Magnesium, Vitamin D, Fluoride (1997) edited by Institute of Medicine,Washington, DC, National Academy Press, pp 146–189
- Frank S, Lawrence A, Prentice M, Warren M (2013) Bacterial microcompartments moving into a synthetic biological world. Journal of Biotechnology 163:273-279
- Gehrmann W, Elsner M (2011) A specific fluorescence probe for hydrogen peroxide detection in peroxisomes. Free Radical Research 45:501-506
- González-Parra E, Gracia-Iguacel C, Egido J, Ortiz A (2012) Phosphorus and Nutrition in Chronic Kidney Disease. International Journal of Nephrology 2012:1-5
- Gray, M. J., Jakob, U. (2015). Oxidative stress protection by polyphosphate — new roles for an old player. Current Opinion in Microbiology 24, 1–6. Elsevier Ltd.

- Grima R. (2009) Investigating the robustness of the classical enzyme kinetic equations in small intracellular compartments. BMC Systems Biology 3:101
- Guo, H., Zhang, X., Tang, S., Zhang, S. (2013). Effects and safety of lanthanum carbonate in end stage renal disease patients with hyperphosphatemia: a meta-analysis – system review of lanthanum carbonate. Ren Fail 35, 1455–1464.
- Havemann G, Bobik T (2003) Protein Content of Polyhedral Organelles Involved in Coenzyme B12-Dependent Degradation of 1,2-Propanediol in *Salmonella enterica* Serovar Typhimurium LT2. Journal of Bacteriology 185:5086-5095
- Havemann G, Sampson E, Bobik T (2002) PduA Is a Shell Protein of Polyhedral Organelles Involved in Coenzyme B12-Dependent Degradation of 1,2-Propanediol in *Salmonella enterica* Serovar Typhimurium LT2. Journal of Bacteriology 184:1253-1261
- Hruska K, Mathew S, Lund R, Qiu P, Pratt R (2008) Hyperphosphatemia of chronic kidney disease. Kidney International 74:148-157
- Huseby D., Roth J. (2013) Evidence that a Metabolic Microcompartment Contains and Recycles Private Cofactor Pools. Journal of Bacteriology 195:2864-2879
- Ishige K, Noguchi T (2000) Inorganic polyphosphate kinase and adenylate kinase participate in the polyphosphate:AMP phosphotransferase activity of Escherichia coli. Proceedings of the National Academy of Sciences 97:14168-14171

- Ishige K, Zhang H, Kornberg A (2002) Polyphosphate kinase (PPK2), a potent, polyphosphate-driven generator of GTP. Proc Natl Acad Sci USA , 99:16684-16688
- Jeter R.M. (1990) Cobalamin-dependent 1,2-propanediol utilization by *Salmonella typhimurium*. Journal of General Microbiology 136:887–96
- Jeter, R., Olivera B. M., Roth J. R. (1984) *Salmonella typhimurium* synthesizes cobalamin (vitamin B12) de novo under anaerobic growth con- ditions. J. Bacteriol. 159:206–216. 18.
- Johnson R, Redding K, Holmquist D (2007) Water quality with vernier. Vernier Software & Technology, Beaverton, OR.
- Joseph B, Przybilla K, Stuhler C, Schauer K, Slaghuis J, Fuchs T, Goebel W (2005) Identification of *Listeria monocytogenes* Genes Contributing to Intracellular Replication by Expression Profiling and Mutant Screening. Journal of Bacteriology 188:556-568
- Kendrick J, Chonchol M. (2011) The role of phosphorus in the development and progression of vascular calcification. Am J Kidney Dis. 58(5): 826–834
- Kerfeld C. (2005) Protein Structures Forming the Shell of Primitive Bacterial Organelles. Science 309:936-938.
- Kerfeld C., Heinhorst S., Cannon G. (2010) Bacterial Microcompartments. Annual Review of Microbiology 64:391-408.
- Kerfeld C., Sawaya M., Tanaka S., Nguyen C., Philips M., Beeby M., Yeates T. (2005) Protein Structures Forming the Shell of Primitive Bacterial Organelles. Science 309:936-938

- Kerfeld, C., Erbilgin, O. (2015). Bacterial microcompartments and the modular construction of microbial metabolism. Trends in Microbiology 23, 22-34.
- Kidney Disease: Improving Global Outcomes (KDIGO) CKD–MBD Work Group. KDIGO clinical practice guideline for the diagnosis, evaluation, prevention, and treatment of Chronic Kidney Disease-Mineral and Bone Disorder (CKD-MBD). Kidney Int Suppl. 2009;113:S1–S130. International
- Kinney J., Salmeen A., Cai F., Kerfeld C. (2012) Elucidating Essential Role of Conserved Carboxysomal Protein CcmN Reveals Common Feature of Bacterial Microcompartment Assembly. Journal of Biological Chemistry 287:17729-17736
- Klein M., Zwart P., Bagby S., Cai F., Chisholm S., Heinhorst S., Cannon G., Kerfeld C. (2009) Identification and Structural Analysis of a Novel Carboxysome Shell Protein with Implications for Metabolite Transport. Journal of Molecular Biology 392:319-333
- Kofoid E., Rappleye C., Stojiljkovic I., Roth J. (1999) The 17-gene ethanolamine (eut) operon of *Salmonella typhimurium* encodes five homologues of carboxysome shell proteins. Journal of Bacteriology 181: 5317–5329.
- Korbel, J. O., Doerks T., Jensen L. J., Perez-Iratxeta C., Kaczanowski S., Hooper S. D., Andrade M. A., Bork P. (2005) Systematic association of genes to phenotypes by genome and literature mining. PLoS Biology 3:e134.

- Kornberg A, Kornberg S, Simms E (1956) Metaphosphate synthesis by an enzyme from Escherichia coli. Biochimica et Biophysica Acta 20:215-Kornberg A (1995) Inorganic polyphosphate: toward making a forgotten polymer unforgettable. J Bacteriol, 177:491-496. 7.
- Kornberg A, Rao N, Ault-Riché D (1999) Inorganic Polyphosphate : A Molecule of Many Functions. Annu Rev Biochem 68:89-125
- Kulaev I, Kulakovskaya T (2000) Polyphosphate and Phosphate Pump. Annu Rev Microbiol 54:709-734
- Kulaev I, Vagabov V (1983) Polyphosphate metabolism in micro-organisms. Adv Microb Physiol 24:83-171
- Kulaev I, Vagabov V, Kulakovskaia T (2004) The biochemistry of inorganic polyphosphates. J. Wiley, Chichester, West Sussex
- Kulakovskaya, T. V., Vagabov, V. M., Kulaev, I. S. (2012). Inorganic polyphosphate in industry, agriculture and medicine: Modern state and outlook. Process Biochemistry 47, 1–10. Elsevier Ltd.
- Kumble KD, Ahn K, Kornberg A (1996) Phosphohistidyl active sites in polyphosphate kinase of Escherichia coli. Proc Natl Acad Sci USA 93:14391–14395
- Kuroda A (2006) A Polyphosphate-Lon Protease Complex in the Adaptation of Escherichia coli to Amino Acid Starvation. Bioscience, Biotechnology and Biochemistry 70:325-331
- Lee H., DeLoache W., Dueber J. (2012) Spatial organization of enzymes for metabolic engineering. Metabolic Engineering 14:242-251

- Lorenz B, Schröder H (2001) Mammalian intestinal alkaline phosphatase acts as highly active exopolyphosphatase. Biochimica et Biophysica Acta (BBA) - Protein Structure and Molecular Enzymology 1547:254-261
- Martín H, Ivanova N, Kunin V, Warnecke F, Barry K, McHardy A, Yeates C, He S, Salamov A, Szeto E, Dalin E, Putnam N, Shapiro H, Pangilinan J, Rigoutsos I, Kyrpides N, Blackall L, McMahon K, Hugenholtz P (2006) Metagenomic analysis of two enhanced biological phosphorus removal (EBPR) sludge communities. Nat Biotechnol 24:1263-1269
- Massey L (2003) Dietary animal and plant protein and human bone health: a whole foods approach. Journal of Nutrition 133:862S-865S.
- McCabe, K. M., Booth, S. L., Fu, X., Shobeiri, N., Pang, J. J., Adams, M. A., Holden, R. M. (2013). Dietary vitamin K and therapeutic warfarin alter the susceptibility to vascular calcification in experimental chronic kidney disease. Kidney International 83, 835–844. Nature Publishing Group.
- Meyer A (1904) Orientierende Untersuchungen ueber Verbreitung, Morphologie, und Chemie des Volutins. Bot Zeit , 62:113-152
- Morita H., Toh H., Fukuda S., Horikawa H., Oshima K. (2008) Comparative genome analysis of *Lactobacillus reuteri* and *Lactobacillus fermentum* reveal a genomic island for reuterin and cobalamin production. DNA research 15: 151-161.

- Morrissey JH, Choi SH, Smith SA (2012). Polyphosphate: an ancient mol- ecule that links platelets, coagulation, and inflammation. Blood 119, 5972–5979.
- Motomura K, Hirota R, Okada M, Ikeda T, Ishida T, Kuroda A (2014) A New Subfamily of Polyphosphate Kinase 2 (Class III PPK2) Catalyzes both Nucleoside Monophosphate Phosphorylation and Nucleoside Diphosphate Phosphorylation. Applied and Environmental Microbiology 80:2602-2608
- Muller L. (1923) Un nouveau milieu d'enrichissement pour la recherche du Bacille Typhique at Paratyphique. Comptes Rendus des Seances de la Societe de Biologie et de ses Filiales.89:434–437
- Müller, F., Mutch, N., Schenk, W., Smith, S. (2009). Platelet polyphosphates are proinflammatory and procoagulant mediators in vivo. Cell 139, 1143–1156.
- Nahálka J, Gemeiner P, Bučko M, Wang P (2006) Bioenergy Beads: A Tool for Regeneration of ATP/NTP in Biocatalytic Synthesis. Artif Cells Blood Substit Immobil Biotechnol 34:515-521
- Neven, E., Dams, G., Postnov, A., Chen, B., De Clerck, N., De Broe, M. E., D'Haese, P. C., Persy, V. (2009). Adequate phosphate binding with lanthanum carbonate attenuates arterial calcification in chronic renal failure rats. Nephrology Dialysis Transplantation 24, 1790–1799.
- Nocek B, Kochinyan S, Proudfoot M, Brown G, Evdokimova E, Osipiuk J, Edwards A, Savchenko A, Joachimiak A, Yakunin A (2008) Polyphosphate-dependent synthesis of ATP and ADP by the family-2

polyphosphate kinases in bacteria. Proceedings of the National Academy of Sciences 105:17730-17735

- Noori, N., Sims, J. J., Kopple, J. D., Shah, A., Coleman, S., Shinaberger, C. S., Bross, R., Mehrota, R., Kovesdy, C. P., Kalantar-Zadeh, K. (2010). Organic and Inorganic Dietary Phosphorus and Its Management in Chronic Kidney Disease. Iranian Journal of Kidney Diseases 4, 1–
- Obradors, N., Bada J., Baldoma L., Aguilar J. (1988) Anaerobic metabolism of the L-rhamnose fermentation product 1,2-propanediol in *Salmonella typhimurium*. Journal of Bacteriology.170:2159–2162
- Pang A., Frank S., Brown I., Warren M., Pickersgill R. (2014) Structural Insights into Higher Order Assembly and Function of the Bacterial Microcompartment Protein PduA. Journal of Biological Chemistry 289:22377-22384
- Pang A., Warren M.J., Pickersgill R.W. (2011) Structure of PduT, a trimeric bacterial microcompartment protein with a 4Fe-4S cluster-binding site. Acta Crystallographica Section D: Biological Crystallography 67: 91-96.
- Parsons J, Frank S, Bhella D, Liang M, Prentice M, Mulvihill D, Warren M (2010) Synthesis of Empty Bacterial Microcompartments, Directed Organelle Protein Incorporation, and Evidence of Filament-Associated Organelle Movement. Molecular Cell 38:305-315
- Parsons J., Dinesh S., Deery E., Leech H., Brindley A., Heldt D., Frank S., Smales C., Lunsdorf H., Rambach A., Gass M., Bleloch A., McClean K., Munro A., Rigby S., Warren M., Prentice M. (2008) Biochemical and

Structural Insights into Bacterial Organelle Form and Biogenesis. Journal of Biological Chemistry 283:14366-14375

- Pavlov, E., Aschar-Sobbi, R., Campanella, M., Turner, R., Gomez-Garcia, M., Abramov, A. (2010). Inorganic Polyphosphate and Energy Metabolism in Mammalian Cells. Journal of Biological Chemistry, 285(13), 9420-9428.
- Peacock M (2010) Calcium Metabolism in Health and Disease. Clinical Journal of the American Society of Nephrology 5:S23-S30
- Peng, L., Jiang, Q., Pan, J., Deng, C., Yu, J., Wu, X., Huang, S., Deng, X. (2015). Involvement of polyphosphate kinase in virulence and stress tolerance of uropathogenic *Proteus mirabilis*. Medical Microbiology Immunology. 307(5708), pp.416-418
- Penrod, J. T., Roth, J. R. (2006). Conserving a Volatile Metabolite: a Role for Carboxysome-Like Organelles in *Salmonella enterica*. Journal of Bacteriology 188:2865–2874.
- Peters K.R. (1974) Characterization of a phage-like particle from cells of Nitrobacter. II. Structure and size. Archives of Microbiology. 97:129–40
- Potrykus K, Cashel M. 2008. (p)ppGpp: still magical? Annu. Rev. Microbiol. 62:35–51.
- Price-Carter M., Tingey J., Bobik T., Roth J. (2001) The Alternative Electron Acceptor Tetrathionate Supports B12-Dependent Anaerobic Growth of *Salmonella enterica* Serovar Typhimurium on Ethanolamine or 1,2-Propanediol. Journal of Bacteriology 183:2463-2475

- Qunibi W, Hootkins R, McDowell L, Meyer M, Simon M, Garza R, Pelham R, Cleveland M, Muenz L, He D, Nolan C (2004) Treatment of hyperphosphatemia in hemodialysis patients: The Calcium Acetate Renagel Evaluation (CARE Study). Kidney International 65:1914-1926
- Rao NN, Gomez-Garcia MR, Kornberg A. 2009. Inorganic polyphosphate: essential for growth and survival. Annu. Rev. Biochem. 78:605–647.
- Rao NN, Kornberg A: Inorganic polyphosphate supports resistance and survival of stationary-phase Escherichia coli. J Bacteriol 1996, 178:1394-1400.
- Rao, N. N., Gomez-Garcia, M. R., Kornberg, A. (2015). Inorganic Polyphosphate: Essential for Growth and Survival. Annual Review of Biochemistry 78, 605–647.
- Rashid MH, Kornberg A. 2000. Inorganic polyphosphate is needed swimming swarming, and twitching motilities of Pseudomonas aeruginosa. Proc. Natl. Acad. Sci. USA 97:4885–90
- Rondon, M. R., Horswill A. R., Escalante-Semerena J. C. (1995) DNA polymerase I function is required for the utilization of ethanolamine, 1,2-propanediol, and propionate by *Salmonella typhimurium* LT2. Journal of Bacteriology 177:7119–7124
- Roof D.M., Roth J.R. (1992) Autogenous regulation of ethanolamine utilization by a transcriptional activator of the eut operon in *Salmonella typhimurium*. Journal of Bacteriology 174:6634–6643.

- Sagermann M., Ohtaki A., Nikolakakis K. (2009) Crystal structure of the EutL shell protein of the ethanolamine ammonia lyase microcompartment. Proceedings of the National Academy of Sciences 106:8883-8887
- Samborska B., Kimber M. (2012) A Dodecameric CcmK2 Structure Suggests β-Carboxysomal Shell Facets Have a Double-Layered Organization. Structure 20:1353-1362
- Sampson E., Bobik T. (2008) Microcompartments for B12-Dependent 1,2-Propanediol Degradation Provide Protection from DNA and Cellular Damage by a Reactive Metabolic Intermediate. Journal of Bacteriology 190:2966-2971
- Schmid M., Paredes A., Khant H., Soyer F., Aldrich H., Chiu W., Shively J. (2006) Structure of *Halothiobacillus neapolitanus* Carboxysomes by Cryo-electron Tomography. Journal of Molecular Biology 364:526-535
- Schulz, H., Schulz, H. (2005). Large Sulfur Bacteria and the Formation of Phosphorite. Science, 307(5708), pp.416-418.
- Science Learning Hub: Soil, Farming and Science (2013) University of Waikato www.sciencelearn.org.nz
- Shinaberger C, Greenland S, Kopple J, Van Wyck D, Mehrotra R, Kovesdy C, Kalantar-Zadeh K (2008) Is controlling phosphorus by decreasing dietary protein intake beneficial or harmful in persons with chronic kidney disease?. American Journal of Clinical Nutrition 88:1511-1518

- Shively J, Ball F, Brown D, Saunders R (1973) Functional Organelles in Prokaryotes: Polyhedral Inclusions (Carboxysomes) of *Thiobacillus neapolitanus*. Science 182:584-586
- Shively J, Bradburne C, Aldrich H, Bobik T, Mehlman J, Jin S, Baker S (1998) Sequence homologs of the carboxysomal polypeptide CsoS1 of the thiobacilli are present in cyanobacteria and enteric bacteria that form carboxysomes - polyhedral bodies. Canadian Journal of Botany 76:906-916
- Singh, R., Singh, M., Arora, G., Kumar, S., Tiwari, P., Kidwai, S. (2013). Polyphosphate Deficiency in *Mycobacterium tuberculosis* Is Associated with Enhanced Drug Susceptibility and Impaired Growth in Guinea Pigs. Journal of Bacteriology, 195(12), 2839-2851.
- Sinha S, Cheng S, Sung Y, McNamara D, Sawaya M, Yeates T, Bobik T (2014) Alanine Scanning Mutagenesis Identifies an Asparagine–Arginine–Lysine Triad Essential to Assembly of the Shell of the Pdu Microcompartment. Journal of Molecular Biology 426:2328-2345
- Smith, S. a, Mutch, N. J., Baskar, D., Rohloff, P., Docampo, R., Morrissey, J. H. (2006). Polyphosphate modulates blood coagulation and fibrinolysis. Proc Natl Acad Sci U S A 103, 903–8.
- Smolke C (2010) The metabolic pathway engineering handbook. CRC Press, Boca Raton
- Snoeck V, Goddeeris B, Cox E. (2005) The role of enterocytes in the intestinal barrier function and antigen uptake. Microbes Infect. 7:997–1004.

- So, A. K.-C., Espie G. S., Williams E. B., Shively J. M., Heinhorst S., Cannon G. C. (2004) A novel evolutionary lineage of carbonic anhydrase (epsilon class) is a component of the carboxysome shell. Journal of Bacteriology 186: 623–630.
- Sriramulu, D., Liang, M., Hernandez-Romero, D., Raux-Deery, E., Lunsdorf, H., Parsons, J., Warren, M., Prentice, M. (2008). *Lactobacillus reuteri* DSM 20016 Produces Cobalamin-Dependent Diol Dehydratase in Metabolosomes and Metabolizes 1,2-Propanediol by Disproportionation. Journal of Bacteriology 190:4559-4567.
- Stojiljkovic I, Baumler A.J., Heffron F. (1995) Ethanolamine utilization in *Salmonella typhimurium*: nucleotide sequence, protein expression, and mutational analysis of the cchA cchB eutE eutJ eutG eutH gene cluster. Journal of Bacteriology 177:1357–66 66.
- Takenoya M, Nikolakakis K, Sagermann M (2010) Crystallographic insights into the pore structures and mechanisms of the EutL and EutM shell proteins of the Eut-BMC. Journal of Bacteriology 10:610-652.
- Tanaka S, Kerfeld C, Sawaya M, Cai F, Heinhorst S, Cannon G, Yeates T (2008) Atomic-Level Models of the Bacterial Carboxysome Shell. Science 319:1083-1086
- Tanaka S, Sawaya M, Phillips M, Yeates T (2008) Insights from multiple structures of the shell proteins from the β-carboxysome. Protein Science NA-NA
- Tanaka S., Sawaya M.R., Yeates T.O. (2010) Structure and mechanisms of a protein-based organelle in *Escherichia coli*. Science 327:81-84.

- Thiennimitr P, Winter S, Winter M, Xavier M, Tolstikov V, Huseby D, Sterzenbach T, Tsolis R, Roth J, Baumler A. (2011) Intestinal inflammation allows *Salmonella* to use ethanolamine to compete with the microbiota. Proceedings of the National Academy of Sciences 108:17480-17485.
- Tocheva, E., Dekas, A., McGlynn, S., Morris, D., Orphan, V., Jensen, G. (2013). Polyphosphate Storage during Sporulation in the Gram-Negative Bacterium *Acetonema longum.* Journal of Bacteriology*,* 195(17), 3940-3946.
- Tsai Y, Sawaya M, Cannon G, Cai F, Williams E, Heinhorst S, Kerfeld C, Yeates T (2007) Structural Analysis of CsoS1A and the Protein Shell of the *Halothiobacillus neapolitanus* Carboxysome. PLoS Biology 5:e144
- Tsai Y, Sawaya M, Yeates T (2009) Analysis of lattice-translocation disorder in the layered hexagonal structure of carboxysome shell protein CsoS1C. Acta Crystallography 65:980-988
- Valsami-Jones E (2004) Phosphorus in environmental technologies. IWA Pub., London
- Varela C, Mauriaca C, Paradela A, Albar J, Jerez C, Chávez F (2010) New structural and functional defects in polyphosphate deficient bacteria: A cellular and proteomic study. BMC Microbiol 10:7
- Vendeville A, Larivière D, Fourmentin E (2011) An inventory of the bacterial macromolecular components and their spatial organization. FEMS Microbiology Reviews 35:395-414

- Von Heijne G (2006) Membrane-protein topology. Nature Review Molecular Cell Biology 7:909–918
- Wheatley N, Gidaniyan S, Liu Y, Cascio D, Yeates T (2013) Bacterial microcompartment shells of diverse functional types possesses pentameric vertex proteins. Protein Science 22:660-665
- Whitehead M, Eagles L, Hooley P, Brown M (2014) Most bacteria synthesize polyphosphate by unknown mechanisms. Microbiology 160:829-831
- Wiame JM: The metachromatic reaction of hexametaphosphate. JAm Chem Soc 1947, 69:3146. 18.
- Winger R, Uribarri J, Lloyd L (2012) Phosphorus-containing food additives: An insidious danger for people with chronic kidney disease. Trends in Food Science & Technology 24:92-102
- Winter S, Thiennimitr P, Winter M, Butler B, Huseby D, Crawford R, Russell J, Bevins C, Adams L, Tsolis R, Roth J, Bäumler A (2010) Gut inflammation provides a respiratory electron acceptor for *Salmonella*. Nature 467:426-429
- Winter, S., Bäumler, A. (2013). Why related bacterial species bloom simultaneously in the gut: principles underlying the 'Like will to like' concept. Cell Microbiology 16:179-184.
- Wood HG, Clark JE: Biological aspects of inorganic polyphosphates. Annu Rev Biochem 1988, 57:235-260

- Yeates T, Crowley C, Tanaka S (2010) Bacterial Microcompartment Organelles: Protein Shell Structure and Evolution. Annual Review of Biophysics 39:185-205
- Yeates T, Thompson M, Bobik T (2011) The protein shells of bacterial microcompartment organelles. Current Opinion in Structural Biology 21:223-231
- Zhang H, Ishige K, Kornberg A (2002) A polyphosphate kinase (PPK2) widely conserved in bacteria. Proceedings of the National Academy of Sciences 99:16678-16683
- Zhu Y, Huang W, Lee S, Xu W (2005) Crystal structure of a polyphosphate kinase and its implications for polyphosphate synthesis. EMBO Rep 6:681-687
- Zoccali C, Mallamaci F, Tripepi G, et al: Adiponectin, metabolic risk factors, and cardiovascular events among patients with end-stage renal disease. J Am Soc Nephrol 2002;13:134–141.

Chapter II

A study of polyphosphate kinases and phosphate uptake in *Lactobacillus* and *E. coli.*

Contents

2.0. Abstract

2.1. Introduction

2.2. Materials & Methods

2.2.1. Bacterial strains and culture conditions

2.2.2. Preparation of lyophilized bacteria

2.2.2.1 E. coli culture preparation

2.2.2.2. Lactobacillus culture preparation

2.2.2.3. Media composition

2.2.3. Molecular methods

2.2.2.2. Vectors

2.2.3.2. Primer design & PCR conditions

2.2.3.3. DNA modification protocols

2.2.3.4. Electrophoresis

2.2.3.5. PCR

2.2.3.6. p18 targeting sequence

2.2.3.7. Microcompartment genes

2.2.3.8. Chromosomal integration

2.2.3.9. Lactobacillus transformation

2.2.4. Expression & Phenotype of constructs

2.2.2.3. Neisser strain protocol

2.2.5. Polyphosphate observations in native lactobacilli

2.2.6. Phosphate assay test and conditions

2.2.6.1. Assay design

2.2.6.2. Assay preparation

2.2.6.3. Phosphate analysis of samples

2.2.6.2.2. Orthophosphate

2.2.6.3.2. Polyphosphate

2.2.7. Graphs

2.3. Results & Discussion

2.2.2. Molecular results

2.3.2 Neisser Staining

2.3.2.1.Wild-type Lactobacillus strain imaging

2.3.2.2. Recombinant strain imaging

2.3.3. Phosphate assays

2.3.2.2. Phosphate assays : live cultures

2.3.3.2. Phosphate assays : freeze-dried cultures

2.3.3.4. Polyphosphate measurements

2.4. Conclusion

2.5. References

2.0. Abstract

Phosphate granules, or volutin granules have been observed in lactobacilli since the 1950s. Phosphate is an essential ion for bacterial cells, and polyphosphate is a means of storing phosphate residues as a polymer connected by high-energy phosphoanhydride bonds such as that in ATP (Brown & Kornberg, 2004). Cellular metabolism depends on the appropriate concentration of intracellular inorganic phosphate (Pi) (Dick *et al.,* 2011) in response to the presence of pyrophosphate (PPi) and can also be influenced by molecules produced during synthesis of cellular polymers such as DNA or RNA (Chen *et al.,* 1990). Through various mechanisms, it can be taken up from the surrounding environment or culture media, and utilized in the cell as orthophosphate (Henry & Cosson, 2013). Orthophosphates are the inorganic forms of phosphate, such PO_4^-, HPO_4^- and $H_2PO_4^-$, and the most common form used for fertilizers (Johnson *et al.,* 2007).

In lactobacilli, the reactive process from phosphate to polyphosphate is a highly dynamic process. This process has been observed to fluctuate greatly during cell cycle, and it has been hypothesized that phosphate metabolism is intrinsically linked to the stress response of the cell. This is particularly noteworthy during the transition stages from cell starvation to glycolysis (Alcantara *et al.,* 2014), (Levering *et al.,* 2012),

This chapter describes manipulation of phosphate uptake and polyphosphate accumulation by *Lactobacillus reuteri* DSM20016, a commensal of the mammalian gut, by cloning and expression of recombinant polyphosphate kinase genes (*ppk1*) from *E. coli* and *L. reuteri*. In addition, the effect of adding a

microcompartment targeting sequence to *ppk1* from *L. reuteri* was assessed. Cloning steps towards expressing an empty recombinant microcompartment from *L. reuteri* genes are described.

For this study two host strains were used; *Lactobacillus reuteri* DSM 20016 and *Escherichia coli* BL21. The wild-type characteristics of the strains were noted, and compared against recombinant constructs utilizing the polyphosphate kinase 1 gene (*ppk1).* Recombinant constructs were analyzed for polyphosphate formation and phosphate uptake against backgrounds of rich media, minimal media, and single sugar sources.

Incubation in media known to induce the Pdu microcompartment operon increased polyphosphate formation in *L. reuteri.* Recombinant *ppk* expression enhanced polyphosphate formation and phosphate uptake in both *L. reuteri* and *E. coli*. Recombinant *E. coli ppk* was functional when expressed in *L. reuteri* and was achieved more phosphate uptake than expression of the recombinant *L. reuteri ppk.*

2.1. Introduction

Phosphate, or phosphorus is one of the fundamental elements essential to the survival and propagation of the prokaryotic cell (Brown & Kornberg, 2004). The mechanisms of phosphate uptake and the transition into polyphosphate have not been directly studied in many bacterial species. This study particularly focused on the strains *Lactobacillus reuteri* DSM 20016, and *Escherichia coli* BL21.

L. reuteri is a Gram-positive, facultative anaerobic bacterium, typically associated with gut fermentation of mammals, particularly cattle (Kullen & Klaenhammer, 2000) It has a GRAS (Generally Regarded As Safe) status, and has displayed probiotic effects in the gastrointestinal tract. It has a naturally occurring bacterial microcompartment (MCP*)*, which is produced in response to the presence of 1,2-propanediol (Pdu microcompartment*)* (Sriramulu *et al.,* 2007).

L. reuteri also produces the antimicrobial substance reuterin by using the Pdu microcompartment for metabolism of glycerol (Rodriguez *et al.,* 2003), (Sriramulu *et al.,* 2007) (Santos *et al.,* 2011). Reuterin is a compound that consists of a variety of hydrated, non-hydrated, and dimeric forms of 3-hydroxypropionaldehyde (3-HPA) (Stevens *et al.,* 2011). Its antimicrobial activity is due to a number of beneficial attributes; it is water-soluble, active across a wide range of pH values and resistant to proteolytic and lipolytic enzymes (Schaefer *et al.,* 2010). Originally identified in the 1950s, the first patent for its usage as an antimicrobial compound was filed in the 1980s (Dobrogosz & Lindgren, 1988). It has been identified to induce oxidative stress

within cells, where the aldehyde interacts with thiol groups of small molecules, leading to inhibition of bacterial growth (Schaefer *et al.,* 2010).

An association between the presence of bacterial MCP and polyphosphate accumulation was suggested (Iancu *et al.,* 2010) on observation of the fact that carboxysomes (carbon-fixing microcompartments) cluster near polyphosphate granulations within *Halothiobacillus neapolitanus* cells.

The bacterial microcompartment is a unique structural organelle that has been identified in 400 genera of bacteria, via genome sequencing (Kerfeld *et al.,* 2010). Bacterial microcompartments are small proteinaceous structures originally observed within bacterial cells in the 1950s (Drews & Niklowitz, 1956). They possess a distinct polygonal shape, which triggered their identification by electron microscopy. Initially observed in the cyanobacterium *Phormidium uncinatum* in 1956 (Drews & Niklowitz, 1956), their distinct polygonal shape has been identified in many more bacterial species, primarily cyanobacteria including *Nostoc punctiforme* (Yeates *et al.,* 2010). However since the early 1970s, they have been studied in approximately 20% of all bacterial genera, including diverse genera such as *Klebsiella, Lactobacillus* and *Salmonella* (Kerfeld *et al.,* 2010).

It is known that *E. coli*, a bacterium which does not normally accumulate polyphosphate, can do so if the native polyphosphate kinase enzyme is over expressed (Kato *et al.,* 1993), (Keasling *et al.,* 1998).

During the period of polyphosphate accumulation, orthophosphate is taken up from the culture medium. However, as the cell cycle progresses polyphosphate is degraded and phosphate returned to the culture medium. Work in the Prentice

laboratory has shown that if polyphosphate kinase is targeted to a recombinant microcompartment, intracellular polyphosphate can be stabilised in *E. coli* with prolonged retention of phosphate (Liang *et al.,* 2015). One of the aims of the thesis was to engineer the same genetic constructs in the GRAS organism *L. reuteri* for potential therapeutic applications of enhanced phosphate retention. In addition, due to the aforementioned association between the presence of the bacterial MCP and an increased accumulation of polyphosphate in a bacterial cell, it was hypothesized that the induction of the native microcompartment within *L. reuteri* could lead to increased polyphosphate formation and hence phosphate uptake from an environmental source, versus a lower phosphate uptake without microcompartment induction.

The planned strategy was to create an empty *L. reuteri* recombinant micocompartment from *L. reuteri pduABJKNU* genes to facilitate expression in *L. reuteri* and compare the phenotype of constructs with microcompartment targeted PPK from *E. coli* and *L. reuteri*. Because of issues regarding vector integrity and difficulties in obtaining an original sequenced vector, the integration of a recombinant microcompartment in *L. reuteri* could not be achieved so this chapter reports progress in constructing an empty microcompartment from *L. reuteri pdu* genes and the effects on polyphosphate formation and phosphate uptake of native microcompartment induction in *L. reuteri* and overexpression of recombinant PPK1 from *L. reuteri* and *E. coli* in *E. coli*. Because the planned *in vivo* experiment (Chapter III) required lyophilized bacteria suspended in water for oral administration of fresh daily suspensions, the effect of prior lyophilisation on these phenotypes was assessed. Supplementation of sorbitol to cultures before the freeze-drying process has been

found to increase storage viability (Carvalho *et al.,* 2003) As the immediate substrate for polyphosphate is ATP (Chapter 1b) optimizing energy generation in bacterial hosts could also be important and the effect of suspending bacteria in isotonic solution containing different carbon sources was assessed.

Both *E. coli* and *L. reuteri* can use gluconate, through the fermentation by the 6-phosphogluconate/phosphoketolase (6-PG/PK) pathway. Here it is transported by an inducible gluconate-PTS, and the resulting 6-phosphogluconate enters the pathway (Jenkins, 2005). This is unavailable in mammals therefore gluconate was assessed as a potential additive for animal administration (Jones *et al.,* 2008), (Jenkins, 2005). Sorbitol was also tested in water.

A previous construct from our collaborators in the University of Kent was also used; this construct contained the structural genes associated with the Pdu MCP from *Citrobacter freundii* (Parsons et al., 2008).

Using shuttle vectors, a number of constructs were made – a recombinant MCP from *Citrobacter*, and *Lactobacillus,* along with a recombinant *ppk* enzyme from *Lactobacillus reuteri*.

In addition, we observed the effect of the p18 targeting sequence on the functionality of *ppk.* The p18 sequence is an 18-amino acid long sequence initially identified in the N-terminal of the PduP protein (Fan *et al.,* 2010) (Chapter 1b).

2.2. Methods & Materials

In order to observe potential differences in gene expression of *ppk* in *E. coli* and *L. reuteri* hosts, a number of different constructs were created to observe phosphate uptake both strains. These constructs were made in collaboration with Dr. Mingzhi Liang, University College Cork. This work has been accredited accordingly throughout the thesis. For the majority of constructs, shuttle vectors were used to enable the constructs to be expressed in both *E. coli* and *L. reuteri* hosts.

2.2.1. Bacterial strains and culture conditions

Bacterial strains used in this study are listed in Table 2.1.

Strain	Origin	Genotype
Lactobacillus reuteri DSM20016	National Collection of Dairy Organisms, Reading, UK	*Pdu+*
Lactobacillus delbrueckii subspecies bulgaricus ATCC11842	DPC, Dairy Products Research Centre, Moorepark, Fermoy, Co. Cork culture collections.	*n/a*
E. coli MG1655	Dr. Mingzhi Liang, University College Cork	*F- λ- ilvG- rfb-50 rph-1*
E. coli JM109	Dr. Mingzhi Liang, University College Cork	*endA1 glnV44 thi-1 relA1 gyrA96 recA1 mcrB+ Δ(lac-proAB) e14- [F' traD36 proAB+ lacIq lacZΔM15] hsdR17(rK-mK+)*
E. cloni 10G Electrocompetent cells	Lucigen, Wisconsin, USA	*F- mcrA D(mrr-hsdRMS-mcrBC) endA1 recA1 f80dlacZDM15 DlacX74 araD139 D(ara,leu)7697 galU galK rpsL (StrR) nupG l- tonA*
E. coli EC1000	J. W. Sanders, Groningen University, The Netherlands (Cotter *et al,* 2001)	*F– mcrA Δ(mrr-hsdRMS-mcrBC) ϕ80dlacZΔM15 ΔlacX74 recA1 endA1 araD139 Δ(ara, leu)7697 galU galK λ– rpsL nupG. repA-*
E. coli BL21 (DE3)	Novagen, Merck Biosciences	*F^- ompT gal dcm lon $hsdS_B(r_B^- m_B^-)$ λ(DE3 [lacI lacUV5-T7 gene 1 ind1 sam7 nin5])*

Table 2.1. *Table indicating strains used.*

Escherichia coli was routinely cultured in Luria-Bertani (LB) broth (Merck, Darmstadt, Germany) at 37°C. *Lactobacillus reuteri* was routinely cultured in de Man-Rogosa-Sharpe (MRS) broth (Merck, Darmstadt, Germany) in static anaerobic conditions at 37°C. For minimal growth conditions, *E. coli* was cultured in 1X MOPS minimal media (Neidhardt *et al.,* 1974) supplemented with K_2HPO_4 and glucose (Sigma Aldrich), whilst *L. reuteri* was cultured in Minimal Lactobacillus Media (Hebert *et al.,* 2004) which was a formation of essential amino acids supplemented with glucose, sodium acetate, K_2HPO_4 and $MgSO_4$ (Sigma Aldrich). Breakdown of media composition is indicated below section 2.2.2.3. All other chemicals from Sigma Aldrich unless indicated.

2.2.2. Preparation of lyophilized bacteria

2.2.2.1. E. coli culture preparation

Luria Bertani (LB) broth, 50mL, supplemented with antibiotics was inoculated with -80°C bacterial stock. Culture was grown overnight at 37°C shaking, and subcultured into 1L LB broth, supplemented with antibiotics. Culture was grown until OD 600nm 0.4-0.6. Culture was then spun down by centrifugation using Beckman Coulter JA10 rotor, at a speed of 7000xg. Supernatant was removed and pellets were washed twice with Ringers buffer solution, to clean the pellet and remove excess media residue. Pellets were then inoculated into 1X MOPS minimal media (*Table 2.6*) supplemented with antibiotics and IPTG to induce present genes. At OD 600nm 1.0, cells were spun down by centrifugation and washed twice again with Ringers solution. These pellets were then frozen for 1 hour minimum at -80°C and lyophilized for 8-12 hours.

2.2.2.2. Lactobacillus culture preparation

MRS broth, 50mL *(Table 3.3)* supplemented with antibiotics, was inoculated with -80°C bacterial stock. Culture was grown anaerobically overnight at 37°C shaking, and subcultured into 1L MRS broth, supplemented with antibiotics. Culture was grown until OD 600nm 0.4-0.6. Culture was spun down by centrifugation using Beckman Coulter JA10 rotor, at a speed of 7000xg. Supernatant was removed and pellets were washed twice with Ringers buffer solution, to clean the pellet and remove excess media residue. Pellets were inoculated into Minimal Lactobacillus Media *(Table 2.7)*. At OD 600nm 1.0, cells were spun down by centrifugation and washed twice again with Ringers solution. These pellets were frozen for 1 hour minimum at -80°C and lyophilized for 8-12 hours.

Post-lyophilisation, the bacterial pellets were kept at 4°C, until use.

2.2.2.3. Media Composition

Material	Quantity
Tryptone from casein	10g/L
Sodium chloride	10g/L
Granulated Yeast Extract	5g/L
Deionized Water	1L

Table 2.2. *Recipe for Luria Broth (LB) for the growth of E. coli*

Material	Quantity
MRS broth	55g/L
Deionized Water	1L

Table 2.3. *Recipe for de Man-Rogosa-Sharpe (MRS) for the growth of lactobacilli*

Material	Quantity
Bacto-peptone	5g/L
Lab-Lemco	4g/L
Granulated Yeast Extract	2g/L
Tween 80	0.5mL/L
K_2HPO_4	1g/L
$NaH_2PO_4.H_2O$	3g/L
CH_3COONa	0.6g/L
$MgSO_4.7H_2O$	0.3g/L
$MnSO_4.H_2O$	0.04g/L
**** Supplemented with 40mM 1,2-propanediol and 200nM B12 to induce the pdu microcompartment***	

Table 2.4. *Recipe for MRS-Modified (MRS-MOD) for the growth of L. reuteri*

Material	Quantity
MOPS	83.72g/L
Tricine	7.17g/L
0.01M $FeSO_4.H20$	10mL/L
1.9M NH_4Cl,	50mL/L
0.276M K_2SO_4	10mL/L
0.02M $CaCl_2$-$2H_2O$	0.25mL/L
2.5M $MgCL_2$	2.1mL/L
5M NaCl	20mL/L
Micronutrient stock	0.2mL/L

Table 2.5 *Recipe for 10X MOPS minimal media.*

Material	Quantity
10X MOPS	50mL/L
Glucose	10g/L
1M K_2HPO_4	10mL/L
Thiamine	5*u*L/L

Table 2.6. *Recipe for 1X MOPS minimal media.*

Material	Quantity
Glucose	10g/L
Sodium acetate	5g/L
K_2HPO_4	3g/L
$MgSO_4.7H_20$	0.2g/L
L-Alanine	0.10g/L
L-Arginine	0.10g/L
L-Aspartic Acid	0.20g/L
L-Cysteine	0.20g/L
L-Glutamic Acid	0.20g/L
L-Histadine	0.10g/L
L-Isoleucine	0.10g/L
L-Leucine	0.10g/L
L-Lysine	0.10g/L
L-Methionine	0.10g/L
L-Phenylalanine	0.10g/L
L-Serine	0.10g/L
L-Tryptophan	0.10g/L
L-Tyrosine	0.10g/L
L-Valine	0.001g/L
Nicotinic acid	0.001g/L
Pantothetic acid	0.001g/L
Pyridoxal	0.002g/L
Riboflavin	0.001g/L
Cyanocobalamin	0.001g/L
Adenine	0.01g/L
Guanine	0.01g/L

Table 2.7*. Recipe for Minimal Lactobacillus Medium (MLM) for the growth of lactobacilli.*

Different carbon compounds were assessed for effect on viable counts when used in aqueous isotonic solution to re-suspend lyophilized constructs. Phosphate uptake from added phosphate was determined to identify which would aid most in sustained viability of the lyophilized culture over the necessary extended time period. Sorbitol (a sugar alcohol) and sodium gluconate (an organic acid) were

the chosen carbon sources, utilized at a concentration of 2% (Zhan *et al.,* 2011), (Santivarangkna *et al.,* 2006) and supplemented with 15, 10 or 5mM phosphate. 1mL samples were then taken at hourly intervals and tested with molybdovandate as previously described.

Compound	Concentration of solution	Reference
Sorbitol **(MW 182.17)**	20g in 1L (2%)	Carvalho *et al.,* 2003
Sodium Gluconate **(MW 196.16)**	20g in 1L (2%) 8g in 1L (0.8%)	Jones *et al.,* 2008

Table 2.8: *Table illustrating the chosen carbon sources.*

2.2.3. Molecular Methods

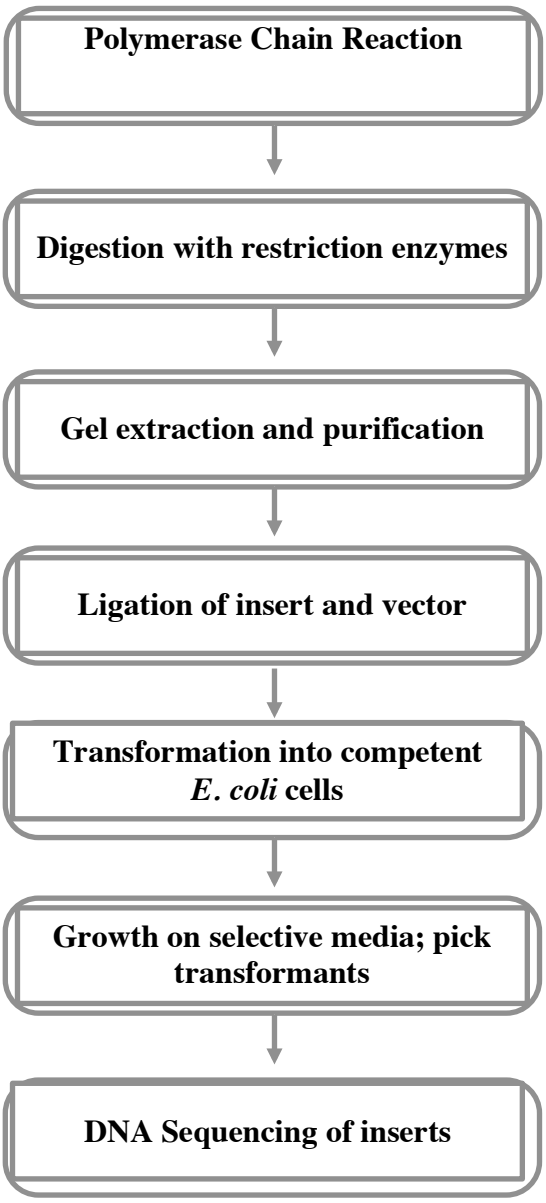


Figure 2.1*. Flow chart indicating the cloning process utilized for the development of the constructs in this study.*

2.2.2.2 Vectors

As previously mentioned, in order to allow direct expression of the inserted genes in both *E. coli* and *Lactobacillus reuteri*, a number of shuttle vectors were studied *(Table 2.9)* in particular pNZ44, which is a vector in the well-known

pNZ series of lactobacilli vectors (Kok, 1991). pNZ44 was created in University College Cork (McGrath *et al.,* 2001) from the backbone of the pNZ8048 vector, replacing the inducible nisin promoter with the constitutive p44 promoter from *Lactococcus lactis* (van der Vossen *et al.,* 1987). For *E. coli*-based cloning, the pET23 vector was also used for cloning purposes. For integration, the pORI280 vector was utilized.

Vector	Size	Antibiotic selection	Replicon Type	Original reference
pNZ44	3.394kb	Chloroamphenicol 10mg/mL	pNZ8048	McGrath *et al.,* 2001
pET23	3.666kb	Ampicillin 100mg/mL	pBR322	Studier and Moffatt, 1986
pORI280	5.263kb	Erythromycin 200mg/mL	pWV01	Leenhouts *et al,* 1998
pEX-A	2.450bp	Ampicillin 100mg/mL	pUC18	n/a

Table 2.9*. Table indicating vector information.*

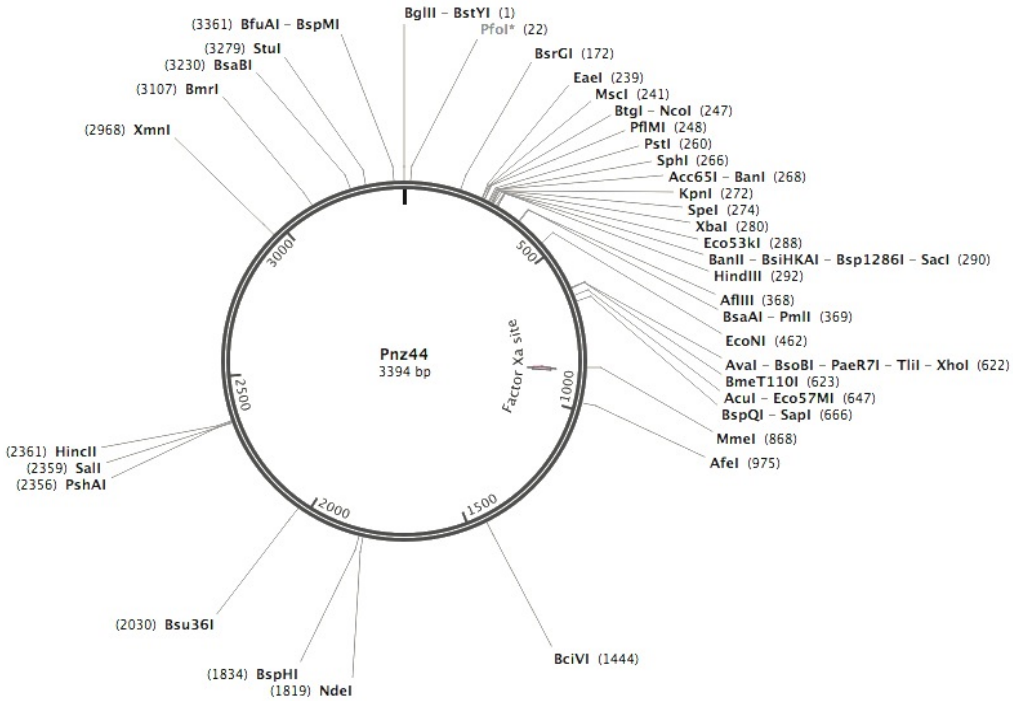


Figure 2.2. *Vector map for pnZ44 (credit: Dr. Lorraine Draper, University College Cork)*

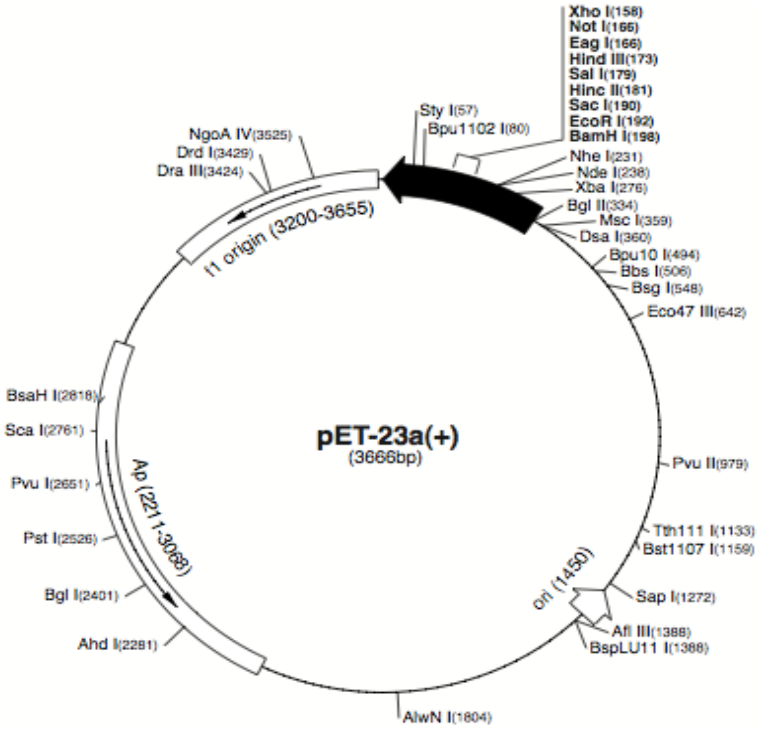


Figure 2.3. *Vector map for pET-23a (credit: Novagen, Merck Biosciences)*

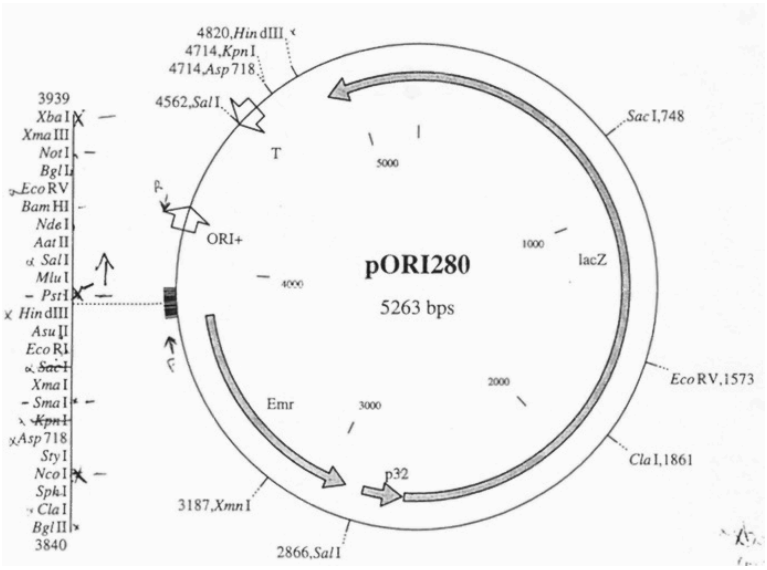


Figure 2.4. *Vector map for pORI280 (credit: Dr. Lorraine Draper, University College Cork)*

2.2.3.2. Primer design & PCR Conditions

All primers utilized in this study were designed by the author (unless specifically indicated otherwise) and produced by MWG Eurofins. Primers mostly adhered to a maximum length of 30bp, and a melting temperature of between 57°C and 70°C, unless specific requirements challenged this.

PCR reactions were performed using a pre-prepared program as indicated in Table 2.11. All reactions utilized the Fermentas Phusion High-Fidelity DNA polymerase (#M0530S). Phusion has 5'-3' polymerase activity and a 3'-5' exonuclease activity, and generates blunt-ended products. The reason for the use of a high-fidelity enzyme was to alleviate the frequency of amplification errors during the reaction.

Step	Temperature	Duration
Denaturation		
1	95.0°C	2 minutes
2	95.0°C	30 seconds
Annealing		
3	62°C	30 seconds
4	72°C	2 minutes 30 seconds**
Return to Step 2 and repeat cycle 29 times		
Extension		
5	72°C	10 minutes
Storage		
6	4°C	Infinity loop
***For amplification of L. reuteri ppk, time is extended to 3 minutes*		

Table 2.10. *PCR program for amplification of E. coli and L. reuteri DSM20016 ppk gene.*

Reagent	Quantity	Final Concentration
Polymerase Buffer	10µL	5X
dNTP	2.5 µL	200µM per dNTP
Primers (MWG)	1	1µM per primer
Genomic template	1 µL	<250ng
Phusion DNA Polymerase	1 µL	1X
Deionised water	33.5 µL	-

Table 2.11. *PCR reaction mix.*

Primer name	Sequence 5-3’	Restriction Sites	Predicated Amplicon Size
KMC1A (L. reuteri ppk Forward)	5’- GGC **CCATGG** ATG TAT AAG GAG TTT TAT AAG -3’	NcoI	2.2kb
KMC1B (L. reuteri ppk Reverse)	5’-GCC **AAGCTT** TCA AGA AAG TTA GAT CGA CGG-3’	HindIII	2.2kb
KMC2A (E. coli ppk Forward)	5’-GCC **CCATGG** ATGGGTCAGGAAAAGC-3’	NcoI	2.0kb
KMC2B (E. coli ppk Reverse)	5’-GCC **AAGCTT** TTATTCAGGTTGTTCGA-3’	HindIII	2.0kb
KMC3A (BamHI.pORI28 Forward)	5'-TGA CT**G GAT CC**T AAG TTC TTT GGA ATA CTT CAA ACC-3'	BamHI	1.3kb
KMC3B (EcorRI.pORI28 Reverse)	5'-TGA CT**G AAT TC**G TTC AAG AAG CAT TTG AGC GTC-3'	EcoRI	1.3kb
KMC3C (HindIII.pORI28 Reverse)	5'-TGA CT**A AGC TT**G TTC AAG AAG CAT TTG AGC GTC-3'	HindIII	1.3kb
KMC4A (SacI.p44 Forward)	5'-GCC **GAG CTC** GGG CAT GCG TTA GTT GAA GAA-3'	SacI	2.6kb
KMC4B (SphI.ABJKNU Reverse)	5'-GCC **GCA TGC** TAT GTT CGT GTA ATT TCA-3'	SphI	2.6kb
KMC4C (SphI.LRppk Reverse)	5'-GCC **GCA TGC** TTA CTC ATC CTT TCG CTC-3'	SphI	2.2kb
KMC5A (Citrobacter pdu-SphI Forward)	5'-GAT **GCA TGC** ATG CAA CAA GAA GCG TTA G-3'	SphI	2.2kb
KMC5B (Citrobacter pdu-SacI Reverse)	5'-GAA **GAG CTC** TTA TGT CCG GGT GAT GGG-3'	SacI	2.2kb
139Pr1 (10023IntegForward)	5’-TG ACT **GGA TCC** TAA GTT CTT TGG AAT ACT TCA AAC C-3’	BamHI	1.3kb
139Pr2 (10023IntegReverse)	5’-TG ACT **GAATTC** GTT CAA GAA GCA TTT GAG CGT C-3’ *	EcoRI	1.3kb
KMC6C (10023IntegReverse)	5’-TG ACT **AAGCTT** GTT CAA GAA GCA TTT GAG CGT C-3’	HindIII	1.3kb
KMCV1 (pNZ44 Forward)	5’-ATG AAT CGT GAT GTG TGA GG-3'	n/a	3.3kb
KMCV2 (pNZ44 Reverse)	5’-TCA ACT AAC GGG GCA GGT TAG TG-3'	n/a	3.3kb
P18 sequence (L. reuteri) ***(purchased double stranded)***	5’-A TGC AGA TTA ATG ATA TTG AAA GTG CTG TAC GCA AAA TTC TTG CCG AAG AAC TA– 3’	n/a	110bp
P18 sequence (E. coli) ***(purchased double stranded)***	5’–ATG AAC ACT TCA GAA CTT GAA ACC CTT ATT CGT AAC ATT TTG AGT GAG CAA CTT GCC-3’	n/a	110bp

Table 2.12. *Table indicating primers used during this study. All produced by MWG Eurofins. Restriction sites shown in bold*

2.2.3.3. DNA Modification Protocols

Extraction of the whole genomic DNA of both *L. reuteri* and *E. coli* was achieved using the Wizard Genomic DNA Purification Kit (Promega, Madison, USA) with protocol followed as per manual provided for Gram positive/Gram negative bacteria. This kit utilizes a series of lytic enzymes, protein precipitation and isopropanol to elucidate high quality DNA from the bacterial cell. 1mL of overnight (approximately stationary phase) culture was pelleted for extraction. Following this procedure, the isolated genomic DNA was stored in the -20ºC freezer for future use in PCR. Confirmation of gene size was obtained using gel electrophoresis. Sequenced plasmids were extracted and purified using a plasmid purification kit (Fermentas GeneJet Plasmid Extraction kit #12703194). This kit utilizes lytic enzymes, RNAase and silica-based membranes for centrifugation purification. 1mL of culture is pellet for plasmid extraction purposes. Digested PCR products were extracted from agarose gels, and purified using using a PCR purification kit (Fermentas GeneJet PCR Purification kit #12790091). This purification kit utilizes silica-membrane-based purification to remove any traces of agarose or other debris from PCR products.

2.2.3.4. Electrophoresis

For this study, 0.48g of powdered agarose was added to 60mL of 10x TAE buffer to create a 0.8% gel, which offers the best resolution of DNA fragments <10kb. This solution was mixed with approximately 1µL of ethidium bromide (Sigma Aldrich E1510) and allowed to set in a loading tray. 3-5µL of DNA sample was added, with 4µL of marker dye to facilitate loading. A 1kb DNA

ladder (N3232S New England Biolabs) was also added to the gel as a standard DNA size marker. Samples are run for 20 minutes at 100mV.

2.2.3.5. PCR

L. reuteri ppk1 was amplified from *L. reuteri* genomic DNA using primers KMC1A and KMC1B**.** The *E. coli ppk* gene was amplified from *E. coli* MG1655 by PCR with primers KMC2A and KMC2B (*PCR protocol Table 2.12, primers Table 2.12)*.

Following confirmation of gene size, the *ppk* gene amplicons and pnZ44 vector were digested and single bands excised from agarose. pNZ44 is a *Lactobacillus-E. coli* shuttle vector (obtained from Dr. Lorraine Draper, UCC) and uses a constitutive p44 promoter and has chloramphenicol resistance (Cm 10mg/mL); (*Table 2.9)*. The *ppk* genes and the pNZ44 vector were digested respectively using 1µL *NcoI* (Fermentas FastDigest #FD0574) and 1µL *HindIII* (Fermentas FastDigest #FD0504), along with 4µL of buffer reagent and 30µL of sample

Following this purification step, the *ppk* gene and the pNZ44 vector were ligated together, to create a new genetic construct. The ligation reaction was carried out in PCR tubes, which are placed in a thermocycler on a specially calibrated ligation programme. 4µL of T4 ligase (Invitrogen #15224-017) is added to the reaction mixture, along with 10µL of the insert DNA and 5µL of the vector DNA.

The resulting ligate was electroporated in E.cloni 10G electrocompetent cells (#60107-1 Lucigen, Wisconsin, USA). After plating on chloramphenicol selective agar, colonies were sequenced to confirm presence of *L. reuteri ppk-pNZ44*. DNA sequencing was obtained by the Value Read service, MWG-

Eurofins. This sequencing service utilizes provided primers to confirm the presence of genes of interest, along with a BLAST analysis.

The resulting plasmid was then further transformed into *L. reuteri* DSM20016 using a specific protocol provided by Prof. J.P. van Pijkeren *(section 2.2.3.9.).*

2.2.3.6. p18 targeting sequence

To observe the potential effect of the p18 targeting sequence with the *E. coli ppk-pNZ44* and *L. reuteri ppk-pNZ44*, a new construct was made with suitable restriction sites (MWG Eurofins). This double stranded DNA construct, or synthetic gene, consisted of an *NcoI* site, followed by 54 bases encoding the 18 amino acid sequence of the p18 linker, ending in a *PstI* site (*Figure 3.5*) To allow ligation with both *E. coli ppk and L. reuteri ppk*, a *BamHI* site followed the *PstI.* This allowed observation of the effect of the linker on both the *E. coli ppk* and also the *L. reuteri ppk.*

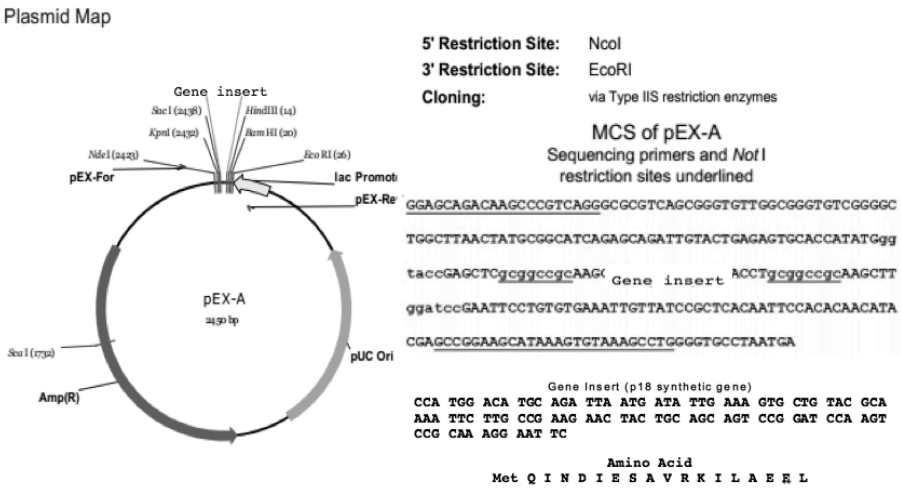


Figure 2.5. *Plasmid map for the synthetic p18 linker gene, obtained from MWG Eurofins. The construct was initially provided on the pEX-A vector.*

2.2.3.7. Microcompartment genes

The Citrobacter propanediol microcompartment (Pdu MCP) consists of a 22 kb operon, which contains a number of shell genes. These shell genes encode for the assembly of the proteins required to form the functional MCP shell. Previous subcloning has shown that the minimal gene set required for empty shell assembly is *pduA, pduB, pduJ, pduK, pduN* and *pduU* (Parsons *et al., 2010*).



Figure 2.6. *Map indicating the minimal genes required for empty microcompartment synthesis.*

Because it was planned to use *E. coli* and *Lactobacillus* hosts for operons encoding for this minimal shell assembly, two different cloning approaches were used to provide recombinant microcompartment operons of Gram positive and Gram negative origin suitable for co-expression with targeted PPK. Approach 1 involved the use of two primers; a forward *pduAB* primer and a reverse *pduU* primer *(Table 2.12)* applied to the existing recombinant vector assembled using genes of *Citrobacter* origin (Parsons et al 2010). Approach 2 involved the amplifying the individual shell genes from the *L. reuteri* DSM20016 genome by PCR. The individual genes were linked on one after another using the "link and lock" multiple cloning strategy (McGoldrick *et al.,* 2005) which was previously used by (Parsons *et al.,* 2010) in the cloning of the empty Citrobacter *pdu* microcompartment.

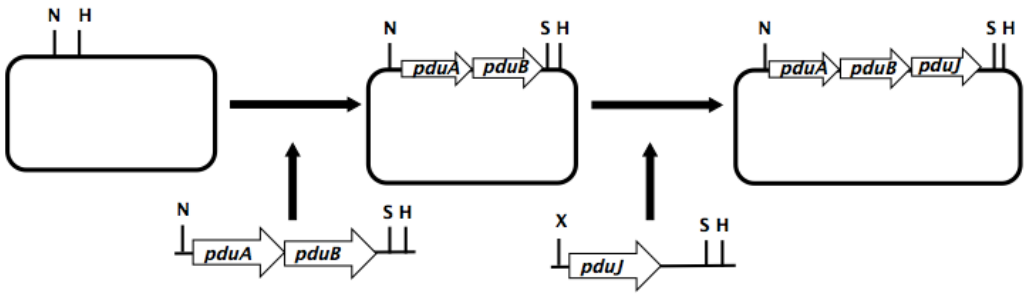


Figure 2.7. *Plasmid construction using Link and Lock method. N represents NdeI, S represents SpeI, X represents XbaI and H represents HindIII. The compatibility of SpeI and XbaI sites, which when ligated together do not reform a restriction site, means that these sites can be reused in successive rounds of cloning, allowing additional genes to be added on one after another.*

2.2.3.8. Chromosomal Integration

In order to co-express a targeted *ppk* gene stably along with the key structural genes required for the MCP assembly in the murine strain *L. reuteri* 100-23, chromosomal integration was attempted. In the first instance the chromosomal integration of the structural genes *pduABJKNU* was attempted with the *ppk* gene remaining on a plasmid.

A method for the chromosomal integration of Lactobacilli had been previously established using the temperature sensitive pVE6007 and the *pORI280* vector to induce chromosomal integration (Russell & Klaenhammer, 2001). Internal fragments of the target genes were amplified by PCR, using specific primers (*Table 2.12*) and inserted into pORI28 (an Em^r *repA*-negative derivative of pWV01) by directional cloning using E. coli EC1000 (which contains a copy of the pVW01 repA gene in the chromosome) as the host. The next step would be the purification of the plasmids and electroporation into *L. reuteri 100-23*, containing the temperature sensitive *pVE6007* (a Cm^r *repA*-positive derivative of pWV01), with 35°C being the optimal temperature for phenotypic expression.

Lactobacilli carrying both plasmids are propagated overnight at 35°C in the presence of erythromycin and chloramphenicol. Through selection on erythromycin plates and an increased temperature of 44°C, transformants are recovered and propagated successively in MRS minus antibiotic for 90 generations to assess stability of integration.

For constructs, the p44 constitutive promoter was also required, to allow constitutive expression of the MCP structural genes on integration.

2.2.3.9. Lactobacillus transformation

A protocol for the transformation of *L. reuteri* was kindly provided by Prof. J.P. van Pijkeren, of Michigan State University.

Day 1 :

5mL MRS was initially prepared in a 15mL tube, and inoculated with *L. reuteri* DSM 20016 from glycerol stocks. Inoculate was grown statically and anaerobically for 16-24hrs at 37°C until stationary phase.

Day 2 :

After overnight growth and stationary phase has been reached, the culture must be accurately sub-cultured to an OD 600 of 0.1. This can be approximately calculated via the following *e.g.* if OD 600 of o/n culture is 1.25 then (4.57/0.1)= 45.7. For a total volume of 40mL MRS, you need to add (40/45.7) = 0.875mL inoculation. This volume must then be once again verified by spectrophotometer readings.

After 1.15 hours, OD 600 was measured again. Once an OD 600 of between 0.55 and 0.65 (early exponential phase) was reached, cells must be cooled

immediately for 5 minutes. Once cooled, cells can be centrifuged in a precooled centrifuge for 5mins at 5000rpm. It is essential to keep the cells on ice at all times.

Supernatant was removed and cells gently resuspended in 20mL ice-cold buffer (0.5M sucrose/10%v/v glycerol). Once resuspended, an additional 20mL buffer was added to reset the volume back to 40mL. Tubes and buffer were again maintained on ice and centrifugation repeated as above.

Again, supernatant was removed, and cells resuspended in 20mL buffer before a final centrifugation.

After final centrifugation, supernatant was carefully removed and adequate buffer added in order to set a total volume 1/50 of initial culture volume *e.g.* 40mL/50=0.8mL. Cells were resuspended gently, and aliquoted out in 100ul volumes.

For transformation, approx. 1ug plasmid DNA was added to one aliquot of cells. Cells were electroporated at 2500V, 25uF, 400Ω with anticipated time constants at approx. 8-10msec. Immediately after electroporation, 1mL MRS (room temp) was added to cells, which were then allowed to recover statically and anaerobically for 2.5hours at 37° C. After recovery, 100ul undiluted culture was plated on antibiotic selective MRS in an anaerobic jar for approx. 24-48hours.

2.2.4. Expression & Phenotype of constructs

2.2.2.3. Neisser stain protocol

Neisser stain is a staining process which highlights intracellular polyphosphate granulations under a bright-field microscope (Machnicka, 2005). The stain

protocol involves three distinct stains, used in a particular order. Neisser Stain A consists of 0.1g methylene blue, 5mL glacial acetic acid and 5mL 96% ethanol to 100mL dH_2O. Neisser Stain B consists of 3.3mL of 10% crystal violet (suspended in 96% ethanol) and 6.7mL 96% ethanol to 100mL dH_2O. Neisser Stain C consists of 33.3mL 1% aqueous chrysodin Y to 100mL dH_2O.

The actual stain protocol is based upon using the aforementioned stains to stain and counterstain polyphosphate. Initially fix a 10µL volume of the culture on a glass slide. Prepare a solution of 2 parts stain A with 1 part stain B. Apply this solution to the glass slide for 10-15 seconds. Rinse and dry. Apply stain C for 45 seconds, rinse and dry. Allow the slide to dry, and view under 100x bright field microscopy. If there is polyphosphate present in the culture, purple accumulations will be observable within the bacterial cells.

2.2.5 Polyphosphate observations in native lactobacilli

Through the process of observing phosphate uptake and polyphosphate retention in *L. reuteri,* it was also possible to observe these processes in other wild-type lactobacilli, such as *Lactobacillus delbrueckii* subspecies *bulgaricus* ATCC11842. This was achieved using Neisser stain. In particular, for the observation of wild-type *L. reuteri,* samples were obtained from both *pdu*-induced and un-induced cultures. Induced cultures were grown over a period of 2 days in MRS, with 1,2-propanediol and vitamin B12 (cyanocobalamin) supplemented during growth *(Table 3.5)* to induce the presence of the Pdu microcompartment as described (Sriramulu *et al.,* 2008). Un-induced cultures were grown exclusively in MRS without supplementation.

2.2.6. Phosphate Assay Test and Conditions

2.2.6.1. Assay Design

In order to identify and quantify the ability of the recombinant constructs to remove and uptake extracellular phosphate, it was necessary to establish a series of phosphate assays. The purpose of the phosphate assay was to establish i) the ability of the constructs to uptake extracellular phosphate and ii) to identify the factors that may enhance or retard the ability of the constructs to uptake phosphate.

2.2.6.2. Assay Preparation

As mentioned, assays were performed with washed cells in Ringers solution supplemented with a defined amount of K_2HPO_4. This was necessary because of the difficulty of measuring phosphate levels in rich media. Strains were grown initially in either defined media (Luria Bertani Broth for *E. coli,* MRS for *L. reuteri*) or minimal media (Supplemented MOPS media for *E. coli,* Minimal Lactobacillus media for *L. reuteri*). Minimal media was used for initial growth where possible to restrict the amount of phosphate provided to the culture pre-assay.

In order to grow the cells to stationary phase, 15mL defined/minimal media, supplemented with relevant antibiotics, was inoculated with the construct of interest and incubated overnight at 37°C. The overnight culture was subcultured in a volume of 500mL defined/minimal media and antibiotics, which was grown to an OD 600nm of 0.4. This would typically take 4-5 hours to occur, and would result in the cells being in early exponential stage. Cells were then pelleted by

ultracentrifugation using the J10 rotor at 7,000G for 5 minutes (Beckman Coulter).

The pellet was washed twice with Ringers solution to remove excess media residue, which may affect the phosphate uptake. Following this washing step, the pellet was resuspended and inoculated into 100mL Ringers solution supplemented with K_2HPO_4. Samples were then obtained every hour for the initial 6-hour duration for testing.

2.2.6.3. Phosphate Analysis of Samples

2.2.6.2.2. Orthophosphate

Orthophosphate content of the supernatant was determined by pelleting 1mL of culture, removing the supernatant and testing with molybdovanadate (#2076032, Hach, Colorado, USA) using a spectrophotometer at OD 430nm. Molybdovanadate is a reagent that binds to orthophosphate in solution, with the degree of yellow color formation quantitative to the amount of phosphate present (Fiske & Subbarow, 1925). Results were then plotted against a KH_2PO_4 standard curve.

2.2.6.3.2. Polyphosphate

Intracellular polyphosphate of the bacteria was tested by pelleting 4mL culture, where the pellet was then frozen for 24 hours at -80°C to induce softening and lysis of the cell membrane. Measurements of intracellular polyP were measured using the DAPI (4',6-Diamidino-2-phenylindole) fluorescence method established by the McGrath lab (Kulakova *et al.,* 2011). Samples were obtained hourly along side phosphate measurements, and were frozen at -80°C for minimum 24 hours. DAPI measurements were done by Dr. Mingzhi Liang.

Briefly, cells were harvested by centrifuging at 5000g for 10 min at 4° C. After washing in 50mM HEPES buffer (pH7.5) the cell pellet or microcompartment fraction was frozen at -80° C followed by defrosting at room temperature. Cell pellets/microcompartment fractions were resuspended in HEPES buffer at an appropriate dilution to ensure that the cellular polyP concentration was in the linear range of the DAPI assay (0-6 mg polyP/mL). Total assay volume was 300µL which included 100 µL of polyP containing samples and 200 µL of DAPI assay buffer containing 150 mM KCl, 20 mM HEPES-KOH (pH 7.0) and 10 µM DAPI solution. After a 10 min incubation at room temperature DAPI fluorescence was measured with a platereader equipped with excitation and emission filters of 420 nm and 550 nm respectively. A polyphosphate standard curve was prepared using sodium phosphate glass Type 45 (S4379 Aldrich) and sodium hexametaphosphate (SX0583). Protein content of the bacterial culture was tested via Bradford assay (Bradford, 1976).

2.2.7. Graphs

All graphs were prepared using Microsoft Excel. Where present, error bars indicate standard deviations calculated from the use of three biological replicates.

2.3. Results & Discussion

2.3.1. Molecular results

Name	Inserts	Final size
pKMC001	*E. coli ppk+pNZ44*	5.3.kb
pKMC002	*L. reuteri ppk + pNZ44*	5.5kb
pKMC003	*E. coli p18+ppk + pNZ44*	5.3kb
pKMC004	*L. reuteri p18+ppk + pNZ44*	5.5kb
pKMC005	*E. coli p18 + pNZ44*	3.3kb
pKMC006	*L. reuteri p18 + pNZ44*	3.3kb
pKMC007	*L. reuteri pduABJKNU + pNZ44*	6.0kb
pKMC008	*P44+xylA + pORI280*	6.5kb
pKMC009	*L. reuteri pduAB + pet23*	4.6kb
pKMC010	*L. reuteri pduABJ + pet23*	4.9kb
pKMC011	*L. reuteri pduABJK + pet23*	5.5kb
pKMC012	*L. reuteri pduABJKN + pet23*	5.9kb
pKMC013	*L. reuteri pduABJKNU + pet23*	6.3kb

Table 2.13. *Table indicating plasmids created during this study.*

The *ppk1* gene was amplified from *E. coli* MG1655, by PCR, using primers KMC2A and KMC2B containing the restriction sites *NcoI* and *HindIII* (MWG Eurofins). The amplicon was the predicted size of approx. 2kb (*Fig. 2.8*) and confirmed by sequencing.

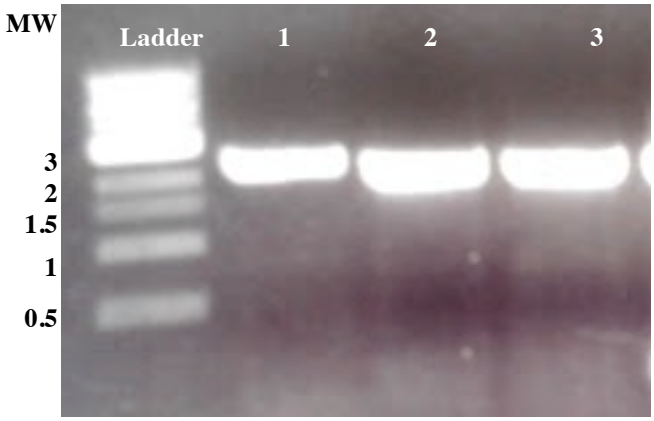


Figure 2.8. *Gel electrophoresis image indicating E. coli ppk amplicon in Lane 2&3. Lane 1 indicates an unrelated PCR product. The brightest MW in the ladder indicates the 3kb mark.*

The *ppk* gene was amplified from the obtained *L. reuteri* DSM 20016 genomic DNA PCR with primers KMC1A and KMC1B *(Table 2.12)* containing the

restriction sites *NcoI* and *HindIII*.. The amplicon was the predicted size of approximately 3.2kb via gel electrophoresis (*Fig. 2.9*) and confirmed by sequencing.

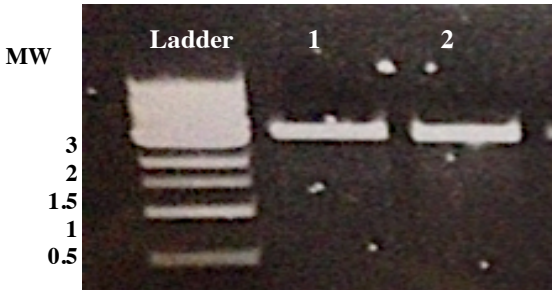


Figure 2.9*. Gel electrophoresis image indicating ppk amplicon (L. reuteri) in Lane 1 & 2. The brightest MW in the ladder indicates the 3kb mark.*

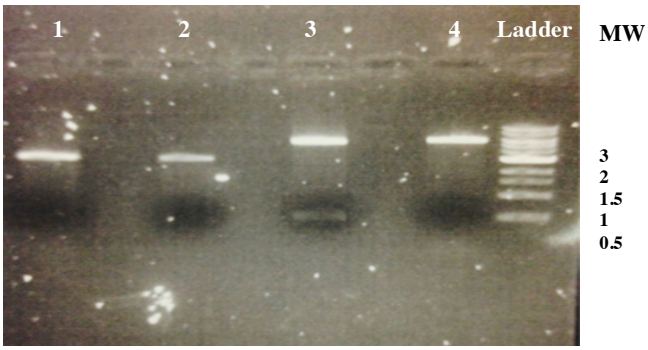


Figure 2.10. *Gel image indicating empty vectors pNZ8048 (Lane 1) and pnZ44 (Lane 2) digested with NcoI. The brightest MW in the ladder*

The p18 sequence was designed and produced as a synthetic gene (MWG Eurofins), (*Figure 2.5*). It was flanked by additional restriction sites, which allowed ligation in multiple vectors for multiple fusions.

On excision from the provided pEXa vector, the gene of interest was approx. 100bp. Due to the small size of the *L. reuteri* p18 gene construct, gel visualization was difficult and therefore frequent sequencing was necessary to ensure its continued presence.

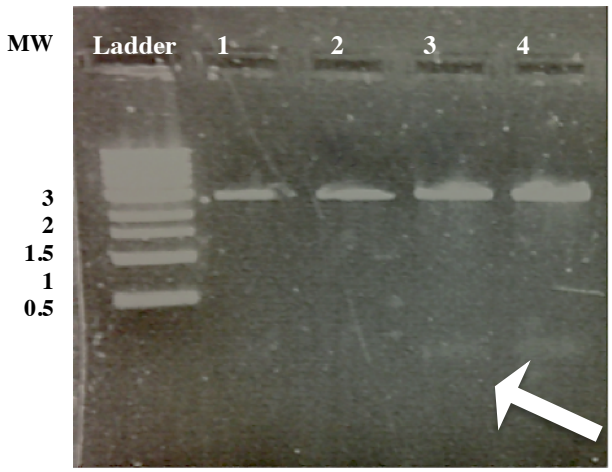


Figure 2.11. *Gel image illustrating plasmid pKMC005 pnZ44 (3kb) containing the E. coli p18 linker (100bp) in lane 3 & 4 after restriction digestion (arrow indicated). Lane 1 & 2 illustrate the pnZ44 vector without the linker.*

To produce an empty MCP, the minimum genes required for MCP expression were amplified and transformed into one vector. *PduAB* was amplified from the *L. reuteri* genome and ligated into the pET23 vector. It was excised from the vector via *NdeI,* which allowed inclusion of the ribosome binding site region of pET34, and a *HindIII* site. *pduJ* was then fused onto the *pduAB* gene via *SpeI/XbalI*, which have compatible ends, and *HindIII*, creating *pduABJ-pET23* (pKMC010).

The compatibility of *SpeI* and *XbaI* sites, which when ligated together do not reform a restriction site, means that these sites can be reused in successive rounds of cloning, allowing additional genes to be added on one after another *(Figure 2.7 for further information), (plasmids pKMC010-013)*. This resulted in the creation of *pduABJK-pET23* (pKMC011), *pduABJKN-pET23* (pKMC012) and *pduABJNU-pET23*(pKMC013).

Once DNA sequencing confirmed the presence of the insert of interest, it was excised from pET23 and transformed into pNZ44, to allow dual expression in *E. coli* and *L. reuteri.*

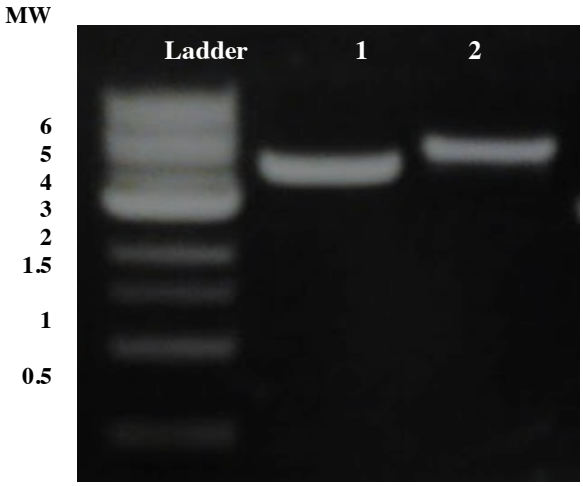


Figure 2.12. *Gel image illustrating L. reuteri pduAB pet23 (pKMC009) (Lane 1) and pduABJ pet 23 (pKMC010) after restriction digest. These genes were individually added on in pet23 before final transformation into pNZ44 (below).*

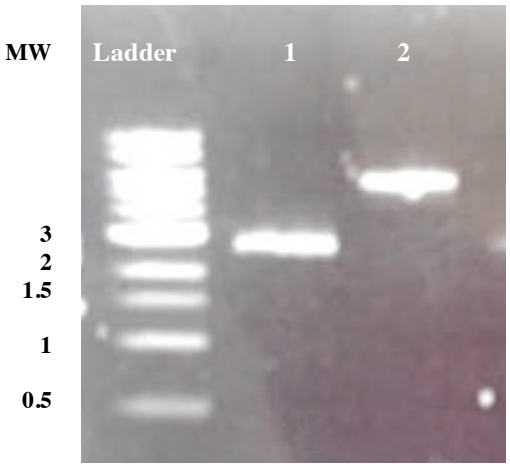


Figure 2.13. *Gel image illustrating L. reuteri pduABJKNUpNZ44 (pKMC007) (Lane 2) after restriction digest with SphI. E. coli ppk. Lane 1 is an unrelated DNA fragment*

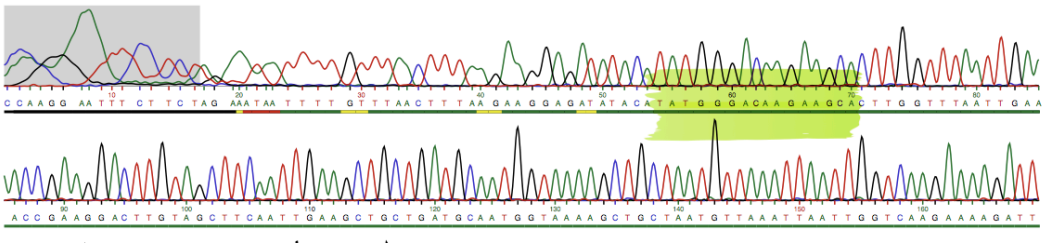


Figure 2.14. *Sequencing read out indicating the presence of L. reuteri pduABJKNU in pET23 (pKMC013). This highlighted sequence is the beginning of the pduA sequence.*

Regarding the use of the integration vector, a method for the chromosomal integration of Lactobacilli had been previously established using the temperature sensitive pVE6007 to induce chromosomal integration (Russell & Klaenhammer, 2001). The xylose isomerase gene (*xylA)* was chosen as the candidate gene to be knocked out, allowing our genes of interest to be integrated in its place. This gene was selected due to previous literature (Walter *et al.,* 2005) identifying this gene as nonessential to successful colonization of the murine gut by *L. reuteri* 100-23. Using primers presented in the Walter study *(Table 2.12),* the *xylA* gene was amplified from the *L. reuteri* 100-23 genome using primers KMC3A and KMC3B (*Table 2.12,)* containing the restriction sites *BamHI* and *EcoRI*. The gene was then ligated into the pNZ44 vector and transformed into Ecloni *E. coli* 10G cells (Lucigen).

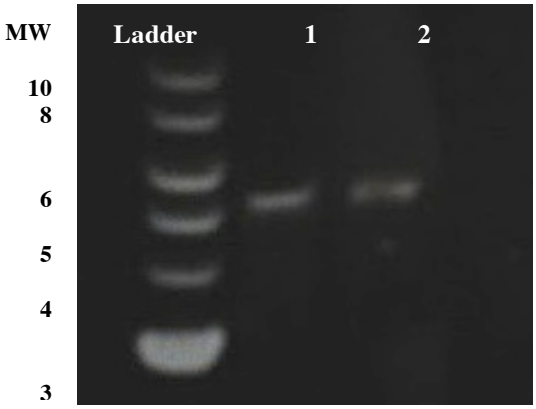


Figure 2.15. *Gel image illustrating empty vector pORI280, a band of approximately 5.3kb, in both lane 1 and 2. Band was digested once with BamHI.*



Figure 2.16. *Gel image illustrating xylA amplicon, a band of approximately 1.3kb, in lane 1. Band was amplified using primers KMC008.*

The p44-*xylA* construct was ligated into the suicide vector pORI280 (EmR *rep-A* negative derivative of pWV01) using *E. coli* EC1000 cells (which contain a copy of the pVW01 *repA* gene). However after successive unsuccessful attempts to obtain a clone with the insert, this protocol was abandoned. The pORI280 vector in our possession did not appear to match the vector map as digestion with the *SphI* restriction sites consistently resulted in an additional cut, indicating the presence of a second *Sph* site in the vector. At this point in the study, difficulties in obtaining an original sequenced pORI280 vector, which would facilitate the use of the required restriction sites, prevented further use of the integration technique and full integration was not achieved.

2.3.2. Neisser stain imaging

In order to observe polyphosphate accumulation and retention in the bacterial strains (wild-type and recombinant), samples of culture were obtained at various time points during growth for optimal observation and treated with Neisser stain.

2.3.2.1. Wild-type Lactobacillus strain imaging

A recent study (Alcantara *et al.,* 2014) noted polyP accumulation in a number of different lactobacilli. *Lactobacillus delbrueckii* subspecies *bulgaricus* ATCC11842 is a milk-adapted lactobacillus, particularly associated with dairy and yogurt production, whilst *L. reuteri* is a commensal bacterium typically associated with the mammalian gut.

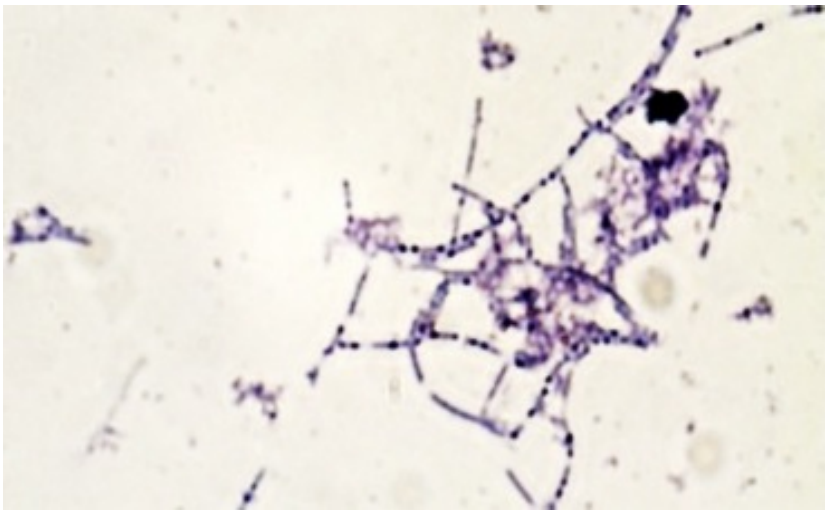


Figure 2.17: *Image of L. delbrueckii subspecies bulgaricus ATCC11842, grown in unsupplemented MRS and stained with Neisser stain. Purple granulations indicate the presence of polyphosphate in the cell. Image taken after 8 hours of growth in MRS.*

Large quantities of polyP accumulations can be observed within the bacterial cells in image 2.17. The observation of an elongated cell shape is also a distinctive feature associated with intracellular polyP accumulation, and previously observed by (Alcantara *et al.,* 2013).

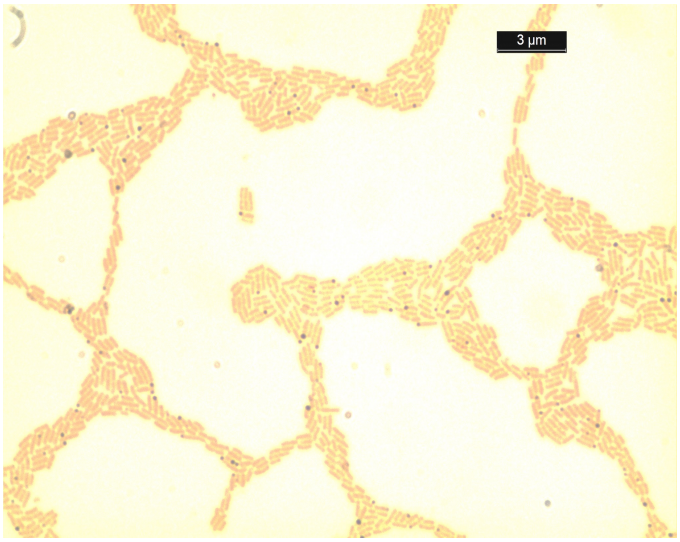


Figure 2.18: *Image of L. reuteri DSM20016 (grown in unsupplemented MRS) stained with Neisser stain. Image taken after 8 hours growth in MRS*

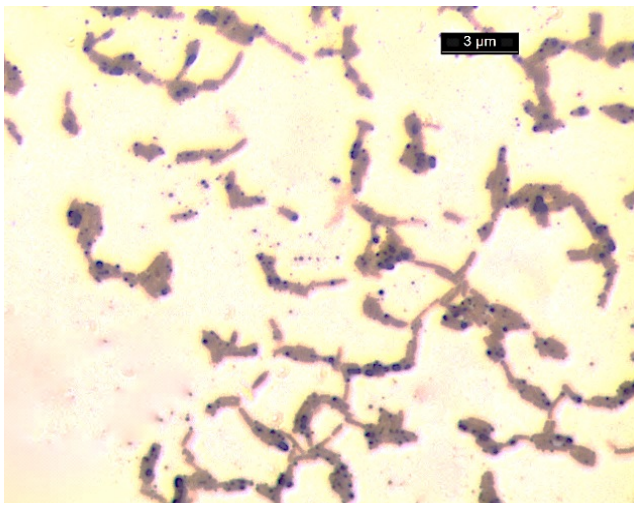


Figure 2.19: *Image of L. reuteri DSM20016 (grown in MRS supplemented with 1,2-propanediol and B12) stained with Neisser stain. Image taken after 8 hours of growth.*

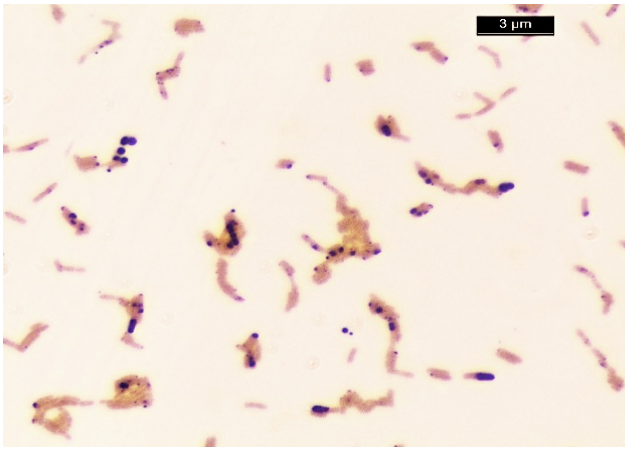


Figure 2.20: *Image of L. reuteri DSM20016 (grown in MRS supplemented with 1,2-propanediol and B12) stained with Neisser stain. Image taken after 15 hours of growth.*

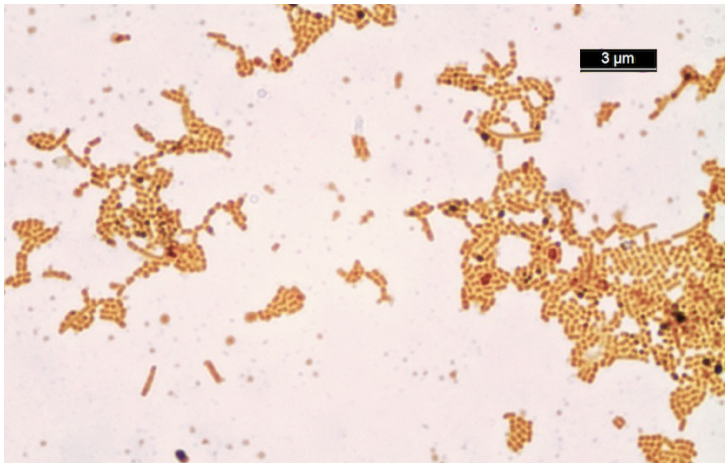


Figure 2.21: *Image of L. reuteri DSM20016 (grown in MRS supplemented with 1,2-propanediol and B12) stained with Neisser stain. Image taken after 30 hours of growth.*

In particular, in *L. reuteri* DSM20016, I observed a correlation between the induction of the wild-type *Pdu* microcompartment via the supplementation of 1,2-propanediol and B12, and polyP formation detected by Neisser staining. This can be observed in the difference between Figures 2.18 and 2.19, 2.20. This accumulation of polyphosphate can be observed to reverse over time, decreasing after approximately 30 hours *(*Figure 2.21*)*.

2.3.2.2. Recombinant strain imaging

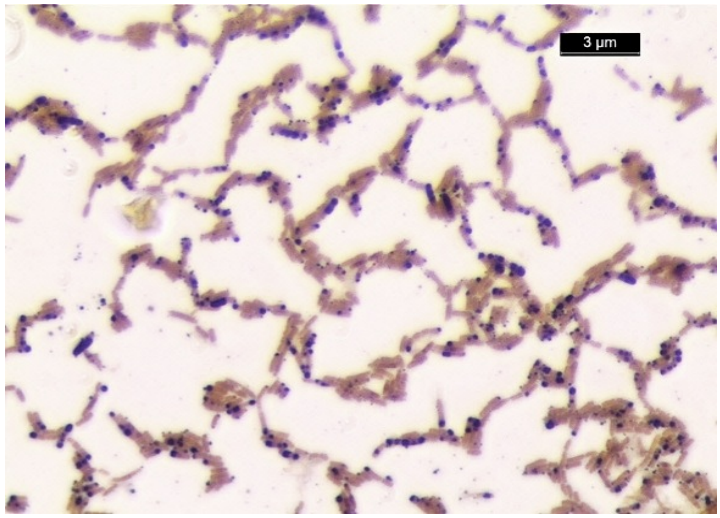


Figure 2.22. *E. coli ppk-pNZ44 (pKMC001) expressed in L. reuteri DSM20016. Cultured in MRS with chloramphenicol. After 9 hours of growth, purple granulations within bacterial cell indicate presence of polyphosphate granulation*

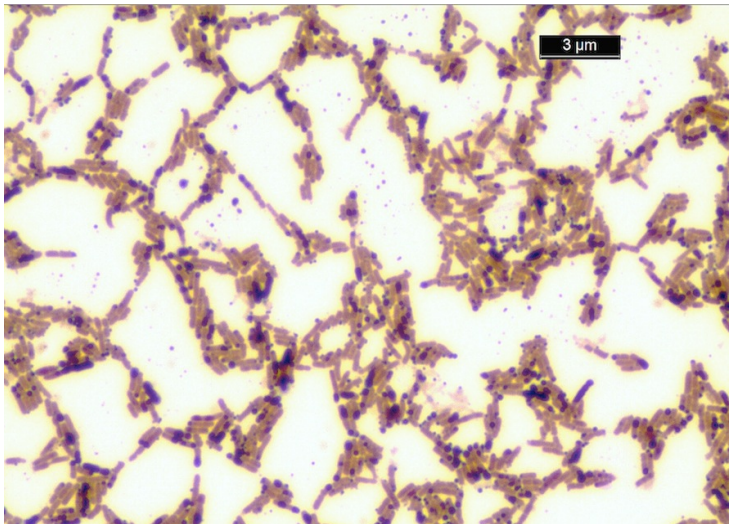
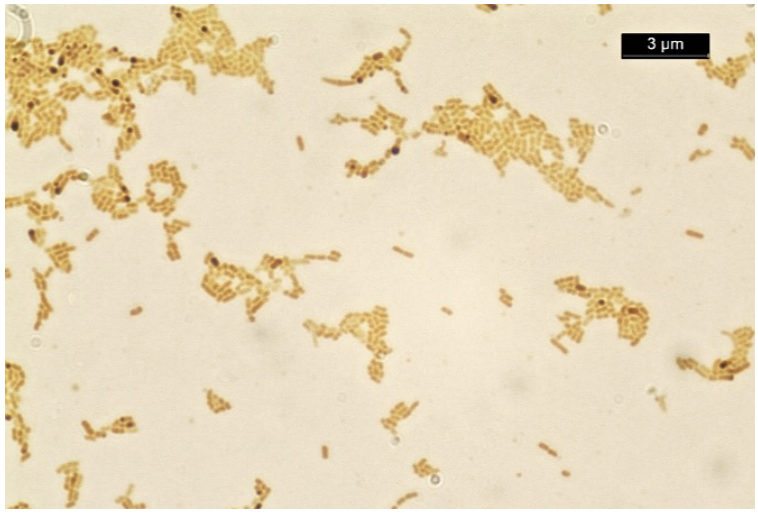


Figure 2.23. *E. coli ppk-pNZ44 (pKMC001) expressed in L. reuteri DSM20016. Cultured in MRS with chloramphenicol. After 15 hours of growth, purple granulations within bacterial cell indicate presence of polyphosphate granulation.*



.***Figure 2.24.*** *E. coli ppk-pNZ44 (pKMC001) expressed in L. reuteri DSM20016. Cultured in MRS with chloramphenicol. After 30 hours of growth, polyphosphate granulations have decreased.*

As observed in the wild-type *L. reuteri,* dynamic fluctuation of intracellular polyP can be seen with expression of the recombinant *E. coli ppk* in *L. reuteri* during different periods of growth *(Figure 2.22-2.24)*. However, the effect of recombinant *L. reuteri ppk* expression in *L. reuteri* is much less marked (*Fig 2.25*).

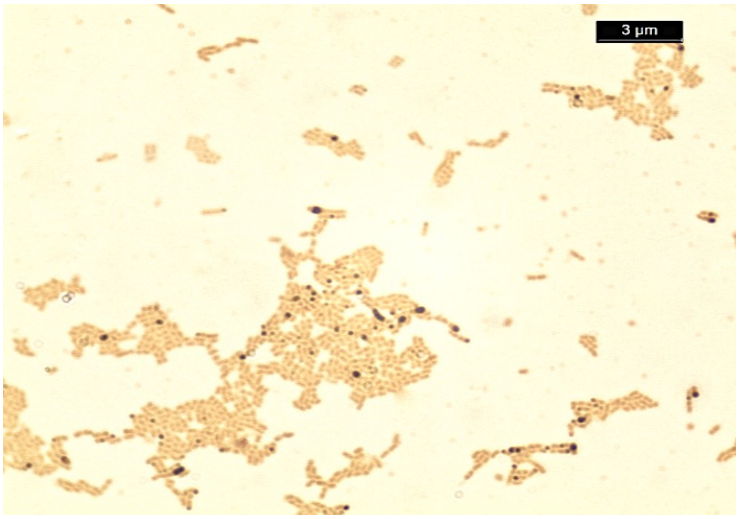


Figure 2.25. *L. reuteri ppk-pNZ44 (pKMC002) expressed in L. reuteri DSM20016 cultured in MRS with chloramphenicol for 9 hours. Purple spots within bacterial cell indicate presence of polyphosphate granulation.*

Polyphosphate levels measured by DAPI fluorescence showed accumulation followed by loss by the *L. reuteri* strain expressing *E. coli ppk* (Figure 2.26).

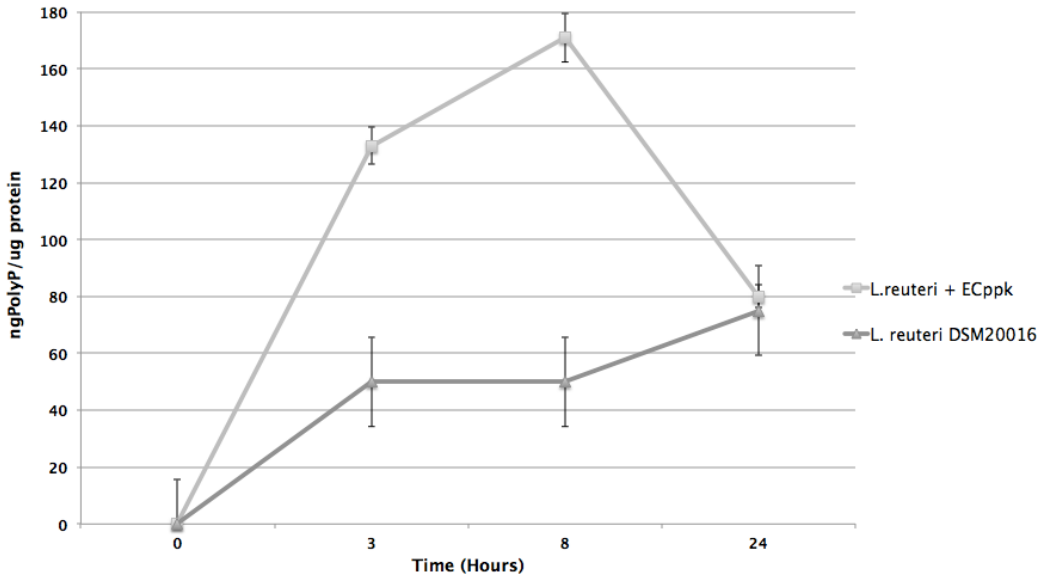


Figure 2.26. *Whole cell polyP assay wildtype L. reuteri 20016 and L. reuteri 20016 expressing the recombinant E. coli ppk gene (pKMC001), grown in MRS. Error bars represent standard deviation of three independent observations*

Therefore, Neisser stain microscopy and both quantitative polyphosphate assays show the expression of the recombinant *E. coli ppk* gene in *L. reuteri* DSM20016 leads to a faster and increased accumulation of polyP in the cell compared with the wild-type strain, however retention time is ultimately not extended beyond that of the wild-type.

2.3.3. Phosphate Assays

2.3.2.2. Phosphate uptake assays; live cultures

All live cultures were grown in MRS, with resuspension in Ringer's solution.

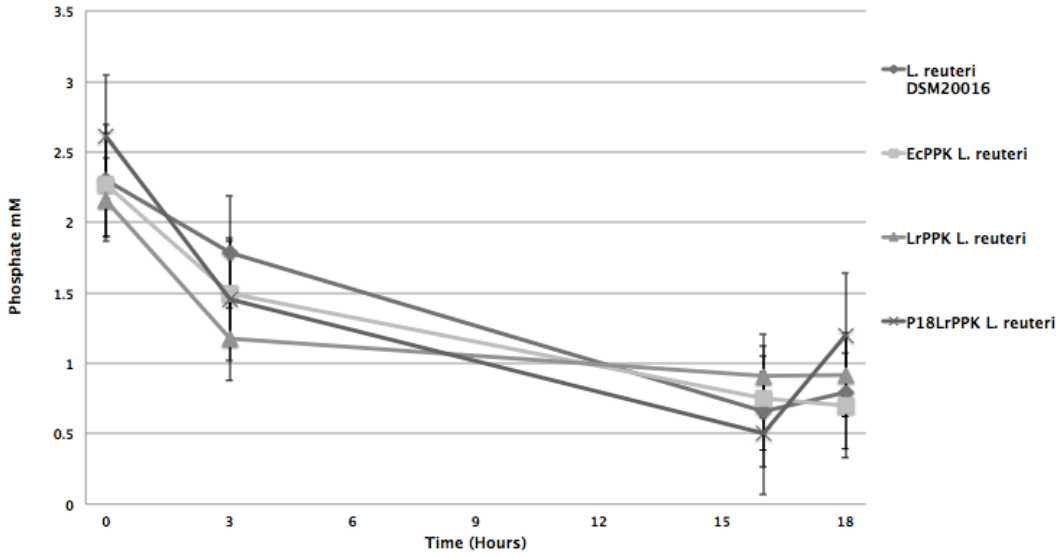


Figure 2.27. *Phosphate levels in supernatant in Ringers solution supplemented with K_2HPO_4, over 18 hour time period. Legend indicates the following constructs : WT wild-type cell ECppk (E. coli ppk pNZ44, pKMC001); LRppk (L. reuteri ppk pNZ44, pKMC002), p18LRppk (p18 targeting sequence plus L. reuteri ppk pNZ44, pKMC004). All constructs expressed in L. reuteri DSM 20016. 0.9g of wet bacteria was added to 100mL solution (per group).*

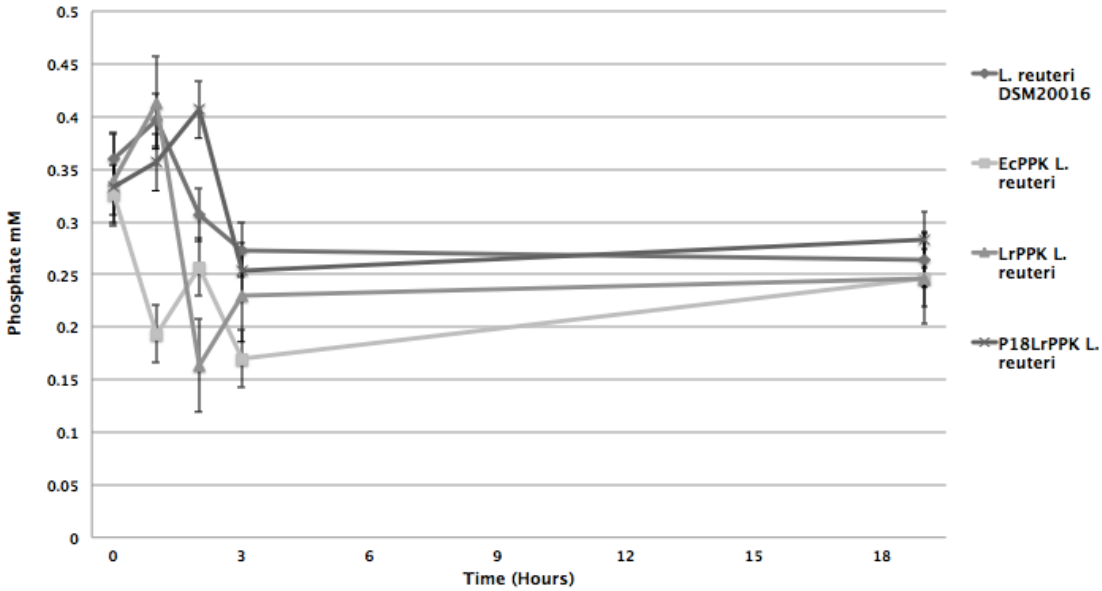


Figure 2.28 . *Graph illustrating phosphate uptake in Ringers solution supplemented with K_2HPO_4, over 17 hour time period. Legend indicates the following constructs i) wild-type cell ii) cell containing E. coli ppk (pKMC001) iii) cell containing L. reuteri ppk (pKMC002) and iv) cell containing the p18 targeting sequence plus L. reuteri ppk (pKMC004). All constructs expressed in L. reuteri DSM 20016. 1.0g of wet bacteria was added to 100mL solution (per group).*

An initial difficulty of measuring phosphate uptake by live cultures was establishing a uniform phosphate starting value i.e. a uniform phosphate concentration in culture from time zero. These difficulties had been observed when strains were grown and tested in rich media e.g. MRS, therefore to alleviate these difficulties, strains were pre-grown for a brief period in MRS to develop initial growth and then assayed in Ringers solution containing an exact amount of phosphate.

2.3.3.2. Phosphate assays; freeze-dried cultures

These assays were performed using freeze-dried bacterial cultures containing the recombinant cultures and a wild-type negative control. Original culture for the *L. reuteri* was in MLM media and *E. coli* in MOPS Media. These were chosen to alleviate the difficulties in using phosphate rich MRS/LB media. The freeze-dried cultures were resuspended in isotonic sorbitol, glucose or gluconate to observe the optimal carbon source for viability after resuspension. These carbon sources were chosen based on previous literature, where the viability of freeze-dried *Lactobacillus* cultures was extended over a long-term period through the usage of these compounds (Carvalho *et al.,* 2004). The selected carbon source was then supplemented with K_2HPO_4 as a phosphate source to assess phosphate uptake properties. Host strains, *E. coli* and *L. reuteri* were used for freeze-dried assays as both strains were considered for *in vivo* studies. Supernatant phosphate and cellular polyphosphate was measured over 6 hours (a period corresponding to the likely duration of orally dosed bacterial presence in the upper

gastrointestinal tract). Higher levels of phosphate than in the first experiments were employed, reflecting post-prandial intestinal levels (Moroz *et al.,* 2011)

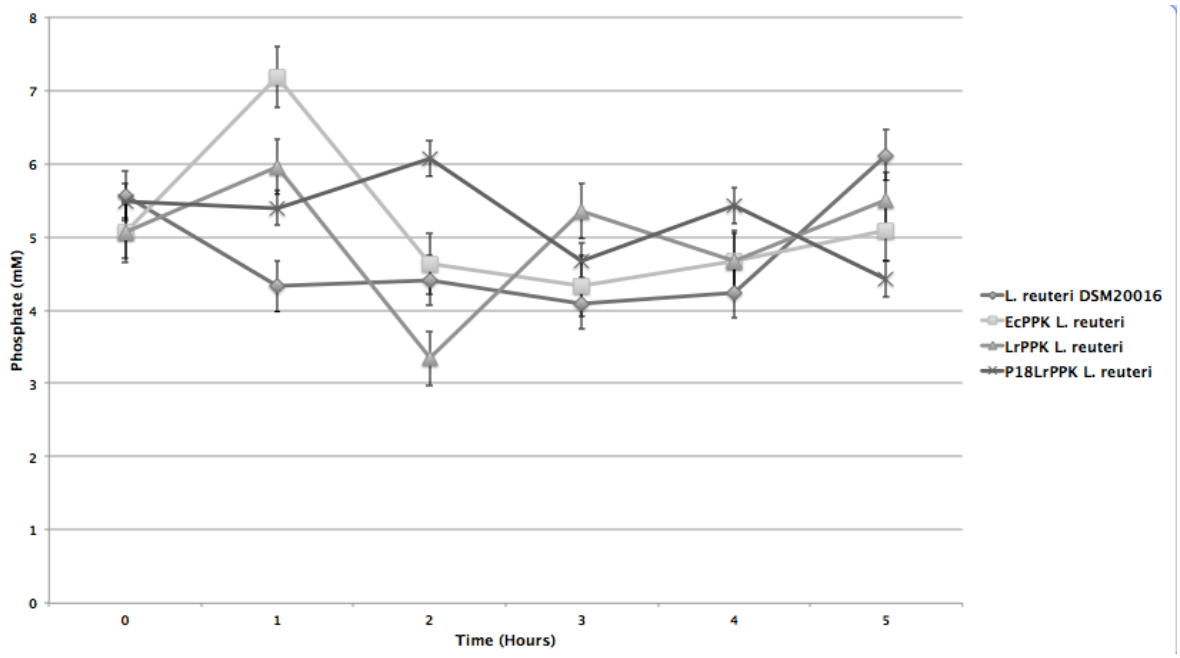


Figure 2.29. *Graph illustrating phosphate uptake over 5 hour time period in aqueous 2% sorbitol plus 5mM K_2HPO_4. Legend indicates the following constructs i) wild-type cell ii) cell containing E. coli ppk (pKMC001) iii) cell containing L. reuteri ppk (pKMC002) and iv) cell containing the p18 targeting sequence plus L. reuteri ppk (pKMC004). All constructs expressed in freeze-dried L. reuteri DSM 20016. 0.0.21g of bacteria was added to 100mL solution (per group).*

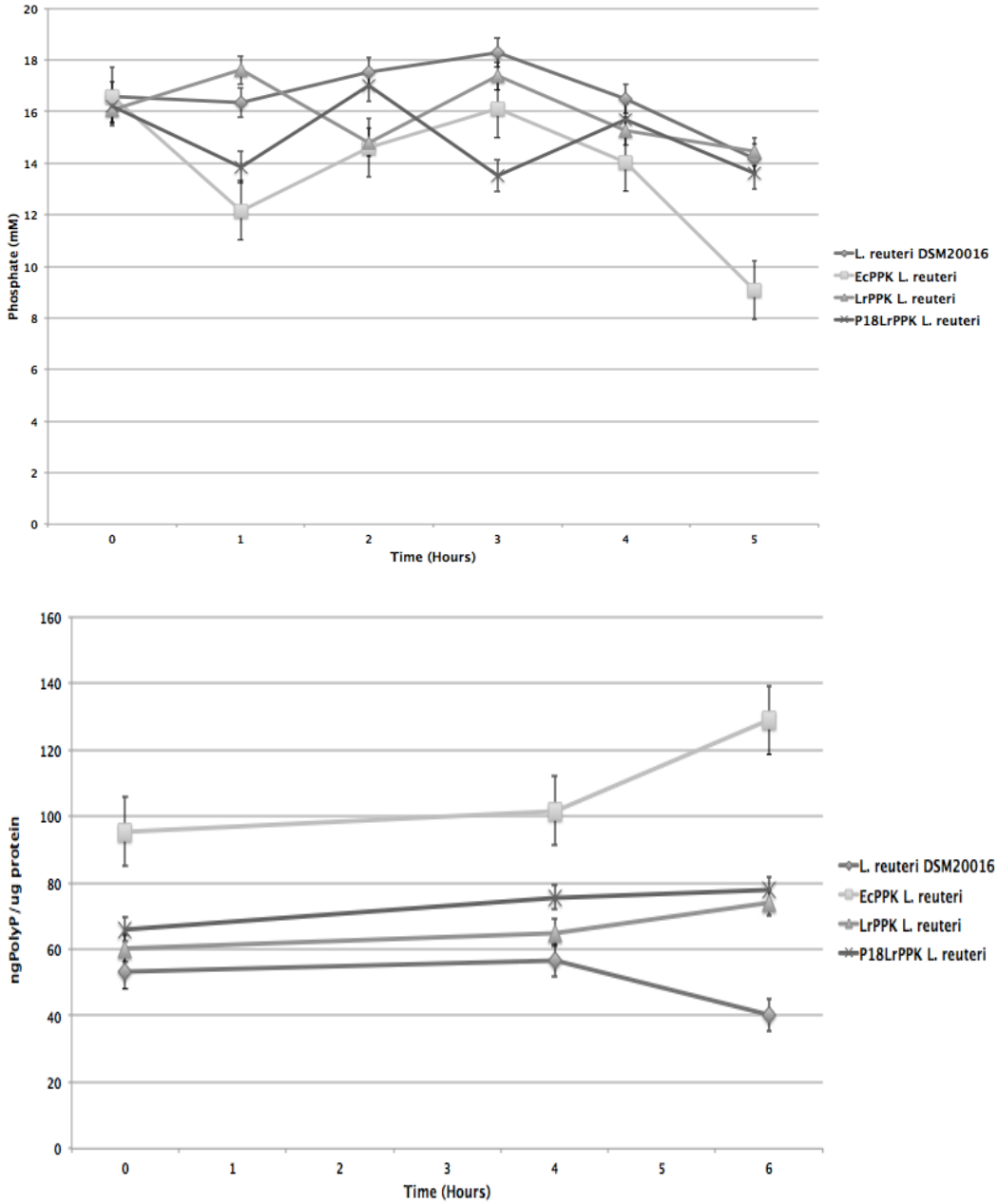


Figure 2.30A&B. *A) phosphate uptake over 5 hour time period in 0.8% gluconate plus 15mM K_2HPO_4 and B) intracellular polyphosphate. Legend indicates the following constructs i) wild-type cell ii) cell containing E. coli ppk (pKMC001) iii) cell containing L. reuteri ppk (pKMC002) and iv) cell containing the p18 targeting sequence plus L. reuteri ppk (pKMC004). All constructs expressed in freeze-dried L. reuteri DSM 20016. 0.018g of bacteria was added to 100mL solution (per group).*

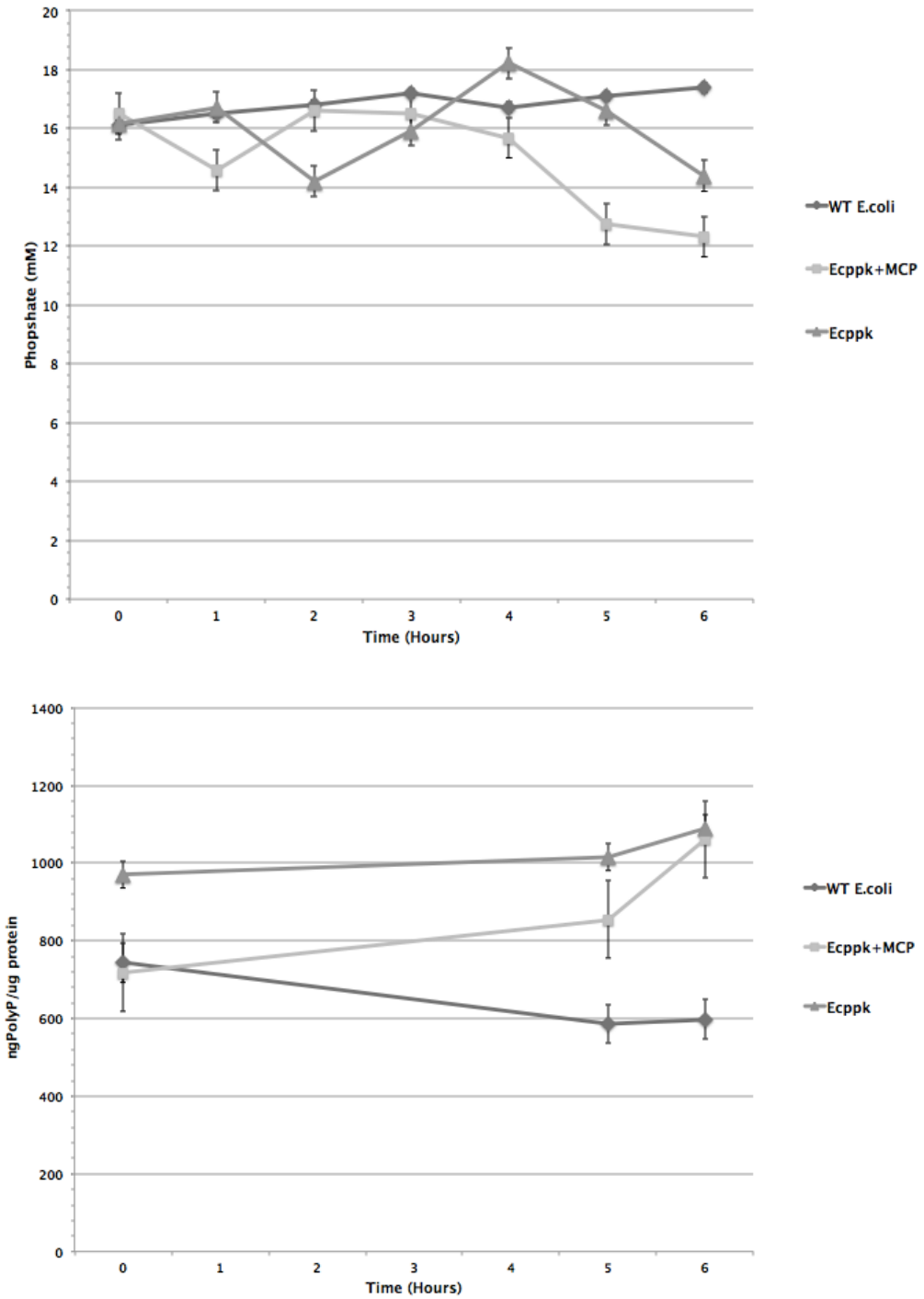


Figure 2.31A&B. *Graph illustrating A) phosphate uptake over 5 hour time period in 2% gluconate plus 15mM K_2HPO_4 and B) intracellular polyphosphate. Legend indicates the following constructs i) wild-type cell ii) cell containing E. coli ppk with pduABJKNU and the empty recombinant microcompartment and iii) cell containing the E. coli ppk. All constructs expressed in freeze-dried E. coli BL21. 0.02g of bacteria was added to 100mL solution (per group).*

Literature had suggested that the supplementation of sorbitol to cultures before the freeze-drying process would lead to increase storage viability (Carvalho *et al.,* 2003). However based upon our study experience, the addition of sorbitol to our cultures disrupted the freeze-drying process and led to sticky, coagulated cultures. As an alternative, sorbitol was added to an aqueous solution and examined for viability post-freeze-drying. Observations of the use of sorbitol with the freeze-dried culture displayed a consistent growth spurt of the cultures, leading to cell death after approx. 6-8 hours (*Figure 4.23*). These observations ultimately led to sorbitol being discontinued as a supplement, as the cultures were required to be viable and sustainable for a longer time period.

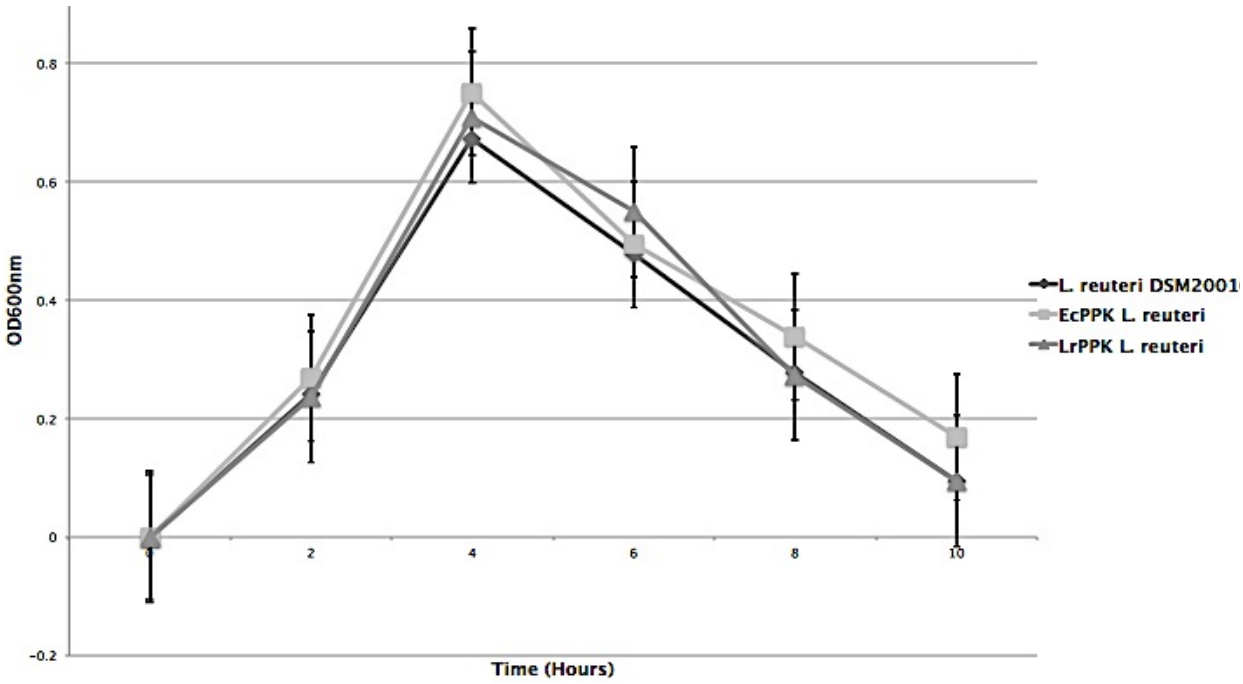


Figure 2.32. *Growth curve of lyophilized cultures resuspended in water with 2% sorbitol.*

In contrast, at concentrations of 0.8% and 2%, gluconate provided positive, stable conditions for good phosphate uptake and sustained growth of the freeze-dried cultures (*Figure 2.29)*. For this reason, gluconate was selected as the most

suitable supplement, as cell viability and phosphate uptake indicated to be at stable levels based on assay results.

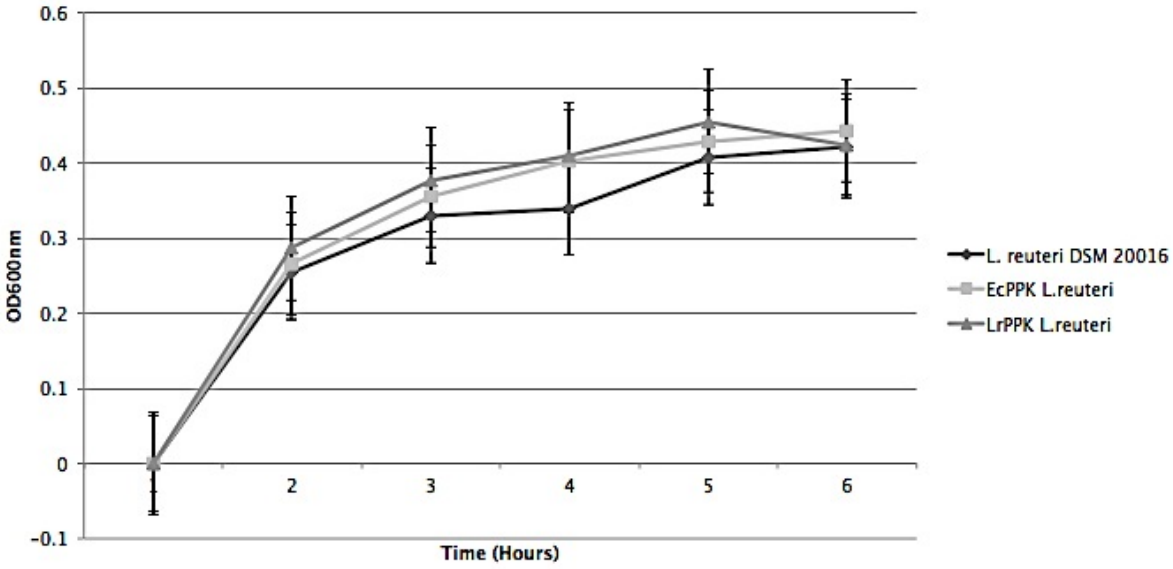


Figure 2.32. *Growth curve of lyophilized cultures resuspended in water with 2% gluconate.*

2.3.3.4.Polyphosphate measurements

No obvious trend for phosphate uptake was seen over time for lyophilized *L. reuteri* WT and clones resuspended in sorbitol solution (*Figure 2.29*). The same clones resuspended in gluconate solution showed a trend for phosphate uptake and polyphosphate accumulation by *L. reuteri* expressing *E. coli ppk* (*Figure 2.30)*. A control experiment with freeze dried *E. coli* BL21 expressing recombinant *E. coli ppk* and *E. coli* expressing recombinant *E. coli* microcompartment targeted *ppk* and an empty microcompartment showed that both clones took up phosphate and accumulated polyphosphate (Figure 2.32) . This would be the predicted phenotype of these clones from longer-term culture experiments (Liang *et al.,* 2015).

2.4. Conclusion

The observation that *Lactobacillus* species differ in their propensity to accumulate visible polyphosphate granules (*Fig 4.8, 4.9*) is in agreement with a recent publication (Alcantara *et al.,* 2013). Polyphosphate granulation has however not previously been reported in the dairy strain *L. delbrueckii subspecies bulgaricus ATCC11842*. This phenotype is reportedly correlated with possession of a *ppk* gene and could contribute to stress resistance because *ppk* knockout simultaneously abolishes this phenotype and decreases stress resistance (Alcantara *et al.,* 2013). However the author found *L. reuteri* DSM20016, which contains a *ppk* gene, was phenotypically granule-free unless the *pdu* operon was induced (*Fig 4.9-11*). This connection between microcompartment induction and polyphosphate production in *L. reuteri* 20016 is novel and intriguing and could result from co-regulation or relate to stress from the production of the microcompartment itself or aldehyde leaks during propanediol metabolism. Further experiments (RNA-Seq, aldehyde challenge) would be required to investigate this. Investigation into the *L. reuteri* 100-23 *pdu*-negative strain would also provide potential analysis.

As stated, the objective of this study was to manipulate phosphate uptake and polyP accumulation in *L. reuteri* DSM20016 and *E. coli*. By using recombinant *ppk* genes, I anticipated an increase in polyphosphate storage and phosphate uptake, and by introducing the empty structural microcompartment with microcompartment-targeted PPK, I anticipated stabilization in phosphate uptake and intracellular polyP accumulation vs. the wild-type strain and the strain with recombinant *ppk* alone.

Initial observations regarding expression of the recombinant *E. coli ppk* in *L. reuteri* indicated that the heterologous enzyme was functional. Increased phosphate uptake and polyphosphate accumulation compared to the wild-type was observed over a 3 to 15 hour time period (*Figure 2.33, 4,17*). Function of *E. coli ppk* in an *L. reuteri* host background has not to the author's knowledge been reported before.

Interestingly, over expression of the *L. reuteri ppk* in the *L. reuteri* host produced a much less marked phenotype (*Figure 2.36, 2.37. 2.38*), suggesting a discrepancy between the efficacies of recombinant *E. coli* and *L. reuteri* ppk when expressed in *L. reuteri*. This discrepancy was identifiable across phosphate uptake assays, and also in microscopy imaging of samples. The reason for this variation in efficacy when expressed in the same host *(L. reuteri)* is unclear and would require further investigation to confirm gene expression and translation of both PPK enzymes. However, the initial hypothesis that polyphosphate content and phosphate uptake can be modified in *L. reuteri* through the application of a recombinant *ppk* gene seems justified.

Ultimately combining the microcompartment targeted PPK and the MCP together, with a view to expression in *L. reuteri,* was an aim of this project. The *ppk* gene from both *L. reuteri* and *E. coli* was cloned and expressed in both host strains respectively, allowing observation of the action of a recombinant PPK within these strains, whilst in parallel the MCP genes *pduABJKNU* of *L. reuteri*, the minimum necessary to form an empty microcompartment, were cloned in shuttle vector pNZ44.

The hypothesis regarding PolyP stabilization could however not be fully observed in *L. reuteri* due to cloning difficulties preventing successful integration of the *pdu* microcompartment and *ppk* gene. These difficulties arose from the selection of the integration vector, which did not allow integration of the empty *pdu* microcompartment into the *L. reuteri* genome due to discrepancies in restriction site availability of the vector in possession versus that of the original vector map.

The instability of polyphosphate resulting from expression of PPK alone in *E. coli* was reproduced in *L. reuteri* in this study (*Figure 2.37*). However, previous studies, confirmed in this thesis (*Figure 4.22*) have shown positive increases in phosphate uptake and accumulation of polyphosphate in the short term by both *ppk* expression and targeted PPK and empty MCP expression in *E. coli* . For future investigations, it would be of interest to pursue successfully the establishment of a *L. reuteri ppk*-MCP expressed in *L. reuteri*, and also to investigate the interaction between the *E. coli ppk-L. reuteri pdu* MCP to see if the initial observations from this study regarding *ppk* discrepancy would continue to be applicable.

Following demonstration of enhancement of phosphate uptake by the recombinant PPK in *L. reuteri,* a decision was made to explore the efficacy of the constructs in an *in vivo* murine study, where the constructs could be tested in an animal model with chronic renal failure and hyperphosphatemia (elevated blood phosphate). This study can be read in detail in Chapter III.

In order for these strains to be delivered daily in water to an animal model, cultures were required to be lyophilized. As such, it was necessary to evaluate

how this process may potentially affect the efficacy and viability of these recombinant strains. Evaluation of lyophilized cultures (*Figure 4.21, 4.22*) identified that the recombinant strains still displayed highly dynamic shifts in phosphate uptake efficacy, with the recombinant *E. coli ppk* again indicating to be more effective versus the *L. reuteri ppk,* when expressed in the *L. reuteri* host. Culture viability and sustainability was identified to be influenced by the sugar source provided post-lyophilisation, with gluconate providing the most stable revitalizing environment for our strains. Estimates of short term orthophosphate in vitro uptake by lyophilized *E. coli* expressing *E. coli* PPK directed to an empty microcompartment and lyophilized *L. reuteri* expressing *E. coli* PPK were of potentially therapeutic levels for the rat model (Chapter III). This depended on carbon source and required resuspension in gluconate solution rather than sorbitol. It is known that sorbitol fermentation results in much higher cytoplasmic levels of NADH in *E. coli* than gluconate fermentation (and this may have global regulatory effects. Lyophilised bacteria would be more practical to administer on a daily basis.

On searching through previous literature, it was difficult to obtain information regarding typical polyP accumulation levels in *Lactobacillus*, therefore this meant a lack of comparison with my findings. Regarding *E. coli*, previous studies have indicated polyP accumulation levels of approximately 48nmol/mg (Rao *et al*., 1998), which is higher than we observed. However my examinations involved the cultures uptaking phosphate in a defined restrictive environment (K_2HPO_4 and gluconate), which may offer an explanation for my observed lower levels. No previous literature could be identified which compared intracellular polyP levels between *E. coli* and *Lactobacillus* species.

Ultimately this study delivered novel observations regarding the role of *ppk* and the microcompartment in phosphate metabolism in *L. reuteri DSM 20016,* and has provided the foundation for further investigative work.

2.5. References

- Alcantara C., Blasco A., Zuniga M., Monedero V. (2013) Accumulation of Polyphosphate in Lactobacillus spp. and Its Involvement in Stress Resistance. Applied and Environmental Microbiology 80:1650-1659
- Bradford MM. (1976) A rapid and sensitive method for the quantitation of microgram quantities of protein utilizing the principle of protein-dye binding. Annual Biochemistry 72:248-254.
- Brown, M. R. W., Kornberg, A., Brown, M. R. W., Kornberg, A. (2004). Inorganic polyphosphate in the origin and survival of species. Proceedings of the National Academy of Sciences of the United States of America 101:16085–16087.
- Carvalho A., Silva J., Ho P., Teixeira P., Malcata F., Gibbs P. (2002) Survival of freeze-dried *Lactobacillus plantarum* and *Lactobacillus rhamnosus* during storage in the presence of protectants. Biotechnology Letters 24:1587-1591
- Carvalho, A. S., Silva, J., Ho, P., Teixeira, P., Malcata, F. X., Gibbs, P. (2003). Protective effect of sorbitol and monosodium glutamate during storage of freeze-dried lactic acid bacteria. Le Lait, 83:203–2

- Carvalho, A.S., Silva, J., Ho, P., Teixeira, P., Malcata, F.X. Gibbs, P. (2004) Relevant factors for the preparation of freeze-dried lactic acid bacteria. International Dairy Journal 14:835–847.
- Chen J., Brevet A., Fromant M., Levequent F., Schmidt J., Blanquet S., Plateau P. (1990) Pyrophosphatase Is Essential for Growth of *Escherichia coli*. Journal Of Bacteriology 5686-5689
- Dick C., Dos-Santos A., Meyer-Fernandes J. (2011) Inorganic Phosphate as an Important Regulator of Phosphatases. Enzyme Research 11:1-7
- Dobrogosz W.J., Lindgren E. (1988) 'Antibiotic reuterin.' US Patent PCT/ US88/01423.
- Drews G., Niklowitz W. (1956) Beitrage zur Cytologie der Blaualgen. Archives of Microbiology 24:147–62
- Fan C., Cheng S., Sinha S., Bobik T. (2012) Interactions between the termini of lumen enzymes and shell proteins mediate enzyme encapsulation into bacterial microcompartments. Proceedings of the National Academy of Sciences 109:14995-15000
- Fiske C., Subbarow Y. (1925) The colorimetric determination of phosphorus. Journal of Biological Chemistry. 66:375-400
- Hall R. H., Stern E.S. (1950) Acid-catalysed hydration of acrylaldehyde: kinetics of the reaction and isolation of 3-hydroxypropionaldehyde. Journal of The Chemical Society 490–498.

- Henry J., Crosson S. (2013) Chromosome replication and segregation govern the biogenesis and inheritance of inorganic polyphosphate granules. Molecular Biology of the Cell 24:3177-3186
- Iancu C.V., Morris D.M., Dou Z., Heinhorst S., Cannon G.C., Jensen G.J. (2010). Organization, structure, and assembly of alpha-carboxysomes determined by electron cryotomography of intact cells. Journal of Molecular Biology 396:105–117.
- Jenkins, J. (2005). Gluconate Metabolism in Lactobacillus and Its Role in Persistence in the Human Intestine. (Electronic Thesis) https://etd.ohiolink.edu/
- Johnson R., Redding K., Holmquist D. (2007) Water quality with Vernier. Vernier Software & Technology, Beaverton, OR.
- Jones S., Jorgensen M., Chowdhury F., Rodgers R., Hartline J., Leatham M., Struve C., Krogfelt K., Cohen P., Conway T. (2008) Glycogen and Maltose Utilization by Escherichia coli O157:H7 in the Mouse Intestine. Infection and Immunity 76:2531-2540
- Keasling, J., Van Dien, S. & Pramanik, J. (1998). Engineering Polyphosphate Metabolism in *Escherichia coli*: Implications for Bioremediation of Inorganic Contaminants. Biotechnology and Bioengineering 58:231-239.
- Kerfeld, C. A., Heinhorst, S., Cannon, G. C. (2010). Bacterial Microcompartments. Annual Review Microbiology 64:391–408.

- Kok, J. (1991). Special-purpose vectors for Lactococci in Genetics and Molecular Biology of Streptococci, Lactococci and Enterococci III Lactococci: Molecular Biology and Biotechnology 97G–102G.
- Kullen, M. J., Klaenhammer, T. R. (2000). Genetic Modification of Intestinal Lactobacilli and Bifidobacteria. Current Issues Molecular Biology 41–50.
- Langa, S., Landete, J. M., Martín-Cabrejas, I., Rodríguez, E., Arqués, J. L., Medina, M. (2013). *In situ* reuterin production by *Lactobacillus reuteri* in dairy products. Food Control 33:200–206.
- Leenhouts K., Venema G., Kok J. (1998) A lactococcal pWV01-based integration toolbox for bacteria. Methods in Cell Science 20:35–50
- Levering J., Musters M., Bekker M., Bellomo D., Fiedler T., de Vos W., Hugenholtz J., Kreikemeyer B., Kummer U., Teusink B. (2012) Role of phosphate in the central metabolism of two lactic acid bacteria - a comparative systems biology approach. FEBS Journal 279:1274-1290
- Liang M., Frank S., Lünsdorf H., Warren M.J., Prentice, M.B. Submitted for publication 2015
- Machnicka, A. (2006). Accumulation of Phosphorus by Filamentous Microorganisms 15:947–953.
- McGoldrick, H.M., Roessner, C.A., Raux, E., Lawrence, A.D., McLean, K.J., Munro, A.W., Santabarbara, S., Rigby, S.E., Heathcote, P., Scott, A.I. (2005). Identification and characterization of a novel vitamin B12 (cobalamin) biosynthetic enzyme (CobZ) from *Rhodobacter capsulatus*,

containing flavin, heme, and Fe-S cofactors. Journal of Biological Chemistry 280:1086–1094.

- Parsons J., Dinesh S., Deery E., Leech H., Brindley A., Heldt D., Frank S., Smales C., Lunsdorf H., Rambach A., Gass M., Bleloch A., McClean K., Munro A., Rigby S., Warren M., Prentice M. (2008) Biochemical and Structural Insights into Bacterial Organelle Form and Biogenesis. Journal of Biological Chemistry 283:14366-14375
- Rao N., Liu S., Kornberg A. (1998) Inorganic Polyphosphate in *Escherichia coli*: the Phosphate Regulon and the Stringent Response. Journal Of Bacteriology 2186–2193
- Rodriguez E., Arques J., Rodriguez R., Nunez M, Medina M (2003) Reuterin production by Lactobacilli isolated from pig faeces and evaluation of probiotic traits. Letters in Applied Microbiology 37:259-263
- Russell, W. M., Klaenhammer T.R. (2001) Efficient system for directed integration into the *Lactobacillus acidophilus* and *Lactobacillus gasseri* chromosomes via homologous recombination. Applied Environmental Microbiology 67:4361–4364
- Santivarangkna C., Kulozik U., Foerst P. (2006) Effect of carbohydrates on the survival of *Lactobacillus helveticus* during vacuum drying. Letters in Applied Microbiology 42:271-276
- Santos F., Spinler J., Saulnier D., Molenaar D., Teusink B., de Vos W., Versalovic J., Hugenholtz J. (2011) Functional identification in

Lactobacillus reuteri of a PocR-like transcription factor regulating glycerol utilization and vitamin B12 synthesis. Microbial Cell Factories 10:55

- Schaefer L., Auchtung T., Hermans K., Whitehead D., Borhan B., Britton R. (2010) The antimicrobial compound reuterin (3-hydroxypropionaldehyde) induces oxidative stress via interaction with thiol groups. Microbiology 156:1589-1599.
- Sriramulu, D. D., Liang, M., Hernandez-Romero, D., Raux-Deery, E., Lunsdorf, H. Parsons, J. B., Warren, M. J., Prentice, M.B., (2008). *Lactobacillus reuteri* DSM 20016 Produces Cobalamin-Dependent Diol Dehydratase in Metabolosomes and Metabolizes 1,2-Propanediol by Disproportionation. Journal of Bacteriology 190:4559–4567.
- Stevens M., Vollenweider S., Meile L., Lacroix C. (2011) 1,3-Propanediol dehydrogenases in *Lactobacillus reuteri*: impact on central metabolism and 3-hydroxypropionaldehyde production. Microbial Cell Factories 10:61
- Van der Vossen, J. M. B. M., van der Leile D, and Venema G. (1987) Isolation and characterization of *Lactococcus lactis* subsp. *cremoris* Wg2-specific promoters. Applied Environmental Microbiology 53:2452–2457.
- Vendeville, A., Larivière D., and Fourmentin E., (2011) An inventory of the bacterial macromolecular components and their spatial organization. FEMS Microbiology Reviews 35(2): p. 395-414.

- Yeates, T. O., Crowley, C. S., Tanaka, S. (2010). Bacterial Microcompartment Organelles: Protein Shell Structure and Evolution. Annual Review of Biophysics 39:185–205.
- Zhan Y., Xu Q., Yang M., Yang H., Liu H., Wang Y., Guo J. (2011) Screening of freeze-dried protective agents for the formulation of biocontrol strains, *Bacillus cereus* AR156, *Burkholderia vietnamiensis* B418 and *Pantoea agglomerans* 2Re40. Letters in Applied Microbiology 54:10-17
- Zhou, H.X., Rivas, G., Minton, A.P., (2008) Macromolecular Crowding and Confinement: Biochemical, Biophysical, and Potential Physiological Consequences. Annual Review of Biophysics 37:375-397.

Chapter III

Investigation into the use of a biological phosphate removal system *in vivo*.

Contents

3.0. Abstract

3.1. Introduction

3.2. Materials & Methods

3.2.1. Experimental Design

3.2.1.1. Strains and culture media

3.2.1.2. Trial diet

3.2.1.3. Group design

3.2.1.4. Pilot Feeding Trial

3.2.2. Preparation and dosage of lyophilized bacteria

3.2.2.1.Bacterial dosage

3.2.2.2. Delivery of bacterial dosage

3.2.2.3. Faecal and water sampling for inoculated bacteria

3.2.2.4. Faecal and water sampling for mineral content

3.2.3. Vascular study and analysis

3.2.3.1. Bloodwork and analysis

3.2.3.2. Tissue preparation

3.2.3.3. Tissue analysis

3.2.3.4. Faecal analysis

3.3 Results & Discussion

3.3.1 Pilot feeding trial

3.3.2. Large-scale trial

3.3.3. Water analysis

3.3.3.1. Water uptake rates

3.3.4. Delivery & Survival Analysis

3.3.4.1. Water survival rates

3.3.4.2. Faecal survival rates

3.3.4.3. Intestinal colonization results

3.3.5. Tissue & Faecal Analysis

3.3.5.1. Faecal mineral analysis

3.3.5.2. Tissue mineral analysis

3.3.6. Statistical Analysis of bloodwork

3.4. Conclusion

3.5. References

3.0. Abstract

The usage of bacteria or probiotics to treat clinical illness is not a new avenue in medicine (Li *et al.,* 2014; Medina *et al.,* 2010). In recent years there has been an increase in the application of probiotics as delivery vehicles for clinical purposes **(**Reid, 2008; Solanki *et al,* 2013). Utilisation of probiotics in this fashion could enable reduction in the required dose of conventional therapeutics, which could be of benefit to patients. (Tomasello, 2008).

The bacterial microcompartment (MCP) has displayed efficacy in providing an enclosed space for chemical or enzymatic retention e.g. the role of the Pdu microcompartment in the reactive process of 1,2-propanediol metabolism. This principle of action, with an associated enzyme targeting system formed the basis for a strategy concerning its use as a novel biological phosphorus removal system utilizing recombinant polyphosphate kinase and empty recombinant microcompartments.

Previous observations (Chapter II) indicated increased phosphate uptake and polyphosphate retention by *E. coli* over expressing *E. coli* microcompartment-targeted *ppk* and a recombinant empty microcompartment, and to a lesser extent by *E. coli* over-expressing *E.coli ppk* alone, and *L. reuteri* expressing *E.coli ppk* alone. The purpose of this study was, firstly, to devise a method to deliver doses of viable recombinant bacteria to the gastrointestinal tract of an experimental animal, sufficient to take up at least half of the phosphate which would normally be absorbed. Secondly the efficacy of these delivered constructs in alleviating hyperphosphataemia in a rat model of chronic renal failure (CRF) and hyperphosphataemia (elevated blood phosphate) was tested. Oral phosphate

absorbing compounds have shown efficacy in such models. Over this period, the experimental groups received a bacterial supplement, which contained the experimental constructs.

Two bacterial strains were used for this study; *Lactobacillus reuteri* DSM 20016 and *E. coli* MG1655, based on Chapter II observations.

Gluconate water was demonstrated to be a suitable re-vitalization agent for lyophilized *E. coli* and *L. reuteri,* which both demonstrated the same levels of phosphate-uptake efficacy post-lyophilisation as they had done pre-lyophilsation. The strains were also successfully delivered to the animal models through the supplementation of gluconate water, and were also recoverable from faeces and intestinal contents. However, confounding factors regarding the baseline blood mineral content of the trial groups led to difficulties in attributing a direct linkage between the bacterial intervention and changes in blood calcium and phosphate, and tissue calcium and phosphate levels.

3.1. Introduction

Hyperphosphataemia is an accumulation of excess levels of the mineral phosphate within the body, and is typically associated with end-stage renal disease (ESRD) (See Chapter 1A). Progressive deterioration of kidney function leads to an inability of the kidneys to excrete phosphate, which in turn can lead to consequential symptoms such as secondary hyperparathyroidism, renal bone disease, and vascular calcification (Guo *et al,* 2013). Typical management of hyperphosphataemia involves dietary intervention and increased medication, which can lead to a decrease in quality of patient life (Albaaj & Hutchison, 2003).

As discussed in Chapter 1A, mammalian phosphate absorption from the diet occurs primarily in the small intestine. Medical interventions in hyperphosphataemia include dietary limitation of phosphate and a variety of different phosphate absorbing materials taken by mouth. Renal failure reduces phosphorus excretion in urine. The normal renal excretion is estimated as 800 mg phosphorus per day (Bleyer *et al.,* 2003), faecal excretion in renal failure taking oral binding agents is about 400 mg phosphorus/day (Sedlacek *et al.,* 2000).

Different animal models have been used to study the efficacy of oral binding agents in renal failure. The commonest non-surgical model of renal failure is through the use of dietary adenine in rats (McCabe *et al.,* 2013); (Neven *et al.,* 2009); (Lacour *et al.,* 2005). Considering the rat model, daily phosphate uptake in a normal rat diet is 1.3 mmoles phosphate (Berndt *et al.,* 2007) approximately 50% of which is absorbed. A target of 625 μmoles phosphate binding per day per rat in a renal failure intervention would therefore be appropriate.

The microcompartment enhanced biological phosphorus removal (MEBPR), system, which involves expression of a phosphate polymerising enzyme (*ppk*) within a MCP inside a bacterium (Chapter 2), offers a potential method of therapy to alleviate this accumulation of phosphate (Hall *et al.,* 2010). By providing an intracellular space for increased polyphosphate storage in a bacterial cell, it was hypothesized that increased uptake of phosphate and retention of polyphosphate by the cell could be achieved. Following on from this, this chapter tested the hypotheses that phosphate retaining bacteria could be delivered in sufficient numbers to the gut that phosphate uptake by the host could be affected, and that this would counteract phosphate retention associated with renal failure.

In this thesis (Chapter II) a number of constructs were created to evaluate the first hypothesis *in vitro*. I observed increased phosphate uptake and polyphosphate retention via the use of the recombinant *E. coli ppk,* and in particular, the 2 plasmid *E. coli ppk-pduABJKNU* construct and *L. reuteri* expressing *E. coli ppk*. Based on the positive results observed *in vitro* and in order to explore the hypothesis further, a murine study was designed to test the constructs *in vivo.*

The optimal constructs were selected from the previous study for *in vivo* studies; these include the aforementioned *E. coli ppk, E. coli ppk-pduABJKNU* (microcompartment) construct and *L. reuteri* expressing *E. coli ppk*. A short pilot study described below was performed prior to the large-scale trial to optimize delivery of the bacteria to the animals, and to observe the survival of the bacteria in a murine host. Due to observations from this trial, it was decided to utilize two

constructs in an *E. coli* strain (*E. coli ppk* and *E. coli ppk-pduABJKNU*) because these were recovered in higher numbers from the murine intestine than *L. reuteri* 20016. A final experimental construct, *L. reuteri* 20016 *expressing E. coli ppk,* was selected

For the purposes of an *in vivo* murine trial, four groups were therefore devised, with three experimental groups and one negative control group. All of the groups would receive an adenine-rich diet, initiating chronic renal failure (CRF) in all groups. The experimental groups would receive a lyophilized bacterial inoculate via their drinking water for a duration of five weeks, after which all groups would be culled and their internal vasculature and organs analyzed. Plasma was taken at set intervals during the trial to monitor renal activity, via fluctuations of phosphorus, calcium and creatinine levels. The strain of rat chosen was Sprague-Dawley, because these had been used for at least three published trials looking at phosphate levels in an adenine induced renal failure model (Shobeiri *et al.,* 2013); (McCabe *et al.,* 2013); (Price *et al.,* 2006).

This work was done under the license of Professor Edward Johns, Emeritus Professor of Physiology, University College Cork, who has previously utilized the rat model for kidney disease observation. His postgraduate student Elaine Barry also collaborated on this work and provided guidance regarding animal handling protocols and dietary feed.

3.2. Methods & Materials

3.2.1. Experimental Design

Experimental procedures were approved by the University College Cork Ethics Committee and carried out under animal licence B/100/3260 held by Professor Edward Johns in accord with EU Directive 86/609/EC. 14-week-old male Sprague Dawley rats (Harlan Laboratories, UK) were used for the experimental trial based on previous literature on renal failure models using 0.25% adenine (McCabe *et al,* 2013); (Lacour *et al,* 2005). Statistical analysis was with SPSS (IBM).

In order to calculate an appropriate sample size, the size requirement for continuous variables such as serum phosphorus is based on the t-test derived formula (Institute for Laboratory Animal Research, 2003):

$$n = 1 + 2C\left(\frac{s}{d}\right)^2$$

Where n= sample size required, s = standard deviation of observation, d = difference to be detected, C is a constant which for power (1-ß) of 90% and a significance level (a) of 5% is 10.51.

Using published lanthanum study data (Neven *et al.,* 2009), where the renal failure group serum phosphorus was 12.07 mg/dl SD +/-3.44 and the treatment group 8.32 mg/dl. To detect a reduction of 3.75 mg/dl in phosphate in a treatment groups compared with a control (this was the reduction seen at 5 weeks with 2% lanthanum treatment) with a power of 90% and a significance level of 5%, $1 + 21(3.44/3.75)^2 = 18.67$ subjects would be required. On this basis, a planned

sample size of 20 per test group to allow for incidental mortality, with 10 in the normal diet control group this makes 70 animals.

3.2.1.1 Strains and culture media

Bacterial strains utilised in this study are listed in Table 3.1.

Strain	Plasmid	Origin	Reference
Lactobacillus reuteri DSM20016	None	National Collection of Dairy Organisms, Reading, UK	Sriramulu *et al.,* 2010
E. coli BL21	*pAR3114 (pduABJKNU+ppk)*	Dr. Joshua Parsons, University of Kent	Parsons *et al.,* 2008
E. coli BL21	*pKMC106 (ppk)*	Dr. Mingzhi Liang, University College Cork	This thesis
Lactobacillus reuteri DSM20016	*pKMC004 (ppk)*	Author	This thesis

Table 3.1. *Table indicating strains used.*

Escherichia coli was routinely cultured in Luria-Bertani (LB) broth (Merck, Darmstadt, Germany) at 37°C. *Lactobacillus reuteri* was routinely cultured in de Man-Rogosa-Sharpe (MRS) broth (Merck, Darmstadt, Germany) in static anaerobic conditions at 37°C.

For minimal growth conditions, *E. coli* was cultured in 1X MOPS minimal media (Neidhardt *et al.,* 1974) supplemented with K_2HPO_4 and glucose (Sigma Aldrich), whilst *L. reuteri* was cultured in Minimal Lactobacillus Media (Hebert *et al.,* 2004) which was a formation of essential amino acids supplemented with glucose, sodium acetate, K_2HPO_4 and $MgSO_4$ (Sigma Aldrich). Breakdown of media composition is indicated below.

Material	Quantity
Tryptone from casein	10g/L
Sodium chloride	10g/L
Granulated Yeast Extract	5g/L
Deionized Water	1L

Table 3.2. *Recipe for Luria Broth (LB) for the growth of E. coli*

Material	Quantity
MRS broth	55g/L
Deionized Water	1L

Table 3.3. *Recipe for de Man-Rogosa-Sharpe (MRS) for the growth of lactobacilli*

Material	Quantity
Bacto-peptone	5g/L
Lab-Lemco	4g/L
Granulated Yeast Extract	2g/L
Tween 80	0.5mL/L
K_2HPO_4	1g/L
$NaH_2PO_4.H_2O$	3g/L
CH_3COONa	0.6g/L
$MgSO_4.7H_2O$	0.3g/L
$MnSO_4.H_2O$	0.04g/L
**** Supplemented with 40mM 1,2-propanediol and 200nM B12 to induce the pdu microcompartment***	

Table 3.4. *Recipe for MRS-Modified (MRS-MOD) for the growth of L. reuteri*

Material	Quantity
MOPS	83.72g/L
Tricine	7.17g/L
0.01M $FeSO_4$.H20	10mL/L
1.9M NH_4Cl,	50mL/L
0.276M K_2SO_4	10mL/L
0.02M $CaCl_2$-2H_2O	0.25mL/L
2.5M $MgCL_2$	2.1mL/L
5M NaCl	20mL/L
Micronutrient stock	0.2mL/L

Table 3.5. *Recipe for 10X MOPS minimal media.*

Material	Quantity
10X MOPS	50mL/L
Glucose	10g/L
1M K_2HPO_4	10mL/L
Thiamine	5*u*L/L

Table 3.6. *Recipe for 1X MOPS minimal media.*

Materia	Quantity
Glucose	10g/L
Sodium acetate	5g/L
K_2HPO_4	3g/L
$MgSO_4.7H_20$	0.2g/L
L-Alanine	0.10g/L
L-Arginine	0.10g/L
L-Aspartic Acid	0.20g/L
L-Cysteine	0.20g/L
L-Glutamic Acid	0.20g/L
L-Histidine	0.10g/L
L-Isoleucine	0.10g/L
L-Leucine	0.10g/L
L-Lysine	0.10g/L
L-Methionine	0.10g/L
L-Phenylalanine	0.10g/L
L-Serine	0.10g/L
L-Tryptophan	0.10g/L
L-Tyrosine	0.10g/L
L-Valine	0.001g/L
Nicotinic acid	0.001g/L
Pantothetic acid	0.001g/L
Pyridoxal	0.002g/L
Riboflavin	0.001g/L
Cyanocobalamin	0.001g/L
Adenine	0.01g/L
Guanine	0.01g/L

Table 3.7. *Recipe for Minimal Lactobacillus Medium (MLM) for the growth of lactobacilli.*

As previously discussed in Chapter II, strains were lyophilized *(Section 3.1.2, Chapter II)* and revitalized using gluconate supplemented water.

Compound	Concentration of solution	Reference
SodiumGluconate	20g in 1L (2%)	Jones *et al.,* 2008
(MW 196.16)	8g in 1L (0.8%)	

Table 3.8: *Table illustrating the chosen carbon sources.*

3.2.1.2. Trial diet

An initial order was made for adenine supplemented purified diet via Harlan Laboratories (Madison, Wisconsin, USA) who are leading providers of adenine-supplemented diets for previously published renal failure studies. (Price *et al.,* 2006); (McCabe *et al.,* 2013); (Diwan *et al.,* 2013).

In March 2014, after the order had been accepted, practical difficulties with shipping the diet became apparent because of enforcement for the first time of legislation requiring an individual import licence arranged by the researcher for every shipment of animal feed from outside the EU from the Irish Department of Agriculture Food and the Marine. In practice this blocked all experimental diet imports from the USA for animal research in Ireland until resolved several months later for rodent diets on a University-wide basis. At this point the experimental animals had been ordered and the cages reserved in the animal facility. The only possibility to obtain the diets in the time frame required was to re-order from a company with a UK manufacturing plant (TestDiet Europe, IPS Product Supplies Ltd, London), but a 6 week delay ensued and in addition a quantitative error, which led to a shortfall in delivered diet, further delayed the start of the trial.

This created a knock-on effect, as the initial animal groups (1 and 2) had begun receiving their adenine diet in a staggered fashion. To avoid disruption to groups which had already begun the trial, Group 4 did not begin their trial until

additional diet had arrived, meaning that they were 18 days older than the other group rats by the trial start date. The rats received a high-adenine diet [0.5% adenine, 1% phosphorus, 1.39% calcium] (TestDiet, UK) for 3 weeks to induce CRF. The use of an adenine-rich diet has been previously utilized in literature to induce CRF (Neven *et al,* 2009). For this study, the adenine dosage was delivered in a gradient amount *(Table 3.9)* decreasing over the period of the trial.

Diet ingredients	Duration of Feed
0.5% adenine **1% phosphorous** **1.39% calcium**	Initial 3 weeks to initiate chronic renal failure (CRF)
0.3% adenine **1% phosphorous** **1.39% calcium**	Additional 3 weeks after confirmed CRF – coincides with beginning of bacterial dosage
0.15% adenine **1% phosphorous** **1.39% calcium**	Final 2.5 weeks of trial – continued bacterial dosage

Table 3.9. *Trial diet composition and dosage schedule*

After the initial three weeks after 0.5% diet, the animals were changed to a lower dosage adenine diet [0.3% adenine, 1% phosphorus, 1.39% calcium], and after an additional three weeks, the animals received an even lower dosage adenine diet [0.15% adenine, 1% phosphorus, 1.39% calcium], *(Figure 3.1)*. The reason for the decreasing adenine percentage diets was to maintain CRF but avoid undue mortality in the animals.

The bacterial intervention consisted of a lyophilized bacterial dosage, which was added to 2% gluconate drinking water at the beginning of the 0.3% diet for the experimental groups (ii, iii and iv). This would be given on a daily basis via the drinking water supply for a period of 5 weeks. Each of the experimental groups would receive 1 of 3 bacterial constructs that were previously assessed *in vitro* in studies from Chapter II. Gluconate was selected as carbon source based upon a

previous study evaluating the most stable sugar source for revitalizing the lyophilized cultures (Chapter II).

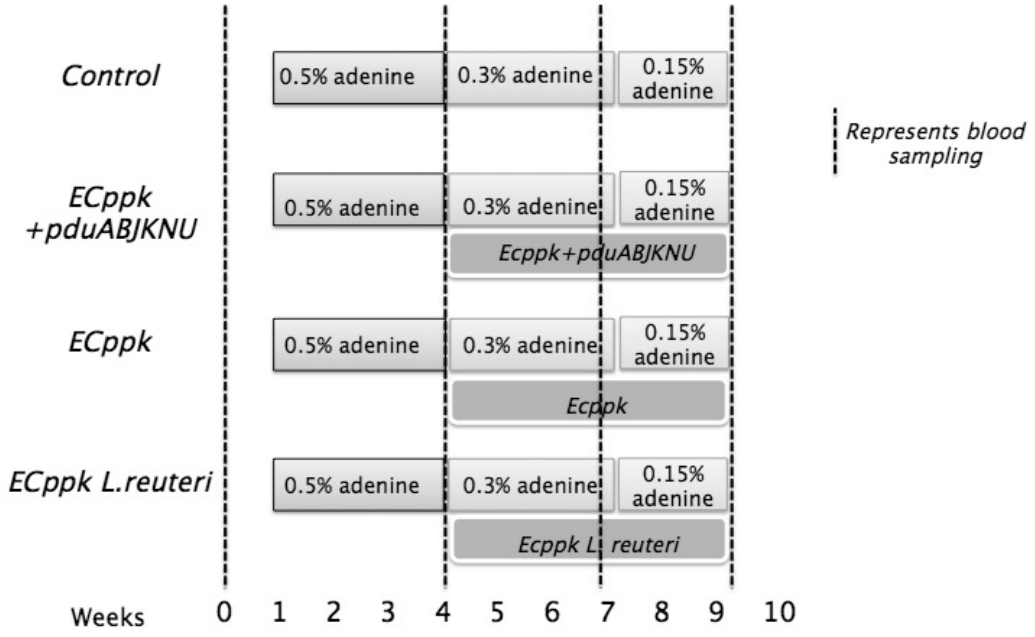


Figure 3.1. *Diagram illustrating the schedule for diet treatment and blood sampling.*

3.2.1.3. Group design

As previously mentioned, there were 4 groups in total, each group containing 20 animals (see power calculation above). These groups consisted of Group 1: a control set receiving no specific bacterial intervention, but receiving gluconate water, Group 2: a set receiving *E. coli ppk+pduABJKNU* expressed in *E. coli* BL21 Group 3: a set receiving *E. coli ppk* expressed in *E. coli* BL21 and Group 4: a set receiving *E. coli ppk* expressed in *L. reuteri* DSM20016. These strains were shown to survive in rats (culturable from faecal pellets following oral consumption) in the Pilot study.

Within each group, there were 4 cages, each containing 5 animals. Each animal was colour-coded and physically marked for identification purposes. In each cage, there were 2 drinking bottles and one communal feeding trough. Each animal was weighed on a weekly basis.

3.2.1.4. Pilot Feeding Study

In order to establish the viability of delivering the bacterial intervention to the animals via a water source, a pilot feeding study was undertaken. This was done over a 7 day period, and utilizing 8 rats. These rats were all Sprague-Dawley rats, but were considerably older than intended for the actual trial (these were surplus animals from the BSU).

From the total of 8 rats, 7 animals received a bacterial dosage, whilst 1 did not. This bacterial dosage of between approximately 0.4-0.5g lyophilised bacteria was delivered over 3 days to 600mLs of 0.8% glucose water, followed by 4 days of glucose water only.

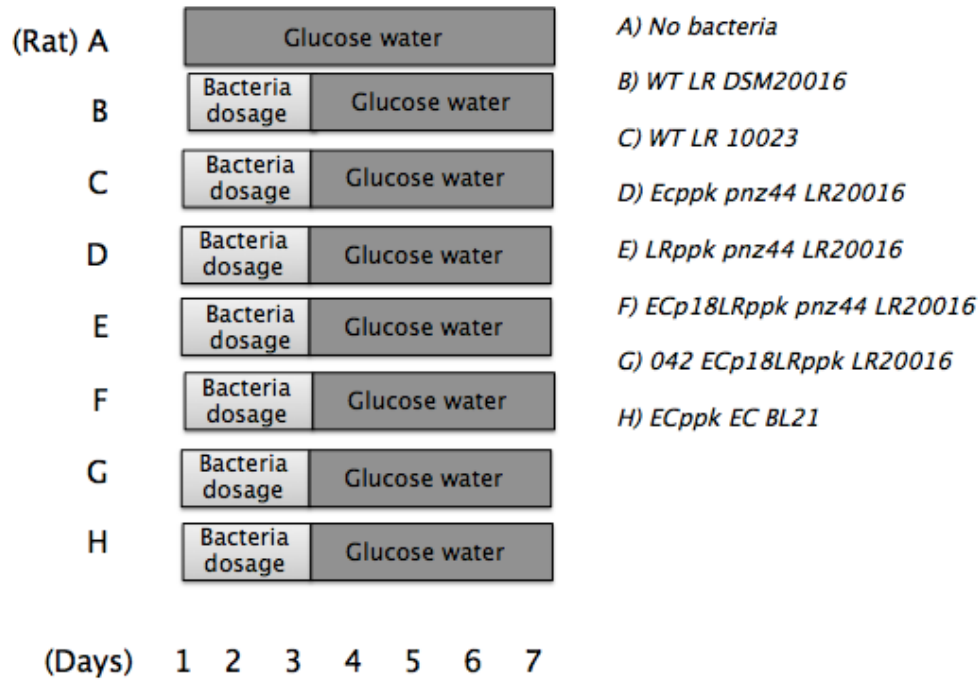


Figure 3.2. *Diagram illustrating the schedule for pilot trial*

1mL water sample was taken from each bottle after addition of bacterial dosage, for subsequent viability count plating. This would allow determination of bacterial survival numbers. Faecal pellets were also collected from each animal to observe successful passage through the animal or indeed potential

colonization. The findings from this pilot trial informed the strains and delivery system utilized for the large-scale trial.

3.2.2. Dosage of lyophilized bacteria

Details of the growth conditions and preparation of the lyophilized bacteria can be read in Chapter II, section 3.1.5 (Materials & Methods). Based upon previous study (Chapter II) bacteria were lyophilized during entry into stationary phase (OD600nm ~0.7) and were weighed prior to lyophilization and again afterwards. As these plasmids can be unstable, in order to ensure that the correct plasmid was present in each strain, multiple repeat cultures were created to avoid over passaging any one original culture. All samples were plated on selective antibiotic agar to confirm presence of plasmid before use and subjected to neisser staining to observe phosphate uptake ability.

3.2.2.1.Bacterial dosage

For rats, daily phosphate uptake is 1.3 mmoles phosphate (Berndt *et al.,* 2007), approximately 50% of which is absorbed, making a requirement of up to 625 µmoles phosphate binding per day in renal failure. An estimate from *in vitro* bacterial growth over 12 hours in vitro found the capacity of the best *E. coli* ppk-pduABJKNU clone 16 µmoles phosphate/mg protein (Prentice, Liang unpublished) suggested 39 mg of final growth of *E. coli* bacterial protein was required to achieve 625 µmoles phosphate uptake corresponding to approximately 98 mg dry weight bacteria. Rat water intake is 10-12 mL/100g (Harkness & Wagner, 1989) or @ 50 mL per day for male rats and this could be achieved with 2 mg/ml bacterial protein in water intake.

Estimates based on shorter-term uptake from high bacterial loads in gluconate water (Chapter II) gave comparable results as follows. An inoculum of 0.0.2 g lyophilised *E. coli* ppk-pduABJKNU clone was able to uptake 0.41 millimoles phosphate from 100mL over a 5-hour period. Likewise, 0.018g lyophilised *E. coli ppk expressed in L. reuteri* took up 0.7 millimoles phosphate over a 5 hour period (*Figure 4.21, Chapter II).*

Using this information, and assuming a baseline population of 1.6e8 bacteria per 100mL resuspended (based upon viability plate counting) this would require a 3.05e+08 bacteria would be required to uptake 0.65mM of phosphate.

Based upon pilot feeding trial data and viability counts, the rats would need to intake a minimum of 18mL per day to achieve a sufficient bacterial intake, which is within the standard average water intake for a rat (John Hopkins University, Animal Care & Usage guidelines).

As such, for the large-scale trial, a daily pellet of approximately 1.5-2g was delivered through cage bottles. The pellet was resuspended initially in 50mL gluconate water, and then transferred to the cage bottle (which typically totaled approximately 1L).

3.2.2.2. Delivery of bacterial dosage

As previously mentioned, the experimental bacterial constructs were delivered to the animals via their drinking water supply. This option was selected due to the constraints of gavaging 80 animals daily and consistently. By supplying the constructs through the water supply and through consistent monitoring of bacterial viability and passage, a baseline level of successful dosage can be deduced.

As mentioned, the bacterial constructs were lyophilized and maintained at 4°C. Each morning, at a consistent time, each water bottle was weighed and noted to monitor water uptake. As there were two bottles per cage, these were totaled together to represent the cage as a whole. The lyophilized pellets, which averaged a weight of between 1.5-2g were resuspended in 50mL 2% sodium gluconate before being added to each individual water bottle (totaling approximately 1L) and once again weighed and noted. This allowed a daily measurement of approximate water uptake, and bacterial uptake.

Twice a week, samples of animal faeces from each cage were collected and plated on selective antibiotic agar to identify successful passage of the bacterial constructs.

Experimentation on delivery of the bacterial solution via the dry feed was tried, but proved unsuccessful due to hard, dry nature of the diet pellets. Soaking them in water supplemented with bacterial cultures led to the pellets become excessively soft (likely unappealing to the animals) and also returned very low bacterial counts on plate culture.

3.2.2.3. Faecal and water sampling for inoculated bacteria

Water samples were obtained from the individual water bottles daily, and serially diluted using Ringers solution. Samples were plated on appropriate antibiotic selective agar, with colonies typically enumerated at 10^{-4} and 10^{-5}. This was to ensure survival and viability of the bacterial in the drinking water.

Faeces were also sampled twice weekly. 1g of homogenized faeces was added to 10mL Ringers solution. The solution was homogenized using a Stomacher 400C (Seward) and 100µl was taken for serial dilution. Dilutions were then plated on

antibiotic selective agar (*E. coli ppk+pduABJKNU* and *E. coli ppk* both display ampicillin 100 mg/ml resistance, whilst *E. coli ppk* expressed in *L. reuteri* displays chloroamphenicol 10 mg/ml resistance). Monitoring the passage of the culture through the faeces allowed the deduction of successful delivery and passage of the bacteria through the animals.

3.2.2.4. Faecal and water sampling for mineral content

Water samples were obtained daily from cage water bottles to confirm the survival of the bacteria in the bottles. 1mL sample was removed approximately 15 minutes after inoculation of bacterial culture, and serially diluted in the lab for plate culture within 3 hours of sample being obtained. Samples were then plated to a dilution factor of 10^{-6}.

In order to measure mineral content (phosphate and calcium) in faeces, samples of faeces were collected on a weekly basis. 1g of faeces was retained and stored at 4°C. However due to issues regarding collection access, inadequate faecal samples for Group 1 and Group 2 were obtained for mineral analysis. Information on mineral analysis can be found in Section 3.1.3.4.

3.2.3. Vascular study and analysis

3.2.3.1. Bloodwork and analysis

Standard tail vein bleeds were obtained at i) the beginning of trial ii) at the end of 0.5% adenine diet/confirmation of CRF iii) mid-way through bacterial intervention and iv) before sacrifice of the animal. Animals were sedated using isofluorine and blood obtained from the tail vein using 1mL syringes (BD plastipak #300013) and 25G needles (BD Microlance #300600). These bleeds

were performed by Elaine Barry from the Department of Physiology, University College Cork. Samples were then sent to the School of Veterinary Pathology, University College Dublin, for plasma serum analysis of phosphorus, creatinine and calcium levels.

At the end of the trial, the groups were sacrificed by cervical dislocation and the major organs, including major circulatory vessels, were obtained for further biochemical and microbiological analysis.

3.2.3.2. Tissue preparation

Tissue samples were obtained at sacrifice. A selection of tissue samples (aortic arch, right carotid, right femoral) were fixed in neutral formalin and cut into 2–3 mm thick rings that were embedded upright in the same paraffin block. This meant that every section contained, on average, 16 cross sections for the aortic arch and 5 cross sections for the carotid and femoral arteries at different sites along the vessel. Selections of μm sections were stained with Von Kossa staining method (Sheehan & Hrapchak, 1980), (Crookham & Dapson, 1991). This staining method utilizes 5% silver nitrate, followed by exposure to bright light for 1 hour, which will cause reduction of calcium present. The silver nitrate will deposit in place of the calcium, allowing visualization of metallic silver sports. Vascular calcifications were then evaluated histomorphometrically with image analysis software at magnification 100×. The absolute areas of tissue and calcified tissue were summed for each animal, and the ratio was expressed as area% calcification. This work was undertaken by Helen McCarthy and Dr. Amr Mahmoud, Department of Pathology, University College Cork.

The small intestine was also harvested on sacrifice, where it was weighted and stored in 10mL Ringers solution. Samples were then homogenized, with 1mL removed for serial dilution in Ringers solution. Dilutions were plated on antibiotic selective agar (ampicillin 100 mg/ml and chloramphenicol 10 mg/ml) to observe if the bacterial constructs had colonized the small intestine. The kidneys were also weighed and recorded on sacrifice.

3.2.3.3. Tissue analysis

Additional vascular vessels (thoracic aorta, abdominal aorta, renal artery, and carotid artery) were weighed and snap-frozen on collection. They were then thawed and homogenized in 0.6 N hydrochloric acid (HCl) for 24 h at 60°C. The samples were spun and the calcium content was determined colorimetrically using an O-cresolphthalein complexone assay kit (Cayman Chemicals #700550).

This assay kit is based upon the principal of the main reagent, O-cresolphthalein forming a purple complex with calcium in samples, with resulting absorbance measured at 540nm (Microplate reader XS Spectrophotometer, Biotek). Samples were homogenized in Phosphate Buffered Solution (PBS) (pH7.4) and centrifuged at 10,000g for 15 minutes at 4°C (Beckman Coulter, rotor JA 25.50). The supernatant was removed, with 10µl of sample placed in test wells, along with 100µl of the detector agent provided by the kit. Samples were incubated for 5 minutes, with absorbance read at 570nm.

The tissue was also used to measure phosphate levels using ammonium molybdovanadate. Samples were initially acid digested with hydrochloric acid, which allowed orthophosphate to be converted to total phosphate (Biologic *et al,* 1967). A solution of 5mL malachite green (0.122%), 3.4mL ammonium

molybdate and 0.2mL Tween 20 was prepared fresh and are added to the samples, and measured at 430nm by spectrophotometry (Heresztyn & Nicholson, 2001), (McCabe *et al,* 2013).

3.2.3.4. Faecal analysis

Faeces samples were also analyzed for phosphate and calcium content, utilizing the O-cresolphthalein complexone assay kit and ammonium molybdovanadate method. However for faecal samples, specimens were divided, with 1 set being ashed in a muffle furnace, and the second set being resuspened as faecal water. This was done in order to obtain the most accurate mineral content (soluble phosphate measurements via faecal water and total phosphate via ashed faeces).

As mentioned, ashing of faeces was done using a muffle furnace oven, and with guidance from Dr. Therese Uniacke, Food Science, University College Cork. Samples were weighed prior to oven treatment (1g maximum) and dry ashed for 8 hours at 550°C. Phosphate was then measured with resuspension in hydrochloric acid.

Faecal water was prepared for analysis by resuspending lyophilized faeces to 25% of its dry weight (to mimic the natural colon conditions). After homogenization, samples were incubated for 1 hour at 37°C, followed by centrifugation at 15,000g for 10 minutes (Govers & Van der Meer, 1993). 10 ul of sample was then removed for assay testing.

3.3. Results & Discussion

3.3.1. Pilot Feeding Trial

As mentioned, an initial pilot trial was undertaken to observe the A) delivery system for the bacterial intervention and B) the success passage of the bacterial strains. This pilot trial provided important information regarding both, ultimately influencing the delivery and strain selection of the main trial. Beyond Day 1, none of the constructs expressed in *Lactobacillus* strains survived in the water source supplemented by glucose after inoculation, with only the *E. coli-ppk* construct, expressed in *E. coli BL21* surviving with counts of $7.0x10^5$ for up to three days. This was a notable result, with the lack of prolonged viability in *Lactobacillus* most possibly due to its more fastidious nature versus *E. coli* (Farnworth, 2008). The water sources and bottles utilized were tested for potential contamination with detergent or other bactericidal substances however no adverse factor was identified.

On Day 1, viable counts were obtained from faecal samples for all strains, however the numbers were extremely low (170 cfu/mL from undiluted cultures). Beyond Day 1, no *Lactobacillus* strains were reobtained from faecal cultures, whilst *E. coli-ppk* was only obtained from undiluted samples.

The results of the pilot study greatly influenced the ultimate delivery and design of the large-scale trial, with the difficulties in ensuring *Lactobacillus* survival and recovery leading to a higher proportion of *E. coli* strains being used for the larger-scale trial, with one *Lactobacillus* strain ultimately used.

Based upon the findings and difficulties encountered with this pilot trial, a number of quality control factors were introduced, to ensure strain delivery and viability and removal of adverse factors. These included use of a different carbon source in drinking water not accessible to the host (Chapter 2), a segregated animal housing room, serviced only by the author and Ms. Barry, the strict use of deionized water (no water of other origin), fresh preparation and delivery of lyophilized bacteria daily and sterile washing of dedicated plastic drinking bottles. A decision was also made to deliver an inoculum of the bacteria on a daily basis, as the pilot trial supported the viability of cultures for a 24 hour period, with problems appearing beyond Day 1. To ensure this did not continue to be an obstacle, each group received a daily dose of the bacterial supplement.

3.3.2. Large-scale trial

The mortality in this study was minimal. One animal of the experimental Group 2 (*E. coli ppk+pduABJKNU)* died 3 weeks after CRF induction, and one animal of the experimental Group 4 (*E. coli ppk L. reuteri)* died the day before sacrifice.

(grams)	Wk 1	Wk 2	Wk 3	Wk 4	Wk 5	Wk 6	Wk 7	Wk 8	Pre-sac
Group 1	321.7	290.2	290.5	289.8	311.8	304.0	308.2	311.9	331.7
Group 2	343.9	300.3	301.5	306.8	314.4	319.0	319.0	311.1	329.1
Group 3	338.8	314.0	314.2	325.6	330.3	338.6	330.2	357.4	355.2
Group 4	367.0	323.6	333.7	332.5	326.4	326.5	316.4	332.3	336.3

Table 3.10. *Table indicating average group weight per week. Pre-sac indicates final weight before sacrifice. Group 1 = Control, Group 2 = E. coli ppk+pduABJKNU, Group 3 = E. coli ppk, Group 4 = E. coli ppk L. reuteri*

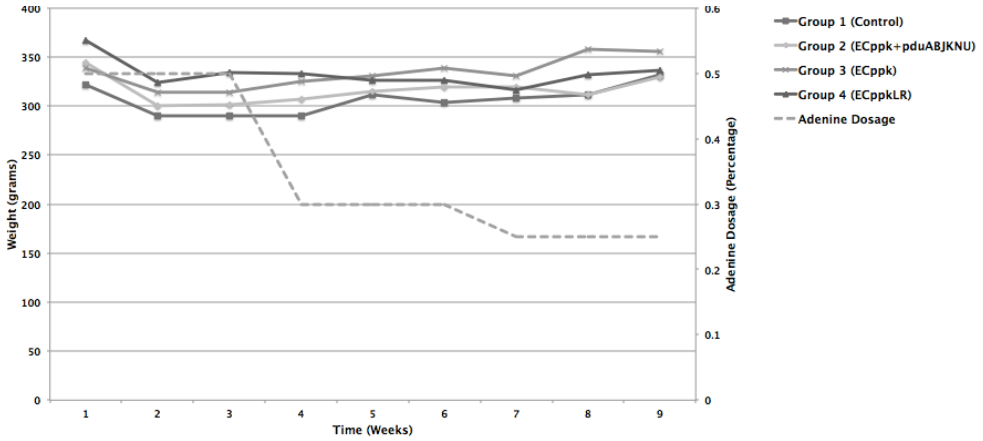


Figure 3.3. *Graph indicating average group weight per week (as in above table).*

Overall no extreme weight shifts can be observed. Across the duration of trial two groups gained weight; Group 1 (control) gained 10g of weight, whilst Group 3 (*E. coli ppk)* gained 16.4g of weight. The remaining two groups both lost weight; Group 2 (*E. coli ppk+pduABJKNU)* lost 14.8g and Group 4 (*E. coli ppk and E. coli ppk L. reuteri)* lost 30.7g. Within the groups themselves there was no clear indication of food dominance in the group *i.e.* all the animals appeared healthy in appearance and weight, with no clear dominant animal in the group.

3.3.3. Water Analysis

Water bottles were monitored daily to observe survival of bacterial dosage and also to allow calculation of daily water uptake per cage, and calculation of an approximate bacterial dosage intake.

3.3.3.1. Water uptake rates

Group 1 *(Control)*

(mLs)	Average intake per cage	Per rat per week	Per rat per day
Week 4	1686	337.2	48.17
Week 5	1772	354.4.	50.62
Week 6	2087	417.4	59.62
Week 7	3259	651.8	93.11
Week 8*	858	171.6	57.2

Table 3.11. *Table indicating water uptake breakdown. Table represents the 5 weeks after confirmed CRF. Week 8 values are smaller due to group sacrifice.*

Group 2 (*ECppk+pduABJKNU*

(mLs)	Average intake per cage	Per rat per week	Per rat per day
Week 4	1650	330	47.14
Week 5	1798	359.6	51.37
Week 6	1754	350.8	50.11
Week 7	1864	372.8	53.25
Week 8	1374	274.8	54.96

Table 3.12. *Table indicating water uptake breakdown. Table represents the 5 weeks after confirmed CRF.*

Group 3 *(ECppk)*

(mLs)	Average intake per cage	Per rat per week	Per rat per day
Week 4	1992	398.4	56.91
Week 5	2082	416.4	59.48
Week 6	2690	538	76.85
Week 7	2244	448.8	64.11
Week 8*	593	118.6	59.3

Table 3.13. *Table indicating water uptake breakdown. Table represents the 5 weeks after confirmed CRF. Week 8 values are smaller due to group sacrifice.*

Group 4

(ECppkLR)			
(mLs)	**Average intake per cage**	**Per rat per week**	**Per rat per day**
Week 4	1898	379.6	54.22
Week 5	2025	405	57.85
Week 6	2188	437.6	62.51
Week 7	2544	508.8	72.68
Week 8*	977	195.4	65.13

Table 3.14. *Table indicating water uptake breakdown. Table represents the 5 weeks after confirmed CRF.*

In all groups, water intake increased per week after confirmed renal failure. This was an expected effect, and illustrated the physiological effect resulting from the adenine rich diet and consequential renal failure.

3.3.4. Delivery & Survival Analysis

3.3.4.1. Water survival rates

	Week 4	**Week 5**	**Week 6**	**Week 7**	**Week 8**
Group 2 (*ECppk+pduABJKNU)*	$1.79x10^7$ cfu/Ml	$1.84x10^7$ cfu/mL	$1.93x10^7$ cfu/mL	$1.46x10^7$ cfu/mL	$1.39x10^7$ cfu/mL
Group 3 *(ECppk)*	$1.79x10^7$ cfu/Ml	$1.84x10^7$ cfu/mL	$1.93x10^7$ cfu/mL	$1.46x10^7$ cfu/mL	$1.39x10^7$ cfu/mL
Group 4 *(ECppkLR)*	$2.89x10^7$ cfu/Ml	$2.94x10^7$ cfu/mL	$2.76x10^7$ cfu/mL	$2.55x10^7$ cfu/mL	$2.54x10^7$ cfu/mL

Table 3.15. *Table indicating viability of bacterial samples in 2% gluconate water source. Values averaged from all cages within a group (4 cages per group). Samples were obtained after 15 minutes post inoculation and cultured within 3 hours.*

3.3.4.2. Faecal recovery rates of orally administered bacteria

	Week 4	**Week 5**	**Week 6**	**Week 7**	**Week 8**
Group 2 (*ECppk+pduABJKNU)*	$1.42x10^6$ cfu/mL	$1.79x10^6$ cfu/mL	$1.64x10^6$ cfu/mL	$1.35x10^6$ cfu/mL	$1.67x10^6$ cfu/mL
Group 3 *(ECppk)*	$1.65x10^6$ cfu/mL	$1.86x10^6$ cfu/mL	$1.12x10^6$ cfu/mL	$1.24x10^6$ cfu/mL	$1.43x10^6$ cfu/mL
Group 4 *(ECppkLR)*	$1.21x10^5$ cfu/mL	$1.34x10^5$ cfu/mL	$1.31x10^5$ cfu/mL	$1.45x10^5$ cfu/mL	$1.49x10^5$ cfu/mL

Table 3.16. *Table indicating viability of bacterial samples from faecal material. Values averaged from all cages within a group (4 cages per group).*

To ensure delivery of the bacterial dosage to the animals, daily 1mL water samples were obtained from the water bottles and serially diluted, with plating on selective antibiotic agar. These values were averaged per group in total, and also per week for tabulating results. Likewise, to identify if the bacterial dosage had been uptaken by the animals, faecal matter was collect twice weekly, and plated on selective antibiotic agar. Based on these results, we can observe that there is an approximate logarithmic difference between the bacterial population present in the water supply (Table 3.15), and that being recovered from the faeces (Table 3.16).

3.3.4.3. Intestinal colonization results

Average values	Small Bowel weight (g)	cfu/mL
Group 1 ***(Control)***	10.54	None of the experimental constructs were identified in the control bowel.
Group 2 **(*ECppk+pduABJKNU)***	10.99	$9.39x10^6$
Group 3 ***(ECppk)***	10.46	$7.29x10^6$
Group 4 ***(ECppkLR)***	9.27	$7.47x10^6$

Table 3.17. *Table illustrating the viability of bacterial intervention in the small intestine of the animals*

After sacrifice, the small intestines of the animals were harvested. Homogenizing and plating these on selective agar further demonstrated the successful delivery of the bacterial dosage from the inoculated water source. These results also indicated the colonization ability of the *E. coli* and *L. reuteri* hosts.

3.3.5. Tissue & Faecal Analysis

3.3.5.1. Faecal mineral analysis

[redacted]

mmol/L Calcium	Group 1 (Control)	Group 2 (ECppk+pduABJKNU)	Group 3 (ECppk)	Group 4 (ECppkLR)
Week 3 (Pre-intervention	N/A	N/A	N/A	7.35
Week 4 (Post-intervention	N/A	N/A	N/A	7.49
Week 5 (Post-intervention	N/A	7.61	7.28	7.86
Week 6 (Post-intervention	N/A	7.39	7.42	7.41
Week 7 (Post-intervention	7.64	7.39	7.56	7.50
Week 8 (Post-intervention	7.47	7.32	7.47	7.43
Week 9 (Post-interventio.n	7.40	7.44	7.31	7.28

Table 3.18. *Table illustrating the calcium content of faecal water. Due to scheduling issues, samples were unavailable pre-intervention for Groups 1-3. Values are in mmol/L.*

[redacted]

mmol/L Calcium	Group 1 (Control)	Group 2 (ECppk+pduABJKNU)	Group 3 (ECppk)	Group 4 (ECppkLR)
Week 3 (Pre-intervention	N/A	N/A	N/A	3.36
Week 4 (Post-intervention	N/A	N/A	8.62	3.79
Week 5 (Post-intervention	N/A	2.74	4.06	2.29
Week 6 (Post-intervention	N/A	3.86	2.66	2.97
Week 7 (Post-intervention	3.08	2.27	3.10	4.29
Week 8 (Post-intervention	2.85	2.82	3.05	3.04
Week 9 (Post-intervention	3.42	3.45	2.96	3.19

Table 3.19. *Table illustrating the calcium content of ashed faeces. Due to scheduling issues, samples were unavailable pre-intervention for Groups 1-3. Values are in mmol/L.*

uM/g Phosphate	Group 1 (Control)	Group 2 (ECppk+pduABJKNU)	Group 3 (ECppk)	Group 4 (ECppkLR)
Week 3 (Pre-intervention	N/A	N/A	N/A	909.62
Week 4 (Post-intervention	N/A	N/A	837.64	1107.99
Week 5 (Post-intervention	N/A	695.83	829.455	1018.93
Week 6 (Post-intervention	N/A	879.54	1052.89	1000.55
Week 7 (Post-intervention	992.27	1111.058	810.72	1154.96
Week 8 (Post-intervention	1132.78	1101.57	1004.76	1149.56
Week 9 (Post-intervention	1109.94	1141.56	842.97	967.95

Table 3.20. *Table illustrating the total phosphate content of ashed faeces from animals. Due to scheduling issues, samples were unavailable pre-intervention for Groups 1-3. Values are uM/g.*

Testing of the water source supplemented with the bacterial constructs indicated that the addition of bacteria to the water source did not cause any detectable effects regarding phosphate/calcium content *i.e.* it did not cause any influential increases to the phosphate/calcium levels of the faeces.

uM/L Phosphate	Group 1 (Control)	Group 2 (ECppk+pduABJKNU)	Group 3 (ECppk)	Group 4 (ECppkLR
On addition to water	0.072	120.56	126.77	131.56

Table 3.21. *Table illustrating the phosphate content of the water plus bacterial addition.*

mmol/L Calcium	Group 1 (Control)	Group 2 (ECppk+pduABJKNU)	Group 3 (ECppk)	Group 4 (ECppkLR
On addition to water	0.084	0.554	0.453	0.284

Table 3.22. *Table illustrating the calcium content of the water plus bacterial addition.*

3.3.5.2. Tissue mineral analysis

mgCa/g	**Group 1 (Control)**	**Group 2 (ECppk+pduABJKNU)**	**Group 3 (ECppk)**	**Group 4 (ECppkLR)**
Femoral	9.63152291 SEM±1.33	13.27904431 SEM ±2.81	11.97732744 SEM ±2.76	6.949422867 SEM ±3.79
Carotid	13.63576929 SEM ±3.06	8.424012727 SEM ±3.74	5.148462475 SEM ±0.96	3.457396171 SEM ±0.89
Abdominal aorta	5.948847415 SEM ±1.80	3.809593197 SEM ±1.06	20.8411949 SEM ±4.08	2.849482631 SEM ±1.06

Table 3.23. *Table illustrating the calcium content of blood vessels.*

On comparing these findings against the published Lanthanum study (Neven *et al.,* 2009), some areas of similarity can be observed. The majority of the Neven samples appeared to test negative for the presence of calcium, however we discuss comparison against those positively testing for calcium.

For the femoral artery, for the Neven study, many of the calcium positive samples within the control (untreated) group fell between the 1.5-2.5g/g range, which is lower than our averaged finding of 9.6mg/g for our control. For the Neven experimental groups, the majority of calcium positive samples were more widely distributed but fell within a range of 1.5-3.5 mg/g, which again is lower than the levels identified in our experimental groups (between 13mg/g and 6.9mg/g).

For the carotid artery, for the Neven study, the calcium positive samples within the control (untreated) group fell between the 5-8mg/g range, which is lower than our averaged finding of 13.2 mg/g. For the Neven experimental groups, the majority of calcium positive samples were between 2-4mg/g, with outliers peaking at 8mg/g. This is comparable with our experimental groups, which fell, on average, within a range of 8.4 to 3.5mg/g.

For the aorta, for the Neven study, the calcium positive samples within the control (untreated) group fell between the 10-15mg/g range, which is slightly higher than our average of 5.9mg/g. For the experimental samples, the average range for the calcium positive samples is between 5-10mg/g, which is comparable to the results of Group 2 and Group 4 (Group 3 has a much higher value of 20.8mg/g).

Whilst it is unclear why the majority of our vessels appeared to show positive for calcium, this may be due to assay sensitivity versus the use of the flame atomic absorption spectroscope.

mM/g	**Group 1 (Control)**	**Group 2 (ECppk+pduABJKNU)**	**Group 3 (ECppk)**	**Group 4 (ECppkLR)**
Femoral	86.13616386 SEM±7.21	40.34270418 SEM ±2.95	73.38034142 SEM ±5.57	94.30335561 SEM ±10.65
Carotid	85.89774594 SEM ±14.08	86.73085369 SEM ±6.98	146.3664643 SEM ±14.39	115.7443526 SEM ±7.71
Abdominal aorta	88.02205976 SEM ±1.97	83.10479652 SEM ±6.65	76.93805125 SEM ±7.27	45.19701866 SEM ±5.61

Table 3.33. *Table illustrating the total phosphate content of blood vessels.*

It is difficult to compare phosphate tissue reading against other literature as many studies focus on serum phosphate level versus tissue phosphate. However on comparison against a previous renal failure study (McCabe *et al.,* 2013), it can be observed that our tissue samples appear to have higher phosphate levels present across the board.

Rat	Artery	# Artery sections sample	# Sections with calcifications	Average % Calcification to Wall Circumference in positive sections	Overall Average % Calcification to Wall Circumference in all sections sampled	Site of Calcifications in the artery	Other
B13	RC	5	1	34.8	7.2	Media	
C16	RF	4	1	1.5	0.66	Media	
D2	AA	20	20	20	20	Intima/Media	70% max
D2	RF	5	5	9.7	9.7	Intima	
D3	AA	15	9	6	3.2	Media	
D3	RF	4	4	8.2	8.2	Media	
D6	AA	18	18	22.9	22.9	Intima/Media	60%
D6	RC	5	5	19.2	19.2	Intima/Media	
D6	RF	4	1	2.8	1.02	Media	
D7	RF	4	4	9	9	Media	
D10	AA	11	2	30.9	9.8	Intima	
D10	RC	7	2	20.7	11.6	Media	
D18	RF	5	4	9.6	8.6	Media	

Table 3.34. *Table illustrating the calcification content of sectioned arterial samples.*

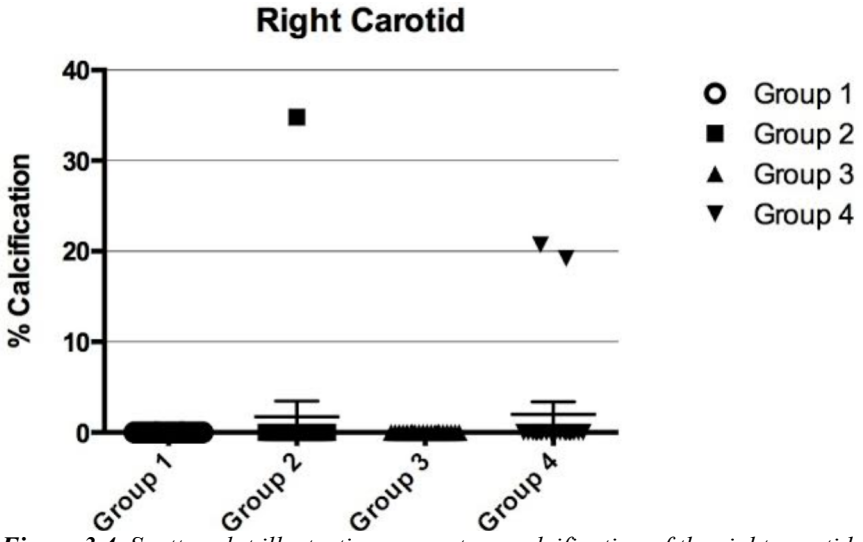


Figure 3.4. *Scatter plot illustrating percentage calcification of the right carotid.*

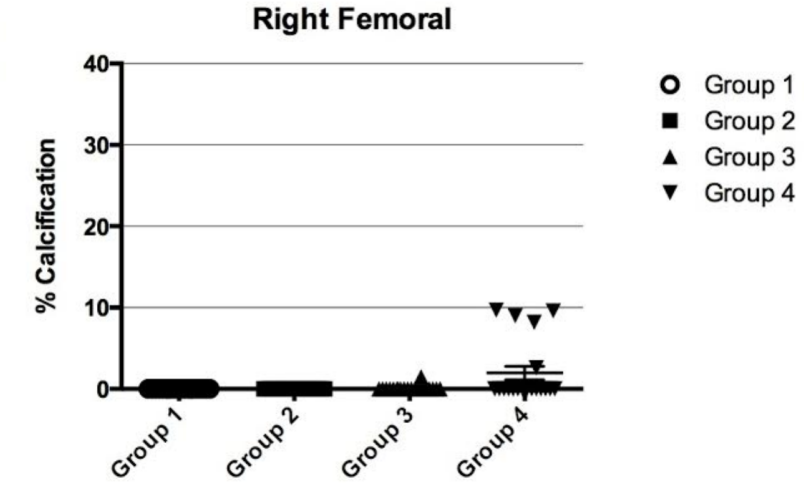


Figure 3.5. *Scatter plot illustrating percentage calcification of the right femoral.*

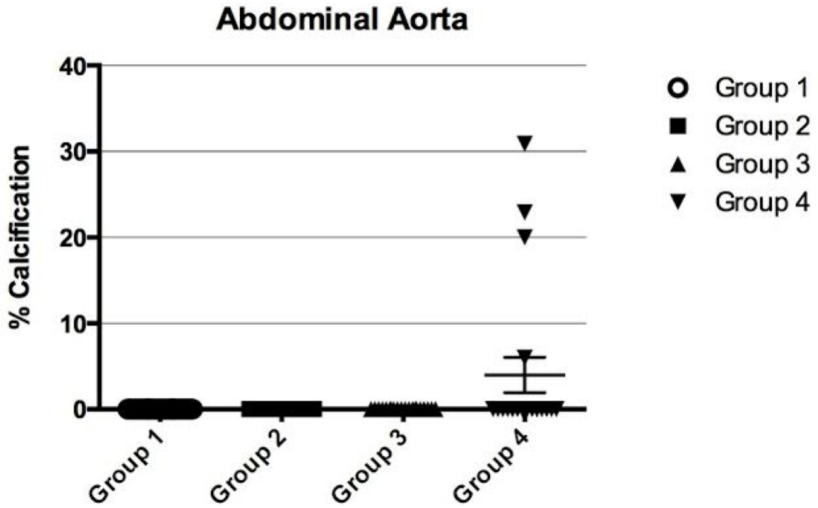


Figure 3.6. *Scatter plot illustrating percentage calcification of the abdominal aorta.*

Based on sectioning, the majority of vessels obtained from the animals did not appear calcified, although there were a number of positive calcified blood vessels from Group 4 (*ECppkLR)*. Calcification can be observed in the right femoral, right carotid and abdominal aorta in 6 animals from Group 4. The reason for this observation of calcification in Group 4 is unclear and may be due to A) the delivery of *Lactobacillus,* although there is no literature indicating a potential link between the two, and B) due to the older age of the rats of Group 4. These animals were 4 weeks older than their counterparts in Groups 1-3 and came from a different batch, however again literature does not indicate excess calcification of rats within their age profile (Kieffer *et al.,* 2000).

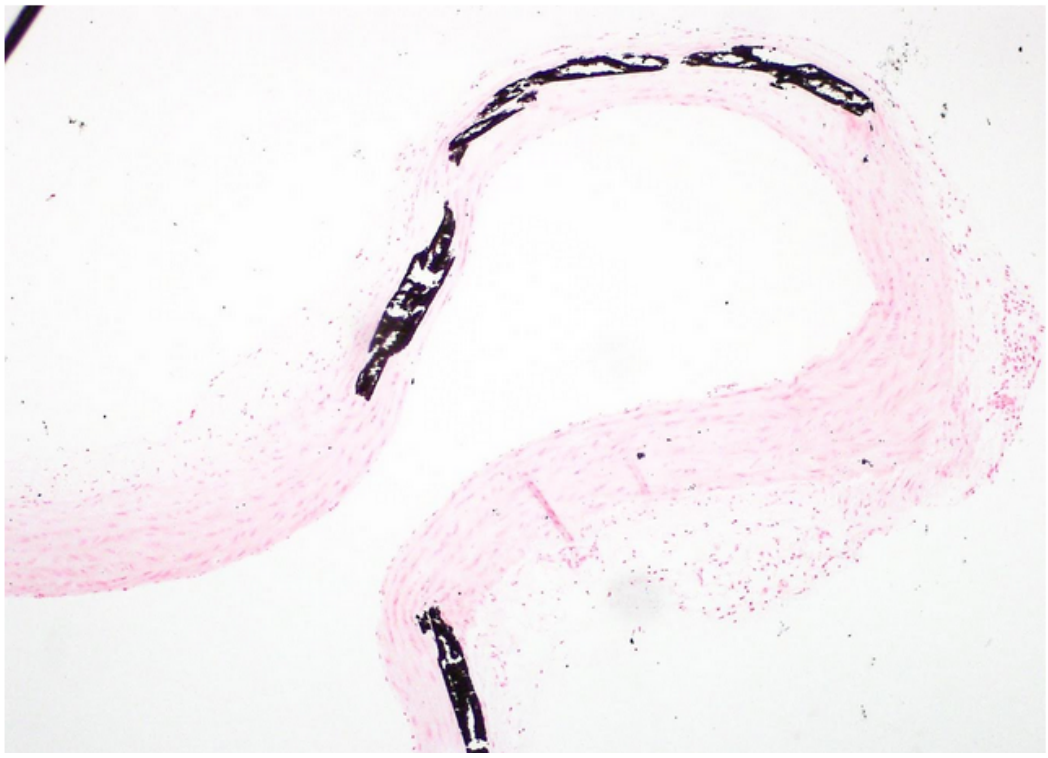


Figure 3.7. *Sagittal section of the right aorta, showing calcification within the media of the arterial wall. Section obtained from animal #6, Group 4 (ECppkLR).*

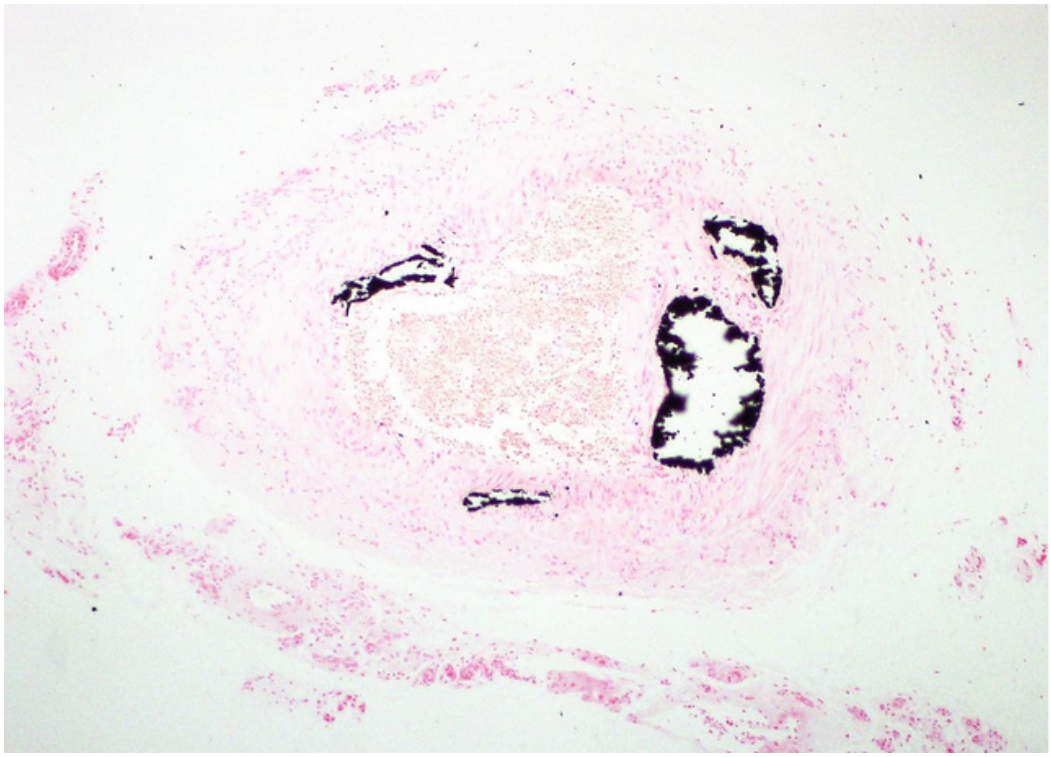


Figure 3.8. *Sagittal section of the right femoral artery, showing calcification within the media of the arterial wall. Section obtained from animal #16, Group 3 (ECppkE).*

3.3.6. Statistical analysis of tail-vein blood samples

Mineral	Group	Equilibration	Established Chronic Renal Failure	After 21 days intervention	After 35 days intervention
Creatinine umol/L	CRF (control)	43.1 ± 3.5	123.7 ± 26.9	315.2 ± 47.7	225.3 ± 38.5
	E. coli ppk+pduABJKNU	47.6 ± 2.8[b]	103.4 ± 26.5	292.9 ± 53.6	226.3 ± 43.2
	E. coli+ ppk	45.1 ± 2.3	82.0 ± 9.2[b]	236.3 ± 59.6[b]	193.4 ± 38.8
	L. reuteri+ECppk	49.5 ± 3.9[b]	151.4 ± 29.9	362.7 ± 57.1	310.8 ± 54.1[b]
Phosphate mmol/L	CRF (control)	2.00 ± 0.21	2.43 ± 0.48	4.52 ± 0.55	3.71 ± 0.78
	E. coli ppk+pduABJKNU	2.12 ± 0.20	2.18 ± 0.40	4.44 ± 0.84	3.67 ± 0.73
	E. coli+ ppk	2.02 ± 0.19	1.66 ± 0.15[b]	3.43 ± 0.84[b]	2.80 ± 0.58[b]
	L. reuteri+ECppk	1.87 ± 0.11	2.76 ± 0.57	4.97± 0.66	4.39 ± 0.73
Calcium mmol/L	CRF (control)	2.27 ± 0.16	2.59 ± 0.09	2.35 ± 0.24	2.42 ± 0.22
	E. coli ppk+pduABJKNU	2.57 ± 0.15[b]	2.65 ± 0.21	2.51 ± 0.28	2.43 ± 0.22[b]
	E. coli+ ppk	2.46 ± 0.09[b]	2.55 ± 0.15	2.47 ± 0.17	2.66 ± 0.16
	L. reuteri+ECppk	2.51 ± 0.12[b]	2.77 ± 0.16[b]	2.46 ± 0.53	2.40 ± 0.36

Table 3.35. *Table indicating values from tail-vein blood samples from animal. Statistical analysis has been preformed. ([b]$P < 0.05$ versus CRF group at the same time point, Independent samples Kruskal-Wallis test).*

As indicated by the tail vein blood samples, initial variation amongst the differing groups already appears large before experimental work had taken place. This variation amongst groups was most likely due to existing genetic variation amongst the Sprague-Dawley rats (Fitzpatrick *et al,* 2013). The Sprague-Dawley breed is traditionally outbred, however the breed is widely used as a renal failure

model (Ye *et al,* 1997; Lacour *et al,* 2005). The large degree of variation therefore made the results of the bacterial intervention on the CRF state difficult to interpret. There appears to be a large decrease in phosphate level at post-intervention for the *E. coli+ppk* group versus the control group, however with initial genetic variation between these two groups, it cannot be proved that this difference is due to the bacterial intervention alone.

3.4. Conclusion

The principle of this study was to observe the effects of the constructs previously examined in Chapter II. These constructs had proven efficacy in an *in vitro* environment, therefore a natural progression of study was to examine this same efficacy *in vivo*. However, the overall results of this study did not show any therapeutic effect of bacterial therapy, but there were large variations between the groups from the initial pre-intervention observations onwards, meaning it was difficult to examine the actual efficacy of the constructs on the CRF state. The published efficacy shown by lanthanum in reducing phosphataemia and vascular calcification in rat renal failure studies (Neven *et al.,* 2009) was not shown by any of the constructs. No toxicity from bacterial delivery was apparent.

In the pilot feeding trial, survival of bacterial samples in glucose supplemented feeding water, was poorer for *Lactobacillus* strains than *E. coli* K12 strains expressing *ppk*. This discrepancy reflects the stress survival effects of PPK (Motomura *et al.,* 2014) because *E. coli* K12 does not generally survive in the rat gut but all the ppk-expressing clones were recovered by viable culture from faeces. *Lactobacillus reuteri* strain survival in the rat gut was improved by addition of a carbon source not accessible to the host. In the final large-scale trial, by changing the carbon supplement to gluconate from glucose we were successfully able to deliver and retrieve as many *Lactobacillus* cells from drinking water and faecal samples and gut samples as *E. coli*. This suggests that *L. reuteri* could be used to deliver therapeutic molecules by the oral inoculation system used in this thesis

The adenine diet successfully induced chronic renal failure in all animals. We observed microscopic calcification in blood vessels from the Group 4 (*EcppkLR)* animals, whilst little to none was observed in the blood vessels of the other groups. However assay results did not indicate any unusually high serum calcium or phosphate results for Group 4 vs. the other assayed Groups. This may be due to assay sensitivity or the sectioning of vessels initially. No consistent variations in calcium or phosphate excretion in faeces were noted with bacterial therapy.

A key observation from the large-scale study was the successful delivery and retrieval of the bacterial strains from supplemented water. In the pilot trial, the difficulties encountered regarding this delivery and viability were improved upon greatly by the strict quality measures implemented for the large-scale trial. Analysis proved viability of bacterial constructs in the supplemented water source, while faecal and intestinal counts demonstrated viable cultures, indicating that the bacteria was indeed delivered from the water source to the animal and passed through the digestive tract.

The behavioural and physiological responses of the animal examined during the study were anticipated in response to the adenine diet and resulting renal failure. However positive aspects of the study included the ability to successfully deliver and recover the bacterial constructs from the faeces and small intestine of the animals without evidence of toxicity, indicating future potential for water and diet delivery as a successful alternative to gavaging.

Moving forward, this trial would ideally be repeated on a smaller scale, with strictly inbred rat models (e.g. Wistar) and with a positive control e.g. lanthanum or sevalamer. This will reduce the genetic variation and allow the effect of the

bacterial intervention to be analyzed independently. Although there was a discrepancy in the age of the initial 3 groups vs the final 4th group, the author could find no evidence indicating this may contribute an influencing factor regarding disease progression as these animals are still considered young rats (Kieffer *et al.,* 2000).

3.5. References

- Berndt, T., Thomas, L., Craig, T., Sommer, S., Li, X., Bergstralh, E. & Kumar, R. (2007). Evidence for a signaling axis by which intestinal phosphate rapidly modulates renal phosphate reabsorption. Proceedings of the National Academy of Sciences 104:11085-11090.
- Biologic E., Foa P., Zak B. (1967) Microdetermination of inorganic phosphate, phospholipids, and total phosphate in biologic materials. Clinical Chemistry 3:326-332
- Bleyer, A. (2003). Phosphate binder usage in kidney failure patients. Expert Opinion on Pharmacotherapy 4:941-947.
- Crookham, J., Dapson, R. (1991) Hazardous Chemicals in the Histopathology Laboratory, 2nd ED, Anatech
- Farnworth E. 2008. Handbook of fermented functional foods. CRC Press, Boca Raton.
- Fitzpatrick C., Gopalakrishnan S., Cogan E., Yager L., Meyer P., Lovic V., Saunders B., Parker C., Gonzales N., Aryee E., Flagel S., Palmer A., Robinson T., Morrow J. (2013) Variation in the Form of Pavlovian Conditioned Approach Behavior among Outbred Male Sprague-Dawley Rats from Different Vendors and Colonies: Sign-Tracking vs. Goal-Tracking. PLoS ONE 8:e75042
- Govers, M., Van der Meet, R. (1993). Effects of dietary calcium and phosphate on the intestinal interactions between calcium, phosphate, fatty acids, and bile acids. Gut 34:365-370.

- Hall E., Monti A., Mohn W. (2010) A comparison of bacterial populations in enhanced biological phosphorus removal processes using membrane filtration or gravity sedimentation for solids–liquid separation. Water Research 44:2703-2714.
- Harkness, J., Wagner J. (1989) The Biology and Medicine of Rabbits and Rodents, Philadelphia: Lea and Fabiger
- Heresztyn T., Nicholson B. (2001) A colorimetric protein phosphatase inhibition assay for the determination of cyanobacterial peptide hepatotoxins based on the dephosphorylation of phosvitin by recombinant protein phosphatase 1. Environ Toxicol 16:242-252
- Institute for Laboratory Animal Research, ed. Guidelines for the Care and Use of Mammals in Neuroscience and Behavioral Research. 2003, The National Academies Press: Washington, D.C.
- Kieffer, P., Robert, A., Capdeville-Atkinson, C., Atkinson, J. Lartaud-Idjouadiene, I. (2000). Age-related arterial calcification in rats. Life Sciences 66, 2371-2381.
- Kulakovskaya T., Vagabov V., Kulaev I. (2012) Inorganic polyphosphate in industry, agriculture and medicine: Modern state and outlook. Process Biochemistry 47:1-10
- Lacour B., Lucas A., Auchere D., Ruellan N., de Serre Patey N., Drueke T. (2005) Chronic renal failure is associated with increased tissue deposition of lanthanum after 28-day oral administration. Kidney International 67:1062-1069.

- Li X., Xing Y., Guo L., Lv X., Song H., Xi T. (2014) Oral immunization with recombinant *Lactococcus lactis* delivering a multi-epitope antigen CTB-UE attenuates *Helicobacter pylori* infection in mice. Pathogens Disease 72:78-86.
- McCabe K., Booth S., Fu X., Shobeiri N., Pang J., Adams M., Holden R. (2013) Dietary vitamin K and therapeutic warfarin alter the susceptibility to vascular calcification in experimental chronic kidney disease. Kidney International 83:835-844
- Medina M., Vintiñi E., Villena J., Raya R., Alvarez S. (2010) *Lactococcus lactis* as an adjuvant and delivery vehicle of antigens against pneumococcal respiratory infections. Bioengineered Bugs 1:313-325.
- Motomura, K., Hirota, R., Okada, M., Ikeda, T., Ishida, T. & Kuroda, A. (2014). A New Subfamily of Polyphosphate Kinase 2 (Class III PPK2) Catalyzes both Nucleoside Monophosphate Phosphorylation and Nucleoside Diphosphate Phosphorylation. Applied and Environmental Microbiology 80, 2602-2608.
- Neven E., Dams G., Postnov A., Chen B., De Clerck N., De Broe M., D'Haese P., Persy V. (2009) Adequate phosphate binding with lanthanum carbonate attenuates arterial calcification in chronic renal failure rats. Nephrology Dialysis Transplantation 24:1790-1799
- Parsons J., Dinesh S., Deery E., Leech H., Brindley A., Heldt D., Frank S., Smales C., Lunsdorf H., Rambach A., Gass M., Bleloch A., McClean K., Munro A., Rigby S., Warren M., Prentice M. (2008) Biochemical and

Structural Insights into Bacterial Organelle Form and Biogenesis. Journal of Biological Chemistry 283:14366-14375.

- Price, P., Roublick, A. & Williamson, M. (2006). Artery calcification in uremic rats is increased by a low protein diet and prevented by treatment with ibandronate. Kidney International 70:1577-1583.
- Proudfoot D., Skepper J., Shanahan C., Weissberg P.(1998) Calcification of Human Vascular Cells In Vitro Is Correlated With High Levels of Matrix Gla Protein and Low Levels of Osteopontin Expression. Arteriosclerosis, Thrombosis, and Vascular Biology 18:379-388
- Reid G. (2008) How Science Will Help Shape Future Clinical Applications of Probiotics. Clinical Infectious Diseases 46:S62-S66.
- Sedlacek, M., Dimaano, F. & Uribarri, J. (2000). Relationship between phosphorus and creatinine clearance in peritoneal dialysis: Clinical implications. American Journal of Kidney Diseases 36:1020-1024.
- Sheehan D., Hrapchak B. (1980) Theory and practice of Histotechnology, Battelle Press, 2nd Ed, 226-227
- Shobeiri, N., Pang, J., Adams, M., Holden, R. (2013). Cardiovascular disease in an adenine-induced model of chronic kidney disease. Journal of Hypertension 31:160-168.
- Solanki H., Pawar D., Shah D., Prajapati V., Jani G., Mulla A., Thakar P. (2013) Development of Microencapsulation Delivery System for Long-Term Preservation of Probiotics as Biotherapeutics Agent. BioMed Research International 2013:1-21.

- Sriramulu D., Liang M., Hernandez-Romero D., Raux-Deery E., Lunsdorf H., Parsons J., Warren M., Prentice M. (2008) *Lactobacillus reuteri* DSM 20016 Produces Cobalamin-Dependent Diol Dehydratase in Metabolosomes and Metabolizes 1,2-Propanediol by Disproportionation. Journal of Bacteriology 190:4559-4567.
- Tomasello S. 2008. Secondary Hyperparathyroidism and Chronic Kidney Disease. Diabetes Spectrum 21:19-25.
- Ye S., Ozgur B., Campese V. (1997) Renal afferent impulses, the posterior hypothalamus, and hypertension in rats with chronic renal failure. Kidney International 51:722-727.

Chapter IV

Investigation into changes in buoyant cell density of bacterial cells following induction of ethanolamine (Eut*)* and propanediol (Pdu) microcompartments

Contents

4.0. Abstract

4.1. Introduction

4.2. Materials & Methods

4.2.1. Bacterial strains & culture conditions

4.2.2. Screening Process

4.2.2.1. Growth analysis

4.2.3. Phenotypic analysis

4.2.3.1. Density gradient & separation

4.2.3.2. Sedimentation & settlement

4.3. Results & Discussion

4.3.1. Plate screening

4.3.2. Growth analysis

4.3.3. Density gradient & separation

4.3.4. Sedimentation & settling

4.3.5. TEM Imaging

4.4. Conclusion

4.5. References

4.0 Abstract

Bacterial microcompartments (MCPs) are small proteinaceous structures originally observed within bacterial cells in the 1950s (Drews & Niklowitz, 1956). They possess a distinct polygonal shape, which triggered their identification by electron microscopy. Their distinctive shape has been identified in genera as diverse as *Klebsiella, Lactobacillus* and *Escherichia* (Kerfeld *et al.,* 2010).

The ethanolamine utilization (Eut) microcompartment and its gene cluster were initially identified in *E. coli* (Stojiljkovic *et al.,* 1995). Ethanolamine is an amino alcohol produced in the gastrointestinal tract of mammals as a product of the degradation of phosphatidyl ethanolamine, which is present in large quantities in eukaryotic membranes.

From the *E. coli* Reference (ECOR) Library strains, I screened 53 strains, with 46% identifying as displaying a Eut-positive phenotype on ethanolamine MacConkey agar. These strains then underwent a selection of phenotypic analysis to observe their phenotypic characteristics.

I hypothesized that strains containing a bacterial microcompartment would display increased buoyant density, and this hypothesis was supported by observations in *E. coli* strains expressing a recombinant *pdu* operon and in both *Yersinia enterocolitica* and *Lactobacillus reuteri* with a native operon. Strains all displayed increased density when grown in the presence of supplemented media to induce the presence of the microcompartment.

In contrast, Eut-positive strains from the ECOR library, displayed the opposite phenotype i.e. they displayed decreased density when grown in ethanolamine-

supplemented media. Expression of recombinant empty microcompartment shells in *E.coli* without an enzyme core, also resulted in decreased buoyant density compared with a complete enzyme-containing Pdu microcompartment, but the ethanolamine-induced ethanolamine-deaminase positive cells should make microcompartments with enzyme cores

This discrepancy between the buoyant densities of cells on induction of the Eut microcompartment versus induced and overexpressed Pdu microcompartments may be hypothesized to be due to the production of ammonia within the Eut microcompartment, increasing buoyancy of the bacterial cell. This hypothesis requires additional investigation.

4.1. Introduction

Ethanolamine is an amino alcohol produced in the gastrointestinal tract of mammals as a product of the degradation of phosphatidyl ethanolamine, which is present in large quantities in eukaryotic membranes. Its association with a bacterial microcompartment was first observed in *E. coli* in 1995 (Stojiljkovic *et al.,* 1995) with the identification of the ethanolamine utilisation (eut) gene cluster.

Since that initial observation, the role of ethanolamine in *E. coli* has been studied sporadically, with a number of studies indicating a relationship between pathogens and the ability to utilize ethanolamine (a readily available source of nutrients in the mammalian gut) (Bertin *et al.,* 2011).

The association between the metabolism and the benefit of the bacterial MCP enclosing the enzymes has not yet been fully elucidated – counter arguments from different studies indicate different hypothesis.

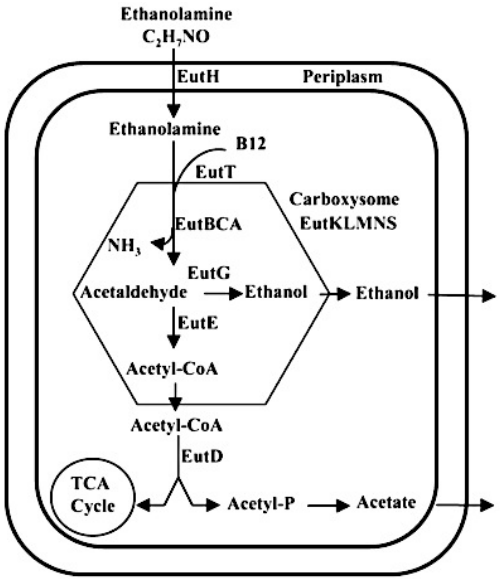


Figure 4.1 *Model of ethanolamine catabolism in E. coli (from Bertin et al., 2011)*

Published literature from (Penrod & Roth, 2006) indicates a potential role in the retention of the volatile aldehyde intermediate, which would otherwise be lost during the gas phase. This is in agreement with additional theories regarding the role of bacterial MCPs (Kerfeld *et al.,* 2010). However studies by (Havemann *et al.,* 2002) have suggested the true role is regarding the mitigation of a toxic intermediate. This theory is supported by deletion mutant results, where the *pduA* mutants displayed interrupted growth at high concentrations of 1,2-propanediol, indicating accumulating toxicity within the cell. However, to date no one clear role has been identified and supported consistently. Both theories are supported by evidence, therefore it is can be hypothesized that the true role involves aspects of both theories and may even support both under differing physiological conditions. Further information on this topic can be found in Chapter 1b.

The ECOR library collection was initially established in 1984 (Ochman & Selander, 1984) and has been widely used since as a standard reference collection of various *E. coli* strains from differing geographical and host backgrounds. Ideally, this reference library was to encompass representatives from the varying natural population. Using this ECOR library to study the presence/absence of the Eut MCP provided adequate strain and background variation to observe the effect of the MCP.

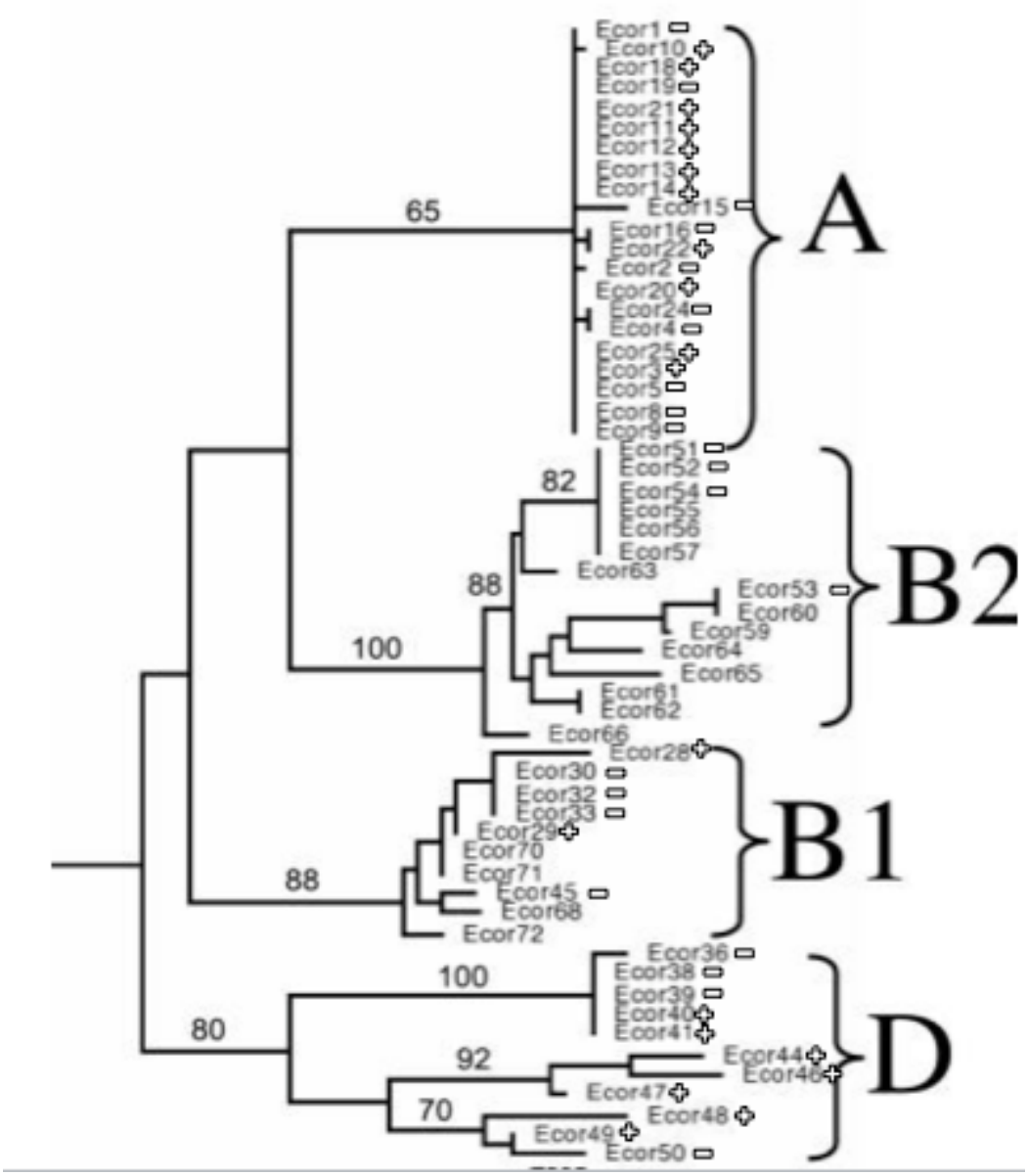


Figure 4.2: *Figure illustrates the phylogenetic relationships amongst the strains of the ECOR library based upon a neighbour joining tree drawn from concatenated MLST data (Wirth, et al 2006). Positive (+) sign indicates strains displaying B-12 dependent ethanolamine metabolism in this study, whilst negative (-) sign indicates strains, which did not display ethanolamine metabolism in this study (see Table 4.1. and 4.2. also) A, B, D are phylogenetic branches determined in the original Wirth study.*

To observe the effect of the Pdu MCP in another Enterobacteria, *Yersinia enterocolitica* was used. In general, virulence-related genes in *Yersinia* spp. can be divided into 3 main groups; Group 1 consists of genes present in all lineages, Group II consists of genes selectively gained or lost by entire lineages and Group III consists of genes specific for single isolates (Reuter *et al.,* 2014).

In *Yersinia* spp., the ability to utilize 1,2-propanediol is a metabolic property encoded by Group II genes on contigs present in the enteric pathogen of mammals *Yersinia enterocolitica* and the majority of other *Yersinia* species. The *Yersinia pdu* operon strongly resembles the *Salmonella pdu* operon (Reuter *et al.,* 2014). This pathway is absent in the *Yersinia pseudotuberculosis/Y. pestis lineage,* and *Y. ruckeri, Y. nurmii, and Y. similis and Y. entomophaga* (none of which apart from *Y. pseudotuberculosis* are enteric pathogens of mammals*).* Therefore it is suggested that the ability of *Y. enterocolitica* to utilise 1,2-PD offers a competitive advantage over other commensal gut bacteria (Reuter *et al.,* 2014).

Cells expressing inclusion bodies or increased polymer production have increased buoyant density (Eroglu & Melis, 2009). It was hypothesized that microcompartment expression, equivalent to an accumulation of organized inclusion bodies or elaborate polymer would have a similar effect. This study investigated whether the buoyant density of bacteria would be increased by the presence of an MCP, compared with an equivalent cell unable to make a microcompartment or in which the microcompartment was not induced.

The analysis performed as part of this study focuses predominantly on phenotypic effects but there is an acknowledgement of the need for genetic investigation to provide a complete overview.

4.2. Methods & Materials

4.2.1. Bacterial strains and culture conditions

Bacterial strains used in this study are listed *(Table 3.1)*. The majority of the *E. coli* strains used in this study were members of the *E. coli* Reference Library Collection (ECOR), kindly provided by Dr. David Clarke, University College Cork, but originating from the Ochman & Selander, 1984 study. An additional *E. coli* strain containing the recombinant Pdu construct, *pAR3114*, was also used. *Yersinia* strains used were provided by Dr. Tamara Ringwood, University College Cork.

Strain	Origin	Reference
ECOR Library (ECOR #1-54)	Dr. David Clarke, University College Cork	Ochman & Selander, 1984
***Yersinia enterocolitica* 53/03**	Dr. Tamara Ringwood, University College Cork	Pathogen Research Group, Nottingham Trent University, Nottingham
***Yersinia enterocolitica* 13/03**	Dr. Tamara Ringwood, University College Cork	Pathogen Research Group, Nottingham Trent University, Nottingham
***Yersinia enterocolitica* NZ3**	Dr. Tamara Ringwood, University College Cork	Pathogen Research Group, Nottingham Trent University, Nottingham
E. coli JM109 pAR3114 (Pdu operon)	Dr. Joshua Parsons, University of Kent	Parsons *et al.,* 2008
E. coli BL21 (DE3) pJP061 (pETpduABJKNU)	Dr. Joshua Parsons, University of Kent	Parsons *et al.,* 2008
Lactobacillus reuteri DSM20016	National Collection of Dairy Organisms, Reading, UK	Sriramulu *et al.,* 2008

Table 4.1. *List of strains utilized in study, indicating strain and origin.*

E. coli strains were cultured on MacConkey agar, supplemented with ethanolamine and B12 *(Table 4.2)*, and LB supplemented with ethanolamine and B12. For minimal growth conditions, *E. coli* was inoculated in ethanolamine minimal media *(Table 4.3)*. Recombinant *E. coli* strains were grown in LB supplemented with relevant antibiotic selection. *Yersinia* strains were cultured on

MacConkey agar supplemented with 1,2-propanediol and B12, and also in LB supplemented with 1,2-propanediol and B12. *Lactobacillus* strains were grown in MRS supplemented with 1,2-propanediol and B12 for the induction of the Pdu MCP. Recombinant *E. coli* strains containing *ppk* were grown in LB supplemented with ampicillin.

Ingredients	Amount (per Litre)
Soy Peptone	20g
Ox-Bile	5g
NaCl	5g
Neutral Red	0.075g
Agar	15g
Adjust to pH 7.4 ±0.2 using 4NaOH	
Ethanolamine (50mM) *	5g
B12 (200nM) *	600µL

Table 4.2. *Recipe list for MacConkey agar, supplemented with either i) ethanolamine ii) ethanolamine and B12 and iii) 1,2-propanediol and iv) 1,2-propanediol and B12 which were added post-autoclave*

Ingredients	Amount (per Litre)
Monopotassium Phosphate	3.94g/l
Dipotassium Phosphate	4.97g/l
Ammonium Sodium Phosphate Tetrahydrate	3.5g/l
Magnesium Sulphate	0.2g/l
Ethanolamine *	3.9g/l
Adjust to pH 7.2 ±0.2 using 4NaOH	
B12 (200nM) *	600µl

Table 4.3. *Recipe list for NCE media, supplemented with ethanolamine, which was added post-autoclave.*

Material	Amount (per Litre)
Tryptone from casein	10g/L
Sodium chloride	10g/L
Granulated Yeast Extract	5g/L
Deionised Water	1L
Ethanolamine (50mM) *	5g
B12 (200nM) *	600µL
1,2-propanediol *	4mLs

Table 4.4. *Recipe for Luria Broth (LB) for the growth of E. coli, supplemented with ethanolamine and B12 or 1,2-propanediol and B12.*

Material	Amount (per Litre)
MRS broth	55g/L
Deionised Water	1L
B12 (200nM) *	600µl
1,2-propanediol *	4mLs

Table 4.5. *Recipe for de Man-Rogosa-Sharpe (MRS) for the growth of lactobacilli, supplemented with 1,2-propanediol and B12.*

4.2.2. Eut utilization screening process

54 strains from the provided ECOR library of 84 strains were used for the screening process. These 54 strains were selected based on their numerical order, with no further traits or attributes contributing to the decision.

E. coli ECOR strains were initially picked from a 96 well plate library and directly inoculated into 50 mL Luria-Bertani broth (LB) (Sambrook *et al.,* 1989) for overnight growth at 37°C with agitation, to confirm their growth ability and rate. Following this initial growth confirmation, selected strains were then streaked on to differential MacConkey agar, supplemented with ethanolamine 50mM and 200nM cobalamin B12. Cobalamin B12 was added in order to determine if the ethanolamine was degraded in a cobalamin-dependant manner, as previously indicated based on work regarding the *pdu* operon in *Salmonella and eut* operon in *E. coli* (Lawrence & Roth, 1996). MacConkey agar plates were prepared fresh daily from a total 500mL flask preparation.

Resulting colonies produced either a red (*eut* positive) or yellow (*eut* negative) colour. This colour difference is triggered by a pH shift due to acid production caused by the utilization of ethanolamine by the enzyme EAL (Ethanolamine ammonia-lyase) (Srikumar & Fuchs, 2011). This colour change can occur

without the addition of cobalamin in the agar, cobalamin dependence is established by more rapid occurrence on cobalamin-supplemented media vs non-supplemented media. As previously mentioned, the EAL enzyme catalyzes the AdoCbl-dependent conversion of ethanolamine to acetaldehyde and ammonia (Bradbeer, 1964).

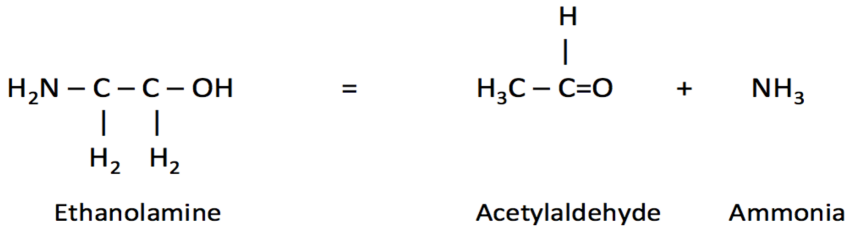


Figure 4.3. *Equation illustrating the conversion of ethanolamine to ammonia and acetaldehyde catalyzed by ethanolamine ammonia lyase (credit: brenda-enzymes.org)*

4.2.2.1. Growth analysis

Following solid culture, colonies were then picked and transferred to liquid broth for further growth screening. In order to determine bacterial growth profiles, 100 µl of LB broth was inoculated with a single colony of a selected *E. coli* strain whilst un-inoculated LB broth was used as a negative control. Cultures were incubated at 37°C for 27 hours with agitation, and the optical density at 600 nm (OD600) was determined during this period at 2 hour intervals using the Biotek plate reader.

4.2.3. Phenotypic analysis

After the identification of potential Eut positive/negative strains, the phenotypic screening processes begun. A number of analyses were applied based upon previous literature.

4.2.3.1. Density gradient and separation

Cell density, or buoyant density is a measure of the tendency of a substance to float in some other substance. This can be measured by density-gradient ultracentrifugation, where samples with a high buoyant density will be found at the bottom of a gradient, whilst samples found near the top of the gradient will have a relatively low density (Mizushima *et al.,* 1967)

To observe this effect, the density gradient media Percoll (GE Healthcare 17-0891-02) was used. Percoll is a cell separation solution consisting of a sodium-stabilized colloid, which is iso-osmotic and pH neutral (Pertoft, 1999) and has been extensively used in literature as a method for *E. coli* cell separation (Makinoshima *et al.,* 2002), (Pertoft, 1999). The principle of a density gradient separation, or isopycnic (meaning "of the same density") centrifugation, is that particles suspended in a fluid whose density varies with depth will move downward until they encounter an area of fluid of the same density as themselves

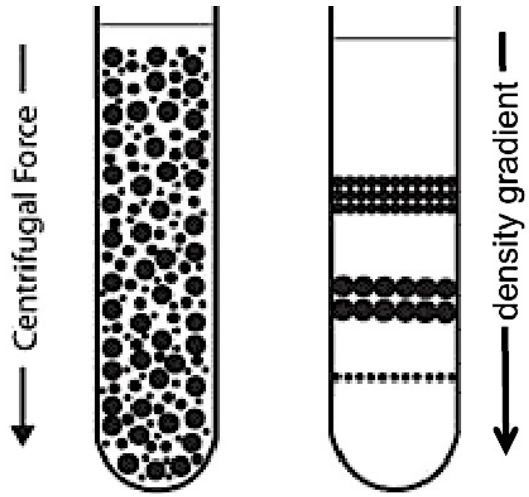


Figure 4.4. *Image indicating the principle of density gradient separation (Frei, Sigma Aldrich)*

E. coli strains displaying a Eut-positive phenotype were induced with ethanolamine and vitamin B12, with a positive control provided by un-induced

strains (i.e. strains grown on plain, un-supplemented media) and a negative control provided by the use of Eut-negative strains. Selected strains were inoculated from MacConkey agar plates into 50mL LB broth supplemented with 50mM ethanolamine and 200nM B12, and grown at 37°C for approx. 18 hours. Eut-negative strains were grown in 50mL LB broth without supplementation. After this overnight growth, cells were harvested by centrifugation at 6,000r.p.m. using the J10 Beckman Coulter rotor, with the resulting pellet washed twice with 10mL PBS. The final cell pellet was then resuspended in 1mL phosphate buffered saline (PBS).

To prepare the density separation gradient, 8 mL of Percoll was added to 1.25mL of PBS and 0.25 mL of density marker beads (supplied by Cospheric, Santa Barbara, CA USA) in PBS for 1 hour at 20,000 r.p.m. at 4°C with a Beckman SW40Ti rotor. 3 different densities of bead were used for the gradient; orange beads 1.04g/mL (UVPMS-BO-1.040 212-250um), red beads 1.10g/mL (REDPMS-1.10 425-500um) and red beads 1.12g/mL (REDPMS-1.12 212-250um) (three different colours were not available).

0.5mL of the bacterial resuspension was added to this prepared density gradient, amounting to a total volume of 10mL. The sample was then centrifuged at 20,000r.p.m for 45 minutes at 4°C, once again using the Beckman SW40Ti rotor. This technique was also applied to observations of the propanediol (Pdu) MCP in *Lactobacillus reuteri* and *Yersinia enterocolitica* strains.

Sample were removed from the Percoll gradient by pipette and sampled for imaging by transmission electron microscopy (see Chapter V for detailed methods).

4.2.3.2. Sedimentation & settling analysis

Previously utilized by (Ramsay *et al.,* 2011) to observe the presence of gas vesicles in *Serratia* spp., the protocol involved the static sedimentation of cultures over a certain time period, to again observe the potential effects of an intracellular body on the buoyant density of the bacterial cell. Cultures were grown overnight in 5mL culture at 37°C (*E. coli* was grown in LB supplemented with ethanolamine and B12; *Yersinia* was grown in LB supplemented with 1,2-propanediol and B12, and *Lactobacillus* was grown in MRS supplemented with 1,2-propanediol). After overnight growth to an OD600nm of 0.8, 1mL of relevant culture was inoculated into 10mL of fresh, unsupplemented broth, in clear open-top tubes that were sealed with paraffin to prevent contamination. Cultures were allowed to stand uninterrupted for a period of 24 hours, with regular visual observation.

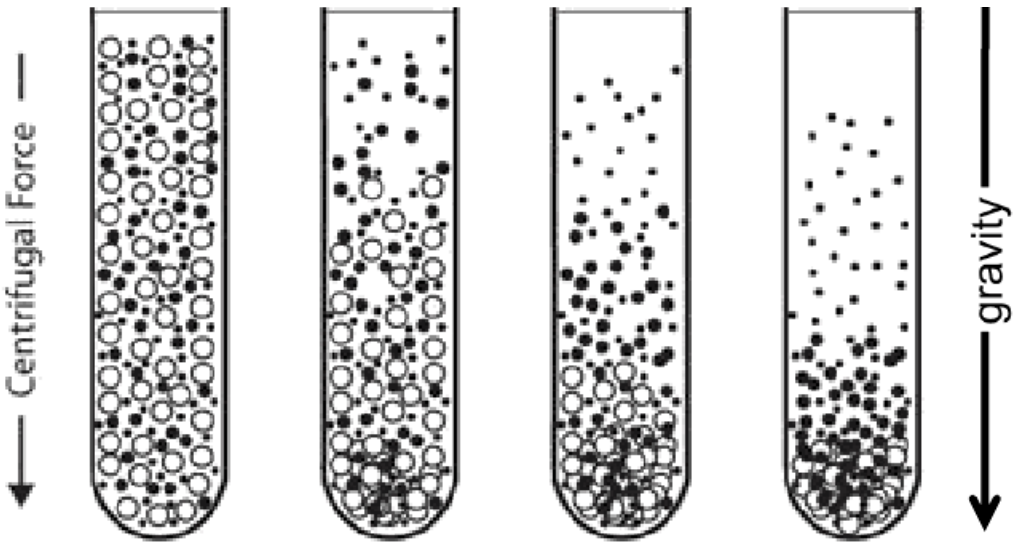


Figure 4.5. *Diagram illustrating the principle of cell sedimentation. A bacterial culture will be allowed stand for a period of time, and the culture will naturally sediment over this time. (Frei, Sigma Aldrich)*

4.3. Results & Discussion

4.3.1. Screening of *E. coli* cultures

54 strains from the ECOR *E. coli* library were screened on MacConkey agar plates supplemented and un-supplemented plates. Of the 54 screened strains, 24 strains produced red colonies more rapidly on MacConkey agar supplemented with ethanolamine and B12 than ethanolamine alone. This indicated the cobalamin-dependant metabolism of ethanolamine, and the potential presence of the *eut* operon.

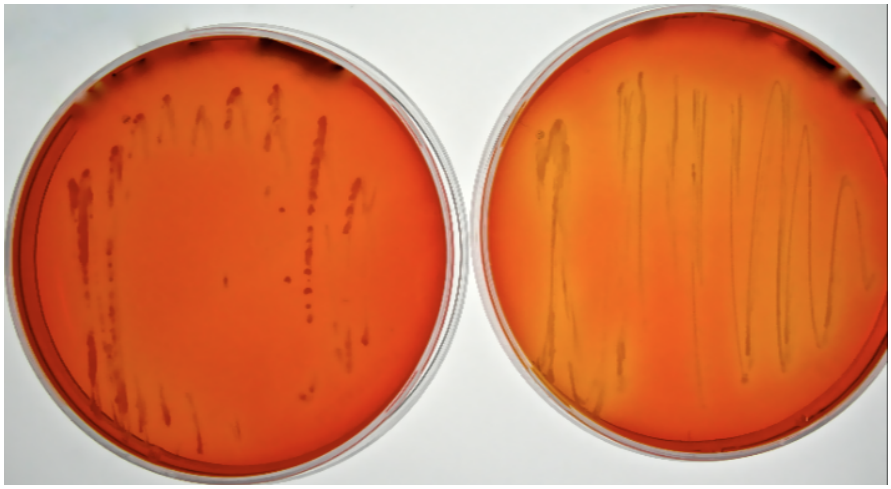


Figure 4.6. *McConkey agar plates cultured with ECOR E. coli #26. Plate on the left has been supplemented with ethanolamine and B12. Red colonies present on plate indicate positivity for the eut metabolism. Plate on the right has not been supplemented, and yellow colonies are present. This indicates cobalamin-dependant ethanolamine metabolism by this strain (Eut positive).*

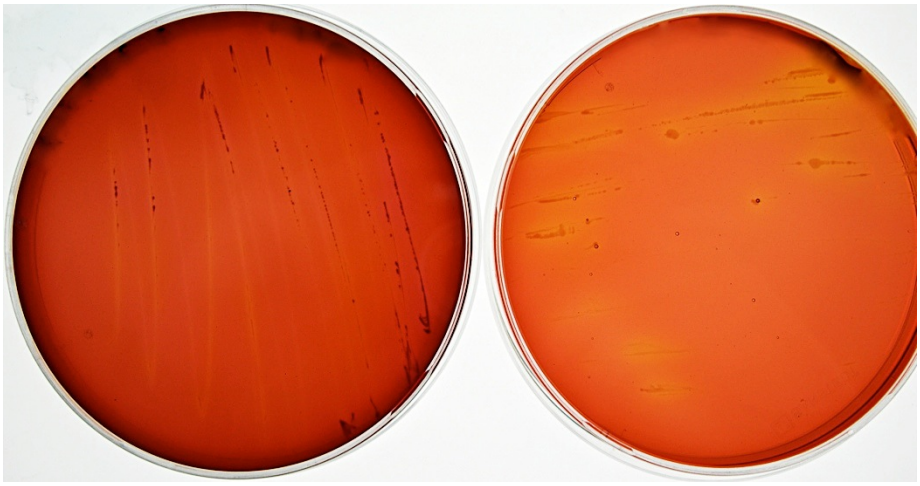


Figure 4.7. *McConkey agar plates cultured with ECOR E. coli #41. Plate on the left has been supplemented with ethanolamine and B12. Red colonies present on plate indicate positivity for the eut metabolism. Plate on the right has not been supplemented, and yellow colonies are present. This indicates cobalamin-dependant ethanolamine metabolism by this strain (Eut positive).*

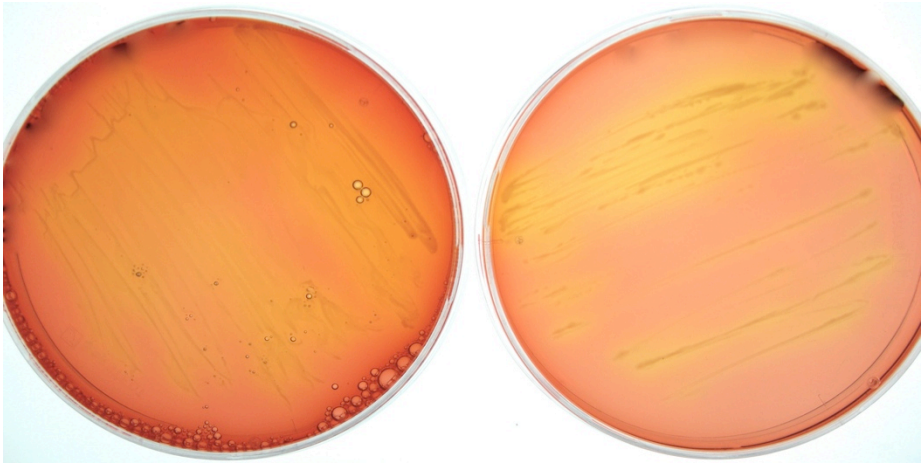


Figure 4.8. *McConkey agar plates cultured with ECOR E. coli #50. Plate on the left has been supplemented with ethanolamine and B12. Plate on the right has not been supplemented, and yellow colonies are present, indicating the strain is phenotypically negative for cobalamin dependent ethanolamine metabolism. (Eut negative)*

Based upon the colony appearance of the *E. coli* ECOR strains on these MacConkey agar plates, they were classified as either Eut-positive or eEut-negative in further analysis. The strains were re-streaked on the supplemented/un-supplemented MacConkey agar plates after each phenotypic analysis to ensure a consistent phenotype from the strain.

As illustrated in Table 4.7., the strains which this study identified as displaying Eut-positive phenotypes are not confined to any one particular branch of the ECOR phylogenetic tree *(Figure 4.2)*. This observance is in agreement with previously published literature (Lawrence & Roth, 1996) which also used the ECOR library. However in comparison with the Lawrence & Roth, 1996 study, we only observed Eut-positive phenotypes in 24 of the 54 analysed strains, wheras Lawrence & Roth observed 47 Eut positive phenotypes testing the same ECOR strain numbers. This difference in the positive:negative ratio is most likely due to *in vitro* selection against the operon, leading to the observation of more negatives than previously noted over a decade ago (Lawrence & Roth, 1996).

ECOR reference number	Strain Origin	Phenotypic Branch
3	Dog, Massachusetts	Branch A
10	Adult human, New York	Branch A
11	Urine, adult human, Sweden	Branch A
12	Adult human, Sweden	Branch A
13	Adult human, Sweden	Branch A
14	Urinary tract, adult human, Sweden	Branch A
18	Celebes ape, Seattle Zoo, Washington	Branch A
20	Steer, Bali	Branch A
21	Steer, Bali	Branch A
22	Steer, Bali	Branch A
25	Dog, New York	Branch A
26	Human infant, Massachusetts	Branch A
27	Giraffe, Seattle Zoo, Washington	Branch B1
28	Adult human, Iowa	Branch B2
29	Kangaroo rat, Nevada	Branch B1
39	Adult human, Sweden	Branch D
40	Urine, adult human, Sweden	Branch D
41	Adult human, Tonga	Branch D
42	Adult human, Massachusetts	Branch D
44	Cougar, Seattle Zoo, Washington	Branch D
46	Celebes ape, Seattle Zoo, Washington	Branch D
47	Sheep, New Guinea	Branch D
48	Urine, adult human, Sweden	Branch D
49	Adult human, Sweden	Branch D

Table 4.7. *Table illustrating the origin of the potential eut-positive strains for the ECOR library. This table references against Figure 2.1 which indicates the phylogenetic relationship of the strains (Modified from Ochman & Selander, 1984)*

ECOR reference number	Strain Origin	Phenotypic Branch
1	Adult human, Iowa	Branch A
2	Adult human, New York	Branch A
4	Adult human, Iowa	Branch A
5	Adult human, Iowa	Branch A
6	Adult human, Iowa	n/a
7	Orangutan, Seattle Zoo, Washington	n/a
8	Adult human, Iowa	Branch A
9	Adult human, Sweden	Branch A
15	Adult human, Sweden	Branch A
16	Leopard, Seattle Zoo, Washington	Branch A
17	Feral pig, Indonesia	n/a
19	Celebes ape, Seattle Zoo, Washington	Branch A
23	Elephant, Seattle Zoo, Washington	n/a
24	Adult human, Sweden	Branch A
30	Bison, Alberta, Canada	Branch B1
31	Leopard, Seattle Zoo, Washington	n/a
32	Giraffe, Seattle Zoo, Washington	Branch B1
33	Sheep, California	Branch B1
34	Dog, Massachusetts	n/a
35	Adult human, Iowa	n/a
36	Adult human, Iowa	Branch D
37	Marmoset, Seattle Zoo, Washington	n/a
38	Adult human, Iowa	Branch D
43	Adult human, Sweden	n/a
45	Pig, Indonesia	Branch B1
50	Urine, adult human, Sweden	Branch D
51	Human infant, Massachusetts	Branch B2
52	Orangutan, Seattle Zoo, Washington	Branch B2
53	Adult human, Iowa	Branch B2

Table 4.8. *Table illustrating the origin of the potential eut-negative strains for the ECOR library. This table references against Figure 2.1 which indicates the phylogenetic relationship of the strains (Modified from Ochman & Selander, 1984)*

4.3.2. Growth analysis

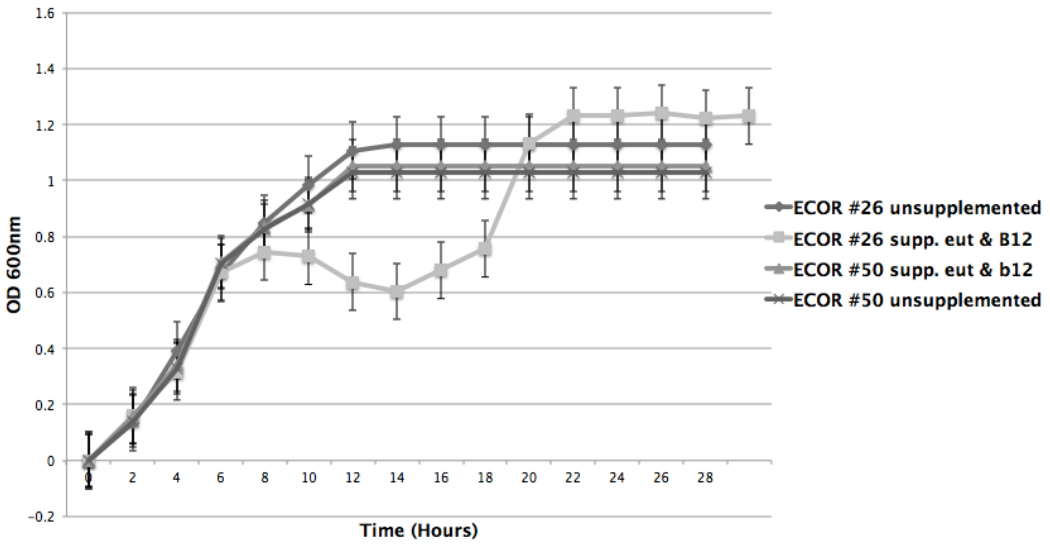


Figure 4.9. *Growth curve indicating the effect of ethanolamine and B12 supplementation. ECOR E. coli #26 (positive eut phenotype) is illustrated grown in LB without supplementation and also with supplementation of ethanolamine and B12. ECOR E. coli #50 (negative eut phenotype) is also illustrated grown in LB with and without supplementation, which appear to have no effect on growth rate.*

Analysis of the growth curves of the ECOR strains grown on LB vs. LB supplemented with ethanolamine and B12 demonstrated no obvious early growth advantage for strains. Selected strains displaying a positive Eut phenotype on plate screening (e.g. ECOR #26) appeared to have a diauxic growth pattern on LB with added ethanolamine, with slower growth and an additional lag phase but an increase in final OD600 compared with LB alone.

4.3.3. Density gradient and separation

For reproducibility and comparability it was necessary to use density marker beads to provide a visual indication of the density for comparison with cell bands for measurement (Woldringh *et al.,* 1981).

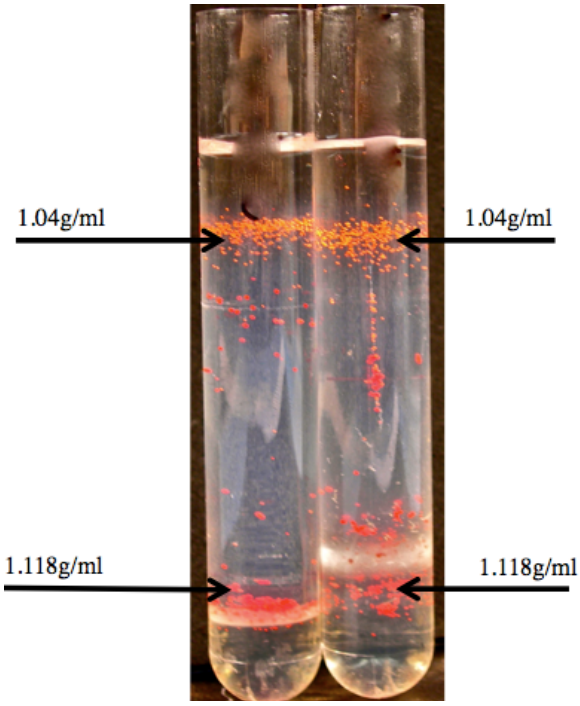


Figure 4.10 *Increased buoyant density of L. reuteri DSM20016 (pdu-positive) in isopycnic (density gradient) centrifugation when grown in Pdu operon inducing conditions. The white band represents bacterial cells. The tube on the left contains L. reuteri DSM20016, which was grown in MRS supplemented with 1,2-propanediol, and B12. The tube on the right also contains L. reuteri DSM20016, which was also grown in MRS, unsupplemented*

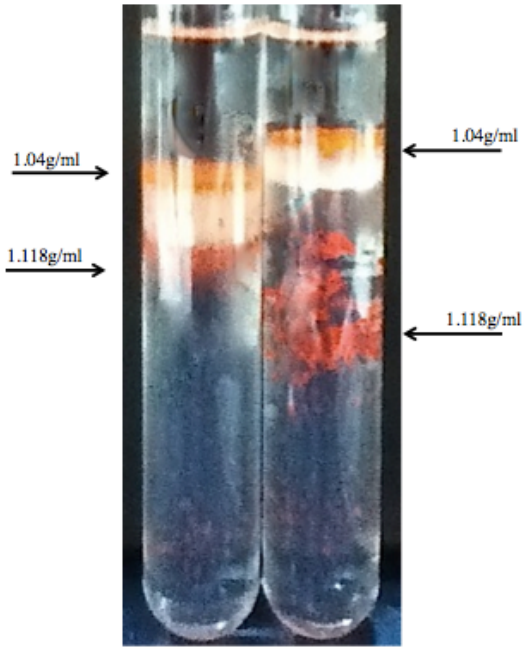


Figure 4.11. *Increased buoyant density of Y. enterocolitica 53/03 (pdu-positive) in isopycnic (density gradient) centrifugation when grown in Pdu operon inducing conditions. The white bands are bacteria. The tube on the left contains Y. enterocolitica 53/03 which was grown in LB supplemented with 1,2-propanediol and B12. The tube on the right also contains Y. enterocolitica 53/03 which was also grown in LB, unsupplemented.*

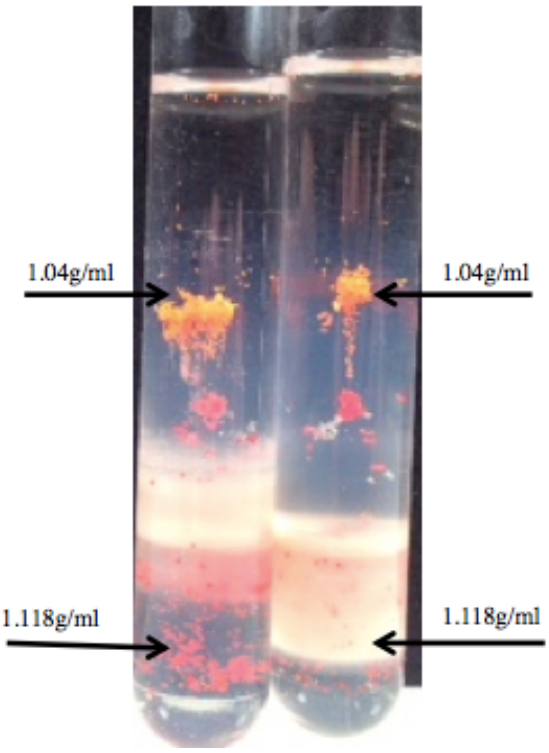


Figure 4.12. *The tube on the left illustrates E. coli expressing the recombinant pduABJKNU (empty MCP shell) which was grown in LB supplemented with ampicillin. The tube on the right illustrates the recombinant Pdu MCP (pAR3114) in E. coli which was grown in LB supplemented with 1,2-propanediol and B12.*

In the instance of the Pdu-MCP samples (*Y. enterocolitica*, *L. reuteri*) the expected effect was observed i.e. the bacterial band from samples grown in microcompartment inducing conditions appears denser (higher buoyant density) than the control (*Figure 4.11, 4.12*). This result supports the original hypothesis that cells containing the MCP would have higher buoyant density than non-MCP containing cells.

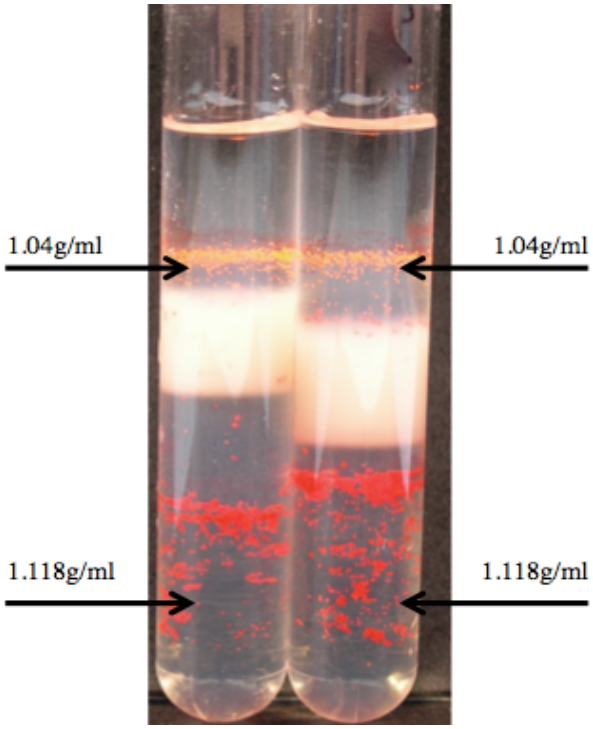


Figure 4.13. *Decreased buoyant density of ECOR E. coli #41 (eut-positive) in isopycnic (density gradient) centrifugation when grown in Eut operon inducing conditions. The tube on the left contains ECOR E. coli #41 that was grown in the presence of ethanolamine and B12. The tube on the right also contains ECOR E. coli #41 that was grown without ethanolamine and B12*

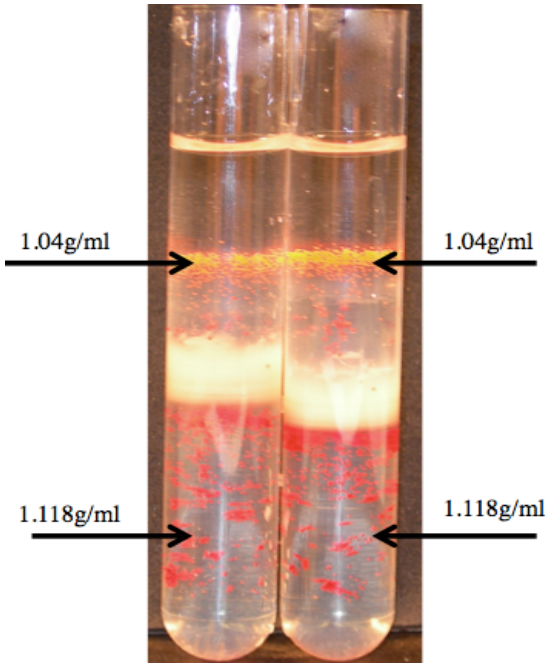


Figure 4.14. *Decreased buoyant density of ECOR E. coli #26 (eut-positive) in isopycnic (density gradient) centrifugation when grown in Eut operon inducing conditions. The tube on the left contains ECOR E. coli #26 that was grown in LB supplemented with ethanolamine and B12. The tube on the right also contains ECOR E. coli #26 which was grown in LB, unsupplemented.*

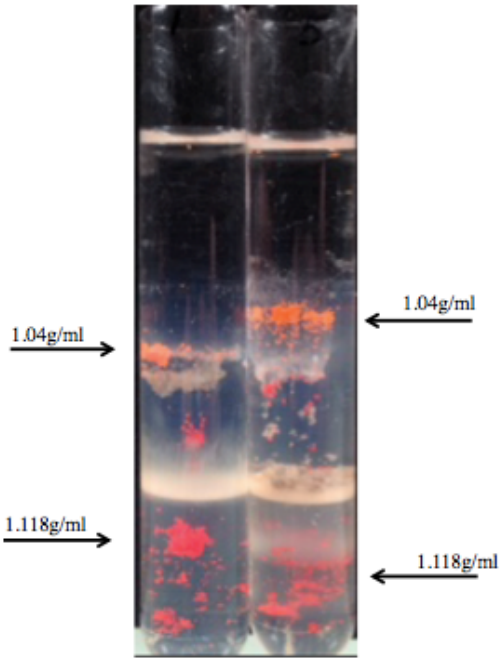


Figure 4.15. *ECOR E. coli #50 (eut-negative) shows no change in buoyant density on isopycnic (density gradient) centrifugation when grown in Eut operon inducing conditions. The tube on the left contains ECOR E. coli #50 that was grown in LB supplemented with ethanolamine and B12. The tube on the right also contains ECOR E. coli #50 which was grown in LB, unsupplemented.*

However, regarding the ethanolamine studies, it was observed in samples containing an induced Eut-positive *E. coli* culture versus a non-induced Eut-positive *E. coli* culture, that the resulting bacterial band appears to be less dense (i.e. lower buoyant density) than its un-induced counterpart (Figure 4.13, 4.14). This trend was observable across examined samples from the ECOR library of Eut-positive strains. With the eut-negative strains, there appeared to be no difference amongst strains grown in the presence/absence of ethanolamine and B12 (Figure 4.15), suggesting a connection between the buoyant density and a functional Eut operon.

4.3.4. Sedimentation & settling analysis

The role of the settling and sedimentation analysis was to observe if the results identified through the isopycnic centrifugation were consistent with another

methodology. These observations were repeated in triplicate to ensure a consistent result.

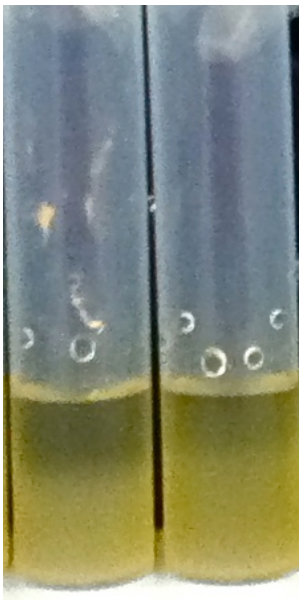


***Figure 4.16**. Increased sedimentation of Y. enterocolitica 53/03 grown in Pdu operon inducing conditions. The tube on the left contains Y. enterocolitica 53/03 grown in LB supplemented with 1,2-propanediol and B12, and allowed to sediment. The tube on the right contains Y. enterocolitica 53/03 which was grown in LB, unsupplemented.*



***Figure 4.17.** Differential E. coli sedimentation with empty and full microcompartment expression. The tube on the left indicates the recombinant Pdu MCP (pAR3114) in E. coli which was grown in LB supplemented with 1,2-propanediol and B12. The tube on the right indicates E. coli expressing the recombinant empty MCP (pduABJKNU) which was grown in LB supplemented with ampicillin.*

As can be observed, the results are consistent and in agreement with previous observations from the isopycnic centrifugation. Pdu-inducing conditions for

Yersinia enterocolitica capable of expressing native MCP (data not shown) result in faster sedimentation or settling than the equivalent non-induced control cells (Figure 4.16).

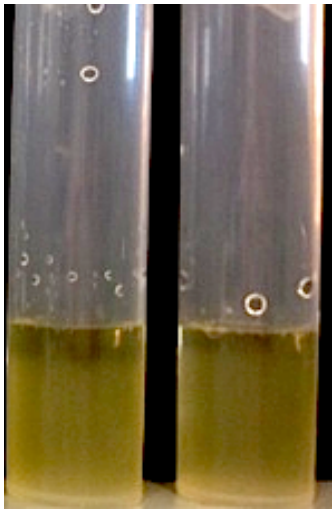


Figure 4.18. *Increased sedimentation of Y. enterocolitica NZ3 grown in Pdu operon inducing conditions. The tube on the left contains Y. enterocolitica NZ3 grown in LB supplemented with 1,2-propanediol and B12, and allowed to sediment. The tube on the right contains Y. enterocolitica NZ3 which was grown in LB, unsupplemented.*



Figure 4.19. *Image illustrating results of ECOR E. coli #26. The tube on the left contains ECOR E. coli #26 grown in the presence of ethanolamine and B12, and allowed to sediment. The tube on the right contains ECOR E. coli #26 grown in standard media conditions and allowed to sediment.*

Again, the results of the sedimentation test agree with the previous isopycnic centrifugation results. The Eut-positive *E. coli* cells (cobalamin-dependent

ethanolamine metabolism phenotype positive) sediment slower after being grown in Eut operon inducing conditions (ethanolamine) than when non-induced. Again, this result was consistent across the various Eut-positive ECOR strains (data not shown, 10 strains tested).

4.3.5. TEM Imagery

Samples from the Percoll gradient were obtained and underwent TEM imaging (see Chapter V for methodology). Samples from the upper part of the buoyant density band from ethanolamine-positive samples were observed under TEM and the presence of dark, electron dense masses could be seen indicative of bacterial microcompartments.

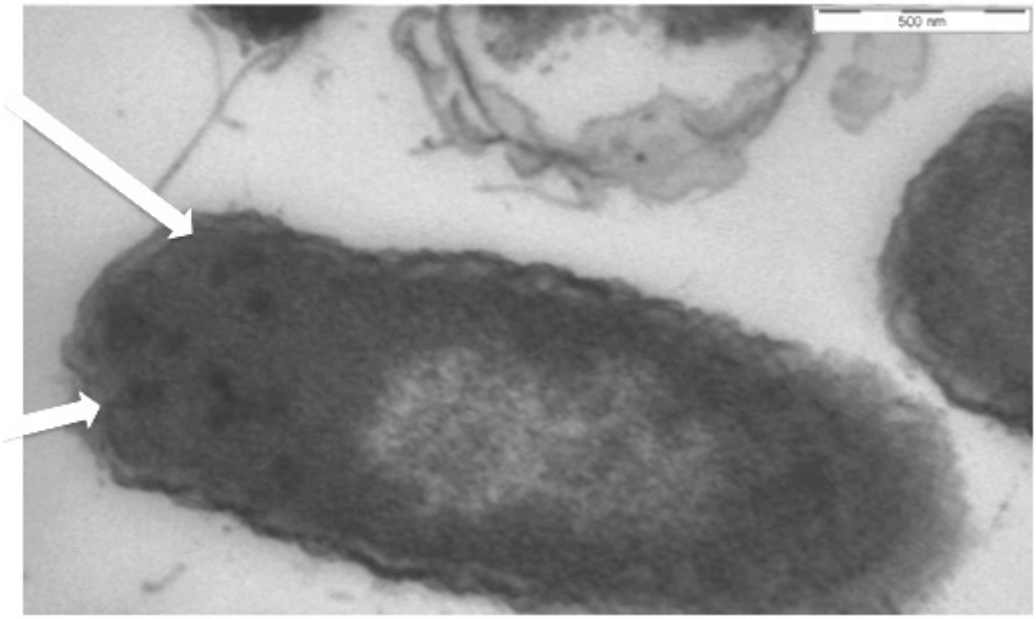


Figure 4.20. *Image illustrating microcompartments under TEM in the ethanolamine positive #ECOR3 sample following ethanolamine induction. This sample was from the upper part of the buoyant band observed in the percoll gradient. Sample at 40k magnification.*

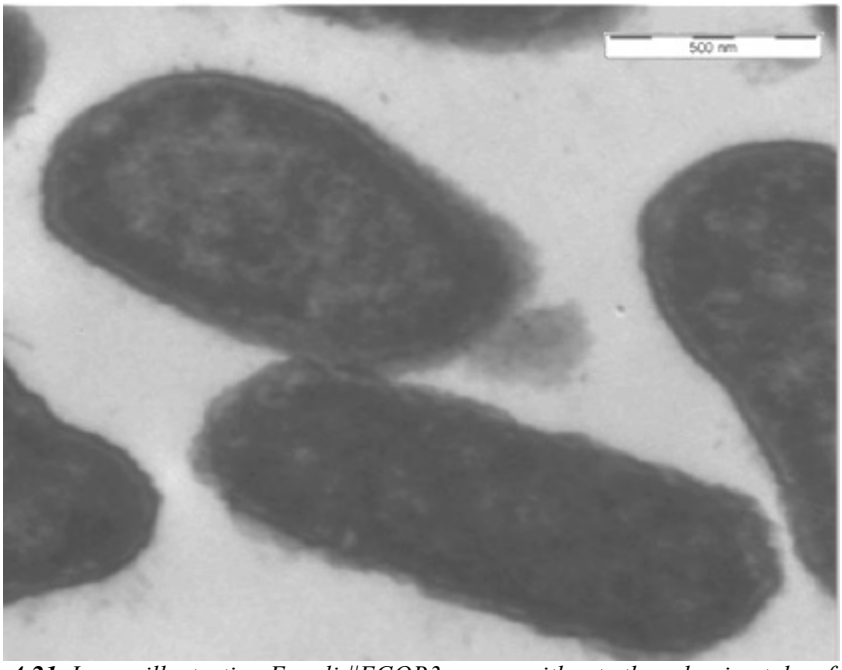


Figure 4.21. *Image illustrating E. coli #ECOR3 grown without ethanolamine taken from the bottom of the density gradient band. No electron dense bodies can be observed.*

4.4. Conclusion

Originally the focus of this study was to investigate the hypothesis that microcompartment expression inside a bacterial cell would affect an intrinsic physical characteristic of the whole cell: buoyant cell density. Due to the unique features of bacterial microcompartments, internal structures containing closely packed enzymes that form only when induced, it was hypothesized that their induction in a bacterial cell would lead to increased buoyant cell density in the same fashion as has been observed for inclusion body formation. To investigate this hypothesis, I made observations of cells with induced native Pdu MCP (*L. reuteri* and *Y. enterocolitica)*, induced native Eut MCP *(E. coli* ECOR strains) and recombinant microcompartments (Pdu MCP and Pdu shell only). Selecting these models also allowed observation of any potential differences between Gram positive *(L. reuteri)* and Gram negative cell *(E. coli, Y. enterocolitica)* cell types.

Growth in conditions known to induce native microcompartment formation resulted in increased buoyant density of *Y. enterocolitica* (Gram negative) (*Figure 4.8*) and *Lactobacillus reuteri* 20016 (Gram positive) (*Figure 4.7*) compared to growth in non-inducing conditions. Corresponding increases and decreases in sedimentation were observed. Increased sedimentation could reflect the known effect of microcompartment gene expression in elongating cells (Liang, Frank, Lunsdorf, Warren and Prentice, submitted for publication), because larger cells should sediment more rapidly, but slower sedimentation was observed for empty microcompartment expressing cells (*Figure 4.14*) which were correspondingly less dense.

This suggests “empty’ microcompartments seen to lack an electron dense core on TEM are indeed lacking some normal cytoplasmic contents and represent a separate enclosure within the cell.

Screening the ECOR library, which provided the majority of the *E. coli* strains utilized in this study, approximately 46% of the tested ECOR *E. coli* strains displaying a Eut-positive phenotype. These positive strains were from various phylogenetic branches of the ECOR library *(Figure 2.2 and Table 4.1)* as in the previous study (Lawrence & Roth, 1996). However, of the 53 strains screened in the current study, 47 were Eut-positive in the previous study whereas in the current study only 24 strains were identified as Eut positive. The strains identified by this study as Eut-negative are also marked on the phylogenetic ECOR tree *(Figure 2.2 and Table 4.2)*. This apparent discrepancy is most likely due to *in vitro* selection against the ethanolamine operon during growth on rich media, leading to the inactivation of the operon in many of the ECOR strains.

Eut-positive ECOR strains grown in the presence of ethanolamine and B12 exhibited diauxic growth (growth in two phases) (Figure 4.4). This trait was not identifiable in eut-negative strains. To identify which aspect of this diauxic growth curve corresponds with ethanolamine metabolism, serial assays (ethanolamine and acetaldehyde) would be required.

These identified strains were observed, alongside the *L. reuteri* and *Y. enterocolitica* strains, for effects relating to the hypothesis regarding buoyant cell density. The Pdu-positive strains displayed expected effects, wherein Pdu-induced samples appeared to be denser, and have a higher buoyant density than un-induced cells. This observance is in agreement with published literature about

recombinant protein expression (Cheng, 1983), (Pandey *et al.,* 2013). Interestingly, empty microcompartments appeared to display decreased cell density vs. the recombinant Pdu MCP, *pAR3114*. A direct comparison with *E. coli* not expressing any microcompartments would be required to show if the empty microcompartments were less dense than normal cytoplasm and the recombinant Pdu microcompartment was more dense than normal cytoplasm.

However, with regards to the native Eut microcompartment, the opposite effect was observed, where the ethanolamine-induced MCP containing cells appear to be less dense, or to have a lower buoyant density that the uninduced cells. This result was consistent across all observed *E. coli* strains.

The reasons for these differing buoyant densities are still unclear. The Eut MCP has been previously linked to pathogenic *E. coli* competitive fitness in the intestines (Thiennimitr *et al.,* 2011) due to the abundance of ethanolamine from membrane cell turnover, in the same way as Pdu microcompartments (Goudeau *et al.,* 2012) but Eut microcompartments have been more difficult to extract and identify than Pdu microcompartments (Choudhary *et al.,* 2012).

If we assume that Eut microcompartments are similarly constructed to Pdu microcompartments, there are two hypotheses based on cell membrane or microcompartment permeability that could explain these unusual results. These relate to the cell membrane permeability of the substrate ethanolamine at ambient pH, or the retention in some form of ammonium ions generated by ethanolamine deaminase activity (Figure 3.1, 5.1).

The bacterial cell membrane permeability of ethanolamine has previously been examined by (Penrod *et al.,* 2004) where they established that ethanolamine

transferred across the cell membrane in a pH-dependant manner. Ethanolamine can pass through the cell membrane when uncharged, with this proportion decreasing at pH below the pKA of 9.4. (Lide, 2004). This diffusion of uncharged ethanolamine is likely facilitated by EutH (ethanolamine permease), which can shift the balance of uncharged ethanolamine.

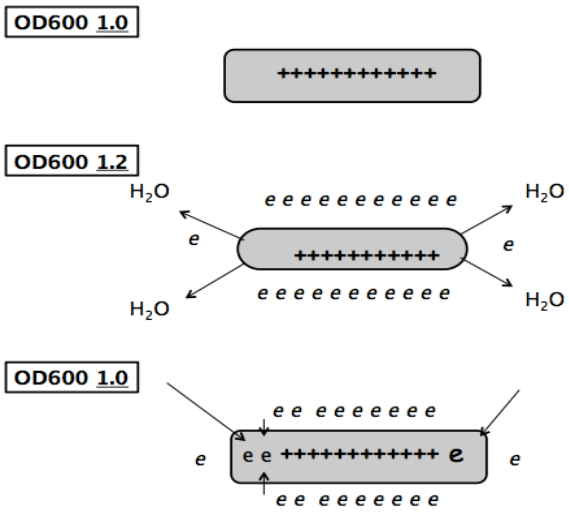


Figure 5.1. *Schematic illustrating the initial shrinkage of the cell due to presence of ethanolamine in the environment. After this initial osmotic shift, balance is restored in the cell, with gradual uptake of ethanolamine.*

This can typically occur at within the pH range of 7-8. This can be illustrated by the observation of a large decrease in ethanolamine uptake in knockout models (Roof & Roth, 1989). Further studies (Penrod *et al.,* 2004) indicated an osmotic pressure associated with the presence of ethanolamine, with cells shrinking initially on addition of ethanolamine at a pH in range 7-8. Therefore it would be expected that ethanolamine-metabolising cells would initially appear less dense (due to shrinkage) before swelling again due to resumption of osmotic balance. In *Salmonella,* this initial shrinkage and then re-swelling can take approximately 10 minutes (Penrod *et al.,* 2004). However in the isopycnic centrifugation, and the sedimentation tests, there was no ethanolamine present in the test medium –

cultures were only exposed to ethanolamine and B12 during initial growth. For testing analysis, cultures were placed in PBS (isopycnic centrifugation) and unsupplemented LB (sedimentation). To explore this discrepancy further, experimentation with a point mutation of the EAL region would be interesting.

Alternatively, the role of ammonia ions in attaining neutral buoyancy has been identified in cephalopods (Seibel *et al.,* 2004). Ammonium (MW 18.03846) is a lighter cation than sodium (MW 22.989769) and replacement of sodium by ammonium in sequestered extracellular compartment fluid decreases buoyant density of the organism.

$$NH_4^+ \rightarrow NH_3 + H^+ \qquad pKa = 9.24$$

Ammonium -> Ammonia + H^+

Figure 5.2. *Equation illustrating the breakdown of ammonium to ammonia, releasing hydrogen.*

At physiological pH most of the total ammonium nitrogen is in the charged ammonium form, for which the cell membrane is impermeable. However, the small fraction of gaseous ammonia is continuously lost via the cell membrane and imposes an ammonium requirement. Ammonia/ammonium ion uptake by *E. coli* is very tightly regulated because ammonia is the preferred nitrogen source for *E. coli* and once taken up a proportion freely diffuses back through the cell membrane in this way (Kim *et al.,* 2012). If large amounts of ammonium were generated by ethanolamine metabolism, the increased ammonium content might displace sodium and reduce density. Additionally, if the microcompartment provided any form of ammonia retention, for example by reduced pH decreasing the proportion of total ammonium nitrogen as ammonia, this could concentrate

ammonium ions relatively to other cations within the microcompartment and potentially decrease cell buoyant density over a longer period.

A mutant disruption of the EAL region, whilst leaving the MCP structure intact, would be the next step in progressing this study and identifying the most probable hypothesis. Another potential progression would be the analysis of single cells, as this study focused on analysis of a population. This could be achieved using the techniques applied by (Godin *et al.,* 2010), where they developed a dynamic fluidic control system which enabled the measurement of cell buoyant mass using a suspended microchannel resonator (SMR). As individual cells transit the microchannel, a shift in the resonant frequency of the SMR can be observed which corresponds to the buoyant mass of the cell (Godin *et al.,* 2010).

A further point of note is regarding cell phase or cell growth. Whilst this was not specifically observed in this study, there has been conflicting evidence regarding variations in cell density and cell growth phase (Makinoshima *et al.,* 2002), (Kubitschek *et al.,* 1984). For this study, incubation time prior to centrifugation was sufficient to enter stationary phase, but more specific study into the potential connection between cell density and cell growth phase would be an interesting progress of this work.

4.5. References

- Bertin Y., Girardeau J., Chaucheyras-Durand F., Lyan B., Pujos-Guillot E., Harel J., Martin C. (2010) Enterohaemorrhagic *Escherichia coli* gains a competitive advantage by using ethanolamine as a nitrogen source in the bovine intestinal content. Environmental Microbiology 13:365-377.
- Bobik T., Havemann G., Busch R., Williams D., Aldrich H. (1999) The Propanediol Utilization (pdu) Operon of *Salmonella enterica* Serovar Typhimurium *LT2* Includes Genes Necessary for Formation of Polyhedral Organelles Involved in Coenzyme B12-Dependent 1,2-Propanediol Degradation. Journal of Bacteriology p. 5967–5975.
- Bradbeer C. (1964) The Clostridial Fermentations of Choline and Ethanolamine. The Journal of Biological Chemistry 240-252.
- Cheng Y. (1983) Increased cell buoyant densities of protein overproducing *Escherichia coli* cells. Biochemical and Biophysical Research Communications 111:104-111
- Choudhary S., Quin M., Sanders M., Johnson E., Schmidt-Dannert C. (2012) Engineered Protein Nano-Compartments for Targeted Enzyme Localization. PLoS ONE 7:e33342
- Drews G., Niklowitz W. (1956) Beitrage zur Cytologie der Blaualgen. Archives of Microbiology 24:147–62
- Eroglu E., Melis A. (2009) Density Equilibrium method for the quantitative and rapid in situ determination of lipid, hydrocarbon, or

biopolymer content in microorganisms. Biotechology and Bioengineering 102:1406-1415

- Godin M., Delgado F., Son S., Grover W., Bryan A., Tzur A., Jorgensen P., Payer K., Grossman A., Kirschner M., Manalis S. (2010) Using buoyant mass to measure the growth of single cells. Nature Methods 7:387-390

- Goudeau D., Parker C., Zhou Y., Sela S., Kroupitski Y., Brandl M. (2012) The *Salmonella* Transcriptome in Lettuce and Cilantro Soft Rot Reveals a Niche Overlap with the Animal Host Intestine. Applied and Environmental Microbiology 79:250-262

- Havemann, G. D., Sampson, E. M., Bobik, T. A. (2002) PduA is a shell protein of polyhedral organelles involved in coenzyme B12 -dependent degradation of 1,2-propanediol in *Salmonella enterica* serovar Typhimurium LT2. Journal of Bacteriology. 184:1253–1261.

- Kerfeld, C. A., Heinhorst, S., Cannon, G. C. (2010). Bacterial Microcompartments. Annual Review of Microbiology 64:391–408.

- Kim, M., Zhang, Z., Okano, H., Yan, D., Groisman A., Hwa, T. (2012) Need-based activation of ammonium uptake in *Escherichia coli*. Molecular System Biology 8:616-630.

- Krouwer J., Babiors B. (1977) Mechanism of Action of Ethanolamine Ammonia-lyase, an Adenosylcobalamin-dependent Enzyme. Journal of Biological Chemistry 252:5004-5009

- Kubitschek H., Baldwin W., Schroeter S., Graetzer R. (1984) Independence of buoyant cell density and growth rate in *Escherichia coli.* Journal of Bacteriology 158:296-299
- Lawrence J., Roth J. (1996) Evolution of Coenzyme BI2 Synthesis Among Enteric Bacteria: Evidence for Loss and Reacquisition of a Multigene Complex. Genetics 142:11-24
- Lide, D. R. (2001) Handbook of Chemistry and Physics (Chemical Rubber Publishing, Cleveland)
- Makinoshima H., Aizawa S., Hayashi H., Miki T., Nishimura A., Ishihama A. (2003) Growth Phase-Coupled Alterations in Cell Structure and Function of *Escherichia coli.* Journal of Bacteriology 185:1338-1345.
- Makinoshima H., Nishimura A., Ishihama A. (2002) Fractionation of *Escherichia coli* cell populations at different stages during growth transition to stationary phase. Molecular Microbiology 43:269-279
- Mizushima S., Miura T., Ishida M. (1967) Fractionation by density gradient centrifugation of membranous organella of *Bacillus megaterium*. Journal of Biochemistry 61(1):146–148.
- Ochman H., Selander R. (1984) Evidence for clonal population structure in *Escherichia coli*. Proceedings of the National Academy of Science 81:198-201.
- Pandey N., Sachan A., Chen Q., Ruebling-Jass K., Bhalla R., Panguluri K., Rouviere P., Cheng Q. (2013) Screening and identification of genetic

loci involved in producing more/denser inclusion bodies in *Escherichia coli.* Microbial Cell Factories 8:12-43

- Parsons J., Dinesh S., Deery E., Leech H., Brindley A., Heldt D., Frank S., Smales C., Lunsdorf H., Rambach A., Gass M., Bleloch A., McClean K., Munro A., Rigby S., Warren M., Prentice M. (2008) Biochemical and Structural Insights into Bacterial Organelle Form and Biogenesis. Journal of Biological Chemistry 283:14366-14375

- Penrod J., Mace C., Roth J. (2004) A pH-Sensitive Function and Phenotype: Evidence that EutH Facilitates Diffusion of Uncharged Ethanolamine in *Salmonella enterica*. Journal of Bacteriology 186:6885-6890

- Penrod, J. T., Roth, J. R. (2006) Conserving a Volatile Metabolite: a Role for Carboxysome-Like Organelles in *Salmonella enterica*. Journal of Bacteriology 188:2865–2874.

- Pertoft H. (2000) Fractionation of cells and subcellular particles with Percoll. Journal of Biochemistry 44:1–30.

- Ramsay J., Williamson N., Spring D., Salmond G. (2011) A quorum-sensing molecule acts as a morphogen controlling gas vesicle organelle biogenesis and adaptive flotation in an enterobacterium. Proceedings of the National Academy of Sciences 108:14932-14937.

- Reuter S., Connor T., Barquist L., Walker D., Feltwell T., Harris S., Fookes M., Hall M., Petty N., Fuchs T., Corander J., Dufour M., Ringwood T., Savin C., Bouchier C., Martin L., Miettinen M., Shubin M.,

Riehm J., Laukkanen-Ninios R., Sihvonen L., Siitonen A., Skurnik M., Falcao J., Fukushima H., Scholz H., Prentice M., Wren B., Parkhill J., Carniel E., Achtman M., McNally A., Thomson N. (2014) Parallel independent evolution of pathogenicity within the genus *Yersinia*. Proceedings of the National Academy of Sciences 111:6768-6773.

- Roof D., Roth J. (1989) Functions Required for Vitamin B12-Dependent Ethanolamine Utilization in *Salmonella typhimurium*. Journal Of Bacteriology 3316-3323

- Sambrook J., Fritsch E.F., Maniatis T. (1989) Molecular Cloning: A Laboratory Manual, 2nd edn. Cold Spring Harbor Laboratory Press, Cold Spring Harbor, NY

- Srikumar S., Fuchs T. (2010) Ethanolamine Utilization Contributes to Proliferation of *Salmonella enterica* Serovar Typhimurium in Food and in Nematodes. Applied and Environmental Microbiology 77:281-290.

- Sriramulu, D. D., Liang, M., Hernandez-Romero, D., Raux-Deery, E., Lunsdorf, H. Parsons, J. B., Warren, M. J., Prentice, M.B., (2008). *Lactobacillus reuteri* DSM 20016 Produces Cobalamin-Dependent Diol Dehydratase in Metabolosomes and Metabolizes 1,2-Propanediol by Disproportionation. Journal of Bacteriology 190:4559–4567.

- Stojiljkovic I., Baumer A.J., Heffron F. (1995) Ethanolamine utilization in *Salmonella typhimurium*: nucleotide sequence, protein expression, and mutational analysis of the cchA cchB eutE eutJ eutG eutH gene cluster. Journal of Bacteriology 177:1357–66.

- Thiennimitr P., Winter S., Winter M., Xavier M., Tolstikov V., Huseby D., Sterzenbach T., Tsolis R., Roth J., Baumer A. (2011) Intestinal inflammation allows *Salmonella* to use ethanolamine to compete with the microbiota. Proceedings of the National Academy of Sciences 108:17480-17485.
- Wirth T., Falush D., Lan R., Colles F., Mensa P., Wieler L., Karch H., Reeves P., Maiden M., Ochman H., Achtman M. (2006) Sex and virulence in *Escherichia coli*: an evolutionary perspective. Molecular Microbiology 60:1136-1151.
- Woldringh, C., Binnerts J., Mans A. (1981) Variation in *Escherichia coli* Buoyant Density Measured in Percoll Gradients. Journal of Bacteriology 148:58-63

Chapter V

Extraction and imaging of bacterial microcompartments.

Contents

5.0. Abstract

5.1. Introduction

5.2. Materials & Methods

5.2.1. Bacterial strains & culture conditions

5.2.2. Microcompartment extraction methodology

5.2.2.1. BPER method

5.2.2.2. YPER method

5.2.2.3. BPER Gram positive cell variation

5.2.3. Imaging & extraction

5.2.3.1. Transmission Electron Microscopy

5.2.3.2. Focused Ion Beam Scanning Electron Microscopy

5.2.3.2.1. Sample Optimization

5.3. Results & Discussion

5.3.1. Microcompartment Extractions

5.3.2. Imaging Extractions

5.3.2.1. Electron Microscopy

5.3.2.2. FIB-SEM Cyro-Imaging

5.4. Conclusion

5.5. References

5.0. Abstract

The ability to identify and extract bacterial microcompartments from bacterial cells is a key to research in this field, and an important aspect in distinguishing microcompartments from gas vesicles or other similarly sized intracellular components. Due to their proteinaceous nature, their extraction from cells is possible by adaptation of standard cell fractionation techniques, but poses technical difficulties. These difficulties include possible contamination from other substances within the bacterial cell, including other proteins and membrane fragments, and failure to obtain intact microcompartments rather than fragments.

A number of different techniques have been described for microcompartment extraction, the majority of which are applicable only to Gram-negative cells. In this study we present the application and adaptation of these different techniques to our strains of focus, including a novel approach to extraction from Gram positive cells.

Following on from these extraction experiments, I endeavoured to image these extracted microcompartments, along with whole cell samples, to identify any potential visual differences in the structure or presence of the microcompartments. This has been undertaken by using transmission electron microscopy (TEM) on extracted microcompartments and also through the novel application of the focused ion beam scanning electron microscope (FIB-SEM) to section whole cells.

Microcompartment extractions were performed on *E. coli* strains containing both recombinant and native microcompartments. Additional novel changes to the

existing extractions methodology facilitated the extraction of the Pdu microcompartment from *Lactobacillus reuteri,* which had been previously unreported. Visualisation of the samples on TEM analysis highlighted putative microcompartments, which were also observable within whole bacterial cells. The use of the FIB-SEM was novel in its application to bacterial samples and required a number of optimisation steps. The use of glycerol protected the cells against excess ice accumulation, but may have led to cell aggregation, which created difficulties in attributing visualised putative microcompartments to individual cells.

5.1. Introduction

Bacterial microcompartments (MCPs) were originally identified within bacterial cells in the 1950s (Drews & Niklowitz, 1956). They possess a distinct polygonal shape, which triggered their identification by electron microscopy. In recent literature, more techniques have emerged to extract whole MCPs from cells, with an increased focus on quantifying the structural proteins (Sinha *et al,* 2012), (Sargent *et al,* 2013).

Extracting the bacterial MCP is a process that heavily depends upon the lysis of the cell. This step can indeed be the most difficult, as failure to correctly lysis will lead to a low quality yield of MCP protein. The majority of MCP extractions in literature have focused on Gram negative cells (Sinha *et al,* 2012), (Havemann *et al,* 2003), which may be potentially due to the difficulties associated with obtaining good quality MCP from Gram positive cells, as the presence of the peptidoglycan wall can prevent sufficient cell lysis.

Following cell lysis, the sample undergoes a procedure similar to a sucrose gradient, with the objective of separating the MCP from the cell. This initial technique has since been refined via the use of detergents and protease inhibitors, to remove the difficulty of contaminating proteins (Sinha *et al,* 2012).

However, whilst it has been possible to view these extracts under the electron microscope, the ability to view the MCP in situ in the bacterial cell would potentially reveal additional information regarding the dimensions and intracellular population of the MCP. To achieve this, collaboration began between the Prentice lab and the Tyndall National Institute. The Tyndall National Institute had recently acquired a focused ion beam scanning electron

microscopy (FIB-SEM), with applications mainly focusing on materials technology, but with a view to experiment with biological samples. This provided an opportunity to explore the various viewpoints available for identifying the MCPs whilst present within in the bacterial cell.

The functionality of the FIB-SEM is based upon its ability to make a deliberate focused cut in the sample. The narrow ion beam, which is typically gallium, cuts into the sample, which has been covered with a platinum-palladium layer. An electron beam is then angled at the ion beam, and scans the resulting cut, producing an image.

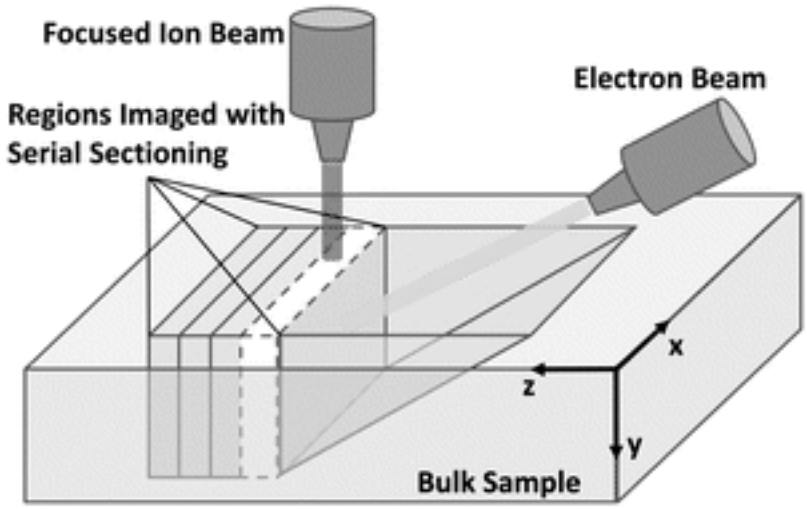


Figure 5.1. *Diagram illustrating the cut technique of the FIB-SEM (credit: Cocco et al, 2013)*

The cut surface is then milled by the ion beam, and a second cut made, allowing the imaging process to be repeated. Through successive cross-sectional cuts, the produced images can be reconciled together, allowing a 3-dimension object to be created using software technology.

As previously mentioned, this technology has been widely used in recent years for materials science (Phelan *et al,* 2012) so a foray into the biological sphere is a recent approach (Alhede *et al,* 2012), (Soares Medeiros *et al,* 2012).

The choice to utilize the FIB-SEM for visualization of the MCPs was to alleviate some of the issues typically associated with standard TEM. The embedding procedure required for TEM usage typically requires the infiltration of the sample with transitional solvent, followed by infiltration with resin, then embedding, curing and finally cutting (Milani *et al,* 2007). This series of processes can lead to disruption and warping of the cell's natural intracellular architecture, and can prevent obtaining reliable insight in to molecular structures (Pilhofer, 2010). The benefit of using cryo-imaging is the removal of these preparative treatments, as the cells are observable in a fully hydrated state. With FIB-SEM, there is also possibility to recreate 3D reconstructions of samples using the previously mentioned ability of the FIB to sequentially slice and image samples (Milani *et al,* 2007).

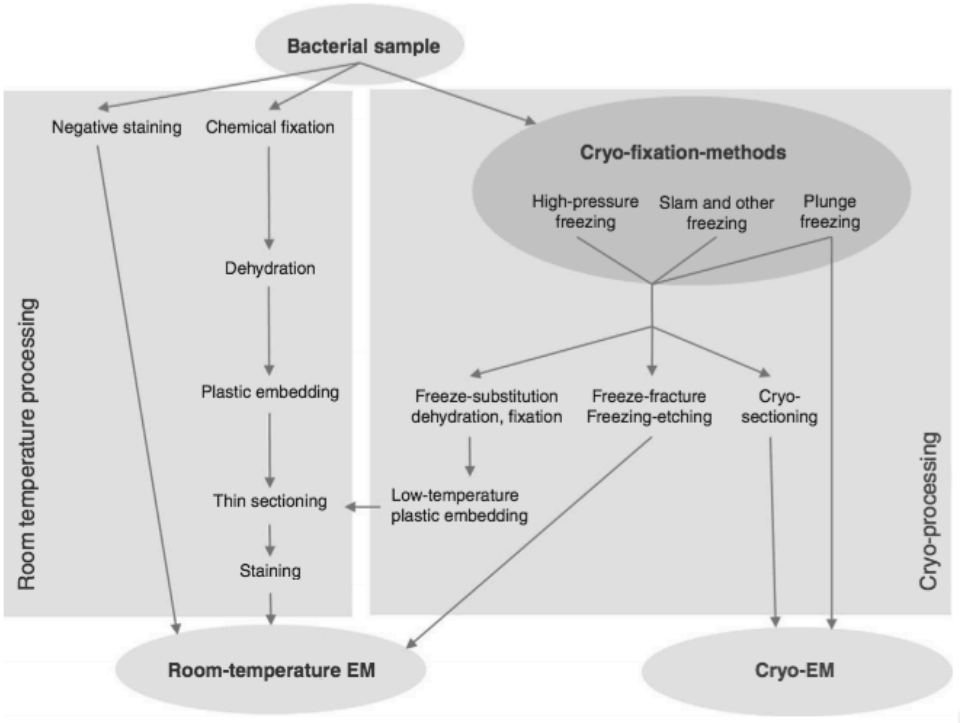


Figure 5.2. *Schematic illustrating electron microscopy imaging methods (credit Pilhofer, 2010).*

5.2. Materials & Methods

5.2.1. Bacterial strains & culture conditions

Bacterial strains used in this study are listed *(Table 3.1).* A variety of different strains, Gram-positive and Gram-negative, native and recombinant, were used in this study.

Strain	Origin	Presence of MCP
ECOR Library (ECOR #1-54)	Dr. David Clarke, University College Cork	Selected strains display positivity on ethanolamine McConkey agar
***Yersinia enterocolitica* 53/03**	Dr. Tamara Ringwood, University College Cork	Display positivity on propanediol McConkey agar, presence of *pdu* operon genes
***Yersinia enterocolitica* 13/03**	Dr. Tamara Ringwood, University College Cork	Display positivity on propanediol McConkey agar, presence of *pdu* operon genes
***Yersinia enterocolitica* NZ3**	Dr. Tamara Ringwood, University College Cork	Display positivity on propanediol McConkey agar, presence of *pdu* operon genes
***Lactobacillus reuteri* DSM 20016**	Prentice lab	Display positivity on propanediol MRS agar, presence of *pdu* operon genes
E. coli* JM109 *pAR3114	Dr. Joshua Parsons, University of Kent	Display positivity on propanediol LB agar, presence of *pdu* operon genes
***E. coli* JM109**	Prentice lab	No Pdu MCP genes present in genome

Table 5.1*. Table indicating strains used in study and their origins.*

E. coli strains with ethanolamine positivity were grown on ethanolamine and B12-supplemented McConkey agar, and in ethanolamine and B12-supplemented LB broth. *pAR3114 E. coli* JM109, which utilizes 1,2-propanediol, was grown in LB broth supplemented with 1,2-propanediol and B12. *Yersinia* strains, which utilize 1,2-propanediol, were grown in 1,2-propanediol supplemented McConkey agar and supplemented LB broth. Finally *Lactobacilli* strains were cultured in

1,2-propanediol supplemented de Man-Rogosa-Sharpe (MRS) and modified MRS (*Table 3.5*) and grown anaerobically at 37°C.

Ingredients	Amount (per Litre)
Soy Peptone	20g
Ox-Bile	5g
NaCl	5g
Neutral Red	0.075g
Agar	15g
Adjust to pH 7.4 ±0.2 using 4NaOH	
Ethanolamine (50mM) *	5g
1,2-propanediol (40mM) $^{+}$	40mL
B12 (200nM)	600µL

Table 5.2. *Composition of MacConkey agar, supplemented with either i) ethanolamine* and B12 or ii) 1,2-propanediol^{+} and B12, which were added post-autoclave.*

Ingredients	Amount (per Litre)
Monopotassium Phosphate	3.94g/L
Dipotassium Phosphate	4.97g/L
Ammonium Sodium Phosphate Tetrahydrate	3.5g/L
Magnesium Sulphate	0.2g/L
Ethanolamine (50mM) *	5g/L
Adjust to pH 7.2 ±0.2 using 4NaOH	
B12 (200nM) *	600µL

Table 5.3. *Recipe list for NCE media, supplemented with ethanolamine, which was added post-autoclave.*

Material	Quantity
Tryptone from casein	10g/L
Sodium chloride	10g/L
Granulated Yeast Extract	5g/L
Deionised Water	1L
Ethanolamine (50mM) *	5g/L
1,2-propanediol (40mM) $^{+}$	40mL
B12 (200nM) *	600µL

Table 5.4. *Recipe for Luria Broth (LB) for the growth of E. coli. Supplemented with either i) ethanolamine* and B12 or ii) 1,2-propanediol^{+} and B12, which were added post-autoclave.*

Material	Quantity
MRS broth	55g/L
Deionised Water	1L
1,2-propanediol (40mM) [+]	40mL
B12 (200nM) *	600µl

Table 5.5. *Composition of de Man-Rogosa-Sharpe (MRS) for the growth of lactobacilli, supplemented with 1,2-propanediol and B12*

Material	Quantity
Bacto-peptone	5g/L
Lab-Lemco	4g/L
Granulated Yeast Extract	2g/L
Tween 80	0.5mL/L
K_2HPO_4	1g/L
$NaH_2PO_4.H_2O$	3g/L
CH_3COONa	0.6g/L
$MgSO_4.7H_2O$	0.3g/L
$MnSO_4.H_2O$	0.04g/L
1,2-propanediol (40mM) [+]	40mL
B12 (200nM) *	600µL

Table 5.6. *Composition of MRS-Modified (MRS-MOD) for the growth of L. reuteri. Supplemented with 1,2-propanediol and B12*

5.2.2. Microcompartment extraction methodology

Initially, two differing methods of MCP extraction or purification were used, both of which utilized detergents to remove the whole MCP.

5.2.2.1. B-PER Method

This method was originally presented in the PhD thesis of Gregory Havemann, of the Bobik lab, and its most current iteration was published in 2012 (Sinha *et al,* 2012) and utilized the proprietary detergent B-PER. B-PER (Bacterial Protein Extraction Reagent, Pierce, Thermo Scientific) is a proprietary detergent product designed to lyse cells obtain high molecular weight proteins without

denaturation. This protocol includes a number of additional steps designed to purify the extraction process via different supernatants and pellets.

400mL of LB (Luria Bertani) broth was inoculated with 2mL of overnight *E. coli* BL21 culture, containing the recombinant pAR3114, which is a cosmid containing an 30-kb construct including the *pdu* operon (Parsons *et al,* 2008). This recombinant construct expresses the *pdu* MCP when induced with 1,2-propanediol and B12.

This overnight culture was incubated at 30°C shaking at 200rpm, until the OD600 reached 0.4. Cells were then harvested at 8000rpm for 10 minutes at 4°C (Beckman Coulter, rotor JA 25.50). Ensuring the centrifugation was pre-chilled to this temperature was essential to obtain a good quality pellet. The cell pellet was then washed twice with 40mL B-PER Buffer A (50 mM Tris-HCl [pH 8.0], 500 mM KCl, 12.5 mM MgCl2).

Approximately 1g wet weight of cells were resuspended in a mixture of 10mL Buffer A and 15mL B-PER solution, supplemented with 5mM β-mercaptoethanol (Sigma Aldrich), one Complete Protease Inhibitor Cocktail (Roche), 25mg lysozyme (Sigma Aldrich) and 2mg DNase I (Sigma Aldrich). The suspension was incubated at room temperature with shaking at 60 rpm for 30 minutes, and then placed on ice for 5 minutes.

Cell debris was removed by centrifugation twice at 12,000g for 5 minutes at 4°C, with the supernatant (containing MCPs) transferred to a new centrifuge tube after each round of centrifugation. Careful transfer of supernatant is essential to avoid contamination with additional proteins and cell debris. The MCPs were then spun from the suspension at 20,000g for 20 minutes at 4°C (Beckman Coulter,

SW40Ti rotor). The MCPs pellet was resuspended in 1000µL Tris-HCL pH 7.5. As with the Y-PER method, an SDS-PAGE protein gel is typically performed afterwards to confirm the quality of the extraction.

5.2.2.2. Y-PER Method

The Y-PER method was originally provided by our collaborator Dr. Stephanie Frank, University of Kent. The method is based upon utilizing the detergent Y-PER (a yeast-specific version of the previously mentioned B-PER), and protein precipitation using varying salt concentration, as protein solubility is affected by ions. At a very high ionic strength, the additional of a neutral salt increases protein-protein interaction. An increase in the salt concentration causes the charges of the proteins to interact directly with the salt, resulting in hydrophobic patches on the protein, and aggregation, eventually resulting in the precipiatation of the protein. This action of protein solubility decreasing as ionic strength increases is a process referred to as 'salting-out' (Lorsch, 2014).

Y-PER (Y-PER Plus Dialyzable Yeast Protein Extraction Reagent, Pierce, Thermo Scientific) is a proprietary detergent product designed to lyse cells obtain high molecular weight proteins without denaturation. Traditionally, cell lysis was achieved using glass beads or sonication, however the use of a detergent-based cell lysis buffer such as Y-PER eliminates this need to use mechanical treatments involving chemicals, pH and temperature extremes to disrupt the proteinaceous cell envelope. This protocol also utilizes a number of additional steps designed to purify the extraction process via different supernatants and pellets.

200mL of LB (Luria Bertani) broth was inoculated with 2mL of overnight E. coli BL21 culture, containing the recombinant pAR3114. This culture was incubated at 37°C, with shaking at 160 rpm until an OD600 of 0.8 was reached. At this point, the Pdu microcompartment was induced via the addition of 1,2-propanediol and B12, and incubated at 37ºC overnight, with shaking at 160 rpm. Following overnight incubation, the cells were harvested by centrifugation for 10 minutes at 4 °C.

Following harvesting, approximately 1g wet cell pellet was re-suspended in 10 mL Y-PER Plus supplemented with 1 tablet of Complete Protease Inhibitor Cocktail (Roche) and 1250 units Benzonase® Nuclease (5 µL per 10 mL Y-PER). The resulting lysate was incubated for 3 hours at room temperature and gently agitated. The lysate was then pelleted for 5 min at 11,00 x g (Beckman Coulter, rotor JA 25.50) at 4°C.

The supernatant and MCP-containing pellet were collected, with the pellet then re-suspended in 2mL of a solution containing 20mM Tris-HCl (pH 8.0), and 20 mM NaCl. This suspension was centrifuged at 4 °C for 5 min at 11,000 x g, with the resulting supernatant now containing the MCPs.

The NaCl concentration of the supernatant was raised to 80 mM by the addition of 5 M NaCl, followed by centrifugation at 4 °C for 5 min at 11,000 x g. This produced another pellet, which now contained the MCPs.

This MCP-containing pellet was re-suspended in 1 mL of 20 mM Tris-HCl, pH 8.0 and clarified by centrifugation (4 °C for 5 min at 11,000 x g). The final supernatant now contained the purest MCPs, as the initial salt precipitation removed any contaminating proteins, whilst the final salt precipitation released

the MCP proteins. In order to ascertain the quality of the extraction, a sodium dodecyl sulfate-polyacrylamide gel electrophoresis (SDS-PAGE) protein gel is typically performed afterwards to visualize individual MCP proteins.

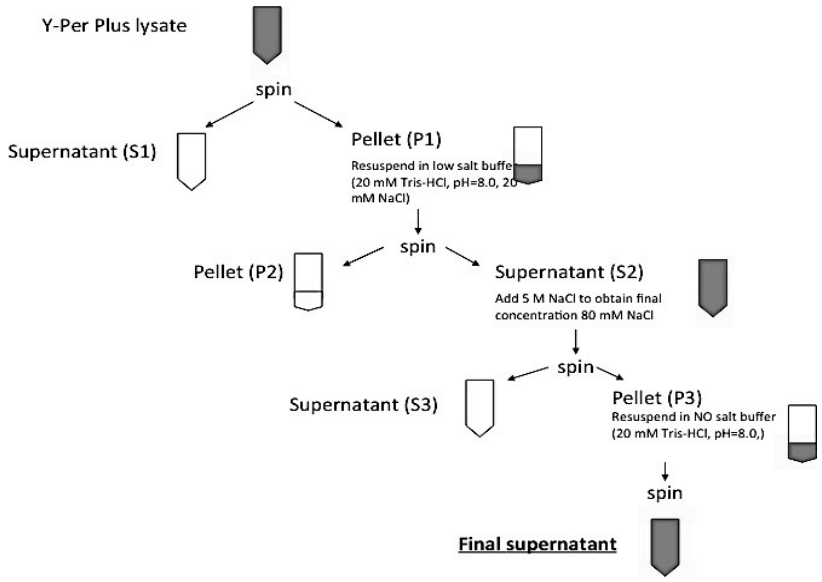


Figure 5.3 *Schematic of Y-PER Method of Microcompartment Extraction as described above.*

B-PER is specifically for bacterial cells however, whilst Y-PER can also be used on yeast cells.

5.2.2.3. B-PER Gram positive cell variation

As previously mentioned, there has been little advancement in MCP extraction for Gram positive cells. To extract the Pdu MCP from *Lactobacillus reuteri* DSM20016, we utilized a variation of the previously mentioned B-PER extraction method. 1L of *Lactobacillus* culture was inoculated with an overnight culture of *L. reuteri* and grown anaerobically at 35°C in MRS media supplemented with 1,2-propanediol and B12 to induce the production of the Pdu MCP, until an OD600nm of 0.5 was reached. Cells were centrifuged as

previously and the pellet washed with washed twice with 40mL B-PER Buffer A (50 mM Tris-HCl [pH 8.0], 500 mM KCl, 12.5 mM $MgCl_2$).

In a novel change to the protocol, 1g of cells were resuspended in 100mL of protoplast buffer). Protoplast buffer is typically used for genome extraction of Gram positive bacteria (Lee-Wickner & Chassy, 1984) and consists of 20 mM Tris-HCL (pH 7.5), 5 mM EDTA, 0.75 M Sucrose, 10 mg/mL Lysozyme and 50 U mutanolysin. The cells were then allowed to incubate in the protoplast buffer for 45 minutes at 37°C. Following this incubation, the protocol reverted to the original protocol, and the cells underwent incubation in a mixture of 10mL Buffer A and 15mL B-PER-II solution (a 2X version of the original B-PER detergent), supplemented with 5mM β-mercaptoethanol, one Complete Protease Inhibitor Cocktail, 25mg lysozyme and 2mg DNase I. The suspension was again incubated for 30 minutes at room temperature, followed then by ice chilling. Centrifugation protocols were the same as the previously mentioned protocol *(Section 3.1.2.1*).

5.2.3. Imaging & electron microscopy

5.2.3.1. Transmission Electron Microscopy (TEM)

After extraction, the samples were then brought for electron microscopy imaging. In University College Cork, the BioSciences Imaging Centre (BSIC), which is located in the Department of Anatomy & Neuroscience, BioSciences Institute provided access to the electron microscopy suite. Extracts were negatively stained using freshly prepared 1% Uranyl Acetate.

For each sample, a drop of bacterial extract suspension was placed onto parafilm and a 400-mesh carbon film copper grid (Agar Scientific, Essex, UK) was

inverted onto the drop for 2 minutes. Excess moisture was wicked away with filter paper. A droplet of 1% Uranyl Acetate stain was placed onto parafilm and the grids were inverted onto the drop for 2 minutes, removed and excess moisture was again wicked away with filter paper. Specimens were then examined using a JEOL Transmission Electron Microscope (TEM) JEM 2000FXII (Jeol Ltd., Tokyo, Japan), operated at 80 kV. Electron micrographs were obtained of areas of interest using a Megaview-III digital camera and AnalySIS software.

5.2.3.2. Focused Ion Beam Scanning Electron Microscopy (FIB-SEM)

As previously mentioned, the FIB-SEM (FEI Helios NanoLab™ 600i DualBeam) was a recent acquisition by the Tyndall National Institute, and as such, its application to biological samples was experimental. Sample preparation and imaging underwent a number of changes to optimize the protocol for our samples.

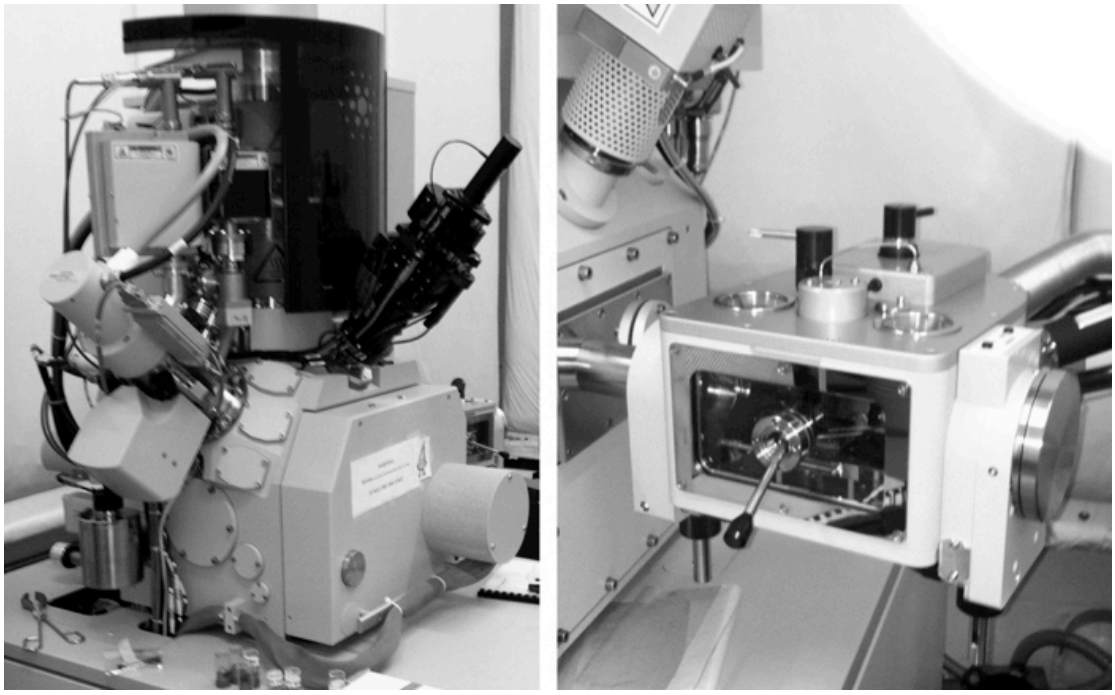


Figure 5.4. *Image of the FEI Helios NanoLab™ 600i DualBeam FIB-SEM and cryo chamber (credit:WormAtlas Database)*

For the purposes of the FIB-SEM, whole cell samples were used. A control sample (*E. coli* JM109, not expressing microcompartments when grown in these conditions*)* was grown in 20mL Luria-Broth (LB) was grown overnight at 37°C with shaking. This was then subcultured to an OD0.1 and allowed to incubate until an approximate OD0.8 was achieved. This culture was then pelleted via centrifugation at 4,000rpm (Beckman Coulter Allegra 64R).

For an experimental culture, the recombinant pAR3114 construct expressing recombinant microcompartments was used as before. 20mL of LB (Luria Bertani) broth was inoculated with 2mL of overnight pAR3114 *E. coli* JM109 culture. This culture was incubated overnight at 37°C, with shaking. This was then subcultured and the Pdu microcompartment was induced via the addition of 1,2-propanediol and B12, and incubated at 37 ºC until an approximate OD0.8 was achieved. This culture was pelleted via centrifugation at 4,000rpm.

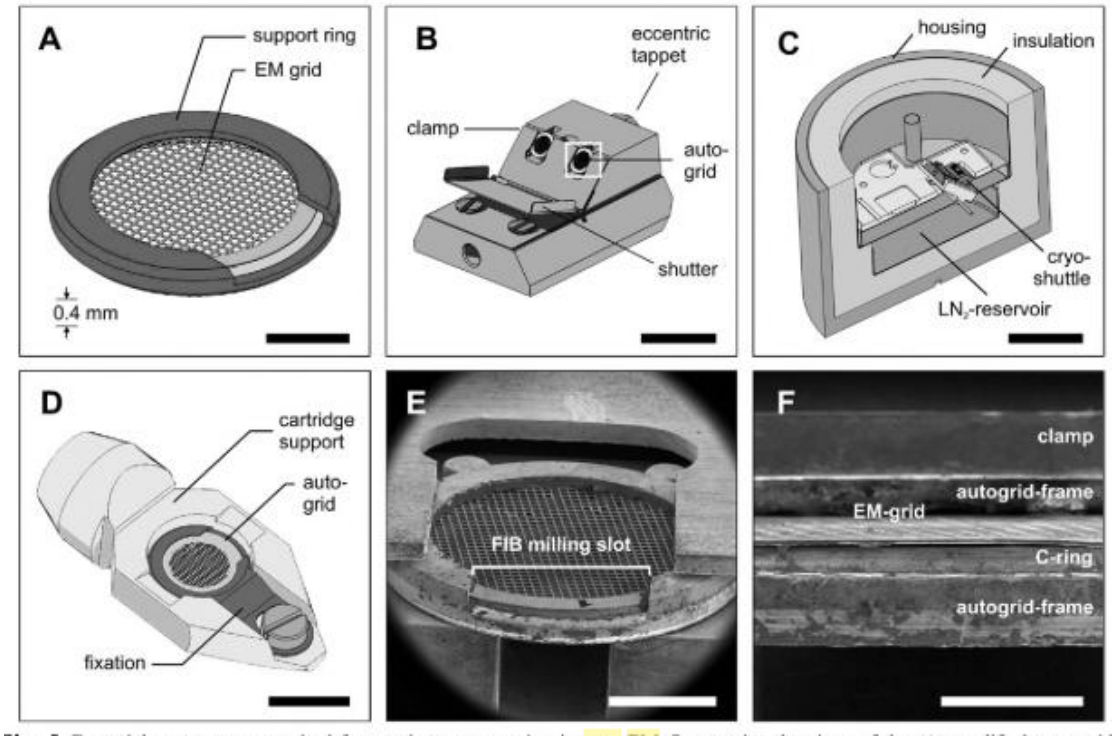


Figure 5.5. *Image illustrating the sample holder required for cryo FIB-SEM*

(Credit:Muller-Reichert & Verkade, 2012)

Approximately 10ul of the sample was loaded onto an aluminum holder, which was then plunge-frozen in liquid nitrogen, as previously mentioned. The frozen sample was then transferred under vacuum to the cryo-preparation chamber of the FIB-SEM. This initial preparation of the stage is delicate process – the stage can require 4 hours of cooling to reach the appropriate temperature, and is highly sensitive to vibration, which can lead to distortion of images. The high vacuum of the cryo-chamber is also another point of contention, as disruption or breaking of the vacuum can lead to the machine becoming unavailable for the rest of a session, therefore a skilled technician is essential for a successful imaging session (Rubino *et al,* 2014).

Following successful loading of the sample into the cryo-chamber, the temperature was then raised to −95ºC for 30 minutes sublimation. Sublimation is a process that removes condensed ice from the sample, which can accumulate

from the plunge-freeze process. Typically sublimation is done for approximately 3 minutes, however on previous imaging sessions, it was observed that the excess ice accumulation obscured viewing of the sample, preventing any quality view of the bacterial cells. The sublimation was gradually increased in 5 minute increments to obtain an optimal sample, with the final 30 minute sublimation providing the clearest view and the least ice accumulation.

In order to avoid excess charge on the sample, and to make the surface electrically conductive, a layer of gold-palladium sputter coating was deployed over the sample to a thickness of 20nm. SEM imaging was taken from number of different sites within the samples, whilst the FIB was utilized on the sites deemed most promising. The electron beam and ion beam can be turned on simultaneously yet operate independently, which allows fine control over sample imaging.

5.2.3.2.1. Sample optimization

As the FIB-SEM is typically used for materials technology, the process of sample optimization was important in determining the success of the use of the machine. Initially, samples were prepared as previously described, and loaded directly into the cryo-chamber of the machine. A key aspect of cryo-EM is the facility to allow samples to be observed without addition of contrast-enhancing agents (Pilhofer *et al,* 2010). Following the use of an un-stained sample, cells were then prepared using 2mL toluidine blue stain. This stain has been used for general bacterial staining for brightfield microscopy (Morris & Groves, 2013).

Due to excess ice accumulation on the sample from the cryo-preparation process, glycerol was also experimentally added to the culture-stain solution, again in a

1:1 ratio. The cryo-preparation is typically achieved via a process called plunge-freezing, where the sample is quickly submerged in liquid nitrogen at approximately −210ºC (Umrath, 1974). However optimization of the sublimation process greatly reduced this ice accumulation. The addition of glycerol, coupled with possible surface tension interaction (Tanner *et al,* 2012), lead to excessive aggregation of the bacteria cultures, preventing the identification of a singular bacteria cell for FIB slicing. To alleviate this, bacitracin, a protein disulfide isomerase inhibitor that prevents cell-cell adhesion (Chapin *et al,* 2001) was added to the sample solution. Bacitracin has been previously utilised as a cell wetting agent to reduce surface tension associated with microscopy samples (Dykstra, 1992). It was added in a 1:1 ratio with the sample culture and toluidine blue.

Previously prepared resin samples of pAR3114 (prepared by Don O'Leary, BSIC) were also sectioned and imaged using the scanning transmission electron microscope) to try and identify optimal contrast/stain levels for usage in the cryo-SEM.

5.3. Results & Discussion

5.3.1. Microcompartment Extractions

As previously described, after extraction, protein samples were run on an SDS-PAGE protein gel to identify the structural and enzymatic proteins indicated through previous analysis as being associated with the presence of the microcompartment. It is typically quite difficult to identify the structural proteins, as these are the smallest and travel to the bottom of the SDS-PAGE gel (Parsons *et al*, 2010).

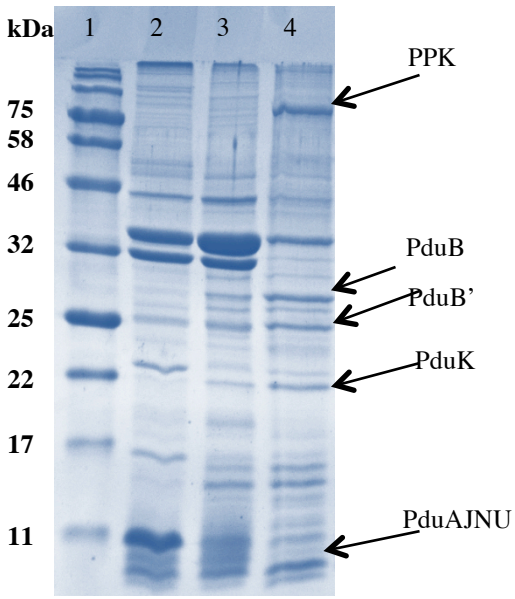


Figure 5.6. *SDS-PAGE illustrating the extraction of the Pdu MCP from pAR3114 using the BPER extraction method. Lane 1 represents the molecular ladder standard (Biolab P7706L). Lane 2 represents the MCP extract containing the enzyme PPK and the structural proteins PduA-PduU. Lane 3+4 are unrelated products.*

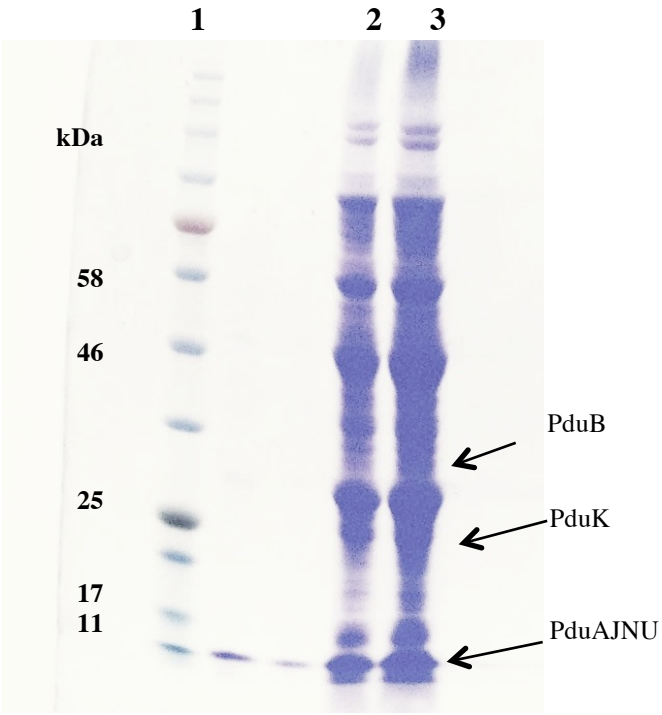


Figure 5.7. *SDS-PAGE illustrating the extraction of the Pdu MCP from L. reuteri using the modified BPER Gram positive extraction method. Lane 1 represents the molecular ladder standard (Biolab P7706L). Lane 2 and 3 represents the MCP extract containing the structural proteins PduA-PduU*

MALDI analysis of these observed proteins was not performed due to the unavailability of the instrument during the required time period, however it can be observed that the positioning of the bands in the protein gels are similar to those previously published (Parsons *et al*, 2010).

5.3.2. Imaging Extractions

5.3.2.1. Electron microscopy

A number of varying microcompartment extractions were imaged by technician Suzanne Crotty of the Bioscience Imaging Centre (SC), while whole sections of samples were imaged by Dr. Don O'Leary (DoL) of the Bioscience Imaging Centre. FIB-SEM images were taken by Dr Michael Schimdt (MS) and Dr

Patrick Carolan (PC) of the Tyndall National Insitutite. Microscopist indicated per image.

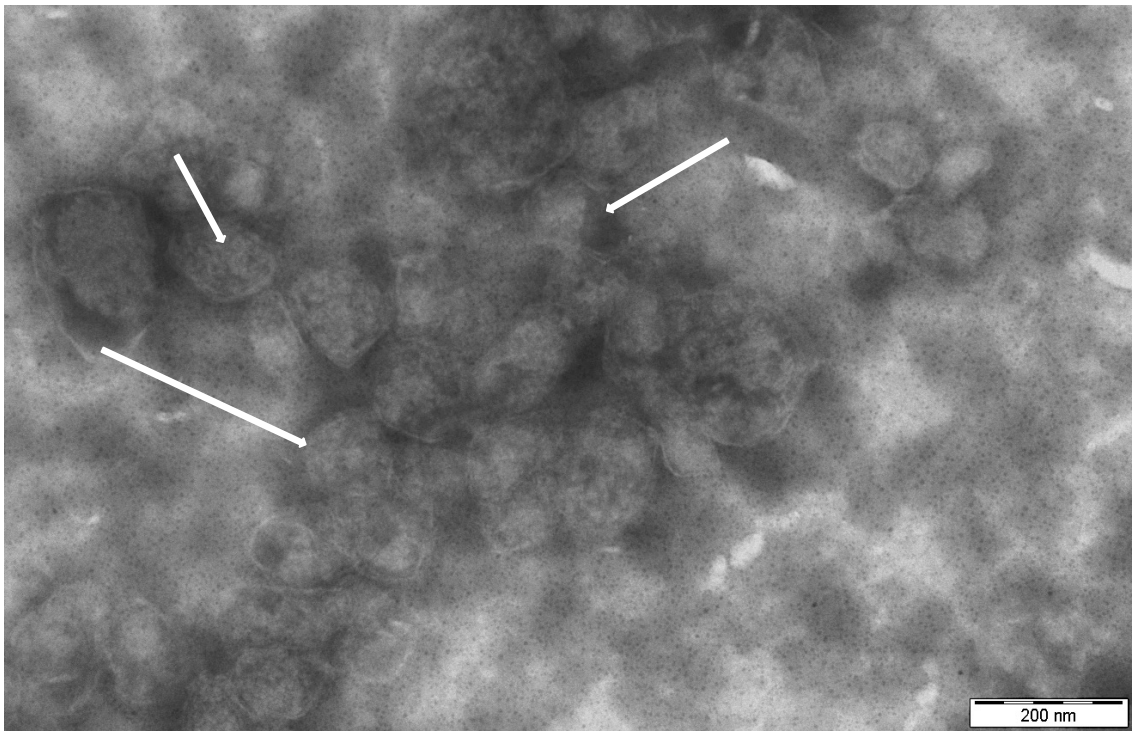


Figure 5.8. *TEM image of the recombinant microcompartment extraction from E.coli (containing genes encoding functional Pdu MCP). Image taken at 80k magnification. (image by SC)*

The above image Figure 5.8 represents a microcompartment extraction from the recombinant *E.coli* JM109 pAR3114, which encodes the Citrobacter propanediol (Pdu) microcompartment. In this image, a number of potential microcompartments can be observed, and are identifiable by their thin electron-dense shell which is often linear. These microcompartments are approximately 100nm in diameter, which is a typical size for these recombinant structures (Parsons *et al,* 2010).

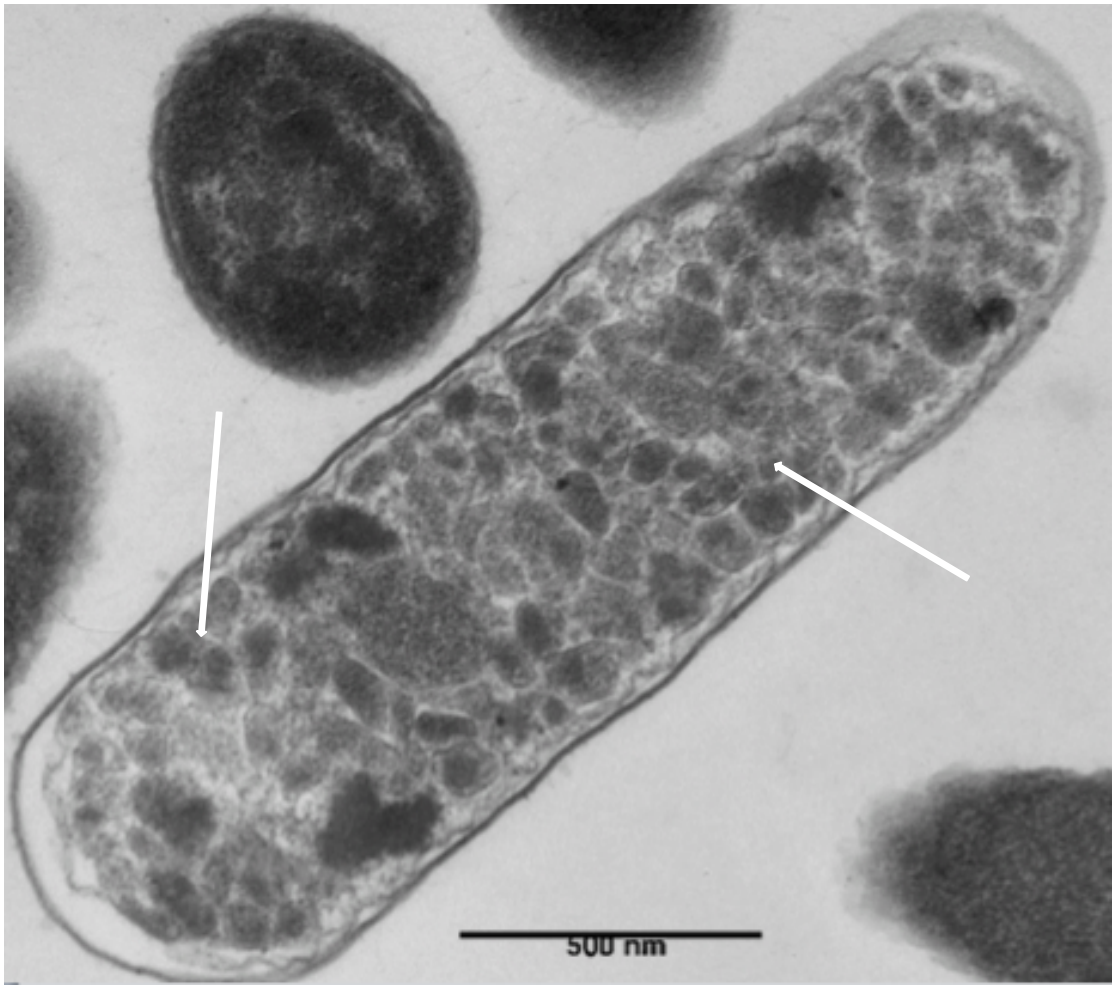


Figure 5.9. *TEM image of the recombinant E.coli JM109 pAR3114 (containing genes encoding functional Pdu MCP) microcompartment extraction. Image taken at 40k magnification. (image by DoL)*

The above image represents a whole cell sample of the pAR3114 recombinant sample, which has been sectioned using a diamond knife, and negatively stained with osmium tetroxide. Obvious electron dense masses, typical of microcompartments, can be observed within the cell, whilst the cell itself is also elongated.

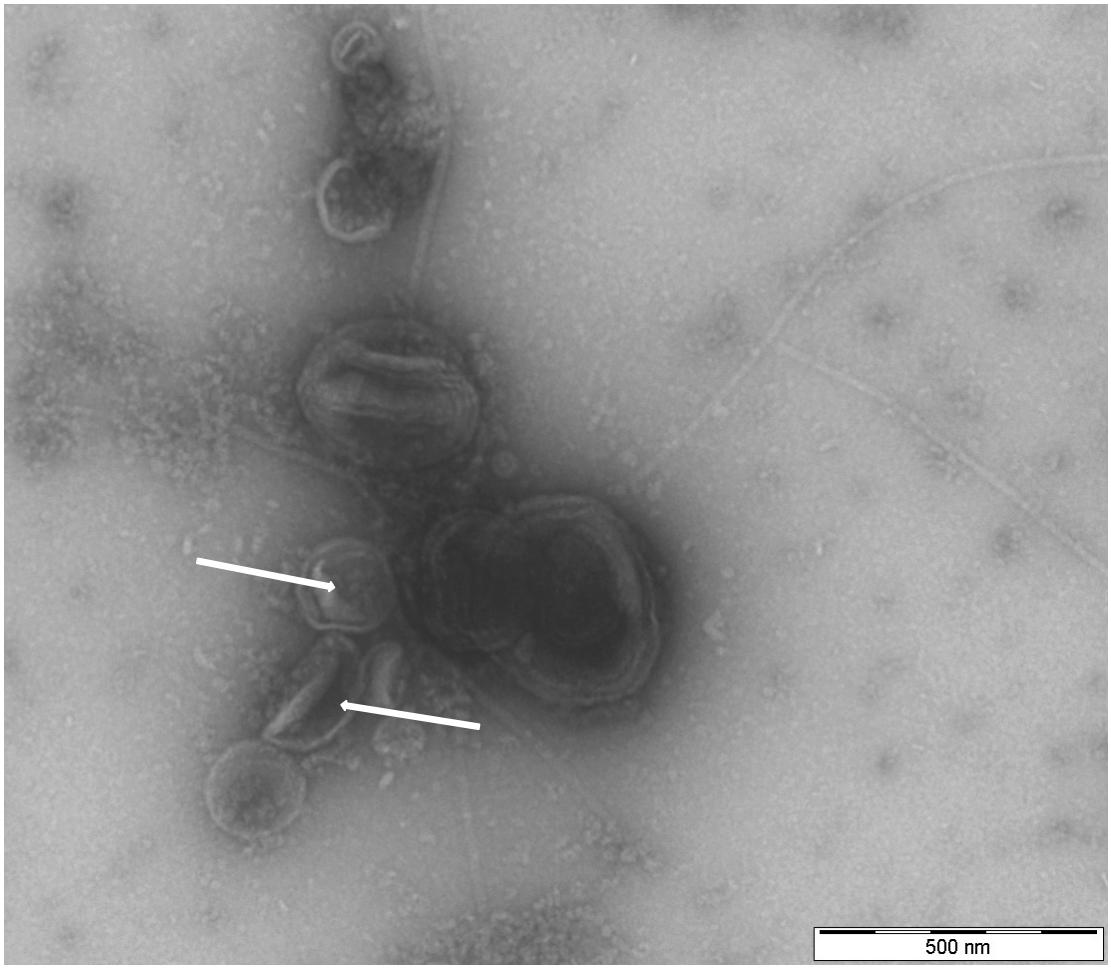


Figure 5.10. *TEM image of the E.coli ECOR#10 Eut microcompartment extraction. Image taken at 40k magnification. (image by SC). Arrows indicate putative microcompartments*

In contrast to the previous extraction image, the microcompartments associated with the metabolism of ethanolamine (Eut) appear more spherical, and less rigid. However (Choudhary *et al*, 2012), previously described this appearance with Eut microcompartments. Again, the Eut microcompartments are approximately 100nm in diameter.

5.3.2.1. FIB-SEM Cyro-Imaging

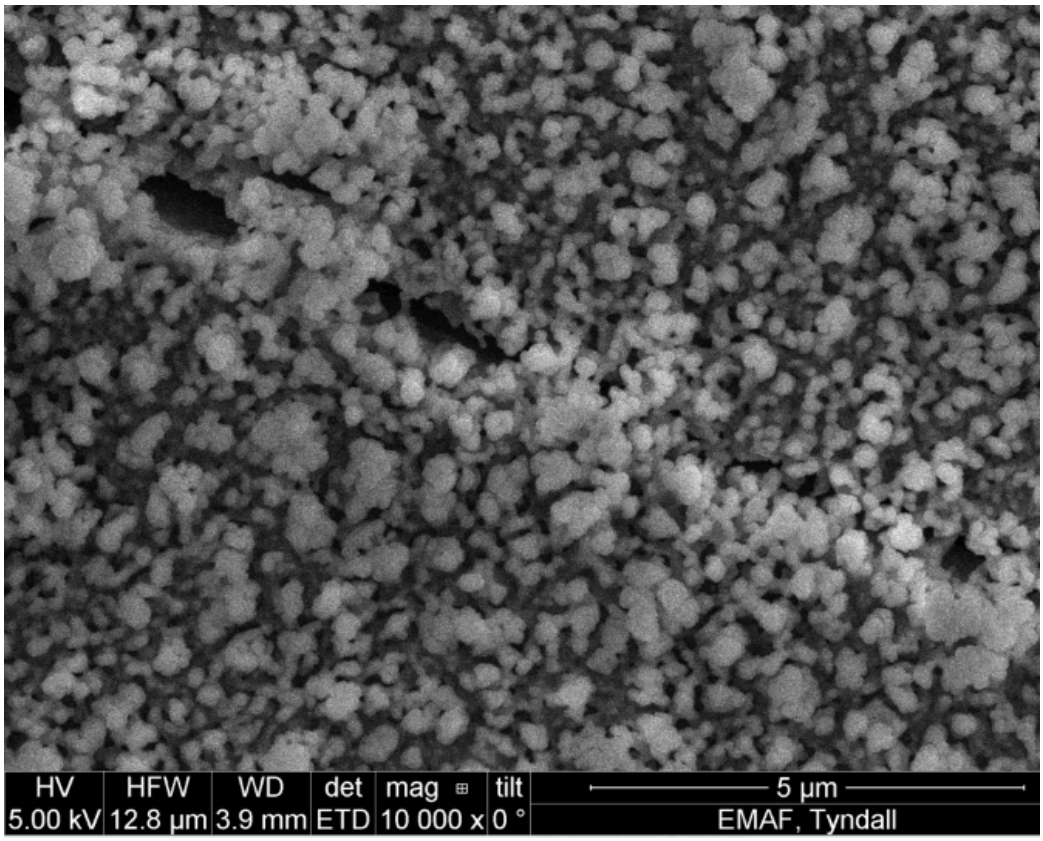


Figure 5.11. *FIB-SEM image of recombinant E.coli JM109 pAR3114 (containing genes encoding functional Pdu MCP), unstained. Excess ice accumulation can be observed all over the plane of view (MS)*

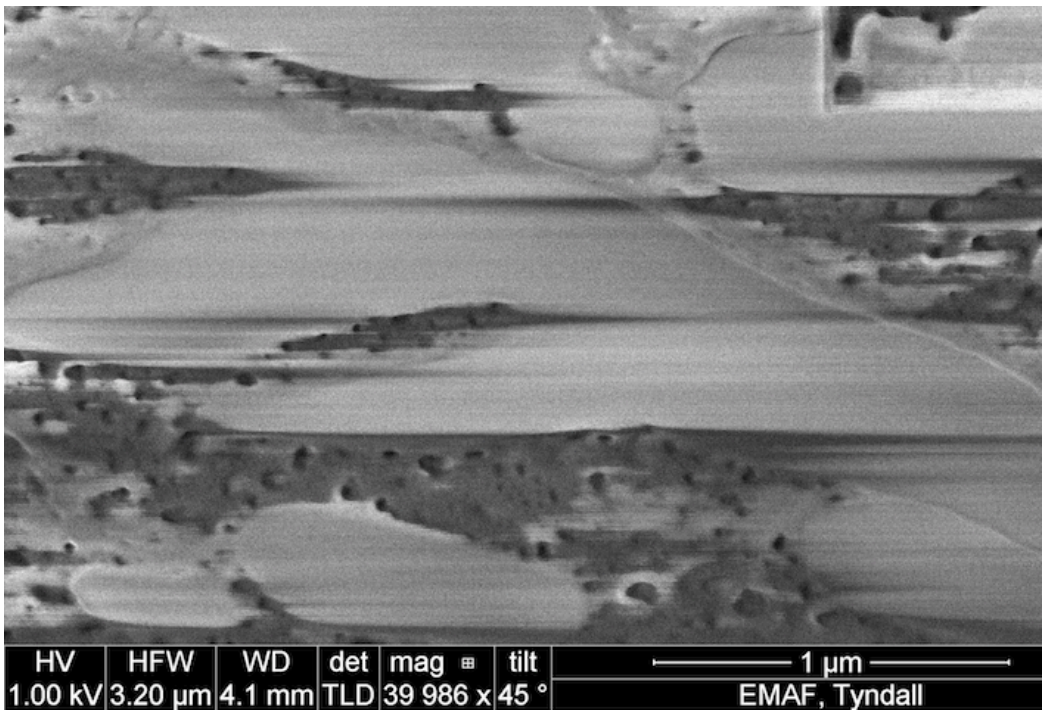


Figure 5.12. *FIB-SEM image of recombinant E.coli JM109 pAR3114 (containing genes encoding functional Pdu MCP), unstained. Vibration of the stage results in poor image resolution (POC).*

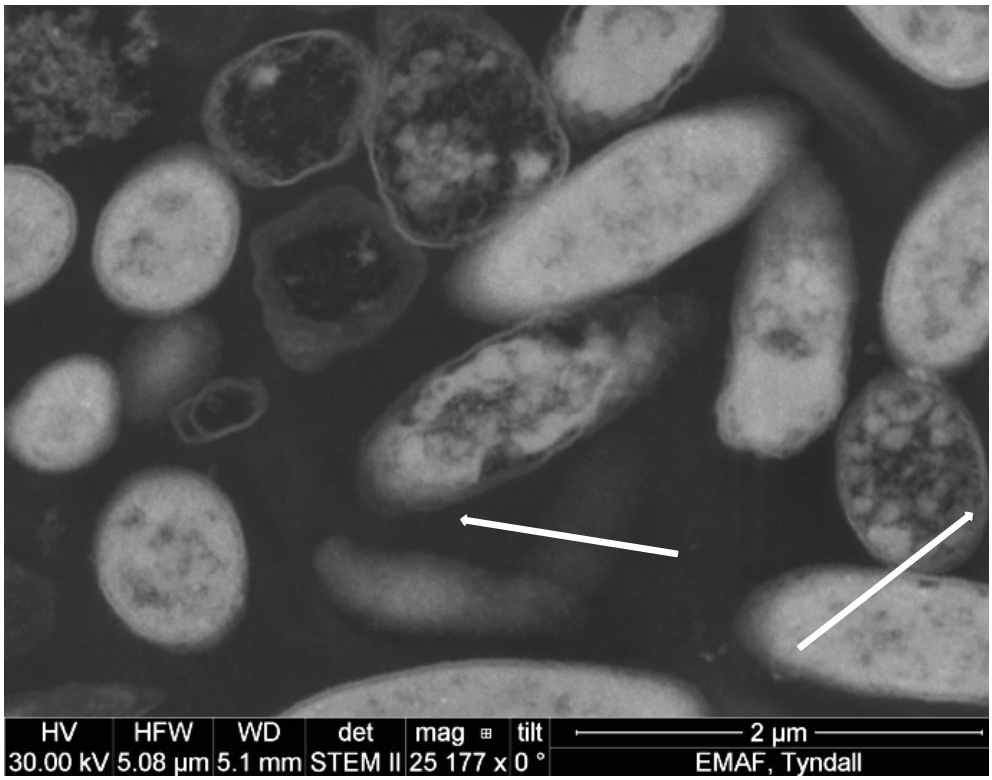


Figure 5.13. *STEM image of recombinant E.coli JM109 pAR3114 (containing genes encoding functional Pdu MCP), resin embedded sectioned and negatively stained with osmium. Light areas indicate electron light, dark areas indicate electron dense.*

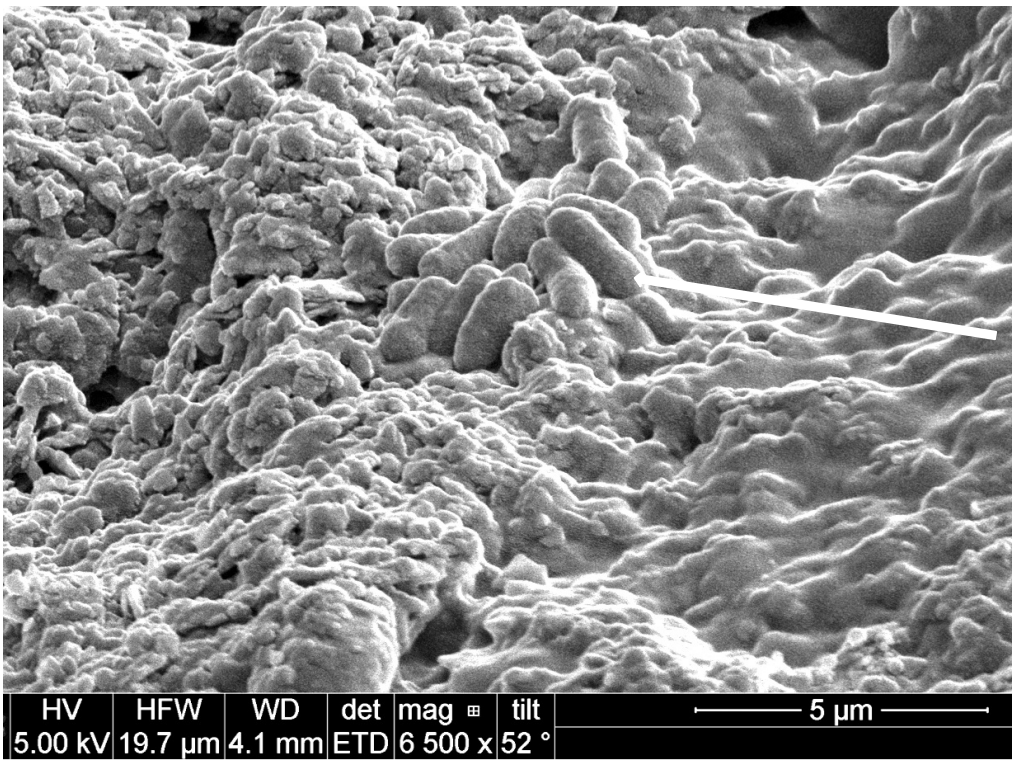


Figure 5.14 *FIB-SEM image of the recombinant E.coli JM109 pAR3114 (containing genes encoding functional Pdu MCP), stained with toluidine blue and glycerol, with bacterial cells identifiable on the surface (image by PC).*

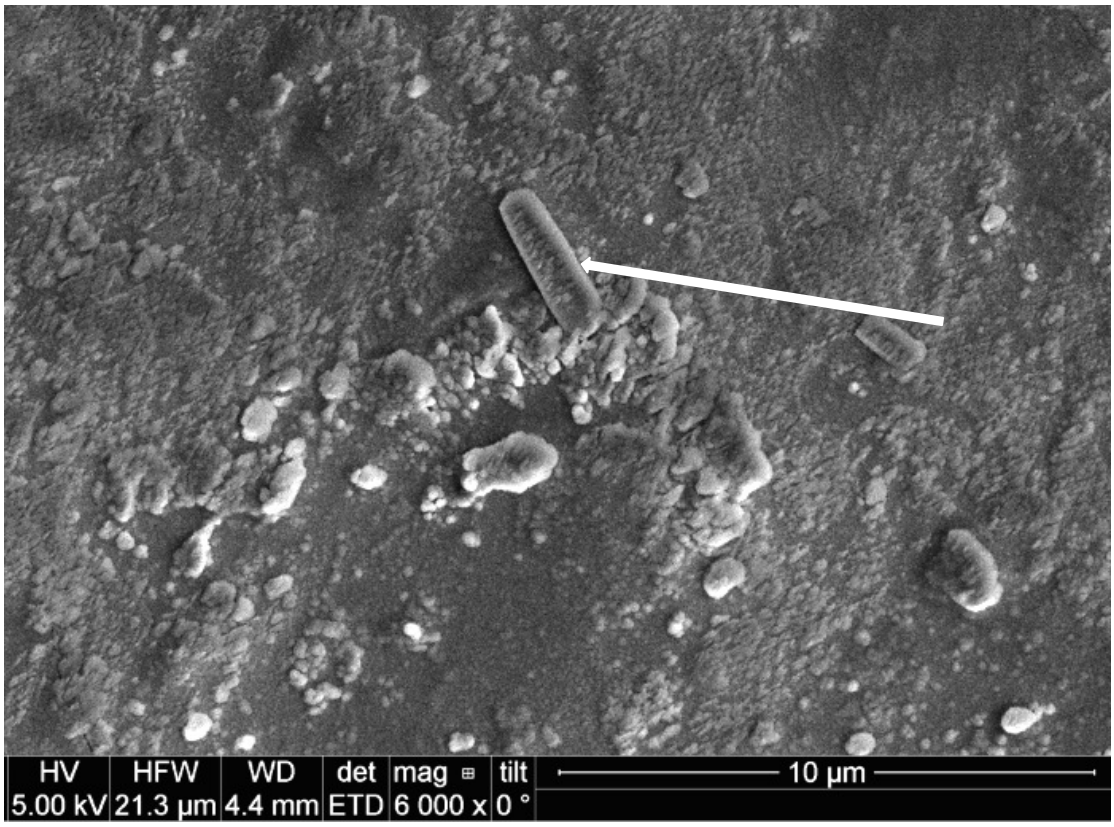


Figure 5.15. *FIB-SEM image of the recombinant E.coli JM109 pAR3114 (containing genes encoding functional Pdu MCP), stained with toluidine blue and bacitracin, with bacterial cells identifiable on the surface (image by PC).*

As previously mentioned, one of the largest difficulties with regards to utilizing the FIB-SEM was optimizing the quality of the field of view. Issues with ice accumulation and cell aggregation made identification of individual cells (necessary for FIB slicing) difficult. Experimentation with different agents (glycerol, bacitracin) provided information but no one agent proved to improve the sample resolution greatly. Due to a lack of individual cells, FIB cut locations were selected in the presence of identifiable cell clusters, which unfortunately made reconciling any observable intracellular structures with the corresponding individual cell highly difficult.

Typically, once a suitable location is identified, the FIB aspect is engaged, and milling of the sample begins. The next three images illustrate a site being milled inward.

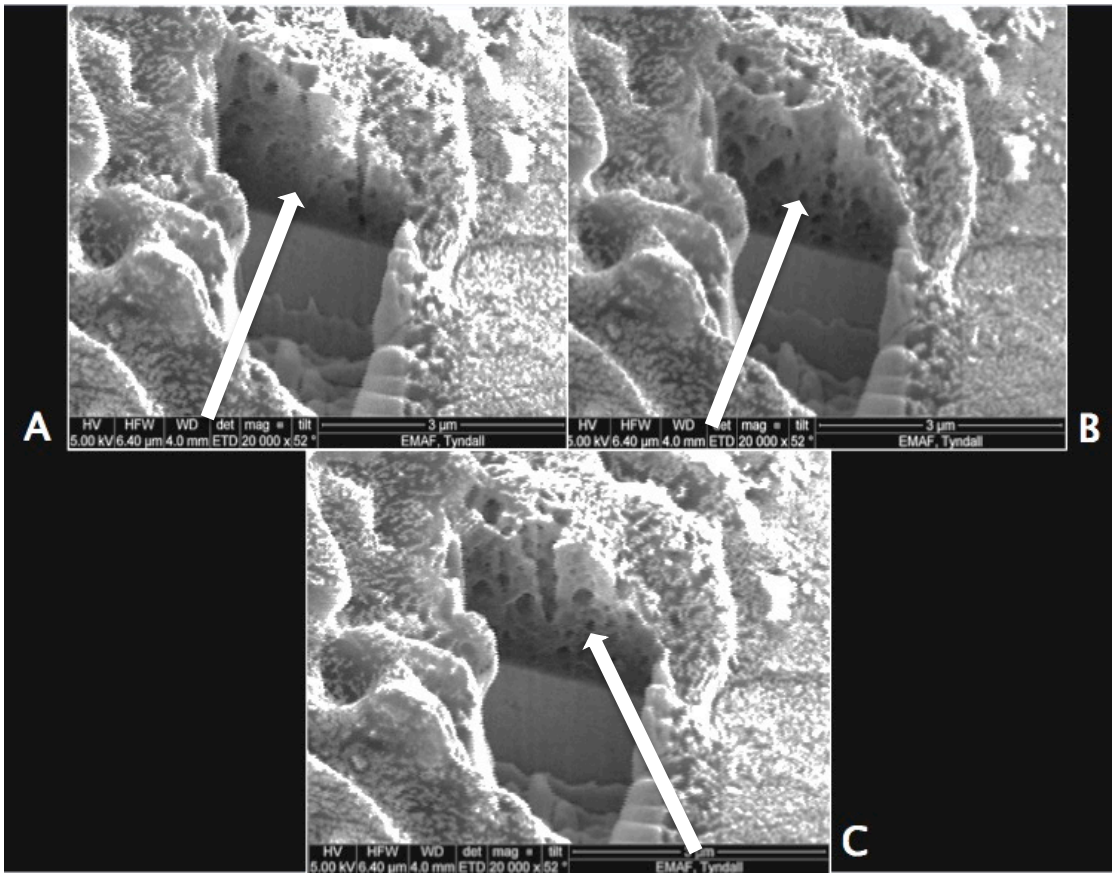


Figure 5.16. *FIB-SEM image of the recombinant E.coli JM109 pAR3114 (containing genes encoding functional Pdu MCP), whole cell sample being sectioned by FIB.*
Image A illustrates an initial cut site.
Image B illustrates view after 100nm milling upwards in the sample.
Image C illustrates view after an additional 100nm milling upwards in the sample (image by PC). Glycerol was supplemented to this sample in a 1:1 ratio. Arrows illustrate putative microcompartments observed within cells.

As can be viewed from the images, it is possible to see defects approximately 100-200 nm across typical of the size of bacterial microcompartments, of varying dimensions within the bacterial cell sample. However because of the difficulties in identifying individual cells, it is not possible to quantify the number of these putative intracellular compartments per bacterial cell.

5.4. Conclusion

Extraction of microcompartments from Gram negative bacterial cells has been optimized over the years since the first description (Cannon & Shively, 1983), and the need for a full cell fractionation procedure with sucrose density gradient centrifugation has been reduced by the use of proprietary detergent based lysis and solubilization systems. However development of microcompartment extraction from Gram positive cells has been more stagnant, most likely due to difficulties associated with high quality lysis of the Gram positive membrane and cell wall (Mahalanabis *et al,* 2012). The successful extraction of the Pdu microcompartment from *Lactobacillus reuteri* DSM20016 using novel adaptations has potential applications for other Gram positive microcompartments and for future protein extractions from Gram positive bacteria.

The experimentation into the extraction and imaging of the bacterial microcompartment was to act as a compliment to the previous studies of this thesis. Through this study, a number of different extraction methods were utilized in order to identify the optimal method. Through these methods, we achieved a number of successful microcompartment extractions, which enabled imaging studies. The resulting images correlated with previously published imagery of the microcompartments, with noticeable difference between the visual appearance of the Pdu microcompartment versus the Eut microcompartment.

The application of the FIB-SEM to the study of microcompartments has not previously been reported and was made possible by the Tyndall National

Institute's National Access Program (NAP), which provided funding and access to the FIB-SEM facilities. However the application of a technique typically utilized for materials science to biological samples led to a number of technical difficulties. Various iterations of the sample preparation protocol were utilized, with obstacles such as excess ice accumulation and a difficulty in creating sufficient contrast.

SEM-FIB has the potential to image microcompartments in native cells if the difficulties in sample optimization were achieved. Good progress had been made on this issue during the course of this study, and further optimization should include further study on the use of wetting agents such as bacitracin and bovine serum albumin (BSA), which when used in combination with an additional agent, may prevent the excess cellular aggregation which prohibited viewing individual cells (Michen *et al,* 2015). The extension of the sublimation time proved to be highly useful in reducing ice accumulation, and perhaps a further extension of this time to 40-45 minutes may remove the need for additional cryoprotectants such as glycerol. A key area of optimization also lies in the need to generate intracellular contrast. Although a key aspect of the FIB-SEM is the apparent non-requirement for stains to generate contrast, this did not translate well to our study, where more intracellular contrast would be essential to highlight the interior of the bacterial cells. In addition, the use of a cryogenic stage, while in theory allowing native structures tobe imaged without fixation arfetfact reduces the number of specimens which can be observed, because it requires several hours to achieve operating temperature.

Finally to progress this project, a multidisciplinary technical team would be utilized to provide wider expertise on the nature of the technology along with the nature of the biological sample. The FIB-SEM is a technology that has been primarily applied to the field of materials chemistry and electronics, which is very different from the study of biological material. However, technician expertise is required for the FIB-SEM capabilities to be used fully, and distinctly from a standard SEM. An increased knowledge of biological sample preparation and staining methodologies would provide greater insight and build on the foundation of optimization developed in this study.

5.5. References

- Alhede M., Qvortrup K., Liebrechts R., Høiby N., Givskov M., Bjarnsholt T. (2012) Combination of microscopic techniques reveals a comprehensive visual impression of biofilm structure and composition. FEMS Immunology & Medical Microbiology 65:335-342
- Cannon G., Shively J. (1983) Characterization of a homogenous preparation of carboxysomes from *Thiobacillus neapolitanus*. Archives of Microbiology 134:52-59
- Chapin R., Wine R., Harris M., Borchers S.C., Haseman J. (2001) Structure and Control of a Cell-Cell Adhesion Complex Associated With Spermiation in Rat Seminiferous Epithelium. Journal of Andrology 22:1030-1035
- Cocco A., Nelson G., Harris W., Nakajo A., Myles T., Kiss A., Lombardo J., Chiu W. (2013) Three-dimensional microstructural imaging methods for energy materials. Physical Chemistry Chemical Physics 15:16377
- Drews G., Niklowitz W. (1956) Beitrage zur Cytologie der Blaualgen. Archives of Microbiology. 24:147–62
- Dykstra M. (1992) Biological electron microscopy. Plenum Press, New York
- Havemann G., Bobik T. (2003) Protein Content of Polyhedral Organelles Involved in Coenzyme B12-Dependent Degradation of 1,2-Propanediol

in *Salmonella enterica* Serovar Typhimurium LT2. Journal of Bacteriology 185:5086-5095

- Lee-Wickner L., Chassy B. (1984) Production and Regeneration of *Lactobacillus casei* Protoplasts. Applied And Environmental Microbiology 994-1000
- Lorsch J. (2014) Laboratory methods in enzymology, 541: 85–94
- Mahalanabis M., Al-Muayad H., Kulinski M., Altman D., Klapperich C. (2009) Cell lysis and DNA extraction of gram-positive and gram-negative bacteria from whole blood in a disposable microfluidic chip. Lab on a Chip 9:2811
- Michen B., Geers C., Vanhecke D., Endes C., Rothen-Rutishauser B., Balog S., Petri-Fink A. (2015) Avoiding drying-artifacts in transmission electron microscopy: Characterizing the size and colloidal state of nanoparticles. Scientific Reports 5:9793
- Milani M., Drobne D., Tatti F. (2007) How to study biological samples by FIB/SEM. Modern Research and Educational Topics in Microscopy
- Morris V., Groves K. (2013) Food Microstructures. Elsevier Science, Burlington
- Muller-Reichert T., Verkade P. (2012) Correlative light and electron microscopy. Elsevier/Academic Press, Amsterdam, Netherlands
- Parsons J., Dinesh S., Deery E., Leech H., Brindley A., Heldt D., Frank S., Smales C., Lunsdorf H., Rambach A., Gass M., Bleloch A., McClean K., Munro A., Rigby S., Warren M., Prentice M. (2008) Biochemical and

Structural Insights into Bacterial Organelle Form and Biogenesis. Journal of Biological Chemistry 283:14366-14375

- Parsons J., Frank S., Bhella D., Liang M., Prentice M., Mulvihill D., Warren M. (2010) Synthesis of Empty Bacterial Microcompartments, Directed Organelle Protein Incorporation, and Evidence of Filament-Associated Organelle Movement. Molecular Cell 38:305-315

- Phelan, R., J.D. Holmes, N. Petkov (2012) Application of serial sectioning FIB/SEM tomography in the comprehensive analysis of arrays of metal nanotubes. Journal of Microscopy 246:33-42.

- Pilhofer M. (2010) Bacterial TEM: New Insights from Cryo-Microscopy. Elsevier

- Rubino S., Melin P., Spellward P., Leifer K. (2014) Cryo-electron Microscopy Specimen Preparation By Means Of a Focused Ion Beam. Journal of Visualized Experiments 10.3791/51463

- Sargent F., Davidson F., Kelly C., Binny R., Christodoulides N., Gibson D., Johansson E., Kozyrska K., Lado L., MacCallum J., Montague R., Ortmann B., Owen R., Coulthurst S., Dupuy L., Prescott A., Palmer T. (2013) A synthetic system for expression of components of a bacterial microcompartment. Microbiology 159:2427-2436

- Sinha S., Cheng S., Fan C., Bobik T. (2012) The PduM Protein Is a Structural Component of the Microcompartments Involved in Coenzyme B12-Dependent 1,2-Propanediol Degradation by *Salmonella enterica*. Journal of Bacteriology 194:1912-1918

- Soares Medeiros L., De Souza W., Jiao C., Barrabin H., Miranda K. (2012) Visualizing the 3D Architecture of Multiple Erythrocytes Infected with Plasmodium at Nanoscale by Focused Ion Beam-Scanning Electron Microscopy. PLoS ONE 7:e33445
- Umrath, W. (1974) Cooling Bath For Rapid Freezing In Electron Microscopy'. Journal of Microscopy 101.1:103-105.
- Weber, K., Osborn M. (1969) The Reliability Of Molecular Weight Determinations By Dodecyl Sulfate-Polyacrylamide Gel Electrophoresis. Journal of Biology Chemistry 244.16: 4406-12.

Chapter VI

Conclusions and Future Directions

6.0 Conclusions

This thesis describes investigations into the function of native bacterial microcompartments, with a particular focus on the ethanolamine utilization microcompartment (Eut) and the propanediol utilization microcompartment (Pdu), and on a hypothesis of a biotechnological application of recombinant microcompartments linked to polyphosphate metabolism. In recent years, the potential of the bacterial microcompartments to act as a biotechnological tool has been increasingly discussed, and this thesis explored the possibility of their application in a clinical setting.

In Chapter 1 the literature background for bacterial microcompartments and phosphate metabolism was reviewed, centred on the role of polyphosphate kinases .

The main biotechnological goal of the thesis was establishing the potential application of bacteria expressing microcompartment targeted polyphosphate kinases and bacterial microcompartments as a tool to remove phosphate from the environment, with a potential clinical application. The model organisms *E. coli* and *Lactobacillus reuteri* 20016 were used as expression hosts because of their non-pathogenic status and known capacity to make microcompartments. A link between microcompartment inducing conditions and polyphosphate formation was found in *L. reuteri.* Through the creation of constructs utilizing microcompartment-targeted *E. coli* polyphosphate kinase enzyme (PPK1) alone this research (Chapter 2) demonstrated an increase in short term phosphate uptake and polyphosphate storage by *Lactobacillus reuteri* and *E. coli in vitro*, utilizing lyophilized bacterial cultures added to sugar-supplemented water over 5

hours (Chapter II). *E. coli* cells co-expressing an empty microcompartment and microcompartment targeted PPK1 retained more polyphosphate and removed more phosphate from the supernatant than those expressing PPK1 alone.

Gluconate proved to be the optimal carbon source to be added to water in these experiments to create a salt free isotonic solution, promoting revival after lyophilisation and phosphate uptake without overgrowth. It also has the advantage that it is not utilized as a carbon source by rats. Quantitative estimates (Chapter III) suggested that deliverable numbers of bacteria in gluconate water could be capable of taking up comparable amounts of phosphate to that normally absorbed in the rat gut. *E. coli* and *L. reuteri* constructs overexpressing *E. coli* PPK1 alone and *E. coli* expressing microcompartment-targeted PPK1 with an empty microcompartment, were applied to an animal model study (Sprague-Dawley rats) evaluating their *in vivo* effect on reducing hyperphosphatemia of renal failure (Chapter III).

Whilst the results of this animal study on calcium and phosphate balance were difficult to interpret due to baseline variation in the study groups arising before therapeutic intervention, the ability to successfully deliver lyophilized bacterial cultures through a supplemented sugar-water source as viable bacteria, and successful recovery of bacterial cultures from animal faeces, and the intestines post-sacrifice was demonstrated. Interestingly, *E. coli* K12 MG1665 strains over expressing *E.coli* PPK1 persisted longer than the control MG1655 strain following single in vivo oral inoculations and were recovered in large numbers from rat faeces during the continuous dosing experiment. *E. coli* K12 strains

generally require streptomycin treatment to colonise rodents (Miranda *et al.,* 2004) and PPK1 overexpression seems to enhance their gut survival.

For further work, the use of an inbred rat strain model would likely provide more interpretable inter-group difference that would allow extension of the observed *in vitro* observations in an *in vivo* model. The creation of a chromosomally integrated *ppk-pduABJKNU* (empty microcompartment) in *Lactobacillus*, as originally intended, would also likely provide interesting information regarding the uptake capacity of the *Lactobacillus* strain *in vivo.* Validation of this ability for the *ppk* and Pdu microcompartment constructs to remove phosphate from surrounding environments may have future applications regarding clinical care via the use of probiotic strains such as *Lactobacillus*, or indeed further development of the MEBPR (Microcompartment Enhanced Biological Phosphorus Removal) system for environmental uses.

Additional thesis research regarding the properties of the native Pdu and Eut microcompartment has contributed to current knowledge regarding these two microcompartments. No previous literature, to the author's knowledge, exists discussing the effects on buoyant density of the cell of microcompartment expression, and the observable difference between the Pdu and Eut microcompartments regarding this (Chapter IV). This observation indicated a number of potential research avenues regarding the cause of this difference, and may be due to the production of ammonia gas or membrane permeability. Further investigation into these properties may provide interesting information and clarify the functional advantages conferred by Pdu and Eut microcompartments.

Eut extraction samples under EM appear to be electron-dense, indicating that the Eut microcompartment is not empty during these observations.

This investigation into the properties of the Pdu and Eut microcompartment, and the encountered difficulties in identifying quality imagery of microcompartments both *in situ* in the bacterial cell and also on extraction from the cell, led to experimentation with various cell fractionation and microscopy techniques (Chapter V). This research attempted to apply FIB-SEM to characterise microcompartments in situ within the cell without fixation using a cryogenic stage. The optimization of the extraction of bacterial microcompartments from the cell, particularly from the Gram-positive *Lactobacillus* cell, allowed improved sample quality, which in turn contribute to better sample imagery.

The use of the FIB-SEM in particular was a novel application regarding the study of microcompartments, and image quality was refined by the use of glycerol suspension, 3D reconstruction of sectioned native microcompartments by SEM-FIB may in future contribute to research regarding the development of synthetic microcompartment constructs. Whilst difficulties were encountered regarding the image quality after cryo-processing, this study represented a new avenue of exploration for identifiying bacterial microcompartments *in situ*, and potentially reconstructing these sectioned images into a 3D form using tomographical software if problems with cell clumping can be eliminated by addition of surface active compounds.

Overall, this thesis explores novel functional aspects of native bacterial microcompartments, and the possible uses of the properties of recombinant

microcompartments as a synthetic metabolic hub, as a clinical/environmental intervention.

6.1. References

- Miranda, R., Conway, T., Leatham, M., Chang, D., Norris, W., Allen, J., Stevenson, S., Laux, D. & Cohen, P. (2004). Glycolytic and Gluconeogenic Growth of Escherichia coli O157:H7 (EDL933) and E. coli K-12 (MG1655) in the Mouse Intestine. *Infection and Immunity* 72, 1666-1676.
- Penrod, J. T., Roth, J. R. (2006). Conserving a Volatile Metabolite: a Role for Carboxysome-Like Organelles in *Salmonella enterica*. Journal of Bacteriology 188:2865–2874.

Acknowledgements

Firstly, I would like to thank my supervisor Prof. Michael Prentice for his guidance and support during the course of this research, and the writing of this thesis. Secondly, an enormous thank you to our postdoc, Dr. Mingzhi Liang. Without Mingzhi's support, advice and guidance, my research experience would have been much more difficult. Plus he introduced me to the best Chinese food in Cork, to make him more invaluable! Also to the former members of 403, Tamara and Kamila, for being so friendly and supportive.

To the School of Microbiology – a great place to spend my college years, with a great academic and research team, plus the friendliest community of people. Huge thanks to Maire for constant order demands, to Morris for much rat advice, to Dan for saving computers and of course to Paddy for enormous help and advice regarding the mass lyophilisation experiments. To the APC staff also – in particular Catherine who was a great mentor away from the lab, and continues to be now.

A very special thank you must go to Elaine Barry, who is still probably confused as to how she got landed with me, but became a great friend and made a difficult time enjoyable. The light at the end of the tunnel is near! Additional thanks to the rest of the Physiology gang for being so lovely, and to Helen and Amr in Pathology for all their help.

The office of 406 was a great place to be based during this time and always allowed rants and laughs. To Adam, Aoife, Marc, John, Alli, Ian and Emma - all past and present have been great friends and always supportive. Plus a special mention to Jill, for great advice and help throughout.

My second lab home was 335/337 where baked goods were always a given! To Lorraine, Karen and Des – thanks for always alerting me to cakes and creating a laugh! You all continue to be my Christmas desk gurus! Of course a huge sappy thanks to my lab partner-in-crime – to Alicia (Camps) for not only being a great roomie but for also knowing my medical history for those times that the knee won't stay in! I'm returning all those favours to you now – and then we can gloat together!

Away from the lab, I was lucky to have friends who kept things light-hearted but were always there for the tea-times and breaks for freedom – Fiona for the constant trashy tv and nights out, Linda for making sure I didn't look like an urchin, and Lynda for being interested from the other side of the world. Plus fellow foodies Ruth and Cole – #microbiologistsforlife.

Finally, although they probably hadn't (and still haven't) got a clue what exactly I do, I am lucky to have a great family who don't need explanations, just offer tea and laughs. Sarah and Elaine – my two blonde superiors who just get things and always supported the nerd. To my beloved Nan and Granda, who always bought me books. To Aoife, who insists she isn't loved but in fact is the most loved – you are a great babydoll. Most importantly to my parents for always being proud of me and making me proud of them, in every way.

Finally, to Dylan who wouldn't let me quit and who I know won't quit on me.